THE ROLE OF STRESS-DERIVED VESICLES IN THE BYSTANDER EFFECT AND CANCER RELATED CACHEXIA

Thesis is submitted in partial fulfilment of the requirements of the award of Doctor of Philosophy

FINDLAY REDVERS BEWICKE-COPLEY

Department of Biological and Medical Sciences

Degree awarded by

Oxford Brookes University

First submitted for examination:

January 2018

ACKNOWLEDGEMENTS

Thank you to Oxford Brookes for providing funding for my research, and especially to Professor Nigel Groome whose research and generosity has allowed so many to complete their PhDs. I would also like to say thank you to the Cancer and Polio trust for providing some of the funding for my PhD

I would like to thank my Supervisors Dave and Ryan for their support throughout my PhD and for only occasionally saddling me with unrelated projects. Without your guidance and support I would have curled up into a ball in the corner of the office and gently sobbed to myself for the last 5 years. Thanks to Priya for her tireless work ensuring the lab functions correctly and supporting all other members of the lab. I'd also like to thank past members of the lab, Laura Jacobs and Laura Mulcahy for their support throughout both my MSc and my PhD. Sunny Vijen for chatting with me whilst he smoked and making me leave lunch early, so he could have another smoke before going back to work. Thank you to Robbie Crickley for all the lunch time chats. To Lia I would like to say χασμουριέμαι! Thanks to Bianca for all her help getting to know the world of immunocytochemistry. To all members of the lab, thank you for your help, for your camaraderie and for putting up with me mashing the return key with all my might whilst running code.

Thanks to Phoebe for bingeing Psychology and Louie Theroux documentaries on the days I was writing, as well as for her support through the hardships and breakdowns during the writing up phase. To Mum and Dad for reluctantly having their own live-in tech support and "getting things off tall shelves" support for the last 5 years. Sparks, Scruff, Gren, Jester, Jen, Jez and Es thanks for helping me destress by getting mad at video games, and to Babs for all the games of Talisman that ended in network trouble.

Thank you also to the members of the Jiu Jitsu Foundation for trying to break my limbs and dump me into the floor as hard as possible. Especially Edward Mearns, Mark Ham, Natalie Lockyer and Jake Gately for all their help over the past 5 years.

I would also like to thank Big Finish Audio productions, the podcasts: My Dad Wrote a Porno, The Dollop, The Guilty Feminist, Sit Down and Shut Up and many others for the many hours of audio that got me through the long hours in the lab.

Oh, and cheers to Dr. Millard for telling me never to get into academia.

ABSTRACT

Extracellular vesicles are small, lipid bound structures that are involved in intercellular signalling. They are known to be involved in numerous processes within the body, including in disease. One interesting function of EVs appears to be the induction of the bystander effect. The bystander effect refers to the non-targeted effects of stress, whereby stressed cells induce damage in neighbouring cells. EVs released from cells following irradiation have previously been shown to induce the bystander effect. EVs have also been implicated in the induction of cancer-cachexia, a muscle wasting disease. This disease is common in patients with cancer and is often linked to poor prognosis.

In this project the ability of EVs released from heat shocked cells to induce bystander effects has been assessed. EVs released from cancer cells following 45°C treatment induced the bystander effect and the bystander cells were shown to be more resistant to subsequent stress treatment. EVs retained this functionality for up to two weeks when stored at -80°C. EVs released following short, 70°C treatment were also able to induce bystander effects.

The ability of EVs from both stressed (cisplatin) and unstressed cancer cells to induce cachexia was also examined. Cancer EVs were able to reduce differentiation in vitro, but no effects were observed when these EVs were injected into mice. The proteome of these EVs and their parent cells was also identified via liquid chromatography-mass spectrometry and pathway analysis was carried out on these proteins.

These data suggest possible roles for EVs in cell-cell communication during stress and disease, with EVs being able to induce bystander effects and alter muscle development *in vitro*.

PUBLICATION ARISING FROM THIS WORK

Bewicke-Copley F, Mulcahy LA, Jacobs LA, Samuel P, Akbar N, Pink RC and Carter DRF (2017) Extracellular vesicles released following heat stress induce bystander effect in unstressed populations. Journal of Extracellular Vesicles. 6(1): 1340746.

ABBREVIATIONS

AIDS	Acquired immune deficiency syndrome
AP-site	Apurinic/Aprimidinic Site
ARF6	ADP-ribosylation Factor 6
ATF	Activating Translation Factor
ATPase	Adenosinetriphosphatase
BAK	Bcl-2 Homologous Antagonist Killer
BAX	Bcl-2-associated X Protein
BiP	Immunoglobulin heavy-chain binding protein
BE	Bystander effect
Bcl-2	B-cell Lymphoma-2
BER	Base Excision Repair
BID	BH3-interating Domain Death Agonist
BLM	Bloom Syndrome Protein
BMI	Body Mass Index
CAD	Caspase-activated DNase
cAMP	Cyclic adenosine monophosphate
C/EBPβ	CCAAT-enhancer-binding protein β
CCM	Cell Conditioned Media
CD9,63,81	Cluster of Differentiation 9, 63, 81
DISC	Death Induced Signalling Complex
DSB	Double Strand Break
ER	Endoplasmic Reticulum
ESCRT	Endosomal Sorting Complexes Required for Transport
EV	Extracellular Vesicle
EXO1	Exonuclease 1
FADD	Fas-associated Death Domain
hnRNPs	Heterogeneous Nuclear Ribonucleoproteins
HR	Homologous Recombination
Hsps	Heat shock Proteins
ICAD	Inhibitor of caspase-activated DNase
LCMS	Liquid chromatography-mass spectrometry

IGF	Insulin-like Growth Factor
IGFBP-3	Insulin-like Growth Factor Binding Protein 3
IL-1β	Interleukin-1β
ILV	Intraluminal Vesicle
IRE1α	Inositol-requiring protein 1α
LFQ	Label Free Quantification
LLC	Lewis Lung Carcinoma
lncRNA	Long Non-Coding RNA
MAC	Membrane attack complex
MAPK	Mitogen-Activated Protein Kinases
MMR	Mismatch Repair
MRN	Mre11-Rad50-Nbs1
MST1	Mammalian Sterile-20 Kinase
MVB	Multivesicular Body
MyHC	Myosin Heavy Chain
NCO	Non-crossover
NER	Nucleotide Excision Repair
NF-κB	Nuclear factor kappa-light-chain-enhancer of activated B cells
NHEJ	Non-Homologous End Joining
PCNA	Proliferating Cell Nuclear Antigen
PERK	PRKR-like ER Kinase
RFC	Replication Factor C
RIDD	Regulated IRE1-dependent decay of mRNA
ROCK 1	Rho-associated coiled-coil-containing protein kinase 1
ROS	Reactive Oxygen Species
RPA	Replication Protein A
SCE	Sister chromatid exchange
SEC	Size-Exclusion Chromatography
SSB	Single Strand Break
TFIIH	Transcription Factor II Human
TNF	Tumour Necrosis Factor
TRAIL	TNF-related Apoptosis Inducing Ligand
TSG101	Tumour Susceptibility Gene 101
UPR	Unfolded Protein Response

VSP4	Variant-specific surface protein 4
XP(A-G)	Xeroderma Pigmentosum Group (A-G)-Complementing Protein
XRCC4	X-ray Repair Cross-Complementing Protein 4
ZFAS1	Zinc finger antisense 1

TABLE OF CONTENTS

TABLE OF FIGURES

TABLE OF TABLES

1 INTRODUCTION

1.1 STRESS RESPONSE

1.1.1 THE CELLULAR RESPONSE TO STRESS

Cells require a controlled environment to ensure optimal function and health of the cells, the tissues they comprise and the organisms they make up. The body has numerous systems to maintain the correct environment which is collectively known as homeostasis. When cells are cultured in a laboratory they need to be maintained in strict conditions, nourished with buffered medium and grown in CO_2 controlled, humidified incubators. Deviation from these conditions can cause problems for the cells; leading to the cells becoming stressed or causing them to die. At high temperatures protein folding begins to collapse, as the hydrogen bonds holding their secondary, tertiary and quaternary structures break, leading to them becoming denatured (Neurath *et al.,* 1944). The temperature at which these problems occur differs for different proteins, with some having evolved to function at extreme temperatures (Feller 2010). At low temperatures chemical reactions will slow and low temperature has also been shown to cause proteins to denature (Privalov & Privalov 1990). Changes to the pH also affect the functioning of cells and organs. Cells attempt to buffer any changes to pH and can pump protons into the extracellular space to control internal pH (Aoi & Marunaka 2014). Blood is maintained at a pH narrow range of 7.36-7.44 and cells at 7.2 through the use of the HCO_3^-/CO_2 buffer (Lee Hamm *et al.,* 2015). Protein kinetics are impaired when not in their optimum pH range and they can even become denatured causing them to malfunction (Jain *et al.,* 2015). Oxidative stress occurs when the regulation of reactive oxygen species (ROS) breaks down. ROS are generated as part of normal cellular metabolism and are utilised in numerous ways by cells such as in iron homeostasis (Ray *et al.,* 2012). However, if the levels of ROS get too high then the cells

will experience damage, therefore the levels of ROS are tightly controlled in cells via the action of molecules known as antioxidants (Ray *et al.,* 2012).

Alteration of the cellular environment is not the only thing that can affect the functioning of cells, there are also numerous exogenous agents that will negatively impact their function. Many drugs are intended to alter or impair cellular functions in order to help the overall health of the organism. Many chemotherapeutic agents aim to kill cells that are undergoing cell division. As cancer cells grow rapidly they are more sensitive to these drugs than normal cells; however, normal cells will inevitably be affected as well (Malhotra & Perry 2003). Radiation is able to cause mutations within DNA leading to errors in protein synthesis (Hutchinson 1966) and it is used in Radiotherapy to cause fatal damage to cancer cells. However, it affects both normal and cancerous cells, but as normal cells divide more slowly than cancer cells it is easier for them to repair DNA damage (Panganiban *et al.,* 2013).

When an organism becomes diseased the affected tissues, their neighbouring sites and even the whole organism can experience a disruption to homeostasis (Brestoff & Artis 2015; Kotas & Medzhitov 2015; Haughey *et al.,* 2002). In cancers numerous physiological processes can become disturbed, leading to numerous stress responses in an attempt to counter the damage being done (Luo *et al.,* 2009). Normal cells contain numerous checkpoints to ensure a tightly-regulated cell cycle and numerous processes that will attempt to repair or kill damaged cells. However, in cancer these systems are subverted and the cells grow out of control (Hanahan & Weinberg 2011; Pflaum *et al.,* 2014). As such, normal physiology breaks down and cancer cells often exist in stressed conditions: e.g. hypoxia due to poor vasculature within the tumour (Ackerman & Simon 2014). On top of the surrounding environment inducing stress, the activity of the tumour cells also induces stress in them. The speed of cancer cell replication leads to high levels of DNA damage as the cell is constantly reproducing its genome (Gaillard *et al.,* 2015). The increased growth

also demands an increase in the levels of proteins produced which can lead to stress in the endoplasmic reticulum (ER) (Ackerman & Simon 2014; Giampietri *et al.,* 2015). Tumour cells also often display high levels of heat shock proteins; chaperones that protect the other proteins within the cell (Mosser & Morimoto 2004). This means that tumour cells rely on numerous stress responses in order to stop themselves from undergoing cell death (Luo *et al.,* 2009). An interesting phenotype in cancer is the unexplained loss of fat and muscle mass known as cancer cachexia (Fearon & Moses 2002; Aoyagi *et al.,* 2015). This wasting is accompanied with very high levels of resting energy expenditure (Mak & Cheung 2006) and an increase in protein catabolism (Jeevanandam *et al.,* 1984; Vaughan *et al.,* 2013) which is implicated in the condition, showing that the breakdown of metabolic homeostasis can have catastrophic effects.

One key regulator of cell survival following damage is the transcription factor p53. First observed in 1979 (Kress *et al.,* 1979; Lane & Crawford 1979) this protein is integral in the choice between repair and apoptosis. P53 is a tumour suppressor and halts the cell's division in G1 phase, should the cell be damaged or stressed in some fashion (Hirao & Kong 2000; Kuerbitz *et al.,* 1992). The mechanism that dictates whether the cell is to be repaired or removed is as yet known but, seems to be related to the presence of pro-apoptotic cofactors and other survival signals that modulate the cell's susceptibility to apoptosis (Vousden & Lu 2002). If the cells goes down the cell death route p53 will activate apoptosis pathways, such as the CD95 (APO-1/Fas) system (Müller *et al.,* 1998), leading to the death and clearance of the cell. This mechanism allows p53 to stop damaged cells from dividing and propagating, which could potentially give rise to tumours.

Without any way to protect themselves from these stresses cells, tissues and organisms would be fragile, unable to survive even slight fluctuations in their environment. They would accumulate damage, become non-functional and perish. The stress response

is therefore integral to the survival of organisms. A brief overview potential stress responses is shown in Figure 1-1.

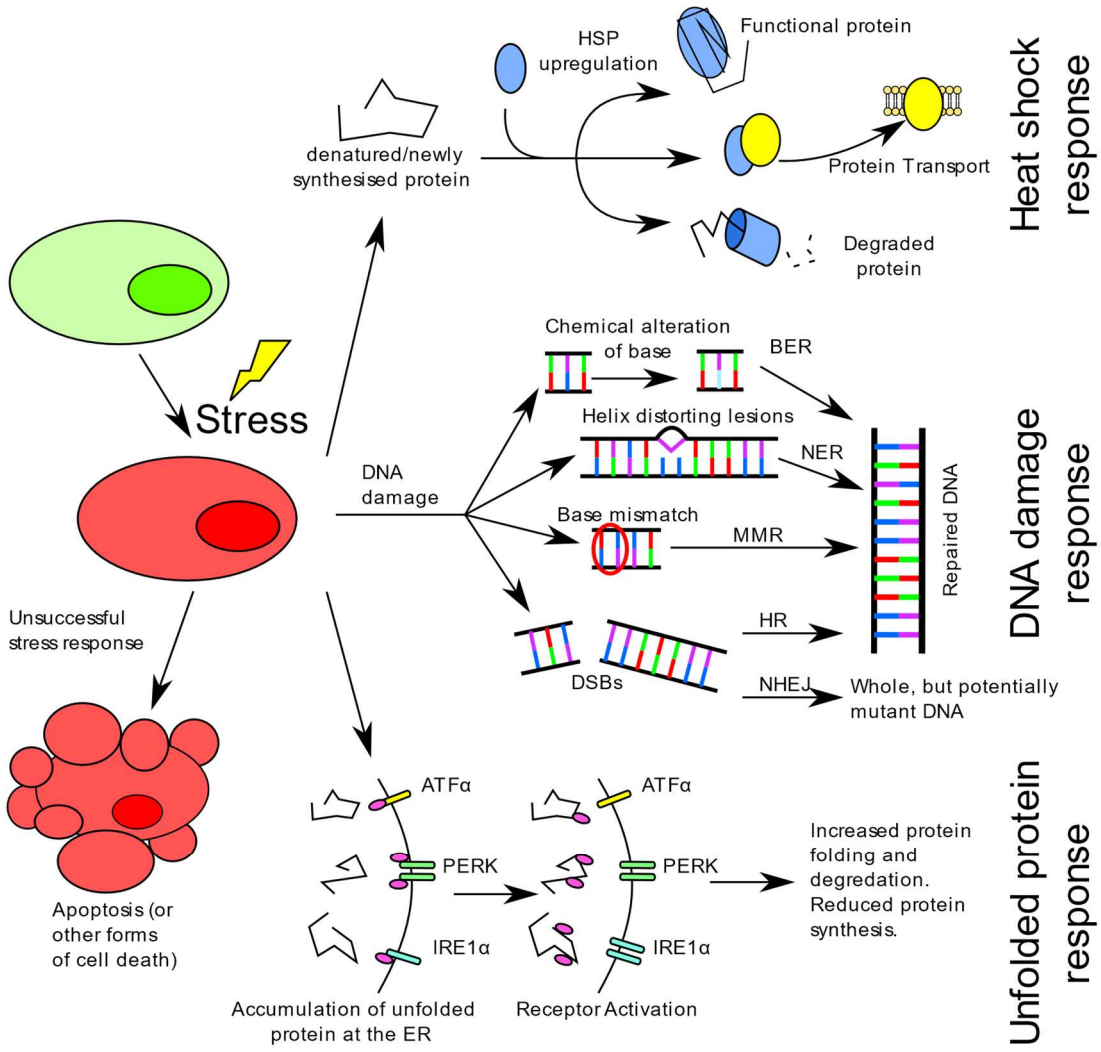

Figure 1-1: Cellular stress responses. *There are numerous different ways in which cells can attempt to mitigate damage caused due to stressful conditions. Stress often inhibits correct protein synthesis and function. Heat Shock Proteins (HSPs) are involved in ensuring that cellular proteins remain functional. Most HSPs are molecular chaperones whose role is to ensure that proteins fold correctly and maintain their structure. However, some have other functions such as transporting proteins or targeting damaged proteins for degradation. Cells that undergo DNA damage have numerous different methods which can be used to try and fix the problem, depending on the type of damage that has occurred. Double strand breaks can be repaired one of two ways. Homologous recombination is where a sister chromatid is recruited to be used as a template strand for repair. Non-homologous end joining does not use a template, and as such is more prone to error. The unfolded protein response is triggered by a build-up of unfolded proteins with in the endoplasmic reticulum. This triggers several cascades which lead to the reduction of the levels of protein by, for example, increasing the rate of protein degradation. If the cell is unable to resist the stress it will undergo cell death.*

1.1.2 THE HEAT SHOCK RESPONSE

Cells are sensitive to differences in temperature with changes of only a few degrees inducing stress response (Richter *et al.,* 2010; Purschke *et al.,* 2010). When outside of the optimal growth conditions the cell's proteins begin to denature, leading to the proteins unfolding and aggregating, inhibiting their correct function (Neurath *et al.,* 1944). As the hydrogen bonds holding the cell's proteins together break, their tertiary and quaternary structure can be altered, potentially leading to loss of function if they lose their active sites (Richter *et al.,* 2010). It is therefore imperative for cells to be able to maintain protein structure during stress. Heat shock proteins (Hsps) are a class of proteins commonly found up-regulated during stress conditions. They earned their name as they were first observed following heat treatment, however they are not solely involved in the heat shock response. In fact, Hsps are induced in most types of stress (Feder & Hofmann 1999) and many are even active in normal physiological conditions (Hartl *et al.,* 2011; Uma *et al.,* 1999; Matts *et al.,* 1992). The majority of Hsps act as molecular chaperones whose role during stress is to ensure the cellular protein maintains a functional structure, stop protein aggregation and to aid the correct folding of newly synthesised proteins (Feder & Hofmann 1999; Whitley *et al.,* 1999; Richter *et al.,* 2010; Bao *et al.,* 2002).

Molecular chaperones are able to distinguish between folded and unfolded proteins as unfolded proteins tend to have a large number of exposed hydrophobic amino acids (Richarme & Kohiyama 1993). They act either by binding to unfolded proteins, halting erroneous interactions within the cells that could cause problems or by helping the proteins fold correctly; these two types are known as holdases and foldases (Richter *et al.,* 2010; Nunes *et al.,* 2015). There is some evidence that holdases and foldases work together to ensure efficient protein refolding (Hoffmann *et al.,* 2004) with the presence of foldases linked to the dissociation of protein from holdases. There are several major classes of molecular chaperones (based on the molecular weight of the proteins) within the Hsps:

Hsp60s, 70s, 90s, 100s and small Hsps. An overview of the Hsps can be found in Figure 1-2. Hsp60 is mainly found within the mitochondria and is able to both hold unfolded protein and provide an isolated environment for the peptide to fold correctly (Calderwood *et al.,* 2006; Cheng *et al.,* 1989; Magnoni *et al.,* 2014). This ring-shaped chaperone surrounds the unfolded protein, separating it from other non-native proteins which might affect the folding process or cause aggregation of unfolded protein (Hartl *et al.,* 2011). Hsp70 is a highly conserved chaperone and is expressed both during stress and normal physiological conditions. It comprises an N-terminal domain involved in regulating conformational changes to the other domains; a substrate binding domain specific for exposed hydrophobic regions of the proteins; and the C-terminal domain which can change position to "close" the substrate binding domain (Hartl *et al.,* 2011). It has a wide range of biological functions such as protein folding, transport and degradation. Whilst the Hsp70s are similar in terms of their structure, their diversity is due to the wide range of cofactors that they interact with, such as Hsp40/J-domain-containing proteins (Kampinga & Craig 2010). BiP is a member of the HSP70 family of chaperones that is involved with protein folding within the ER (Griesemer *et al.,* 2014). This chaperone is also involved in the induction of the unfolded protein response (UPR) as it binds to the intercellular regions of three key proteins within the ER stress cascade, holding them in an inactive state (Bertolotti *et al.,* 2000). Once BiP disassociates from these proteins the UPR cascade begins (Okamura *et al.,* 2000). Hsp90 is found at high levels in the cytosol during normal conditions and increases when cells encounter stress conditions (Buchner & Li 2013). This homodimeric chaperone acts as a foldase and helps to ensure the correct folding of proteins during physiological and stress conditions. Unlike other HSPs it deals with proteins in the final stages of maturation (Buchner & Li 2013; Nathan *et al.,* 1997). It is also involved in regulating numerous facets of cancer progression such as: tumour growth, metastasis and angiogenesis. As such it is a target for anti-tumour therapy (Wu *et al.,* 2017). GRP94 is a HSP90-like chaperone that

operates within the ER in response to incorrectly folded proteins (Kozutsumi *et al.,* 1988). This protein is known to be involved in the innate immune response, with the absence of this protein in B cells leading to internal retention of Toll-like receptors which subsequently stops the B cell from recognising pathogens (Randow & Seed 2001). Hsp100 is a protein disassembler or unfoldase; it unfolds misfolded proteins allowing them to refold correctly and separates aggregated proteins (Saibil 2013). Non-native proteins are pulled through the centre of a ring-like structure causing them to unfold, therefore allowing them to re-fold correctly (Richter *et al.,* 2010; Saibil 2013). Some members of the Hsp100 proteins such as ClpX have proteolytic activity, degrading the proteins as they pass through the ring-like structure (Labreck *et al.,* 2017). Small Hsps range in size from around 12-43 kDa, and are often active as large oligomeric structures (Bakthisaran *et al.,* 2014). They are chaperone proteins that exhibit holdase activity and aim to stop partially folded or unfolded proteins aggregating within cells (Richter *et al.,* 2010; Bakthisaran *et al.,* 2014). Some sHsps have also been shown to be able to aid correct folding for their targeted proteins (Bakthisaran *et al.,* 2014). Several classes of heat shock proteins have been shown to have an anti-apoptotic effect achieved in numerous ways (Hatayama *et al.,* 2001; Wu *et al.,* 2017; Fulda *et al.,* 2010; Takayama *et al.,* 2003; Pasupuleti *et al.,* 2010).

The heat shock proteins are invaluable to the cell, both during normal conditions and whilst attempting to ensure correct protein folding continues under stress conditions. Without these chaperones to ensure the stability of their protein complement, the cells physiological processes would begin to shut down as misfolded, non-functional proteins are created and protein aggregates form overwhelming the cell.

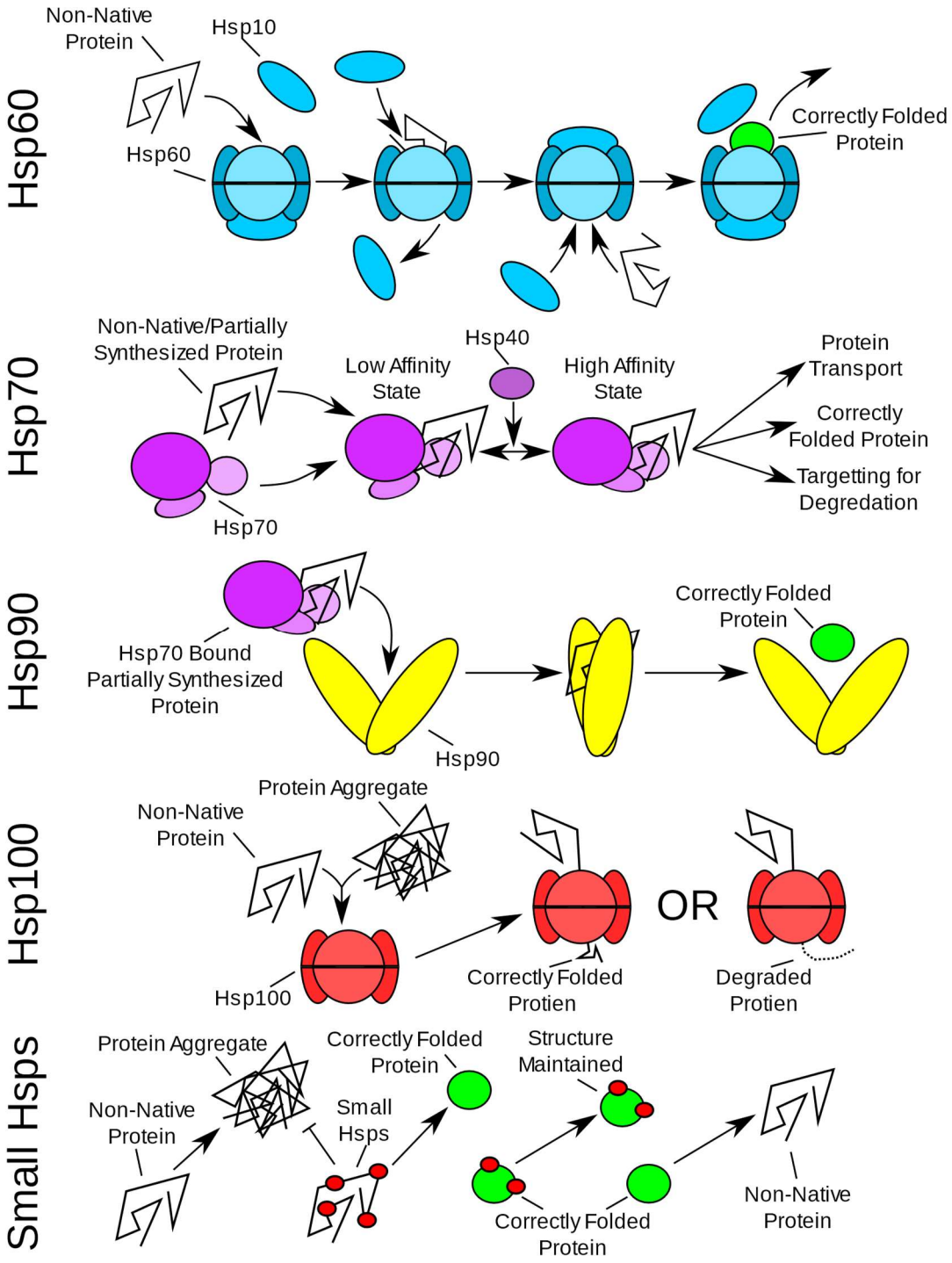

Figure 1-2: The five major classes of heat shock proteins. *The heat shock proteins are a family of proteins that are involved both during normal physiological conditions and during stress conditions. There are five main classes of HSPs: HSP60, HSP70, HSP90, HSP100 and small HSPs. The majority of HSPs expressed within cells act as molecular chaperones whose function is to ensure and maintain the correct folding of cellular proteins. HSP60 acts as a compartment within the cell in which protein folding can occur away from other unfolded proteins, preventing aggregation. HSP70 binds to non-native/partially synthesised protein and prevents aggregation. HSP70 is also known to aid in protein transport, targeting protein for degradation and aiding the correct protein folding. HSP90 is commonly found in normal physiological conditions and is involved with the final maturation of newly synthesised protein. Incorrectly folded protein is passed through HSP100 causing the protein to unfold. Some HSP100s have protease activity and degrades the protein as it passes through. Small HSPs bind with non-native and correctly folded protein in order to prevent protein aggregation and unfolding.*

1.1.3 UNFOLDED PROTEIN RESPONSE

Many proteins are modified post-translationally at the endoplasmic reticulum, such as folding, glycosylation or oligomerization (Braakman & Bulleid 2011). When the cells undergo various stresses, such as glucose deficiency or hypoxia, the ability of the ER to produce correctly assembled proteins is impaired, leading to the accumulation of unfolded proteins in the ER, known as ER stress (Fulda *et al.,* 2010). When the ER is unable to maintain protein homeostasis due to this accumulation the unfolded protein response is initiated. This starts several processes all with the aim of increasing protein transport, folding and degradation, reducing the aggregated protein within the ER whilst also reducing the levels of protein synthesis (Fulda *et al.,* 2010; Wang & Kaufman 2014; Hetz 2012). If the cells are unable to combat the stress successfully then they will undergo apoptosis, via the mitochondrial pathway. Three transmembrane proteins exist within the lumen of the ER that are activated in order to initiate the unfolded protein response: Inositol-requiring protein 1α (IRE1α), PRKR-like ER kinase (PERK) and activating transcription factor 6α (ATF6α) (Hetz 2012). These proteins are held in an inactive state through physical interaction with immunoglobulin heavy-chain binding protein (BiP) (Wang *et al.,* 2009). Build-up of unfolded protein within the ER causes dissociation of BiP with these receptors, leading to their activation (Hetz 2012).

When IRE1α is activated it formers homodimers and begins to splice mRNA coding for the transcription factor X-box binding protein 1 (XBP1) which is then translated (Kawahara *et al.,* 1997). This transcription factor then upregulates various UPR genes such as ER chaperones (Chen & Brandizzi 2014). IRE1α also acts to reduce the levels of cellular mRNA in order to reduce the levels of protein synthesis, a process known as regulated IRE1-dependent decay of mRNA, or RIDD (Maurel *et al.,* 2014). If the ER stress reaches extreme levels, the cell no longer tries to reduce protein synthesis; instead IRE1 α begins to target

the apoptosis repressor Anti-Casp2 miRNA leading to the induction of apoptosis (Hetz 2012; Chen & Brandizzi 2014).

PERK activation leads to the formation of PERK homodimers which phosphorylate the eukaryotic initiation factor 2α (eIF2α), part of the eIF2 trimer (Wang & Kaufman 2014; Harding, *et al.,* 2000). This then leads to reduction of general protein translation and an upregulation of translation of ATF4 (Harding, *et al.,* 2000) which then acts to increase the transcription of ER genes. Phosphorylated eIF2α also affects the translational capabilities of the subunit eIF2β reducing protein synthesis (Nika *et al.,* 2001).

When activated ATF6α travels from the ER to the Golgi where the luminal and cytosolic region of the protein is cleaved by site-1 and site-2 proteases respectively (Sun *et al.,* 2015; Chen *et al.,* 2002). This releases the N-terminal fragment ATF6(N) into the cytosol, which travels to the nucleus and acts as a transcription factor, leading to the upregulation of UPR genes such as BiP, which acts as a molecular chaperone, and protein disulphide-isomerase, which is involved with forming and breaking disulphide bonds in protein folding (Walter & Ron 2012).

Without the UPR cells would be unable to clear blockages in the endoplasmic reticulum leading to protein aggregation in the ER and protein synthesis becoming restricted.

1.1.4 DNA DAMAGE RESPONSE

When a cell's DNA becomes damaged it is important that the cell is able to repair the damage with as few errors as possible to reduce the chances of mutations arising. Numerous factors are able to induce DNA damage in cells such as: irradiation, heat stress, oxidative damage and chemical agents (Hakem 2008; Velichko *et al.,* 2012).

Due to the various different types of DNA damage there are several distinct methods of DNA repair. Base excision repair (BER) removes a single nucleotide that has undergone

minor chemical alterations such as deamination or oxidation (Krokan & Bjoras 2013). The altered base is removed by a DNA glycosylase leaving an AP (apurinic/apyrimidinic) site (Jacobs & Schär 2012). AP endonuclease then creates a strand incision at the location of the AP site which is then either filled with short- patch (single nucleotide) or long- patch (2-13 nucleotides) repair (Hakem 2008). Nucleotide excision repair (NER) occurs when more complex lesions occur which leave the DNA helix distorted (Jackson & Bartek 2009; Ciccia & Elledge 2010), meaning a number of nucleotides must be completely removed and replaced. When the damaged DNA is detected, helicases separate the DNA strands both up- and down-stream from the damage (Coin *et al.,* 2008; Tirode *et al.,* 1999). The damaged section is then excised as a 24-32 nucleotide fragment before the gap is filled and sealed as above (Fadda 2016). Mismatch repair (MMR) is used to fix errors that occur in the newly synthesised strand during normal cell replication (Kunkel 2004; Bridge *et al.,* 2014). When mismatches are found on the daughter strand they are bound by a complex that degrades the erroneous section. Again the missing section is refilled by DNA polymerase and DNA ligase (Bridge *et al.,* 2014; Iyer *et al.,* 2008).

The above can only repair single-stranded breaks (SSBs) however as they require a template strand to re-synthesise and correctly match the excised nucleotides, double-stranded breaks (DSBs) are repaired by different pathways. In non-homologous end-joining (NHEJ) the broken ends of the DNA are ligated together, this is an error prone process (Jackson & Bartek 2009). In contrast homologous recombination (HR) uses a sister chromatid as a template sequence to faithfully repair the DNA (Ciccia & Elledge 2010; Jackson & Bartek 2009). Only around 10% of the DSB in mammalian cells are repaired with HR compared with NHEJ and HR can only occur S/G_2 phase (Hakem 2008; Jasin & Rothstein 2013).

Mutations arising within a cell's genetic code can be disastrous, causing the production of malfunctional proteins, which can lead to diseases such as cancer. It is, therefore, vital for the cell to be able to quickly and efficiently repair damage to its DNA.

1.1.5 APOPTOSIS

If cells are unable to survive stress they will activate cell death pathways, such as the apoptotic pathway. Apoptosis is controlled by the action of several caspases which, when activated, target numerous proteins for degradation, causing cells to be deconstructed from the inside. The nucleus begins to condense and break apart into smaller pieces. The cells then begin to break up into apoptotic bodies, large blebs from the plasma membrane, before being cleared by phagocytes for recycling (Ichim & Tait 2016; Taylor *et al.,* 2008). This controlled approach to cell death prevents damage to the surrounding cells and stops the immune response being triggered due to harmful molecules that may be released when the cells degrade in a less regulated manner, such as occurs in necrosis (Taylor *et al.,* 2008; Iyer *et al.,* 2009).

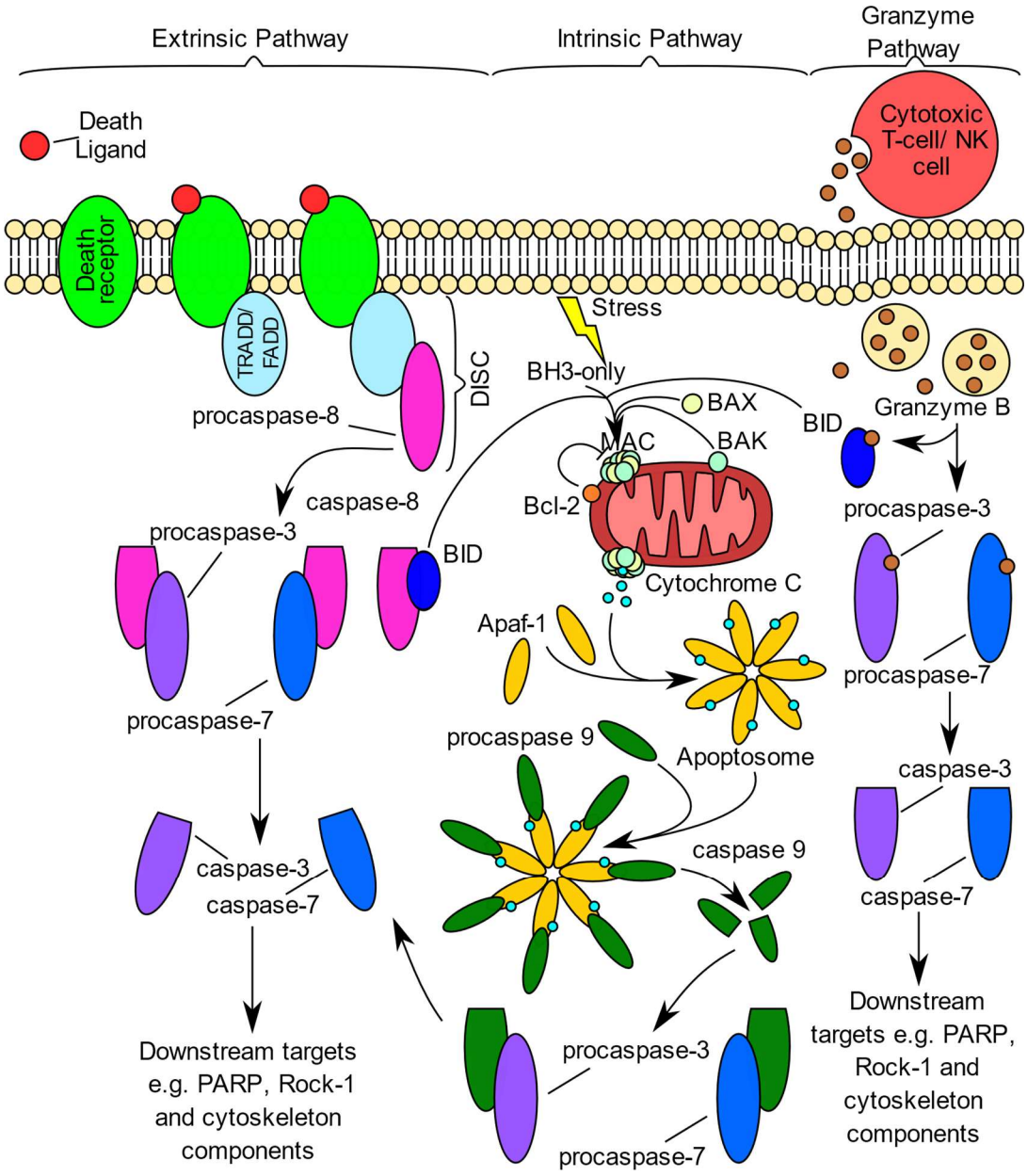

Figure 1-3: The caspase cascade. *There are numerous ways by which apoptosis is controlled, the most common are: the intrinsic pathway which involves the release of cytochrome C from mitochondria and the extrinsic pathway which involves the activation of membrane bound death receptors. The extrinsic pathway is initiated by stress conditions which activate proteins of the BH3-only family. In turn, these proteins activate BAX and BAK which form pores in the mitochondrial membrane allowing the release of cytochrome C. Bcl-2 proteins inhibit the formation of these pores when the levels of active BH3-only proteins are too low. Combined with Apaf-1 this forms the Apoptosome which cleaves procaspase-9, activating it. Caspase 9 then activates the effector caspases-3 and -7. In the extrinsic pathway death receptors (TNF receptor, TRAIL receptor) are activated and recruit death domain containing proteins (TRADD, FADD) to the membrane, which sequester procaspase-8 forming a complex known as the death-inducing signalling complex (DISC). Procaspase-8 is cleaved to active caspase 8 which in turn activates the effector caspases-3 and -7. Caspase 8 is also able to activate the BH3-only protein BID which can induce the intrinsic pathway by inducing BAX/BAK pore formation. Apoptosis is also able to be induced by the introduction of Granzyme B by immune cells. Granzyme B enters the cell via the endocytotic pathway and activates BID leading to the formation of BAX/BAK pores on mitochondria as in the intrinsic pathway. Granzyme B is also able to activate caspase-3 and -7. Caspase-3 and -7 then cleave numerous downstream targets such as other caspases, ROCK 1 and PARP.*

There are two main pathways for apoptosis: Intrinsic and extrinsic. Both pathways seek to activate a family of cysteine proteases known as caspases. These proteins exist in normal conditions within the cell as procaspases and are activated by proteolysis into their active forms following apoptosis signalling (Rastogi *et al.,* 2009). A brief overview of the main steps within the caspase cascade is shown in Figure 1-3. The extrinsic pathway occurs when death receptors such as the tumour necrosis factor receptor (TNFR), or TNF-related apoptosis inducing ligand (TRAIL) receptors are activated by a death ligand, tumour necrosis factor-α (TNFα) or Fas ligand (FasL) respectively. This then causes the recruitment of the TNFR type 1-associated Death Domain (TRADD) or the Fas-associated Death Domain (FADD) (Bodmer *et al.,* 2000; Ermolaeva *et al.,* 2008). FADD sequesters procaspase-8, forming the death-inducing signalling complex (DISC) and leading to the activation of caspase-8 (Ashkenazi 2008). Active caspase-8 targets caspase-3 and caspase-7 for proteolysis (Stennicke *et al.,* 1998; Hirata *et al.,* 1998) as well as BH3- interacting domain death agonist (BID) which, when truncated, activates the intrinsic pathway via the mitochondria (Huang *et al.,* 2016; Martinez-Caballero *et al.,* 2009). Caspase-3 then activates other caspases which then target their substrates for degradation (Slee *et al.,* 2001). TRADD acts by forming a complex with FADD, activating caspase-8 as above (Hsu *et al.,* 1996).

The mitochondria are also able to induce caspase activation by through the release of pro-apoptotic factors inducing caspase activation. (Wang & Youle 2009). Members of the BH3-only protein family are activated by the cells in stress conditions (Puthalakath *et al.,* 2007; Naik *et al.,* 2007). These apoptosis activators are inhibited by a subclass of the B-cell lymphoma-2 proteins (Bcl-2), and can only activate apoptosis if they reach a level sufficient to overcome this inhibition (Cheng *et al.,* 2001; Taylor *et al.,* 2008; Dejean *et al.,* 2006). These proteins then induce the construction of pores called mitochondrial apoptosis-induced channel (MAC) within the mitochondrial membrane made from BAK-

BAX oligomers (Martinez-Caballero *et al.,* 2009; Zong *et al.,* 2001; Dejean *et al.,* 2005). Truncated BID from the extrinsic pathway activates formation of these channels as well. This allows proteins within the mitochondria to enter the cytoplasm of the cell. One such protein cytochrome C binds with apoptotic protease activating factor 1 (Apaf-1) forming a structure known as the apoptosome (Zou *et al.,* 1999; Jiang & Wang 2000). This then recruits pro-caspase-9 and activates it via proteolysis (Zou *et al.,* 1999). Caspase-9 then cleaves and activates caspase-3 and caspase-7 starting the same cascades as in the extrinsic pathways (Slee *et al.,* 1999). Finally, a third way via which apoptosis may be induced is via the introduction of granzyme B into the cell by immune cells (Cao *et al.,* 2007). This protein is able to activate caspase-3 and caspase-7 and cleave BID leading to the formation of BAK-BAX pores in the mitochondrial membrane (Barry *et al.,* 2000; Yang *et al.,* 1998).

Once active, the caspases begin to cleave their many target proteins, eventually leading to the destruction of the cell. Some of the many targets of caspases are the components of the cytoskeleton. The degradation of these proteins leads to a loss of cellular structure producing a rounded appearance (Kothakota *et al.,* 1997; Mashima *et al.,* 1999). Membrane blebbing is induced when caspase-3 cleaves rho-associated coiled-coil-containing protein kinase 1 (ROCK 1) (Coleman *et al.,* 2001). ROCK 1 activity is also implicated in the fragmentation of the nucleus as it no longer occurs when ROCK 1 is silenced (Croft *et al.,* 2005). DNA is broken down by the protein caspase-activated DNase (CAD), which is activated when the inhibitor of caspase-activated DNase (ICAD) is removed by caspases (Liu *et al.,* 1997; Jänicke *et al.,* 1998). Chromosome condensation is caused by the phosphorylation of histones by the mammalian sterile-20 kinase (MST1) following its activation by caspases (Cheung *et al.,* 2003).

Once the cell has completely broken down into numerous apoptotic bodies they are phagocytosed, both by macrophages and neighbouring cells, then broken down for recycling of their contents (Gregory & Devitt 2004). In order for the apoptotic cells to be

cleared they must recruit the phagocytes to their location. In order to do this apoptotic cells release “find me” signals that attract the phagocytes including various secreted and vesicle associated molecules (Hawkins & Devitt 2013; Segundo *et al.,* 1999; Lauber *et al.,* 2003). The phagocytes then travel to the location of the apoptotic bodies and must correctly identify the apoptotic cells. They are aided in this with various “eat me” signals presented by the apoptotic cells, which induce phagocytosis (Ravichandran & Lorenz 2007). One key “eat me” signal is the presentation of phosphatidylserine on the outer leaflet of the membrane (Asano *et al.,* 2004; Hanayama *et al.,* 2002). Once the phagocyte has engulfed the apoptotic bodies they fuse with lysosomes and are subsequently broken down within phagolysosomes (Guo *et al.,* 2010).

The clearance of old or damaged cells, or simply cells that are no longer required needs to be carried out safely to avoid negative impacts in neighbouring cells. The highly controlled nature of apoptosis is beneficial as it means harmful components of the cell can be removed by specialised cells, not simply released into the extracellular environment which can occur when cells undergo necrosis.

1.2 THE BYSTANDER EFFECT

1.2.1 NON-TARGETED EFFECTS OF STRESS

The classical model of stress is that only the cells directly affect by the stress exhibit a stress response, with the surrounding cells and tissues being unaffected. However, there is mounting evidence of non-targeted effects of stress in the form of the bystander effect (Hall 2003; Hei *et al.,* 2008). The bystander effect is, in brief, the raising of a stress response in cells that have not been exposed to stress (Figure 1-4). This effect has been observed in many different cell types and organisms.

The first example of the bystander effect was reported in 1992. When cells were treated with α-particles 30% showed sister chromatid exchange (SCE), but estimates suggested only 1% of nuclei should have been traversed by α-particles (Nagasawa & Little 1992). Additional evidence of off-target effects of radiation was observed in 1994 in rat lung epithelium (Hickman *et al.,* 1994). Subsequent studies found other markers of damage in bystander cells such as P-53 levels and apoptosis (Hickman *et al.,* 1994; Prise *et al.,* 1998). Further work on the off-target effects of α-particles suggested that some extranuclear target of radiation that could explain the difference between the estimated numbers of cells traversed by α-particles and damaged cells (Deshpande *et al.,* 1996). It was suggested that some radiation target located outside of the nucleus existed that, when traversed by an α-particle, could then induce sister chromatid exchange. However a study targeting only 4 individual cells with α-particles observed micronuclei formation and apoptosis in bystander cells. (Prise *et al.,* 1998). As the cells were specifically targeted it could not be α-particles traversing the cytoplasm of the bystander cells that induced these bystander effects. Therefore, some signal must be released from the irradiated cells that is able to induce damage in the bystander cells. It's important to note, however, that there is

evidence of cytoplasmic irradiation leading to similar damage to nuclear irradiation and that this may still play a role in the bystander effect (Zhou et al 2009).

As these experiments were often carried out in cells grown in monolayers it was suggested that gap junction signalling was the mechanism by which bystander cells received these signals. Studies showed that the gap junction signalling inhibitors lindane and octanol were able to reduce the levels of bystander damage, suggesting that a bystander signal is transferred in this manner (Zhou *et al.,* 2000; Zhou *et al.,* 2001; Shao *et al.,* 2003). Further, when gap junction signalling was increased via treatment of cells with 8-Br-cAMP the number of micronuclei increased (Shao *et al.,* 2003).

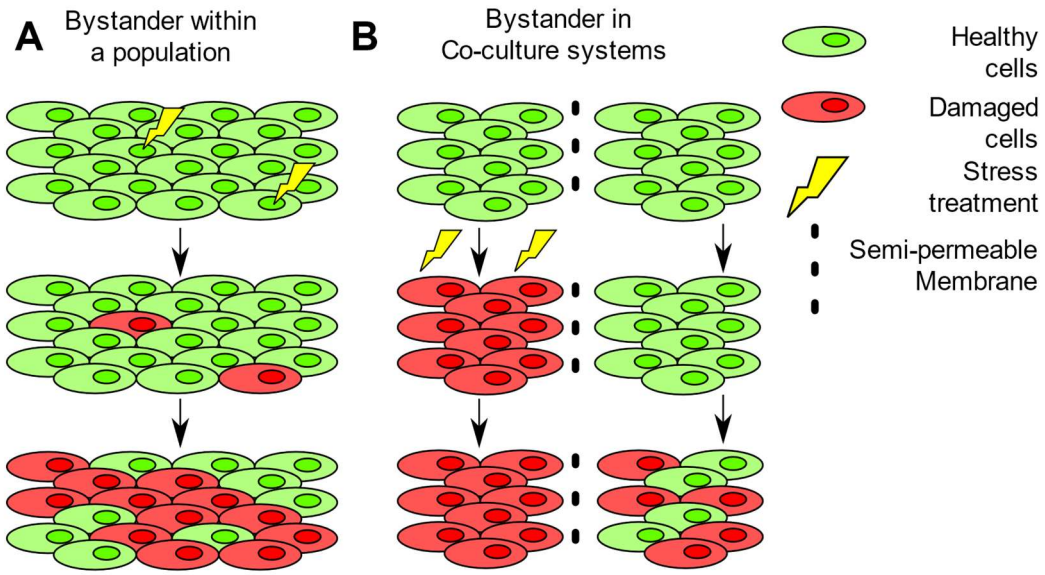

Figure 1-4: Damage occurs in cells that were not affected by a stressor. A *Bystander cells near to stressed cells within a population also become damaged, despite not actually being stressed themselves.* ***B*** *When a population of cells is stressed, and the stressed cells are co-cultured with unstressed cells the bystander cells also show damage, despite there being no cell contact.*

Interestingly the bystander effect is still observed when the medium from irradiated cells is harvested and fresh cells are grown in it (Mothersill & Seymour 1997; Lyng *et al.,* 2000; Mothersill & Seymour 1998). There was some suggestion that the irradiation was affecting the culture medium in some way, which in turn was causing the effects. However, a 2002 study observed no bystander effect when cells were cultured with irradiated medium alone, whilst co-culture with irradiated cells did show the effect (Zhou et al 2002).

As these cells are not in direct contact these data suggest that there is some extracellular signal that is released by stressed cells that induce these effects. It has more recently been shown that bystander cells treated with extracellular vesicles (EVs) extracted from irradiated cells show a higher level of DNA damage, apoptosis and chromosomal aberration than cells treated with EVs from non-irradiated cells (Al-Mayah *et al.,* 2012; Al-Mayah *et al.,* 2015).

1.2.1.1 IN VIVO STUDIES

Whilst much of the work on the bystander effect has been done in cell culture models there has also been work *in vivo* showing bystander occurring within organisms, see Figure 1-5. A study in 2008 irradiated radiosensitive *Patched-1*$^{+/-}$ mice whilst their heads were covered by a lead shield. There was an increase in medulloblastomas, DNA damage and apoptosis in the cerebellum of shielded mice compared to mice that were sham irradiated, or left untreated (Mancuso *et al.,* 2008). Another study showed DNA hypomethylation in the spleen, when the head of the animal head was irradiated (Ilnytskyy *et al.,* 2009). This work highlights that bystander can occur in whole animals and that the effect is not simply an artefact from cell culture systems. It also shows that the signals that induce the bystander effect are able to travel quite far from the original site of stress, with damage being observed in organs nowhere near the treatment site. This suggests a stable molecule is responsible for this effect, as it must travel quite a distance before reaching bystander cells, probably carried within the blood stream.

There is also evidence that bystander effects can occur between organisms. Studies in zebrafish and rainbow trout have shown that fish grown within the same tank as irradiated fish, or in water that previously contained irradiated fish, showed bystander effects when organs were removed and examined (Mothersill *et al.,* 2006; Mothersill *et al.,* 2007). There was also an effect seen between fish species (zebrafish and medaka) and even

when non-irradiated rainbow trout were fed with irradiated California blackworms. In both cases explant conditioned medium reduced clonogenic survival in the reporter cells (Smith *et al.,* 2013). This data suggests that bystander is able to occur between animals of different species and even between an animal and its food.

Bystander effects were originally just studied within populations of cells; however, these data show that bystander signals are able to travel far from the irradiated site and even between organisms. This suggests that this signal must be stable and resistant to degradation.

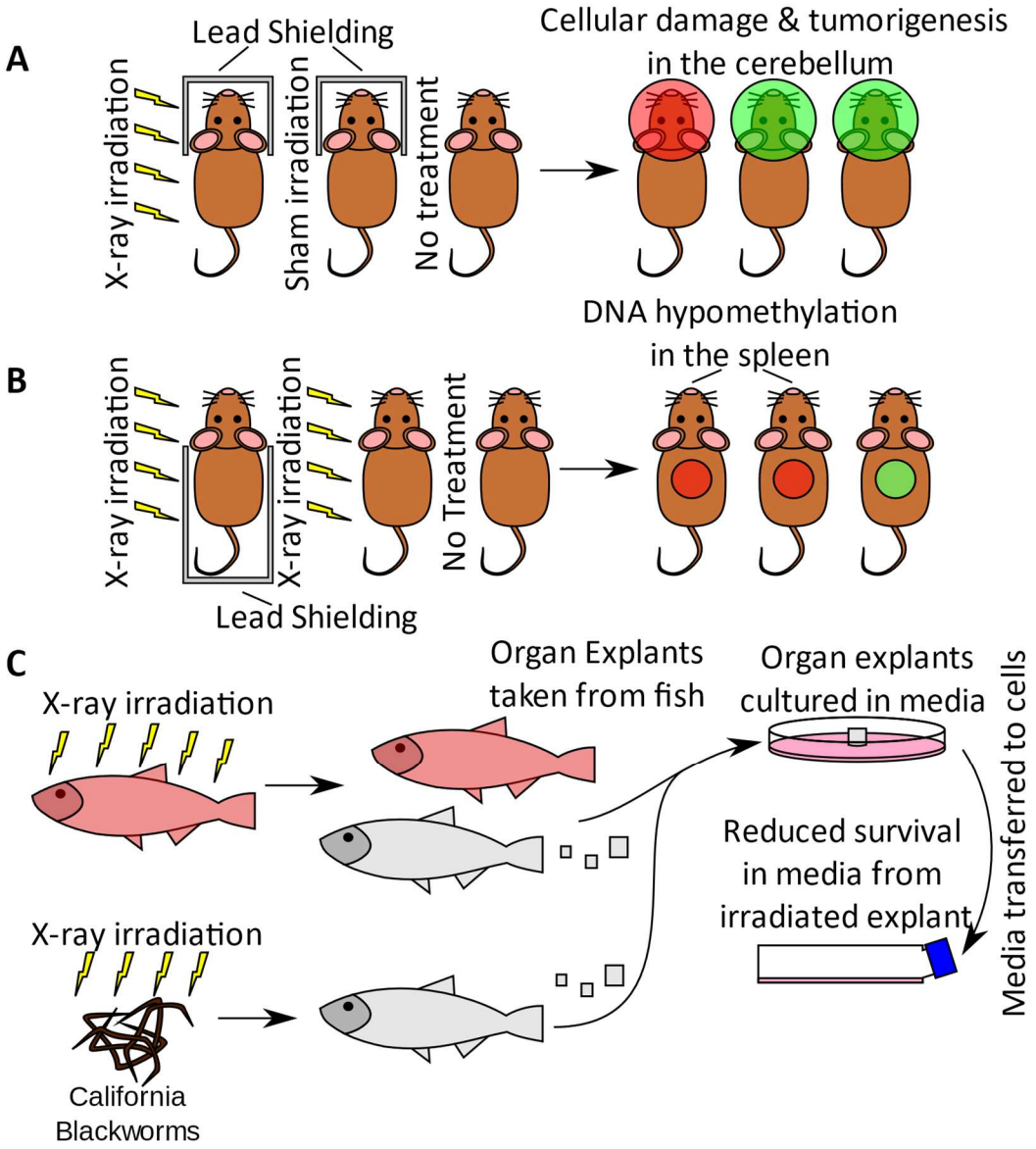

Figure 1-5: Bystander effects observed* in vivo.** *Studies in rodents have shown that cellular damage and tumorigenesis can be observed following x-ray treatment in areas of the body that were shielded from the treatment.* ***A) *Mice were subjected to X-ray treatment whilst the head was behind a lead shield. These mice were found to have increased levels of DNA damage, apoptosis and medulloblastomas in their cerebellum.* ***B)*** *Mice subjected to the X-rays whilst the body was shielded showed increased hypomethylation in the spleen. These two examples demonstrate that bystander effects are able to occur* in vivo *and that bystander signals are able to travel large distances within the organism, head to spleen for example.* ***C)*** *Fish were placed in the same tank with fish that had previously been subjected to x-rays. Explants were removed from the bystander fish and cultured in medium. This medium was removed and used to culture HPV-G reporter cells. These cells showed lower survival than cells grown in medium conditioned by explants from fish not exposed to irradiated fish. Similar experiments were carried out when fish were fed irradiated California blackworms. Again, reporter cells showed lower survival when cultured in medium conditioned by explants from fish fed the irradiated worms. These examples all demonstrate that stable signals must be involved in the induction of bystander effects as they are able to travel within the body of irradiated organisms, between an organism and its food and even remain active in the water when released by the irradiated fish.*

1.2.1.2 THERMAL BYSTANDER

The vast majority of work on the bystander effect has been carried out using irradiation as the stressor, but it has also been demonstrated in different stress types (Asur *et al.,* 2009; Dąbrowska *et al.,* 2005). Several studies have shown that heat treatment induces bystander effects. The effect was first observed following lethal heat doses. Cells co-cultured with cells that had been heat shocked at 75^{o}C showed a loss of adhesion in the bystander cells as well as a reduction in cell growth (Dąbrowska *et al.,* 2005). At such high temperatures, it is likely that the directly shocked cells were probably dead. However, studies have been carried out at lower temperatures that also show bystander effects when the directly stressed cells were still alive (Purschke *et al.,* 2010; Purschke *et al.,* 2011). Again, bystander cells were co-cultured with directly shocked cells (37-70^{o}C) and the levels of micronuclei, apoptosis and cell viability were assayed. A significant bystander effect was observed at 46 and 50^{o}C that occurred even if the donor cells were washed prior to co-culture, in order to remove any debris from dead cells (Purschke *et al.,* 2010). These data demonstrate that the bystander effect seems to be an active process, not simply the result of factors released from degraded cells, as live cells are able to produce a signal that drives bystander damage.

1.2.1.3 CHEMICAL BYSTANDER EFFECT

The effects of chemical stresses on neighbouring cells have also been studied. As any chemical treatment will be added to the medium the cells are growing in it is difficult to accurately state that any observed effect is due to bystander signalling and not simply residual levels of the test chemical. An interesting paper in 2004 used co-culture of two cell lines, one of which could metabolise ganciclovir into its genotoxic metabolite (Chinese hamster) and one that could not (3T3), to demonstrate a bystander effect (Thust *et al.,* 2004). This system allowed the cells to share the same medium containing the test chemical

whilst only one cell line should have been affected by it. The 3T3 cells showed an increase of SCE when co-cultured with the ganciclovir sensitive cells (Thust *et al.,* 2004). Interestingly increasing the number of directly stressed cells compared to the bystander cells, therefore potentially increasing bystander signalling, did increase the number of SCE/cell observed in the bystander population. The dose of ganciclovir had slightly less effect on the number of SCEs but the rate did increase in line with the dose (Thust *et al.,* 2004). However, whilst the 3T3 cells cannot metabolise ganciclovir, it's possible that the genotoxic product of its metabolism could have been passed between the cells.

Media transfer experiments have also been conducted following chemical treatment. It is important that no chemical residue is left within the conditioned medium when it is transferred, as this could cause direct damage to the bystander cells, which would then be recorded as bystander damage. Thorough washing of the cells after treatment has been shown to remove any residual chemical effect left in the medium (Asur *et al.,* 2009; Jin *et al.,* 2011). Media conditioned by cell that had been treated with chemotherapeutic agents like actinomycin D, mitomycin C and Vincristine were shown to induce micronuclei formation, chromosomal aberrations and other markers of cellular damage (Asur *et al.,* 2009; Asur *et al.,* 2010b; Asur *et al.,* 2010a; Testi *et al.,* 2016; Jin *et al.,* 2011). Phleomycin, a radiomimetic agent, has been shown to induce micronuclei formation in bystander cells (Asur *et al.,* 2009; Asur *et al.,* 2010b; Asur *et al.,* 2010a). The method of action of these drugs are varied: Mitomycin C acts by forming DNA crosslinks; vincristine binds tubulin inhibiting chromosomal division during metaphase; actinomycin D binds DNA blocking translation and phleomycin damages DNA through the production of hydroxyl radicals. That the radically different mechanisms all induce bystander damage adds further evidence that BE is a general response to stress. The dose of the chemical treatment has been shown to have an effect on the level of the bystander damage (Asur *et al.,* 2009; Testi *et al.,* 2016; Jin *et al.,* 2011). The effects were seen to plateau at a certain point though, suggesting that

bystander signalling can become saturated at sufficiently high levels of stress (Asur *et al.,* 2009).

The bystander effect is observed following numerous different stresses suggesting that it is a generic response to stress and not only related to irradiation. Most stress responses are triggered based on the effects the stress has on the cell e.g. heat shock proteins being upregulated when there are high levels of non-native proteins. Therefore, it follows that the bystander effect is a response to damage within the cells, rather than the specific stress inducing that damage.

1.2.1.4 The mechanism of Bystander effect

The mechanism by which the bystander effect occurs is not yet fully understood, but there are two commonly suggested ways the cells could signal to unstressed cells and induce bystander effects. Either the cells are communicating with neighbouring cells via gap junction signalling, or cells release a signal into the external environment that is then taken up by the bystander cells (Hall 2003; Hei *et al.,* 2008). Studies have shown that reduction or increase in the levels of gap junction signalling alter the levels of bystander damage accordingly (Zhou *et al.,* 2000; Zhou *et al.,* 2001; Shao *et al.,* 2003) as mentioned above. Media transfer experiments suggest that there is also some factor secreted by stressed cells that is then able to be taken up by bystander cells (Mothersill & Seymour 1997; Lyng *et al.,* 2000; Mothersill & Seymour 1998). This is also supported by *in vivo* studies where the effects of stresses such as radiation are seen at sites distant from the area treated (Mancuso *et al.,* 2008; Ilnytskyy *et al.,* 2009), or even separate animals grown in the same environment (Smith *et al.,* 2013), suggesting the signal involved here is able to travel quite far through the organism, which would be difficult if the effect is solely controlled via gap junctions. There are data showing that extracellular vesicles (EVs) released from the irradiated population are sufficient to drive the bystander effect in

unstressed cells (Al-Mayah *et al.,* 2012; Al-Mayah *et al.,* 2015; Jella *et al.,* 2014; Xu *et al.,* 2015). Bystander cells treated with EVs extracted from medium conditioned by irradiated cells showed higher levels of DNA damage and chromosomal aberrations. Interestingly there is no such increase when the supernatant from the ultracentrifugation is used to treat cells, suggesting that the factor inducing the damage is found only in the EV pellet (Al-Mayah *et al.,* 2012). These data show that EVs are involved in the induction of the bystander effect in naïve cells. It seems most likely that the bystander effect is propagated via both gap junction signalling and secretion of soluble factors.

1.2.1.5 The molecular mechanism of the Bystander Effect

Molecular analysis of the bystander cells has found a few targets of interest for the bystander effect (Zhou et al 2005). Transcription of *COX-2,* a gene coding for cyclooxygenase-2, was increased 3 fold in bystander cells, and inhibition of cyclooxygenase-2 was shown to reduce levels of the bystander effect (Zhou *et al.,* 2005). This implicates *COX-2* expression as a target of bystander signalling. Interestingly inhibition of NF-κB, which acts as a transcription factor for *COX-2,* was shown to reduce the levels of damage in bystander cells (Zhou *et al.,* 2008). NF-κB is controlled by exogenous tumour necrosis factor α (TNFα) and interleukin-1β (IL-1β) and again bystander damage was reduced following suppression of TNFα (Zhou *et al.,* 2008). The levels of the insulin-like growth factor binding protein 3 (IGFBP-3) in bystander cells was reduced 7 fold in bystander cells (Zhou *et al.,* 2005). IGFBP-3 is an inhibitor of insulin-like growth factor (IGF) signalling. The reduction of IGFBP-3 RNA in the bystander cells implicates IGF signalling in the bystander effect. Addition of exogenous IGFBP-3 into bystander cells did slightly abrogate the bystander effect, hinting that IGF repression reduces bystander damage (Zhou *et al.,* 2005). IGF is a cytokine that targets the MAPK/ERK pathway, which is linked with *COX-2* expression via the phosphorylation of ERK. Activation of the MAPK signalling cascade was demonstrated in

bystander cells via western blotting (Zhou *et al.,* 2005). The phosphorylation of key proteins in the MAPK/ERK pathway and changes of expression in 18 MAPK/ERK gene targets has been demonstrated in both radiation and chemically-induced bystander cells (Asur *et al.,* 2010b; Asur *et al.,* 2010a). Oxidative metabolism is also thought to play a role in the induction of bystander effects. There is a large amount of evidence pointing to the involvement of ROS in the induction of bystander effects (Chen *et al.,* 2009; Azzam *et al.,* 2003; Zhou *et al.,* 2000; Lyng *et al.,* 2006).

However as of yet a full model of the bystander effect has not been constructed. Further, most of the data presented in these studies were solely from irradiated cells grown together, so these pathways may only be involved in the induction of bystander effects via gap junction signalling. Further work is needed to know whether the mechanism of the bystander effect is conserved across stress types and whether medium and EV induced bystander uses the same mechanism to induce cell damage and death.

1.3 CACHEXIA

Cachexia is an unexplained loss of skeletal muscle and weight loss found in patients with cancer as well as other chronic disorders such as AIDS (Fearon & Moses 2002; Aoyagi *et al.,* 2015). The disease is characterised by numerous symptoms; skeletal muscle wasting, loss of body mass, inflammation, increased catabolic metabolism (Aoyagi *et al.,* 2015). The disorder often also shows wasting of adipose tissues (Bing *et al.,* 2006; Rydén & Arner 2007), however it is not seen necessarily as a marker of the disease (Aoyagi *et al.,* 2015). The chances of a patient developing cachexia is dependent on the type of cancer that a patient suffers. Patients suffering lung or pancreatic cancers have a much higher incidence of developing cachexia than those with breast tumours (Dewys *et al.,* 1980). However this distinction does appear to depend on the specific definition of cachexia being used (Fox *et al.,* 2009). The term ‘cachexia’ has been used for some time with no consistent clinical

definition (Vanhoutte *et al.,* 2016; Little 2003; Fox *et al.,* 2009). Most definitions focus on weight loss observed in the patient, with the following definitions often used: involuntary weight loss of >5 %; Body Mass Index (BMI) of <20 kg/m^2 with >2 % weight loss or sarcopenia with any weight loss (Vaughan *et al.,* 2013). Many studies have suggested that the appearance of cachexia is a marker of poor long term survival for the patient (Vanhoutte *et al.,* 2016; Aust *et al.,* 2015; Deans & Wigmore 2005). Further, some evidence suggests it can be indicative of a poor response to chemotherapy (Dewys *et al.,* 1980; Ross *et al.,* 2004; Prado *et al.,* 2009) with cachexic patients being more likely to show toxicity following treatment or fail to complete the programme of chemotherapy. However this is disputed, with some studies suggesting the appearance of cachexia does not mean a worse outcome for therapy (Evans 2010; Srdic *et al.,* 2016). Whilst the reasons and mechanisms by which cachexia progress are not fully understood there are some therapies available, which primarily focus on reducing the symptoms. Many of these treatments attempt to halt further reduction in body mass via increasing appetite or calorific intake (Aoyagi *et al.,* 2015; Kumar *et al.,* 2010). However as cachexic weight loss is related to both adipose mass loss and more predominantly skeletal muscle weight loss this will only be of limited use (Vaughan *et al.,* 2013). Exercise may be suggested to patients as a method to reduce muscle wasting, however fatigue and respiratory difficulties are often also present with cachexia meaning it is difficult for patients to stick to an exercise programme (Kumar *et al.,* 2010). These treatments are only palliative in nature; more work is needed on the molecular mechanisms of cachexia in order for curative therapies to be developed.

Patients with tumour types associated with cachexia tend to display high levels of energy expenditure (Mak & Cheung 2006). This boost in catabolism is likely to be, in part, what is driving the muscle wasting (Aoyagi *et al.,* 2015). There is a net loss of proteins as protein formation is reduced and protein breakdown is increased. Cytokines have been implicated in the induction of cachexia (Argilés *et al.,* 2003; Porporato 2016). Cytokine

production in cancer patients appears to be hijacked by the tumour, promoting the production of cytokines that benefit the tumour (Quail & Joyce 2013; Smith & Kang 2014; Abou El Hassan *et al.,* 2015). Some of the cytokines found in cachexic patients are thought to be involved in increasing the levels of muscle breakdown. For example, TNFα is able to induce muscle catabolism via the upregulation of NF-κB leading to increased proteolytic activity (Reid & Li 2001). These cytokines make an interesting anti-cachexia target, and are well studied as an anti-cachexia therapy (Monk *et al.,* 2006; Penna *et al.,* 2010). One study showed that muscle cells grown in medium conditioned by lung cancer cells showed reduced muscle differentiation (Zhang *et al.,* 2011). It was observed that p38β, a member of a family of mitogen-activated protein kinases (MAPK), activates CCAAT-enhancer-binding protein β (C/EBPβ) leading to the activation of two E3 ubiquitin ligases, UBR2 and atrogin 1 (Zhang & Li 2012; Zhang *et al.,* 2013; Yuan *et al.,* 2015). E3 ubiquitin ligases are part of the ubiquitin-proteasome system, which is involved in normal muscle atrophy related to reduced muscle use (Bonaldo & Sandri 2013).

1.4 Extracellular Vesicles (EV)

Extracellular vesicles are produced constantly by all types of cells and serve a myriad of functions in both normal and stressed cells, often in intercellular communication (Record *et al.,* 2011; Yáñez-Mó *et al.,* 2015). They were originally observed in the late 1940s as particles released from platelets that had procoagulant properties (Chargaff & Randolph 1946). In 1967 a molecule was extracted from blood samples via high speed centrifugation that was high in phospholipids and had the same coagulant effect (Wolf 1967). Work carried out separately in the early 1970s showed sac like structures within platelets that were released from the cells and involved in coagulation (Webber & Johnson 1970; Crawford 1971). The first time vesicles were seen released from tumours was 1981 when medium conditioned by mice and guinea pig tumour cells was ultracentrifuged (Dvorak *et*

al., 1981). In 2005 an attempt to define these microparticles was made by a sub-committee of the International Society on Thrombosis and Haemostasis who agreed that the particles were 0.1-1µm in size, that they lacked nuclei and that they had phosphotidylserine on their outer leaflets (Hargett & Bauer 2013). More recently this definition has been called into question as more has been deciphered about different EV classes and their characteristics (Witwer *et al.,* 2013).

There are three main recognised classes of extracellular vesicle: Apoptotic bodies, microvesicles and exosomes. These different classes of EVs are shown in Figure 1-6. EVs are not just released from mammalian cells but also from fungi (Oliveira *et al.,* 2010) and even prokaryotic cells, which release outer membrane vesicles (Kuehn & Kesty 2005). Many EVs are known to act as signalling molecules, carrying protein and nucleic acids to other cells (Huang *et al.,* 2013; Yáñez-Mó *et al.,* 2015). These signals have been shown to have a wide variety of effects on recipient cells, from priming a pre-metastatic niche for colonisation (Hoshino *et al.,* 2015) to inducing macrophages following stroke (Couch *et al.,* 2017). The fact that EVs are released during resting conditions suggests that they also have some housekeeping effects (Yáñez-Mó *et al.,* 2015).

Distinguishing between the different vesicle subtypes is tricky and is currently a main concern of the field (Witwer *et al.,* 2013). It used to be thought that these vesicles could all be separated by size and morphology, however this dogma has been called into question recently and the field has become much more cautious in using specific terminology to describe extracted particles (Witwer *et al.,* 2013). The International Society of Extracellular Vesicles has published guidelines on how the nomenclature should be used in an attempt to standardise the usage across all EV research (Witwer *et al.,* 2013). An overview of the formation and release of the different classes of vesicles is shown in Figure 1-7.

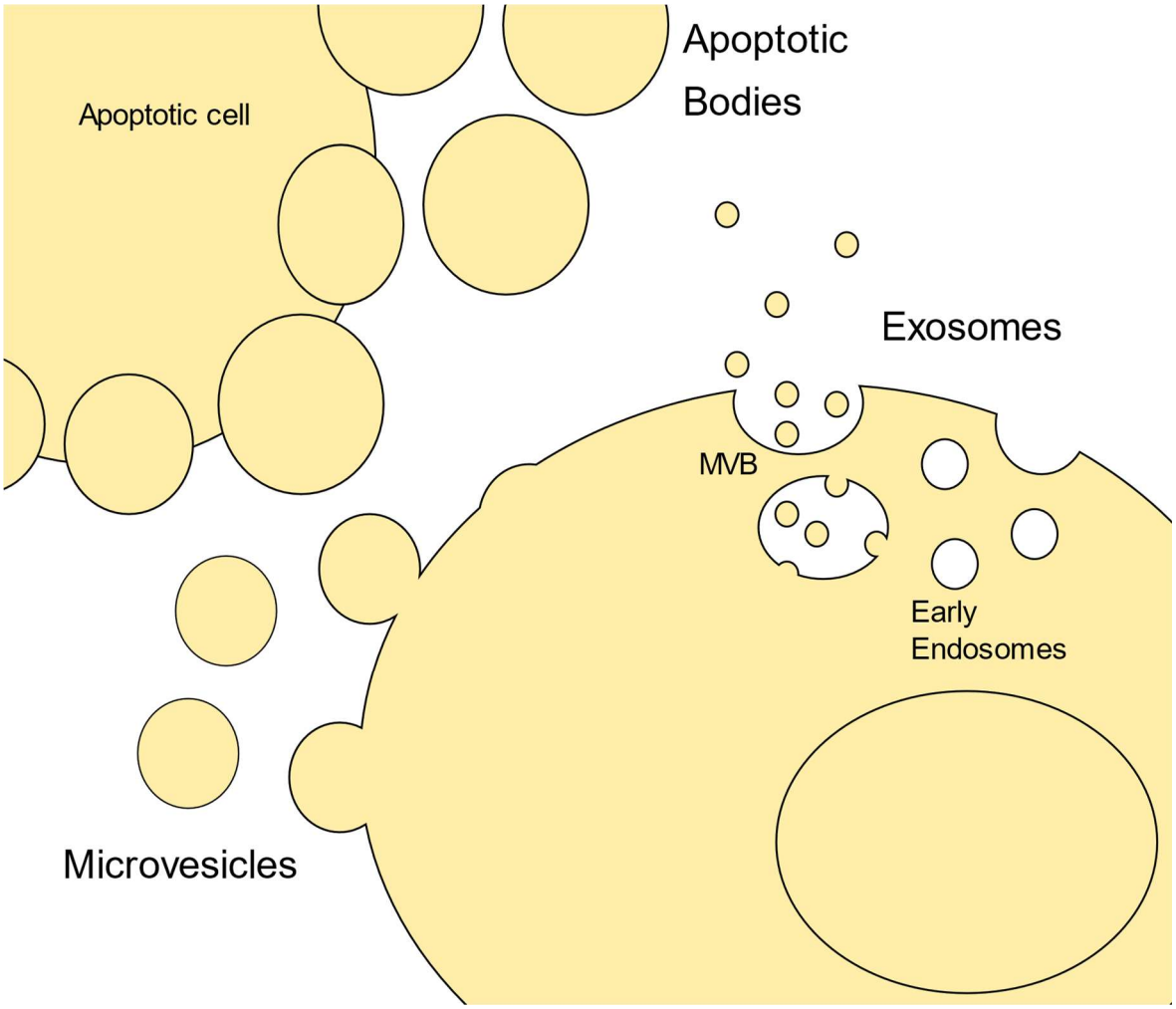

Figure 1-6: The biogenesis of different types of extracellular vesicles. *Apoptotic bodies are formed as the apoptotic cell begins to degrade. Microvesicles are formed via blebbing from the plasma membrane. Exosomes have an endocytotic origin, and form as invaginations into late endosomes, which are then known as multivesicular bodies (MVB). These MVBs either fuse with the plasma membrane (as above) or are degraded by lysosomes.*

1.4.1.1 APOPTOTIC BODIES

Apoptotic bodies are formed when cells undergo apoptosis. They are a highly heterogeneous subset of EVs thought to be around 50-5000nm in size (Kalra *et al.,* 2016). Apoptotic bodies are essentially the end point of apoptosis, with cellular debris contained within apoptotic bodies and then targeted for phagocytosis, disassembly and recycling (Elmore 2007). The formation of apoptotic bodies is driven by actin-myosin contraction induced by ROCK 1. During apoptosis ROCK 1 is cleaved to its active form by caspase-3. ROCK 1 then induces several downstream processes necessary for membrane blebbing (Coleman *et al.,* 2001). It aids the coupling of actin-myosin filaments to the plasma membrane, contraction of myosin light chain via phosphorylation and myosin ATPase

activity. All of this leads to the contraction of the membrane and the formation of apoptotic vesicles (Wickman *et al.,* 2013).

1.4.1.2 MICROVESICLES

Microvesicles (occasionally also known as ectosomes) are formed by outward budding of the plasma membrane. They are commonly larger than exosomes, with a range of about 50-2000nm (Akers *et al.,* 2013). Whist exosomes and microvesicles have often been differentiated by size, it's important to note that it is actually their origin that defines them. The two leaflets that make up the phospholipid bilayer of the plasma membrane have distinct lipid organisation (Hugel *et al.,* 2005). These lipids are held in the correct formation via the action of two molecules known as flippases and floppases. Under resting conditions the flippases ensure that phosphotidylserine and other related lipids like phosphatidylethanolamine are sequestered on the inner leaflet of the membrane, whilst the floppases are switched off (Akers *et al.,* 2013; Hugel *et al.,* 2005; Larson *et al.,* 2012). Increased Ca^{2+} within the cell activates the floppases which works to translocate the phosphotidylserine onto the outer leaflet of the membrane, as well as activating lipid scramblases which induce the redistribution of lipid within the bilayer (Hugel *et al.,* 2005). The activation of both of these molecules lead to the inhibition of flippase activity. An increase of phosphotidylserine on the outer leaflet increases membrane curvature and induces vesicle budding (Muralidharan-Chari *et al.,* 2010; Cocucci & Meldolesi 2015). There are two suggested methods of vesicle release. First ARF6 initiates a signalling cascade involving the phosphorylation of myosin light chain kinase which leads to the contraction of actomyosin (Muralidharan-Chari *et al.,* 2009). The other suggests mechanism is TSG101 inducing the translocation of ESCRT-III to the plasma membrane. ESCRT-III forms a spiral of CHMP4B around the opening of the vesicle (Chiaruttini *et al.,* 2015; Hanson *et al.,* 2008)

which is then constricted by variant-specific surface protein 4 (Vsp4) ATPase leading to vesicle release (Kalra *et al.,* 2016; Muralidharan-Chari *et al.,* 2010).

1.4.1.3 Exosomes

Exosomes are small vesicles of endosomal origin (Théry *et al.,* 2002). Exosomes are formed via invagination into endosomes causes the formation of small vesicles known as intraluminal vesicles within the endosome. These vesicle containing endosomes are known as multivesicular bodies, which can either be targeted to the lysosome for destruction or fuse with the plasma membrane, releasing these small vesicles into the extracellular matrix where they are known as exosomes (Klumperman & Raposo 2014).

Exosomes were originally described in 1987 when vesicles were found to form during reticulocyte maturation (Johnstone *et al.,* 1987). When reticulocytes mature into erythrocytes they lose numerous functions such as transferrin binding activity. Internal vesicles had been seen to be involved in internalisation of the transferrin receptor (Harding *et al.,* 1983; Pan *et al.,* 1985; Pan & Johnstone 1983). Pellets extracted via 100,000 x g centrifugation demonstrated these functions. The surface proteins involved in these functions were undergoing endocytosis and forming multivesicular bodies within the cells that then released them as exosomes. These exosomes contained the surface proteins within their membranes, allowing them reticulocyte-like activity (Johnstone *et al.,* 1987). Whilst they were at one time characterised as being 30-100nm there have been studies suggesting that they can be larger than this, and that other vesicles can, in fact, fall within this spectrum, suggesting size is not a sufficient way to characterise a vesicle population (Witwer *et al.,* 2013). They also were thought to have a cup-shaped morphology, but this was found to be an artefact of their fixation for Electron Microscopy (Witwer *et al.,* 2013).

The fact that the protein cargo of exosomes only contains proteins found in the plasma membrane, the membranes of endocytic compartments and the cytosol suggests

that EVs are derived of an endosomal origin (Théry *et al.,* 2002). Exosomes form as invaginations into endosomes that bud off into the interior of the endosome. The system driving the formation of these intraluminal vesicles (ILVs) is not well understood. It is suggested that the either the ESCRT machinery or a ceramide dependent pathway is used to drive vesicle formation. The ESCRT model suggests that ESCRT-0 through ESCRT-III bind to the outside of the endosome. ESCRT-I and -II are thought to cause vesicle budding and cargo transport whilst ESCRT-III is then used to facilitate ILV scission (Hurley 2010; Nabhan *et al.,* 2012; Raiborg & Stenmark 2009; Baietti *et al.,* 2012). Exosome formation has been observed in cells with no ESCRT expression which suggests this is not the only method of exosome genesis (Stuffers *et al.,* 2009). Another model suggests that conversion of sphingomyelin to ceramide within lipid rafts alters the leaflets and drives inward budding of the endosomal membrane (Trajkovic *et al.,* 2008). The MVBs can then either move to the lysosome and undergo degradation or move to the plasma membrane and release their contents. This distinction is controlled by a class of proteins known as the Rab GTPases (Kalra *et al.,* 2016). The Rab27s are involved with MVB trafficking. Rab27a is required for MVB docking with the plasma membrane and when Rab27b is silenced the vesicles were found to travel towards the nucleus of the cell, rather than the plasma membrane suggesting it is required for vesicle transport (Ostrowski *et al.,* 2010). Other members of the Rab family are also implicated in exosome release (Villarroya-Beltri *et al.,* 2014). Once the MVBs bind to the plasma membrane they fuse and release their exosome contents (Théry *et al.,* 2002; Kowal *et al.,* 2014).

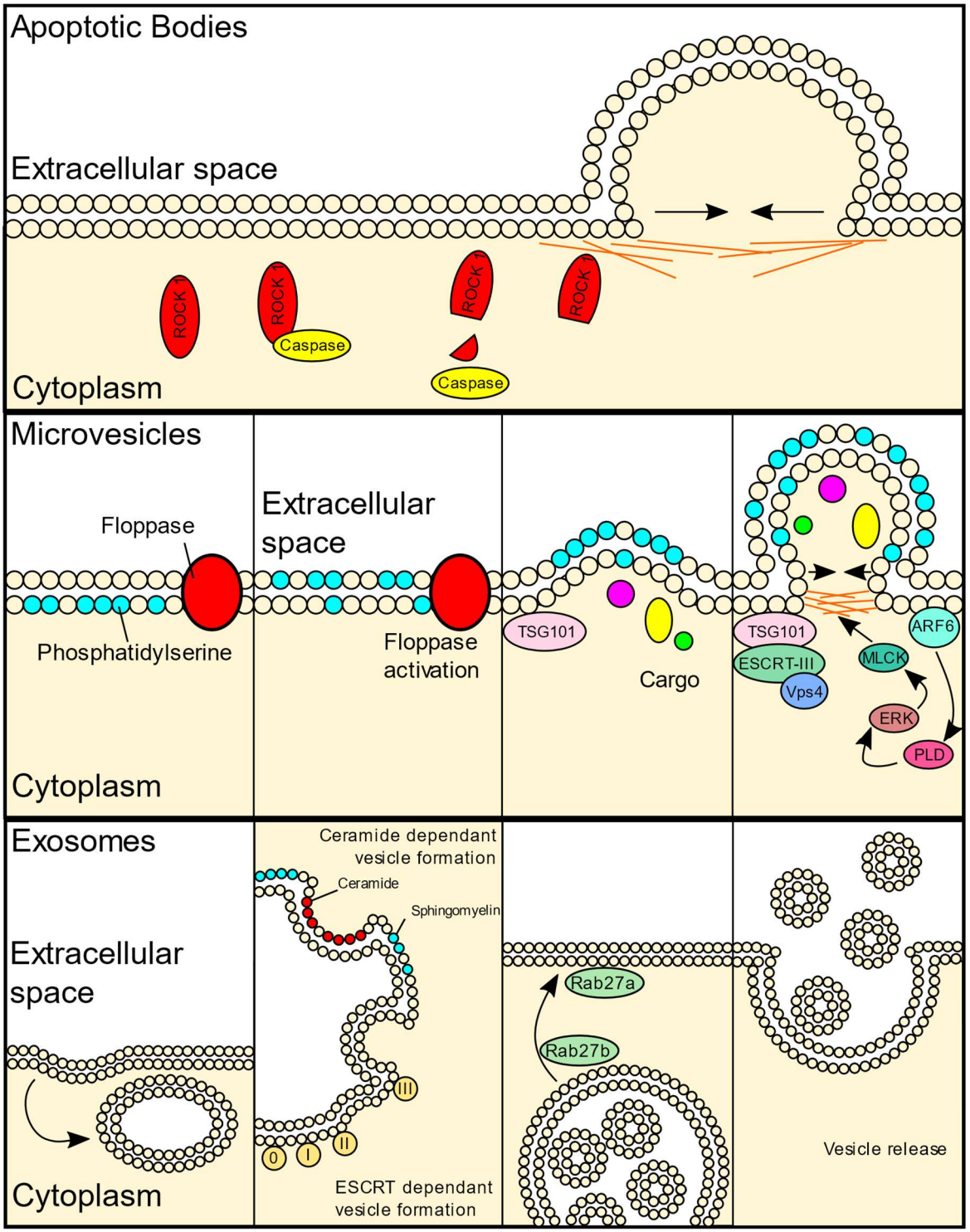

Figure 1-7: The mechanisms underlying extracellular vesicle release. *Apoptotic bodies are formed when activated caspase cleaves ROCK 1 leading to the contraction of the cytoskeleton and the formation of large membrane blebs.* ***Microvesicle*** *budding occurs when the cells move phosphatidylserine to the outer leaflet of their membranes. There are two potential mechanisms by which microvesicles are released from cells. In the first mechanism ARF6 activation leads to the activation of myosin light chain kinase and the contraction of the actomyosin. The other route for vesicle release is the contraction of ESCRT-III spirals by Vps4, which causes the vesicles to separate from the membrane.* ***Exosomes*** *are formed as invaginations into endosomes forming multivesicular bodies (MVBs). This inward budding is carried out either by the ESCRT machinery (0-III) or by conversion of sphingomyelin into ceramide within lipid rafts. MVBs then travel to, and fuse with the plasma membrane with the help of the Rab27 proteins, releasing their vesicle cargo as exosomes.*

1.4.1.4 METHODS FOR THE UPTAKE OF EVS BY RECIPIENT CELLS

EV uptake has been demonstrated via numerous different pathways (Feng *et al.,* 2010; Morelli *et al.,* 2004). One of the most commonly observed method of EV uptake is endocytosis (Montecalvo *et al.,* 2012; Morelli *et al.,* 2004). This refers to a group of pathways that lead the EV invaginate at the plasma membrane (Doherty & McMahon 2009). These endosomes are then 'pinched off' by enzymes such as Dynamin2 which forms a collar at the opening to the endosome and facilitates its release into the cell (Herskovits *et al.,* 1993; Damke *et al.,* 1994). Micropinocytosis involves the extension of the plasma membrane into the extracellular space which then fuse with other extensions, engulfing a section of the extracellular matrix along with any EVs that may be present (Costa Verdera *et al.,* 2017). Phagocytosis is often carried out by specialised cells such as macrophages (Jersmann *et al.,* 2003) but can occur in other types of cells (Gregory & Devitt 2004). The EVs bind to receptors on the cells due to their increased levels of PS in their outer leaflets which triggers invagination and internalisation of the bound molecule (Caron & Hall 1998). It is also possible for the plasma membrane of the EV to fuse to the recipient cell, leading to the internalisation of the EV's cargo (Prada & Meldolesi 2016).

1.4.2 EXTRACELLULAR VESICLES IN DISEASE

EVs are known to act as signalling molecules and are able to travel around the body to carry out their functions. They have numerous in intercellular communication during disease, their unique RNA and protein cargos mean they are promising as biomarkers (Vanni *et al.,* 2017; An *et al.,* 2015; Guo *et al.,* 2017). They have been implicated in the pathogenesis of cancer, with EVs participating in numerous pro-cancer events. Patients with cancer show much higher levels of circulating EVs than healthy patients suggesting they are involved in the disease (Silva *et al.,* 2012). EVs from metastatic tumours have been shown to increase the metastatic potential of other tumours (Tominaga *et al.,* 2015; Becker

et al., 2016). Breast cancer EVs have even been shown to induce non-cancerous epithelial cells to form tumours *in vivo* (Melo *et al.,* 2015). The pre-metastatic niche is an environment within the body that is primed to allow metastasis of a primary tumour (Peinado *et al.,* 2017). Primary tumours are able to condition these sites via the secretion of certain factors from their locations that alter the environment at target sites, and EVs released from numerous tumour types have been shown to travel to known pre-metastatic niche locations *in vivo* (Hoshino *et al.,* 2015).

Despite the specificity of localisation observed here, studies on the biodistribution of EVs *in vivo* following systemic delivery show that large numbers of the EVs are found to localise to the liver soon after introduction to the organism, with the spleen and lungs commonly having the next highest EV burden (Wiklander *et al.,* 2015). The levels of EVs within the liver peaked at around 30 minutes post injection (Wiklander *et al.,* 2015). Further EVs levels have been shown to peak around 60-120 minutes after injection (Lai *et al.,* 2014). This suggests that EVs are being removed from the organism via hepatic circulation shortly after their introduction. The speed with which EVs are removed could mean that they are able to act very quickly *in vivo* or that they need to be continuously secreted over a long period of time in order to induce changes in an organism.

As has already been mentioned, EVs are implicated as being one of the signalling molecules that induce bystander effects in a non-gap junction mediated fashion (Al-Mayah *et al.,* 2012). EVs extracted from irradiated cells are able to induce bystander effects in recipient cells (Al-Mayah *et al.,* 2012; Al-Mayah *et al.,* 2015; Al-Mayah *et al.,* 2017; Jella *et al.,* 2014; Xu *et al.,* 2015). In this context, RNAse treatment abrogated the bystander effect, and suppression of miR-21 in the irradiated cells was also shown to reduce the levels of bystander damage (Al-Mayah *et al.,* 2012; Xu *et al.,* 2015).

Whilst little work has been done on the roles of EVs during heat stress one study found that EVs were significantly enriched in HSPs following sub-lethal heat shock (Clayton

et al., 2005). The heat-treatment also increased the number of EVs that were released from the cells (Clayton *et al.,* 2005). These data suggest that stress may induce the release of specialised EVs, with a different cargo to EVs produced in normal conditions. As these EVs carry HSPs they could potentially be involved in the stress response in their recipient cells. This difference in cargo in the stress-derived EVs could be related to their ability to induce bystander effects in bystander cells.

1.4.3 Extracellular Vesicle Cargo and Loading

EVs are known to carry a wide range of cargo consisting of proteins, RNA and lipids. It is, however, difficult to accurately characterise the content of EVs as current isolation methods tend to produce impure samples, possibly contaminated with other proteins, protein-associated RNA, liposomes or micelles, which are also found in the extracellular space (Abels & Breakefield 2016).

1.4.3.1 Loading of EV cargo

The loading of EVs appears to be an active process; EVs can contain different levels of numerous proteins, nucleic acids and lipids to their donor cells (Villarroya-Beltri *et al.,* 2014). The first discovery of exosomes showed that many of the surface proteins lost during reticulocyte maturation were selectively endocytosed by the cells and released on exosomes (Johnstone *et al.,* 1987). The mechanisms behind the loading of cargo into exosomes are not well understood, though there are several ways it could be controlled. ESCRTs 0-II are known to be involved with sorting ubiquitinated protein into MVBs heading to the lysosome (Raiborg & Stenmark 2009) which suggests they may be involved. In fact silencing certain ESCRT components alters the composition of the released exosomes (Colombo *et al.,* 2013). ESCRT-independent exosome formation must also be able to selectively load cargo. These exosomes are formed due to a restructuring of the membrane to form a ceramide-rich lipid raft (Trajkovic *et al.,* 2008). Inhibition of two other lipids sphinogosine-1-phosphate and diacylglycerol was shown to once again alter the cargo of exosomes (Kajimoto *et al.,* 2013). Many of the proteins linked to these loading mechanisms are tetraspanins such as CD63 and CD81. These transmembrane proteins have also been implicated in protein loading, with their exposed regions interacting with other proteins (Mazurov *et al.,* 2013; Perez-Hernandez *et al.,* 2013; Verweij *et al.,* 2011). It is therefore probable that the tetraspanins incorporated into the forming exosomes are able to

influence the protein cargo that is loaded. Microvesicles also seem to be loaded via the ESCRT machinery (Chiaruttini *et al.,* 2015) and it is thought that plasma membrane anchors target proteins for incorporation into these vesicles (Shen *et al.,* 2011). The miRNAs found in secreted vesicles appear to contain an EXOmotif at their 3' ends that aid their sorting into EVs (Villarroya-Beltri *et al.,* 2013; Villarroya-Beltri *et al.,* 2014). Several heterogeneous nuclear ribonucleoproteins (hnRNPs) were also observed to bind only to exosome miRNAs (Villarroya-Beltri *et al.,* 2013) implicating them in the loading of these miRNAs.

1.4.3.2 PROTEIN

The proteins seem to be selectively loaded into EVs, with differences in the proteomics of vesicles released from different types of cell (Welton *et al.,* 2016). There are, however, several proteins often found within EVs that are commonly used as markers when characterising vesicles. These include tetraspanins, such as CD63 and molecular chaperones like HSP70 (Abels & Breakefield 2016). Tetraspanins are transmembrane proteins that are implicated in protein loading into vesicles as outlined above. The tetraspanins are often used as molecular markers to distinguish between different vesicle sub-populations. Tetraspanins CD9, CD63 and CD81 are found highly enriched within the membranes of exosomes (Andreu & Yáñez-Mó 2014; Kowal *et al.,* 2016) for example. Discovery of markers for EV sub-populations is a very active area of research with many labs trying to find accurate ways to classify EVs from an unknown population. Whilst EV uptake by recipient cells is still poorly understood there is evidence that tetraspanins may play a role in cell binding and fusion (Mulcahy *et al.,* 2014). Proteins involved with the formation and release of EVs are often found enriched in vesicles, such as components of the ESCRT machinery like TSG101 as well as cytosolic proteins such as HSP70 (Yoshioka *et al.,* 2013).

1.4.3.3 NUCLEIC ACIDS

EVs carry a range nucleic acids, usually small RNAs (sRNA), though long non-coding RNA (lncRNA) and messenger RNA (mRNA) have been found within EVs (Ekström *et al.,* 2012; Abels & Breakefield 2016; Valadi *et al.,* 2007). RNA also appears to be selectively loaded into vesicles as numerous differences were observed in the RNA content of EVs from cells before and after irradiation (Yentrapalli *et al.,* 2017). The RNA found in vesicles is a key area of EV study with numerous reports suggesting the functions of EVs are related to their RNA cargo (Al-Mayah *et al.,* 2012; Xu *et al.,* 2015; Pan *et al.,* 2016). As mentioned above, EV associated RNA is implicated in the induction of bystander effect (Al-Mayah *et al.,* 2012) and EVs enriched in miR-21 specifically have been shown to be able to induce damage in bystander cells (Xu *et al.,* 2015). Long non-coding RNAs associated with EVs have also been shown to be able to increase the cell viability of recipient cells (Hewson *et al.,* 2016). The transport of the lncRNA ZFAS1 by EVs is implicated in the progression of gastric cancer with EVs extracted from cells with high ZFAS1 levels were able to induce proliferation and migration in gastric cancer cells (Pan *et al.,* 2016).

1.4.3.4 LIPIDS

The lipid content of the vesicles tend to reflect that of the donor cells that released them, though they are often enriched in sphingomyelin, cholesterol, phosphatidylserine and glyco-sphingolipids when compared to parent cells (Yáñez-Mó *et al.,* 2015; Trajkovic *et al.,* 2008). Microvesicle formation occurs when the phosphatidylserine flipped from the inner to the outer leaflet of cells which explains its enrichment on the outer leaflet of vesicle membranes (Hugel *et al.,* 2005). Similarly ceramide is implicated in ESCRT-independent exosome formation, again explaining why it is often found in EV membranes (Trajkovic *et al.,* 2008). However lipid composition seems to vary based on cell type (Haraszti *et al.,* 2016).

1.5 AIMS

Whilst EVs have been demonstrated to be involved with radiation-induced bystander effect, no such study has been done of the effects of EVs from other stresses on bystander cells. First the role of EVs in the propagation of the thermal bystander effect will be established by answering the following questions:

- Are EVs released during heat shock able to induce stress in bystander cells?
    - EVs will be extracted from medium conditioned by heat-treated cells via ultracentrifugation and will be transferred onto bystander cells. The levels of DNA damage and cell viability in the bystander cells will then be assayed.
- What effect does blocking EV uptake have on thermal bystander effect?
    - By treating cells with inhibitors of EV uptake it should be possible to abrogate the levels of bystander damage and thus test whether EVs are indeed the signal that induces the bystander effect.
- Does the bystander effect occur after very high heat treatment?
    - Cells will be stressed at 70°C high temperatures for 10 seconds and then left to condition their medium. EVs will be extracted from the medium and used to treat bystander cells and the levels of DNA damage and cell viability will be assayed.

The activity of EVs from chemically-stressed cells will also be tested. As stated above chemical stresses are also able to induce bystander effects. It is probable that chemically-induced bystander effects use the same mechanisms to induce damage in bystander cells. Further the ability of cancer cell line EVs to induce cachexia both with and without treatment with the chemotherapeutic cisplatin will be assessed.

- Can chemical bystander effects also be transferred via EVs?

    - EVs extracted from cisplatin-treated cells will be used to treat bystander cells and the levels of damage assayed.

- Do EVs released from cells treated with chemotherapeutic agents affect cancer-associated muscle wasting (cachexia)?
    - EVs from cisplatin-treated cells will be used to treat both muscle cells and rodents and the levels of muscle wastage will be assayed.
- What are the molecular changes in stress-derived EVs and are they responsible for the observed effects?
    - The protein cargo of cisplatin-treated cells and the EVs they release will be analysed via mass spectrometry and compared with control cells and EVs.

This work will help to clarify the role of extracellular vesicles in the stress response and attempt to discover the molecular changes in vesicles that are released during stress conditions.

2 METHODS

2.1 CELL CULTURE

All cells were propagated in a humidified incubator maintained at 37°C and 5% CO_2. Cells were cultured in sterile medium (MCF7, C2C12 and HeLa: DMEM, SLS; K562 and A2780: RPMI, Fisher) supplemented with 10% v/v FCS and 2mM L-Glutamine (MCF7 and HeLa, Fisher) or GlutaMAX (C2C12, Fisher). For EV extractions, cells were grown in medium supplemented with pre-cleared FCS when the cells were conditioning medium. This FCS was cleared via ultracentrifugation for 16 hours at 100,000 g.

For experiments, unless otherwise stated, cells were seeded the day prior to treatment at the following concentrations:

- K562 $5x10^5$ cells/ml of medium
- MCF7 $3.5x10^4$ cells per cm^2 of growth surface
- HeLa $1.58x10^4$ cells per cm^2 of growth surface
- A2780 $4.21x10^4$ cells per cm^2 of growth surface
- C2C12: $2x10^4$ cells per cm^2 of growth surface

2.1.1 SUB-CULTURING CELLS

Cells were split using 1x trypsin whenever the cells reached ~70% confluency. The medium was removed, and the cells washed with PBS. 1x trypsin was added to the cells and allowed to cover the apical surface of the flask or plate. The trypsin was then removed, and the cells were incubated at 37°C for 5 minutes to allow the trypsin to act. The flasks were then removed from the incubator and the cells were washed with complete medium forming a suspension of cells in medium. The cells were then either counted for experiments or split into new flasks at a low starting seeding density.

2.1.2 CELL LINES USED

- MCF7: Human immortalised breast Cancer cell line
- A2780: Human immortalised ovarian cancer cell line
- K562: Human immortalised myelogenous leukaemia cell line
- HeLa: Human immortalised cervical cancer cell line
- C2C12: Mouse immortalised myoblast cell line

2.2 EV EXTRACTION

2.2.1 ULTRACENTRIFUGATION

For EV extractions cells were grown in medium supplemented with EV-depleted FCS. Medium was removed from cells 24 hours after treatment. Medium was centrifuged at 300 g for 5 minutes to pellet cells. The supernatant was aspirated from the pellet and then centrifuged again at 16,500 g for 20 minutes to pellet cell debris and larger vesicles (Tkach *et al.,* 2018). The supernatant was aspirated and filtered through 0.22 µm filters that had been blocked with 0.01% w/v BSA. This medium was then centrifuged again at 100,000 g for 1 hour and 30 minutes to pellet extracellular vesicles. The supernatant was aspirated and discarded. The pellets were then re-suspended in PBS and centrifuged at 100,000 g. Once more the supernatant was discarded, the pellet re-suspended in PBS and stored on ice until use.

2.2.2 MEDIA EV DEPLETION

For EV extractions culture medium was removed from cells and fresh medium supplemented with EV-depleted FCS was added. FCS was depleted of EVs by ultracentrifugation at 100,000 x g for 16 hours at 4°C. The supernatant was saved and then filtered through 0.22 µm filters into 50ml centrifuge tubes and stored at -20°C until it was used to create EV-depleted medium.

2.3 Cell Treatments

Cells were seeded in 6 well plates the day before treatment as outlined above. For medium transfer experiments the medium was removed from cells and discarded. Medium from stressed cells prepared as above was added onto the cells. For EV transfer, the medium was removed from the bystander cells and the EVs extracted as above were suspended in medium and then added to the bystander cells. In both cases the cells were then grown for 24 hours before being assayed.

2.4 Comet Assay

The comet assay is a DNA damage assay, that uses electrophoresis to assess the levels of double strand breaks in individual cells. The cells are embedded in agarose on slides and then lysed to expose the cell's DNA. Electrophoresis is carried out at a high pH, with small fragments of DNA traveling further along the slide than larger fragments or complete DNA. This causes cells with high levels of DSBs to for a comet like appearance with a large amount of DNA fragments forming a "tail" behind the "head" of the comet see Figure 2-1. There are numerous ways to estimate the DNA damage for each cell. One common method is the length of the comet tail; however, this biases the result towards cells that had the shortest fragments not necessarily the most damage. Here I have used tail % DNA, which is based on the proportion of the fluorescent dye found within the tail region compared to the head region. The higher the observed fluorescence in the tail, the more DNA fragments in the tail.

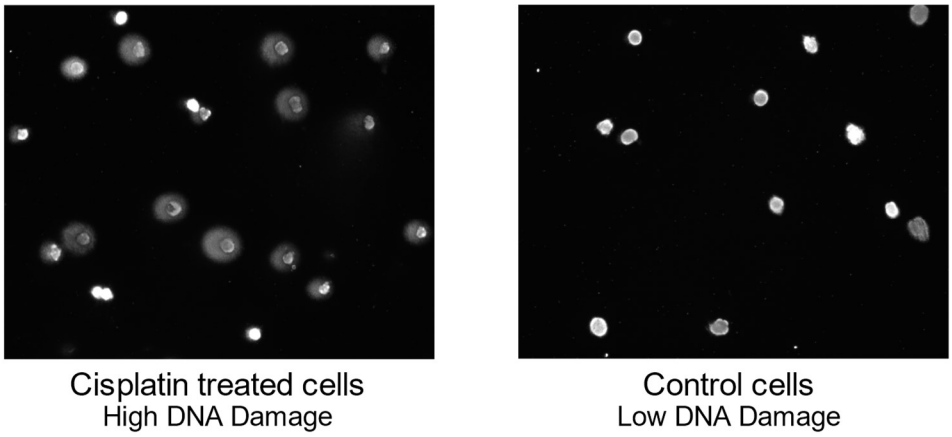

Figure 2-1: Representative images of comet assay slides. *The cells used to create these images were MCF7s. On the left is a representative image of cells treated with 40μM cisplatin, a light trail is seen following the bright circle in the hollow left by the cell where the majority of the DNA still resides. The right shows control cells with little to no DNA damage. There is no trail following the cells, so very few DNA fragments have moved during the electrophoresis.*

20,000 cells were embedded in low melting point agarose (LMPA, *Fisher Biotech: BP165-25*) on slides pre-coated in normal melting point agarose (NMPA, *Sigma: A9539-25G*). These slides were then left in Alkaline Lysis Buffer (2.5M NaCl, 100mM Na_2EDTA pH 8, 10mM Tris-HCl pH 8, 1% v/v TritonX-100, 1% v/v DMSO, adjusted to pH 10) overnight to lyse the cells. The slides were then transferred to Alkaline Electrophoresis Buffer (0.3M Sodium Hydroxide, 1mM NA_2EDTA) and left for 40 minutes to allow the DNA to unwind. The slides were then electrophoresed at 1 V/cm for 30 minutes. Slides were then neutralised with neutralising buffer (0.5M Tris-HCL, pH7.5) four times, before being washed with distilled water a further four times. Slides were then stained with 1x Sybr Gold (*Invitrogen: S11494).* When dry, photos were taken using a ZEISS Axio Imager 2 and around 200 comets per slide were analysed using the comet analysis software CASP (Końca *et al.,* 2003). This number of comets was chosen based on the number of comets that were commonly found sufficiently spaced on the slide to avoid measuring overlapping comets.

2.5 MTT ASSAY

The MTT is a colourimetric assay that estimates the level of a population of cells by the metabolic ability the living cells to reduce the tetrazolium salt MTT (MTT 3-(4,5-

dimethylthiazol-2-yl)-2,5-diphenyltetrazolium bromide) to the purple formazan form. The absorbance at 565-600nm is then used to determine how much formazan has been produced which can be used as an estimate of cell viability.

Cells were grown and treated in 96 well plates. When the cells were ready to be tested for cell viability, 100µl MTT solution at 4mg/ml (Sigma, M5655) was added to each well. The plates were then incubated for 3 hours (MCF7) or 2 hours (K562). After incubation both the MTT solution and medium were carefully removed from each well and 100µl of MTT solvent (4 mMHCl, 0.1% IGEPAL® CA-630) was added. The absorbance at wavelength 595nm of each well was then recorded using a plate reader.

2.6 Protein extractions

Cell and EV pellets were lysed in 1x radioimmunoprecipitation assay (RIPA) buffer via sonication using a probe sonicator for 10 seconds at 30% amplitude in 4°C. Debris and larger vesicles were removed and discarded by centrifugation at 14,000×g for 20 minutes at 4°C.

2.6.1 Bicinchoninic acid (BCA) assay

Proteins extracted above were quantified using the BCA assay (life technologies). Bovine Serum Albumin (BSA) standards were made at set concentrations from the 2000 µl stock ampule provided in the kit. 25 µl (control for cell protein) or 5 µl (control for EV protein) of each standard was added to a 96-well, flat bottom, plate in triplicate. 25 µl of cell protein samples or 5 µl of EV protein samples were also added to the plate. Working reagent was made with 50 parts of BCA reagent A and 1 part BCA reagent B. 200 µl of 40 µl of the working reagent was then added to the cell/standard or EV protein respectively. The plate was the incubated at 37°C for 30 minutes and then the absorbance at 570nm was read on a plate reader. A standard curve was created using the samples of known concentration and this was used to quantify the unknown samples.

3 THE ROLE OF EVS IN THERMALLY-INDUCED BYSTANDER EFFECT

3.1 INTRODUCTION

3.1.1 THE EFFECTS OF HEAT STRESS ON CELLS

When cells become stressed they undergo numerous different biological processes in order to attempt to alleviate of the effects of this stress (Fulda *et al.,* 2010). The optimum temperature for an organism's survival can range widely, though the range within which they can survive is normally small (Feller 2010). Temperatures outside the optimum range for the cell will cause the cell's proteins to operate less efficiently or stop working entirely (Neurath *et al.,* 1944). The peptide structure begins to breakdown as hydrogen bonds holding it together break, causing the proteins to lose their function and they must either be repaired or replaced for the cell to survive.

3.1.2 THE THERMAL BYSTANDER EFFECT

Whilst the majority of work on the bystander effect has been on the radiation-induced bystander effect, BE has been demonstrated following both lethal and sub-lethal levels of heat stress (Dąbrowska *et al.,* 2005; Purschke *et al.,* 2010). Ovarian cells were exposed to heat treatment of 75°C for 10 minutes followed by a cooling period of 10 minutes in cold water, before being cultured with bystander cells. When assayed the bystander cells co-cultured with heat damaged cells showed increased cell detachment and reduced cell density (Dąbrowska *et al.,* 2005). However, this heat treatment is very severe, and as such may have led to the cells undergoing necrosis. Therefore, the observed bystander effect could be due to some factor released from dying cells, rather than in response to the stress.

Subsequent studies have shown that the effect also occurs at sub lethal temperatures where a significant portion of the stressed population was shown to have survived (Purschke *et al.,* 2011; Purschke *et al.,* 2010). Fibroblasts were grown in inserts, heat shocked on a heating plate for 10 minutes to numerous temperatures and then co-cultured with bystander cells for 72 hours. Bystander cells co-cultured with cells heated from 40°C to around 50-55°C were found to have increased micronuclei formation and apoptosis, and lower cell viability (Purschke *et al.,* 2010). Above this temperature a large number of cells were killed by the stress and the bystander effect was no longer observed meaning that the bystander signal is not released by dead cells. Interestingly there was no difference if the cells were washed following stress, hinting that the effect involves the cells continuing to secrete a bystander signal, even after the stress has been removed. Further work on the Active Thermal Bystander effect found dividing fibroblasts and preadipocytes were able to induce bystander effects whilst non-diving fibroblasts and mature adipocytes did not (Purschke *et al.,* 2011). These data all suggest that following sub-lethal stress the bystander signal is released by living cells in response to the stress, rather than dying cells releasing toxic factors into the extracellular environment.

3.1.2.1 HYPERTHERMIA: A NEW CANCER THERAPY

Treatments for cancer, chemotherapy and radiotherapy induce stress in the patients cells, and, in fact, induction of stress response related genes seems to correlate with treatment outcome (Bøhn *et al.,* 2012). Further, *in vivo* studies in rodents have found that irradiating one part of the body leading to damage in distant organs (Ilnytskyy *et al.,* 2009; Mancuso *et al.,* 2008). A greater understanding of how stress induces bystander effects is therefore very important. There is a new cancer therapy that is currently under investigation known as hyperthermia (Mallory *et al.,* 2015). It involves heating the patient to moderate temperatures (40-45°C) in order to induce cell death and has been shown to

increase the effectiveness of chemo and radiotherapy (Habash *et al.,* 2011). It is important to understand whether the mechanism behind thermally-induced bystander is the same as RIBE as it may also need to be considered from a therapeutic standpoint, should it become a viable cancer therapy.

3.1.3 EVs AS BYSTANDER SIGNALS

Previous work on the RIBE has shown that EVs are sufficient to induce damage in bystander cells (Al-Mayah *et al.,* 2012; Al-Mayah *et al.,* 2015). EVs released following irradiation have been shown to induce chromosomal aberration and increase DNA damage in bystander cells, with the effects having been observed even after 20 cell doublings after initial EV treatment (Al-Mayah *et al.,* 2012; Al-Mayah *et al.,* 2015). Interestingly when EVs from irradiated cells were used to treat cells shortly before irradiation they showed slightly higher survival than treatment with control EVs or control cells with no EV treatment (Mutschelknaus *et al.,* 2016). This offers some insight into the benefits to the cell of the bystander effect, as the bystander cells were better able to resist subsequent stress.

3.1.4 AIMS

Thermal Bystander is known to be able to be transferred via a factor secreted into the medium as described above. EVs from Irradiated cells have been shown to be able to induce BE in unstressed cells. In this chapter the hypothesis that EVs released from heat-shocked cells are able to induce the Thermal Bystander effect will be evaluated.

- Determine whether cells treated with EVs from stressed populations show higher levels of damage
- Evaluate the effect of blocking EV uptake on Thermal Bystander effect
- Test whether bystander cells are better able to resist stress treatment
- Assess whether bystander effects occur after very high heat treatments

3.2 METHODS

3.2.1 CELL CULTURE

Cells were cultured as in Chapter 2.1. In brief, cells were cultured in the following medium supplemented with 10% v/v fetal calf serum (Fisher, 10500064): MCF7 and HeLa: DMEM (SLS) supplemented with 2 mM L-Glutamine (Fisher); K562: RPMI, (Fisher). For experiments cells were seeded the day prior to treatment at $3.5x10^4$ (MCF7) and $2.1x10^4$ (HeLa) cells per cm^3 of growth surface or $5x10^5$ cells/ml of medium (K562). For EV extractions cells were grown in medium supplemented with pre-cleared (by ultracentrifugation for 16 hrs at 100,000 g) FCS following treatment.

3.2.2 HEAT TREATMENT

Cells were seeded at the above densities 24 hours prior to heat treatment. For EV experiments medium was removed from cells immediately before treatment and EV-depleted medium was added. Except where stated otherwise cells were heat shocked for in an incubator pre-warmed to 45°C for 1 hour (MCF7 and HeLa cells) or 3 hours (K562 cells). The cells were then returned to 37°C for 24 hours before either being harvested for assays or the medium being removed and EVs extracted. Control cells were maintained at 37°C.

3.2.2.1 70°C HEAT TREATMENT

For 70°C heat treatment the medium was removed from the flasks and the cells were placed into a water bath pre-heated to 70°C. The medium was removed to ensure the cells would heat and cool quickly given the high temperature and short time of the treatment. The cells were then removed from the water bath and allowed to cool for 10 seconds before fresh medium at 37°C was added to the flasks and they were returned to the incubator. The control flasks had their medium removed and were left at room

temperature for 20 seconds before fresh medium was added and the cells were returned to 37°C.

3.2.3 Western Blot

Protein was extracted from EVs and the cells as outlined in the methods section 2.6. Protein was quantified using bicinchoninic acid assay kit (Life Technologies). Ten micrograms of protein were run on 12% w/v precast acrylamide gels (BioRad) and transferred onto polyvinylidene difluoride membrane (BioRad). Membranes were blocked using 5% w/v skimmed milk powder in tris buffered saline with 0.05% v/v tween 20 followed by overnight incubation at 4°C with rabbit or mouse anti-human primary antibodies (Abcam) specific to HSP70 (ab5439) (exosome marker), TSG101 (ab83) (EV marker), cytochrome C oxidase (ab150422) (apoptotic body/mitochondrial marker), GAPDH (ab128915) (cytoplasmic marker), and calnexin (ab22595) (endoplasmic reticulum marker). Secondary Cy3 or horseradish peroxidase (HRP) tagged antibody (Abcam) incubations were then performed for 60 minutes at room temperature. Membranes were imaged using ChemiDoc MP (BioRad).

3.2.4 Nano Particle Tracking Analysis

The NTA was carried out using the NanoSight LM10 with a laser wavelength of 642nm and the NTA 2.3 build 0033 analytical software (Malvern Instruments Ltd, Malvern). The recording took place at room temperature which was monitored manually. The sample was manually added to the chamber and allowed to settle for 30 seconds before each video was taken. There were three 30 second videos recorded for each sample. Camera gain was 300 and the shutter speed was 19.97 ms. For analysis the detection threshold was set to 10 and the type to multi. The blur, min track length and min expected particle size were all set to auto. Calibration was carried out using 100nm silica beads diluted to a known concentration in PBS and then three 30 second videos were recorded.

3.2.5 EV UPTAKE INHIBITION

Cells were treated with EV uptake inhibitors 30 minutes prior to treatment with EVs. The following dose of each inhibitor was used: Heparin 10µg/ml (Franzen *et al.,* 2014), Dynasore 50µM (Newton *et al.,* 2006), Amiloride 50µM (Kälin *et al.,* 2010). These inhibitors were diluted in PBS, and control cells in these experiments were treated with an equivalent volume of PBS.

3.2.6 EV STORAGE

Unless otherwise stated EVs were used on the day of extraction. For the EV storage experiment the EVs were resuspended in PBS, aliquoted at the required volume and moved immediately to the -80°C freezer. Frozen EV samples were thawed on ice prior to use and any excess discarded after one freeze thaw cycle.

3.3 RESULTS

3.3.1 HEAT TREATMENT REDUCES CELL VIABILITY AND INCREASES THE LEVELS OF DNA DAMAGE

In order to determine whether heat shock treatment at 45°C for 1 hour (MCF7) or 3 hours (K562) was sufficient to induce damage in directly treated cells the levels of DNA damage and cell viability following heat treatment were assayed. MCF7 Cells were either heat-treated (45°C, red) or control treated (37°C, green) for 1 hour and then incubated for 24 hours. The levels of DNA damage and cell viability were then assayed using the Comet assay and the MTT assay respectively. Heat treatment increased the levels of DNA damage as shown by the percentage of DNA in the comet tail (Figure 3-1A). Cell viability was shown to have decreased after treatment at 45°C, as shown by a lower optical density following the MTT assay (Figure 3-1B). To further ensure a heat shock response was being triggered by this treatment the levels of HSP70 inside the cells was assessed via western blot (Figure 3-1C). Western blot was performed by Priya Samuel. HSP70 was found to be highly enriched in the MCF7 cells following the heat treatment. K562 cells were heat shocked at 45°C for 3 hours and the levels of DNA damage assayed using the comet assay (Figure 3-1D). Higher levels of damage were observed in the heat-treated cells than in the cells mock shocked at 37°C. These results suggest that the heat treatment is sufficient to induce a stress response in the MCF7 and K562 cells.

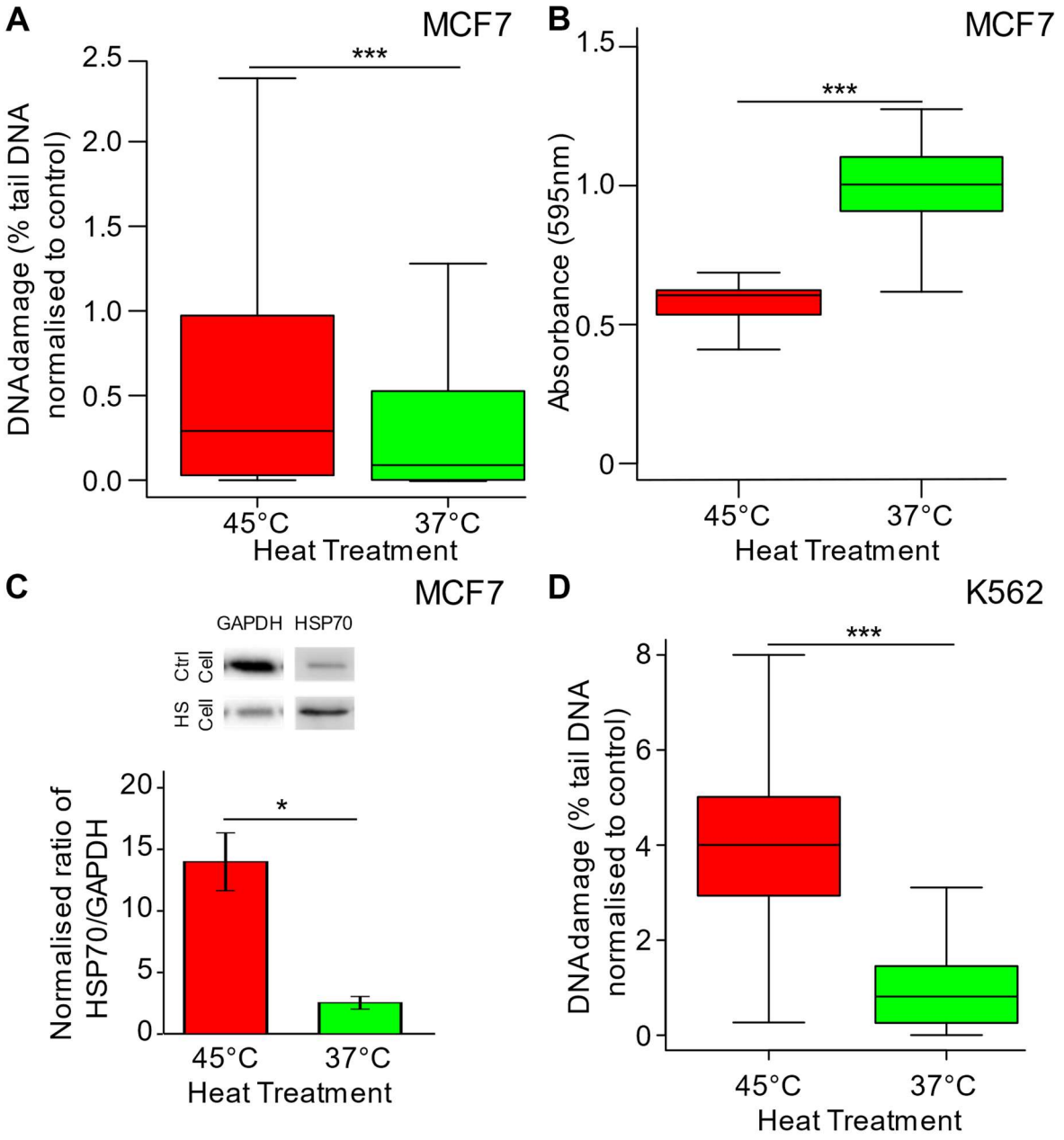

Figure 3-1: Heat treatment reduces cell viability and increases DNA damage. *MCF7 cells were either heat-treated (45°C, red) or control treated (37°C) for one hour then the levels of DNA damage (**A**) and cell viability (**B**) were assayed. **C)** Proteins were extracted from MCF7 cells treated as above and then a western blot was carried out to determine the levels of HSP70 within the heat shocked cells. **D)** K562 cells were heat-treated or control treated at 45°C for 3 hours then left at 37°C for 24 hours and assayed for DNA damage. Box and whisker plots show percentage of DNA in the comet tail normalised to mean control (**A** & **D**) or absorbance (**B**), median, upper and lower quartiles, error bars are 1.5x interquartile range. Bars for western blot **(C)** show standard error of the mean. For comet assay at least 500 comets were scored across two biological replicates. For MTT absorbance was recorded from 30 biological replicates. Statistical significance in comet assay data was assessed using the Mann-Whitney U test, MTT data and western blot was analysed using t-test. * p<0.05, ** p<0.01 and *** p<0.001.*

3.3.2 MEDIA CONDITIONED BY HEAT-STRESSED CELLS IS ABLE TO DRIVE DAMAGE IN BYSTANDER CELLS

Heat-induced bystander effects have been observed in co-culture systems, where cells are not touching but share medium, suggesting that signals able to induce the bystander effect are released into the medium (Purschke *et al.,* 2010; Purschke *et al.,* 2011). I hypothesised that our heat stress protocol would also be able to induce a bystander effect in this manner. To confirm that the medium contained a bystander inducing signal, medium was removed from cells 24 hours after heat treatment (MCF7 and HeLa: 45^{o}C, for 1 hour; K562: 45^{o}C, for 3 hours) and control treated cells (37^{o}C) and centrifuged at 300 x g for 5 minutes to remove any remaining cells and then at 16,500 x g for 20 minutes to remove debris and larger vesicles. It was then filtered through a 0.22 µm filter to remove any cell debris before being added onto bystander cells. These cells were then grown in this conditioned medium for 24 hours before being harvested. MCF7, K562 and HeLa cells were treated in this fashion and then assayed using the comet assay. The DNA damage in the MCF7 cells was assayed by Laura Jacobs. When cells were treated with stressed cell conditioned medium (SCCM) MCF7, K562 and HeLa cells showed higher levels of DNA damage than cells treated with control cell conditioned medium (CCCM) (Figure 3-2A, C-D). These data suggest that SCCM is capable of inducing the bystander effect in all three cell lines.

One potential explanation for the bystander effect could be that some factor within the media is altered during the heat treatment that causes the damage observed in the bystander cells. However a previous study on the bystander effect demonstrated that medium without cells that is irradiated does not induce bystander effects (Zhou *et al.,* 2002). In order to ensure that the bystander effect displayed here is also not influenced by the transformation of factors within the medium MCF7 cells were also treated with medium that had undergone heat treatment at 45^{o}C for 1 hour and the level of cell viability

measured via MTT assay (Figure 3-2B). There was no difference in the level of cell viability in the bystander cells treated with this medium. These data suggest that it is the effects of the heat stress on the donor cells and not on the medium that leads to damage in the bystander cells.

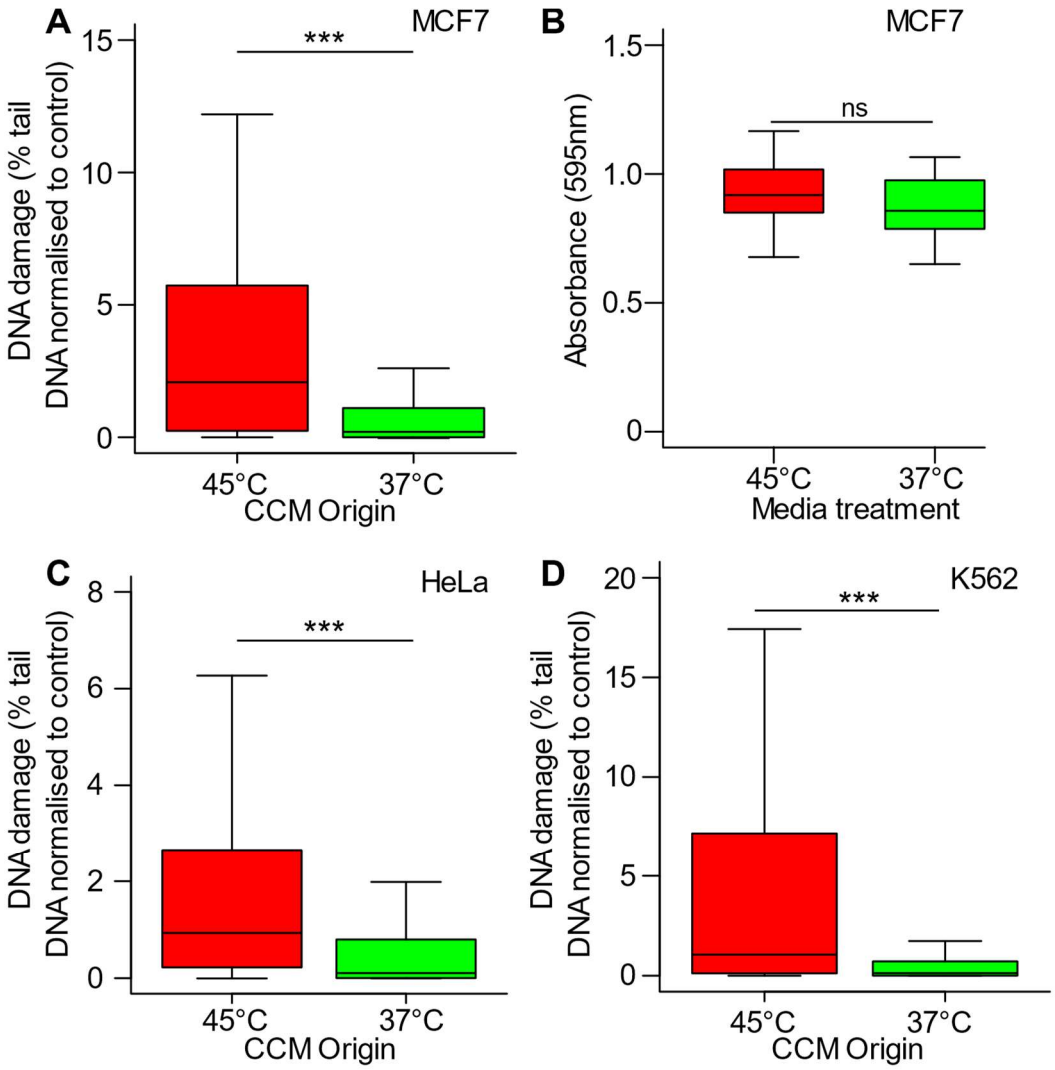

Figure 3-2: The bystander effect is induced by a soluble factor released by cells during stress. *Cells were heat shocked (red, 45°C: HeLa - 1 hour; K562 - 3 hours) or control treated (green) and incubated for 24 hours. The medium was then removed from the cells and used to treat bystander cells.* ***A, C-D*** *The level of DNA damage in bystander cells following treatment with stressed cell conditioned medium (SCCM) (****A****-MCF7,* ***C****-HeLa,* ***D****-K562).* ***B*** *Medium alone was heat-treated and used to treat* ***MCF7*** *cells and the level of cell viability were measured with the MTT assay. Box and whisker plots show percentage of DNA in the comet tail normalised to mean control, median, upper and lower quartiles, error bars are 1.5x interquartile range. At least 200 comets were scored across 2 biological replicates. For MTT absorbance was recorded in 30 biological replicates. Statistical significance in comet assay data was assessed using the Mann-Whitney U test, MTT data was analysed using t-test. * p<0.05, ** p<0.01 and *** p<0.001.*

3.3.3 Extracellular vesicles released during heat stress are able to induce the bystander effect

Previous work has shown that the vesicles released from stressed cells into the medium are sufficient to drive the radiation-induced bystander effect in cell culture (Al-Mayah *et al.,* 2012; Al-Mayah *et al.,* 2015). Here I tested the hypothesis that EVs released by heat treated cells were able to induce bystander effects in unstressed populations. To confirm whether these vesicles are responsible for the observed bystander effect the above experiment was repeated but EVs were harvested from the CCM. Cells were heat stressed as above (MCF7, HeLa: 45°C, for 1 hour) and control treated (37°C) and left for 24 hours to condition the medium, then EVs were extracted from the medium via ultracentrifugation. Remaining cells were pelleted, and the supernatant centrifuged at 16,000 g to pellet cell debris. The supernatant was then filtered and ultracentrifuged at 100,000 g to pellet EVs. Bystander cells were treated with these EVs and incubated for 24 hours before being harvested. Bystander cells were treated with EVs extracted from the same cell line. In order to ensure the EV treatments were comparable, the cells were all treated with the same volume of EVs which had been extracted from the same number of cells. Characterisation of these EVs was carried out by Laura Mulcahy and Naveed Akbar (Figure 3-3A). The presence of EV markers HSP70 (Zhan *et al.,* 2009), TSG101 (Thery *et al.,* 2001); the housekeeping gene GAPDH; Cytochrome C oxidase (CytoC Ox) a mitochondrial inner membrane protein and ER protein Calnexin were assayed via western blot. Both EV markers and GAPDH were both found in the EVs whilst CytoC ox and Calnexin were absent, suggesting the preparation included EVs. MCF7 cells were treated with EVs from heat or control treated cells. After 24 hours these cells were assayed for both DNA damage (comet assay) and cell viability (MTT assay). These cells showed an increase in DNA damage following treatment with stress EVs as well as a reduction in cell viability (Figure 3-3B, C). Bystander HeLa cells were also assayed for DNA damage using the comet assay. HeLa cells

treated with EVs from heat-treated HeLa cells showed higher levels of DNA damage than cells treated with control EVs (Figure 3-3D). These data demonstrate that the EVs released from the heat-stressed cells are sufficient to induce the bystander effect.

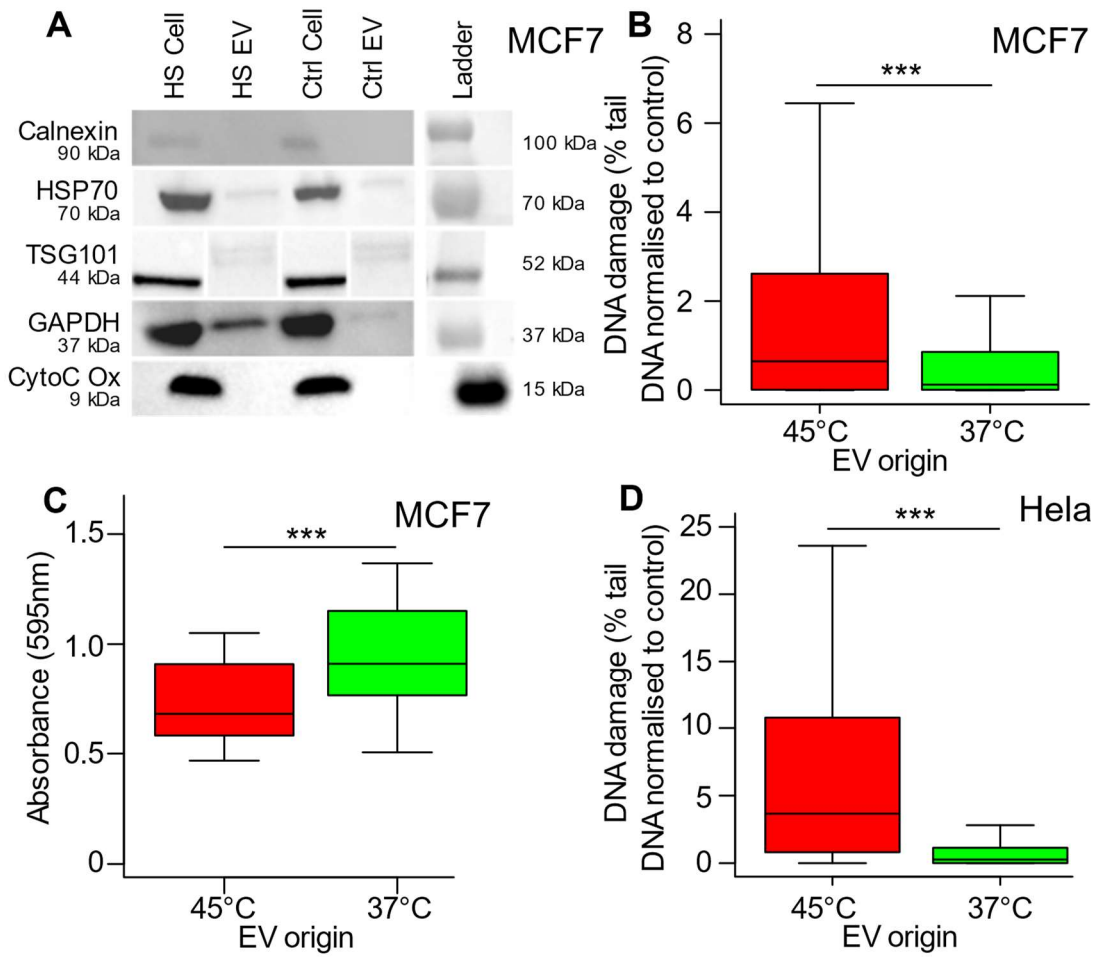

Figure 3-3: EVs released after heat treatment induce the bystander effect. *Cells were heat shocked (red, 45°C: HeLa, MCF7 - 1 hour) or control treated (green) and incubated for 24 hours. The medium was then removed from the cells and EVs were extracted via ultracentrifugation and used to treat cells.* ***A*** *proteomic analysis of heat and control treated* ***MCF7*** *cells and the EVs they released. Work carried out by Laura Mulcahy, Naveed Akbar and myself, image reproduced from Bewicke-Copley et al 2017.* ***B*** *The levels of DNA damage in bystander* ***MCF7*** *cells following treatment with EVs from heat shocked cells.* ***C*** *Estimated cell viability in bystander* ***MCF7*** *cells following treatment with EVs released from heat shocked cells.* ***D*** *The level of DNA damage in bystander* ***HeLa*** *cells following treatment with EVs extracted from heat shocked cells. Box and whisker plots show percentage of DNA in the comet tail normalised to mean control (**B, D**) or absorbance (**C**), median, upper and lower quartiles, error bars are 1.5x interquartile range. For comets at least 250 comets were scored for the HeLa cells, whist at least 300 were scored for the MCF7 across two biological replicates. For MTT absorbance was measured from 30 biological replicates. Statistical significance in comet assay data was assessed using the Mann-Whitney U test, MTT data was analysed using t-test. * p<0.05, ** p<0.01 and *** p<0.001.*

3.3.4 Vesicles released by heat stressed cells appear to reduce cell viability in a dose-dependent fashion.

A previous study has shown that increasing the number of stressed cells relative to bystander cells can increase the severity of the observed bystander effect (Thust *et al.,* 2004), I hypothesised that this could be due to an increase in the quantity of bystander signals present in the media and therefore that treatment with an increased number of EVs would also increase the severity of the bystander effect. In order to see whether a dose response was observed, MCF7 cells were treated with two different relative concentrations of EVs (1x and 2x) and the levels of cell viability and DNA damage were assayed. Cells were treated at either 45^{o}C or 37^{o}C (control) for 1 hour, then incubated at 37^{o}C for 24 hours to condition the medium. Then EVs were extracted from the CCM via differential ultracentrifugation and they were used to treat bystander cells. These cells were incubated for 24 hours before being harvested. The levels of DNA damage and cell viability were both assayed after EV treatment (Figure 3-4). Cells treated with EVs from heat stressed cells showed higher DNA damage and lower cell viability when compared to cells treated with EVs from control treated cells. The level of DNA damage in cells treated with EVs was not significantly different when twice as many EVs were used. However, the level of cell viability dropped significantly more when cells were treated with twice as many EVs. These data suggest that the reduction in cell viability caused as part of the bystander effect might be influenced by the levels of EVs available to the bystander cells. However, the level DNA damage is not affected by the dose.

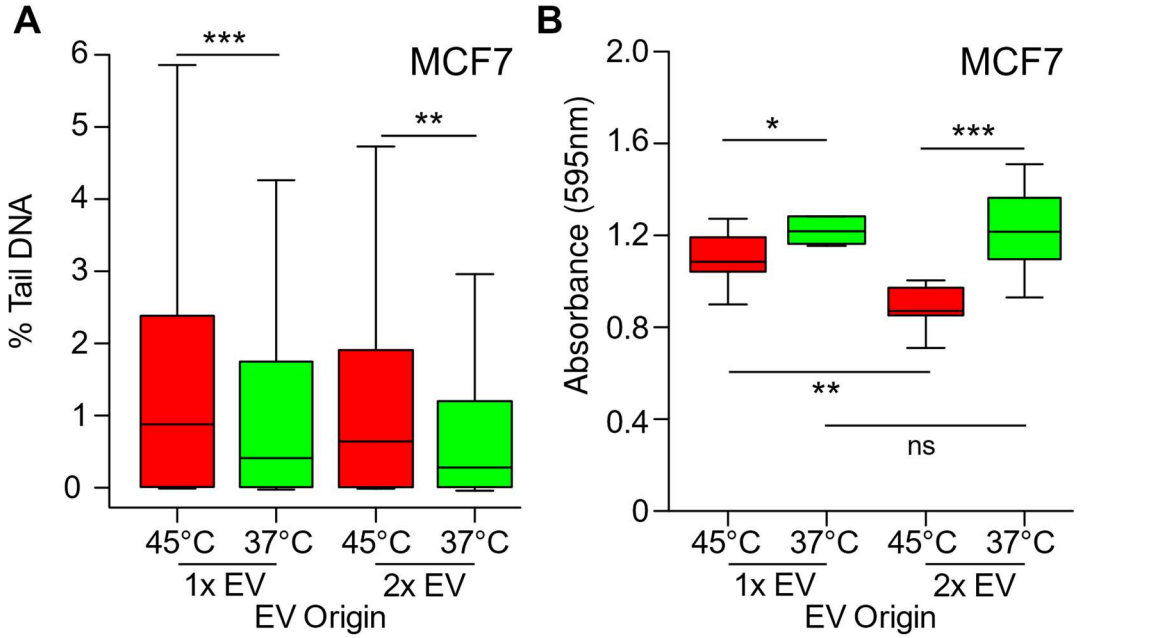

Figure 3-4: The effect of increasing EV dose on damage in bystander cells. *EVs were extracted from MCF7 cells after heat treatment (45°C for 1 hour) or control treatment. Bystander cells were treated with 1x and 2x the relative number of EVs and incubated for 24 hours before the levels of cell viability and DNA damage were assayed.* ***A*** *The level of DNA damage in cells following treatment with 1x or 2x EVs from heat-treated (red) or control treated (green) cells.* ***B*** *The levels of cell viability following treatment with 1x or 2x EVs from heat-treated (red) or control treated (green) cells. Box and whisker plots show median, upper and lower quartiles, error bars are 1.5x interquartile range. For comets at least 500 comets were scored across 2 biological replicates. For MTT, absorbance was measured from 10 biological replicates per treatment. Statistical significance in comet assay data was assessed using the Mann-Whitney U test, MTT data was analysed using t-test. * p<0.05, ** p<0.01 and *** p<0.001.*

3.3.5 EVs stored at -80°C retain the ability to induce bystander damage for around 2 weeks.

The best way to store vesicles is not yet known. ISEV guidelines state that EVs should be store at -80°C, however it has been suggested these conditions maintains EV structure but can cause EVs to lose their function (Witwer *et al.,* 2013; Lőrincz *et al.,* 2014). To assess the stability of EVs in the freezer, EVs extracted from heat and control treated MCF7 cells, resuspended in PBS and immediately frozen at -80°C. These were then thawed on ice and used to treat bystander cells after 0, 1, 2 and 4 weeks (Figure 3-5). Cells treated with EVs that had been frozen for up to 2 weeks still showed a significant increase in DNA damage against control. However, after 4 weeks the EVs no longer had the ability to induce bystander damage. These data imply that EVs are stable at -80°C for a short while after which they may lose their biological function.

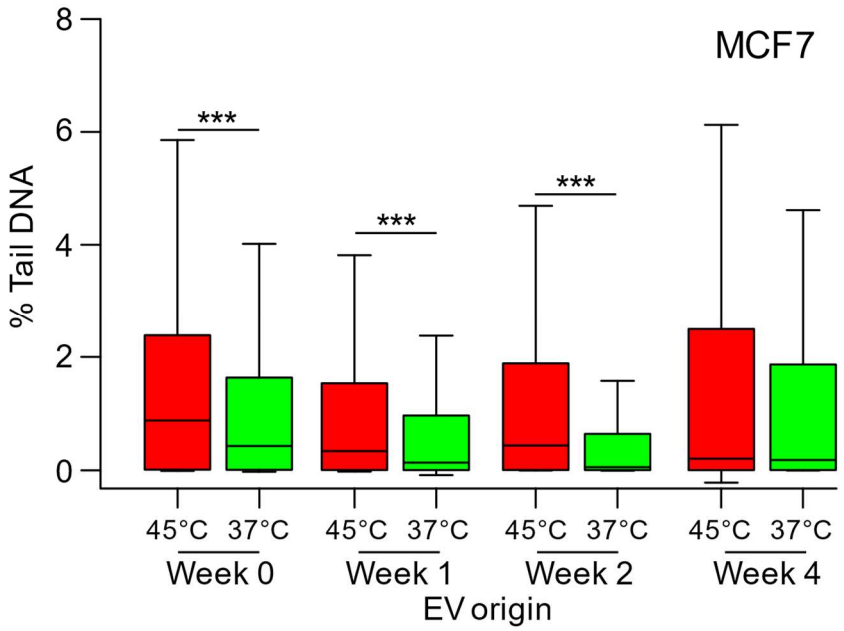

Figure 3-5: The effect of freezing EVs at -80°C on their ability to induce bystander effects. *EVs were extracted from heat-treated MCF7 cells (45°C, 1 hour) and control treated cells. A portion of these EVs were used to treat bystander MCF7 cells (Week 0). The remaining aliquots were then frozen at -80°C. After 1, 2 and 4 weeks an aliquot of the EVs was defrosted and used to treat bystander MCF7 cells, which were then incubated for 24 hours and the cells harvested, and the levels of DNA damage were assayed. Bystander effect was observed at weeks 0, 1 and 2, but no difference was seen in cells treated with 4-week-old EVs. Box and whisker plots show percentage of DNA in the comet tail, median, upper and lower quartiles, error bars are 1.5x interquartile range. At least 300 comets were scored across two biological replicates. Statistical significance was assessed using the Mann-Whitney U test. * p<0.05, ** p<0.01 and *** p<0.001.*

3.3.6 Inhibiting EV uptake has mixed effects on the bystander effect

In order to confirm that it is EVs within the pellet recovered via ultracentrifugation that cause the bystander effect, the effect of two known inhibitors of EV uptake, Heparin (Franzen *et al.,* 2014) and Dynasore (Newton *et al.,* 2006), on the bystander effect were assayed. If EVs are involved in bystander signalling then these inhibitors of EV uptake should abrogate the bystander effect. EVs were extracted from heat and control treated cells as above. Cells were then treated with the inhibitors above prior to treatment with the EVs. Treatment with Dynasore reduced the levels of DNA damage induced by stress-derived EV treatment. However, treatment with heparin had no effect on the level of DNA damage after stress EV treatment (Figure 3-6). Therefore, Dynasore treatment is able to abrogate the damaging effects of HS EVs, whilst heparin treatment has no effect on the bystander effect. Dynasore treatment in fact seems to reduce the levels of damage below

control levels, suggesting it may in fact protect the cells from damage. Heparin treatment on the other hand seems to have no inhibitory effect on the bystander effect with heparin treated bystander cells showing an increased level of damage against control cells.

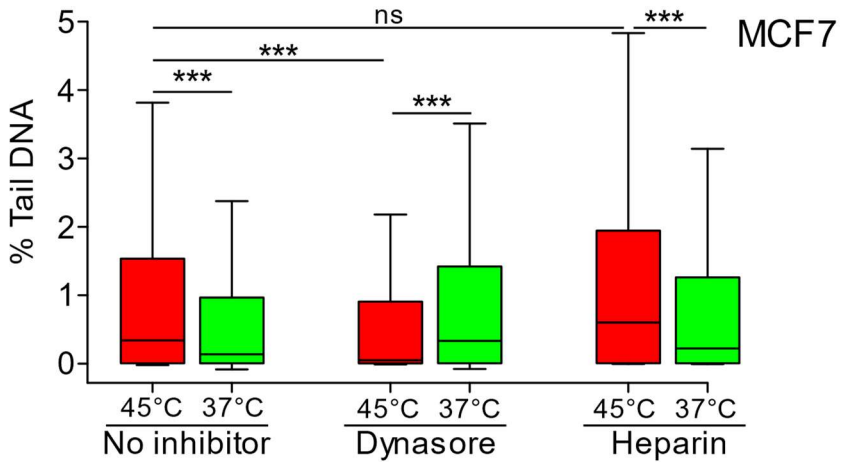

Figure 3-6: The effect of inhibitors of EV uptake on bystander damage and cell viability after direct heat treatment. A *EVs were extracted from Heat-treated MCF7 cells as above. These were then used to treat bystander MCF7 cells that had been pre-treated with inhibitors of EV uptake. These cells were incubated for 24 hours and then harvested for the comet assay. Box and whisker plots show percentage of DNA in the comet tail, median, upper and lower quartiles, error bars are 1.5x interquartile range. For comets at least 450 comets were scored across two biological replicates. Statistical significance was assessed using the Mann-Whitney U test; * p<0.05, ** p<0.01 and *** p<0.001.*

3.3.7 Bystander cells are better able to resist stress

Previous work on RIBE has shown that bystander cells show increased resistance to irradiation (Shankar *et al.,* 2006; Tang *et al.,* 2016; Ojima *et al.,* 2011), I therefore hypothesised that stress EV treated bystander cells would be better able to survive direct stress. Here the ability of stress-derived EVs to confer a protective effect was assayed. Cells were treated with EVs from stressed and unstressed cells and then subjected to heat shock. First MCF7or K562 cells were heat (45°C) or control (37°C) treated (1 hour, MCF7; 3 hours, K562) then returned to 37°C for 24 hours. Then EVs were extracted from the medium via ultracentrifugation and used to treat fresh K562 cells. These cells were grown for 24 hours and then heat shocked at 45°C for three hours and again returned to 37°C for 24 hours. The cells were assayed for DNA damage using the comet assay (Figure 3-7). The MCF7 work shown here was carried out by Laura Jacobs. The levels of DNA damage observed in the cells treated with HS EVs were significantly lower than in the cells treated with control EVs.

This suggests that the bystander cells were more resistant to the heat shock, further adding evidence to the idea that stress-derived EVs aid cells survival during stress.

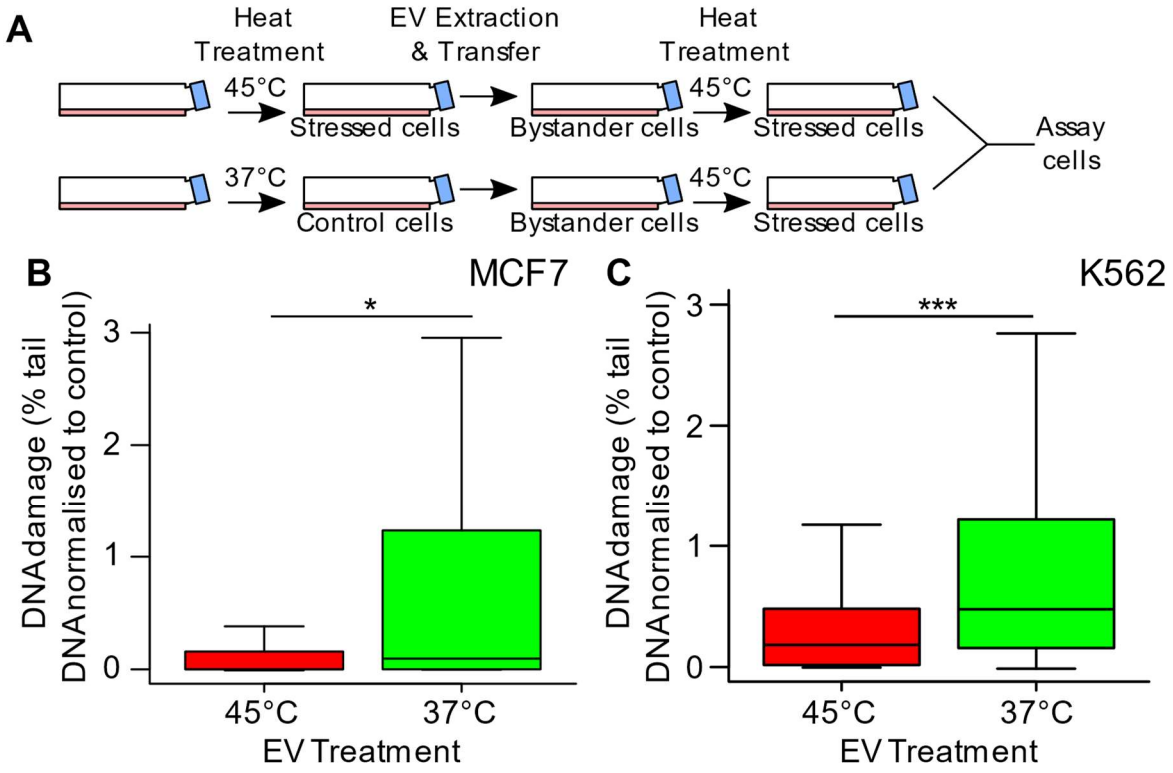

Figure 3-7: Treatment with EVs from heat shocked cells increases stress resistance. *EVs were extracted from heat (45°C) and control (37°C) treated MCF7* ***(A)*** *or K562* ***(C)*** *cells via ultracentrifugation. Cells were treated with these EVs for 24 hours before being heat shocked at 45°C (1 hour, MCF7; 3 hours, K562). 24 hours post heat shock these cells were assayed for DNA damage.* ***A)*** *Diagram of the experiment. Box and whisker plots show percentage of DNA in the comet tail normalised to control, median, upper and lower quartiles, error bars are 1.5x interquartile range. For comets at least 700 comets were scored across two biological replicates. Statistical significance evaluated using the Mann-Whitney U test. * p<0.05, ** p<0.01 and *** p<0.001*

3.3.7.1 *Treatment with inhibitors of EV uptake reduces the level of cell viability post stress.*

As stress-derived EVs are able to induce resistance to subsequent stress, it is possible that one function of stress-derived EVs is to help the population become more resistant to the stress. EVs may play a key role in priming cells to respond to stress. In order to check whether EVs released during stress also affect the population's ability to survive this initial stress, MCF7 cells were treated with the EV uptake inhibitors Heparin, Dynasore or Amiloride (Kälin *et al.,* 2010) prior to heat treatment (45°C, 1 hour) or control treatment. These cells were then incubated for 24 hours before the level of cell viability was assayed using the MTT assay. If stress-EVs induce an adaptive response, then blocking uptake should sensitise the population to the effect of the stress. Both Dynasore and amiloride showed a larger negative fold change in cell viability after heat treatment than in cells that were control treated. Heparin, however, showed no effect on the cell viability following heat stress. These data suggest that EV uptake during stress increases cell viability, as blocking it leads to a reduction in cell survival (Figure 3-8).

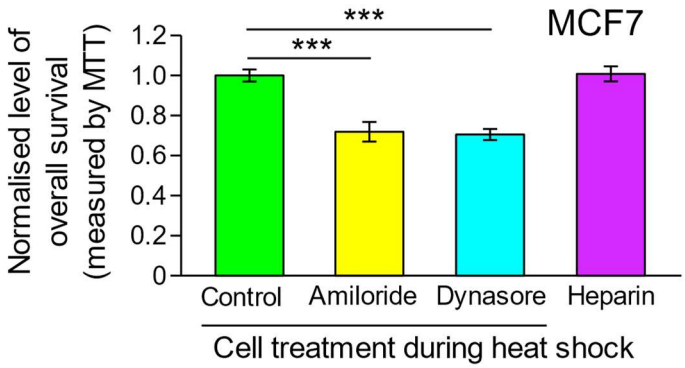

Figure 3-8: Treatment with EV inhibitors reduces cell survival during stress. *MCF7 cells were treated with Amiloride (50µM, yellow), Dynasore (50µM, blue), Heparin (0.01µg/ml, purple) or control treated (green) and then heat shocked as before at 45 and 37°C. The cells were then returned to 37°C and grown for a further 24 hours before being assayed for cell viability using the MTT assay. Readings for each group were normalised to the average reading for the vehicle control of the appropriate treatment group, then the fold change in cell viability following treatment at 45°C was calculated from these data. Bars represent fold change, error bars are standard error of the mean. For MTT, absorbance was measured in 12 biological replicates per treatment. Statistical significance was assessed using an ANOVA and then tested pairwise by tukey test, which is displayed in the figure. * p<0.05, ** p<0.01 and *** p<0.001.*

3.3.8 Bystander effects observed after treatment with EVs released following heat-stress at 70°C

A previous study on thermally induced bystander effect showed effects in bystander cells after treatment at 75°C. Here I hypothesised that EVs released from cells treated with a high temperature would also release EVs capable of inducing bystander effects.

3.3.8.1 There is no difference in the quantity of EVs produced after treatment at 70°C

In the interest of characterising the EVs extracted via ultracentrifugation following short, high heat, treatment the EVs were analysed using the NanoSight LM10 (Filipe *et al.,* 2010). Cells were treated at 70°C for 10 seconds and left for 8 hours to condition medium. EVs were then extracted from this medium via ultracentrifugation as outlined above. These EV populations were then characterised using the NanoSight (Figure 3-9A, B). There was no significant difference in the concentration or size of the EVs release by cells whether they had been heat- or control-treated. These data show that heat treatment does not seem to change the quantity or size of the vesicles released by the cells.

3.3.8.2 The bystander effect occurs after very short treatment at 70°C

Thermal bystander effect has been demonstrated to occur following a 10 minute heat treatment at 75°C (Dąbrowska *et al.,* 2005). To test whether this effect would occur after very short treatments at this temperature MCF7 cells were heat shocked at 70°C for 10 seconds or control treated and then left to condition medium for 3 hours. After this incubation EVs were extracted from the medium via ultracentrifugation. These EVs were then used to treat bystander cells which were then incubated for 3 hours before being assayed for cell viability. The cells treated with EVs from heat stressed cells showed a decline in their viability when compared with cells treated with EVs from control treated cells and cells that received no EVs (Figure 3-9B). These data suggest that short, high temperature treatments can also induce the production of EVs that are able to cause

bystander damage. Further as the cells were only conditioned by the EVs for 3 hours rather than 24 hours as in previous experiments, it also seems that the bystander effect is triggered soon after EV treatment.

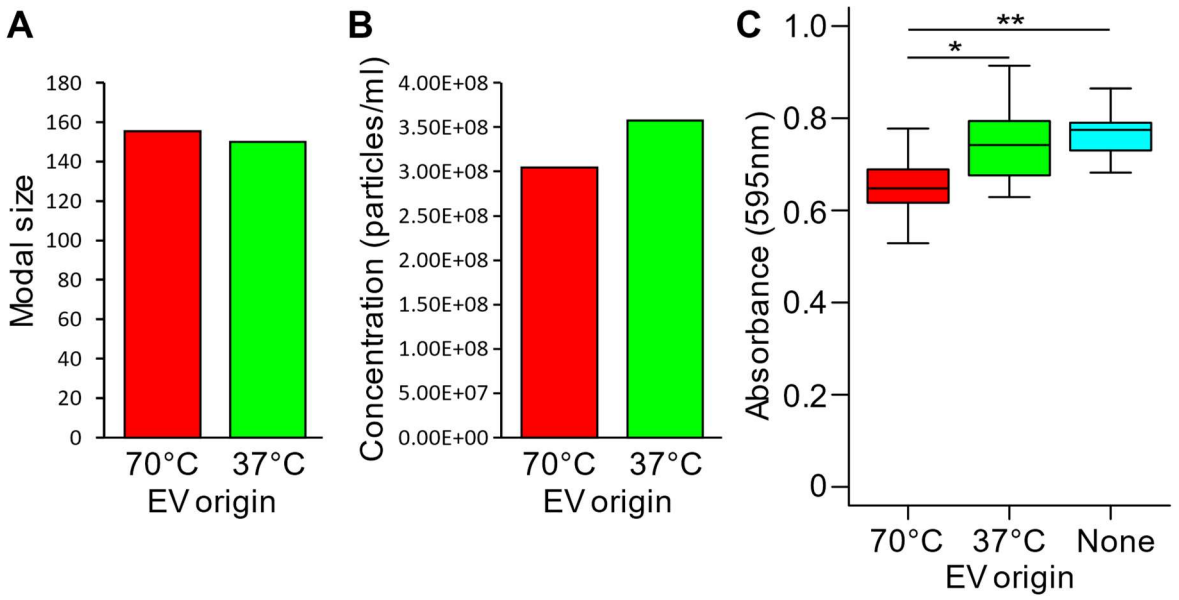

Figure 3-9: EVs from high heat are able to induce bystander effects in non-stressed cells. *MCF7 Cells were heat-treated at 70°C for 10 seconds, or control treated, then incubated for 3 hours. The medium was then removed and EVs were extracted via ultracentrifugation and then vesicle diameter* ***(B)*** *and concentration* ***(C)*** *were assayed using the NanoSight. 3 videos were taken across two biological replicates. Bars represent the average modal size of vesicles and mean concentration across 2 biological replicates.* **C)** *EVs were extracted as above and used to treat bystander MCF7 cells which were subsequently incubated for 3 hours before being assayed for cell viability. Box and whisker plots show absorbance at 595nm as an estimate of cell viability, median, upper and lower quartiles, error bars are 1.5x interquartile range, For MTT data from one biological replicate, 15 separate wells of a 96 well plate. For MTT data statistical significance was assessed using an ANOVA and then tested pairwise by tukey test, which is displayed in the figure. * p<0.05, ** p<0.01 and *** p<0.001.*

3.4 DISCUSSION

In this chapter the ability of EVs released following heat treatment to induce a bystander effect in nearby cells was assessed. EVs released after moderate and extreme heat treatments have been shown to lower cell viability and induce DNA damage in bystander populations.

3.4.1 HEAT-TREATED CELLS EXHIBIT A BYSTANDER EFFECT THAT CAN BE TRANSFERRED VIA EXTRACELLULAR VESICLES

One of the remaining questions surrounding the bystander effect is the mechanism by which stressed cells induce damage in nearby cells. There is evidence that blocking gap junction signalling abrogates the bystander effect, suggesting that the signal might be passed between cells in this fashion (Desai *et al.,* 2014; Shao *et al.,* 2003). However *in vivo* studies have shown bystander effects that occur far from the site of the original stress (Mancuso *et al.,* 2008; Ilnytskyy *et al.,* 2009). On top of this there have been numerous studies *in vitro* where the bystander effect has been observed either after co-culture with stressed cells, or after being grown in medium conditioned by stressed cells (Purschke *et al.,* 2010; Mothersill & Seymour 1997). These studies suggest that, as well as gap junction signalling, there is an alternative mechanism by which the bystander effect can occur, without the need for cell to cell contact. This work confirms that that a bystander effect occurs following medium transfer from heat stressed cells to bystander cells in both K562 and HeLa cell lines, with increased levels of DNA damage seen in cells after growth in stress cell conditioned medium. This agrees with previous findings that show bystander effects occurring after sub-lethal heat shock in co-culture systems (Purschke *et al.,* 2011; Purschke *et al.,* 2010).

There is some evidence that suggests that extracellular vesicles, notably exosomes are able to induce the bystander effect, with EVs extracted from irradiated cells being able

to induce damage in bystander cells (Al-Mayah *et al.,* 2012; Al-Mayah *et al.,* 2015). Here, EVs were extracted from heat-treated cells and used to treat bystander cells. The bystander cells showed higher levels of DNA damage and lower levels of cell viability when treated with heat-induced EVs. These data further the idea that EVs released by stressed cells that are at least one factor released by cells that can cause bystander effects in un-stressed populations. It is important to note that extraction via ultracentrifugation does not provide a clean preparation of EVs (Witwer *et al.,* 2013), though ultracentrifugation is the current gold standard for EV extraction (Gudbergsson *et al.,* 2015). The sample could also contain various proteins and other cellular components and debris that pellet at the same speeds. It is hard to ascertain the level of protein contamination as separating EV-associated protein from free protein would be very difficult. New methods for EV extraction are available which may be able to isolate samples with higher purity (Böing *et al.,* 2014).

The bystander effect was observed in all three cell lines used in this chapter (MCF7, HeLa and K562). It is, however, important to consider that cell lines often differ in numerous ways from physiologically normal cells and other cell lines, and these differences could lead to unexpected results. For example, the MCF7 cell line is deficient in caspase-3 , which is a key component in the induction of apoptosis. This deficiency allows the MCF7 cells to resist numerous different chemotherapeutics, and this resistance is abrogated when caspase-3 is reintroduced into the cells (Yang *et al.,* 2001). Furthermore, whilst these cells lack the apoptotic changes associated with caspase-3 activation, caspase-3 independent pathways can lead to the cells being phagocytosed by macrophages (Turner *et al.,* 2003). MCF7 are also able to utilise caspase-7 to induce cell death (Twiddy *et al.,* 2006). It is therefore important to consider which cell lines to use and appropriate assays for those cell lines when planning bystander experiments. An apoptosis assay that measures cleaved caspase-3, for example, would suggest that no the MCF7 cells undergo apoptosis. For this reason, it is also useful to use more than one assay to assess bystander damage, as if cells are

resistant to one factor, such as apoptosis, they may not be resistant to others, such as DNA damage.

The mechanism by which these EVs induce damage has not been elucidated, however it is probable that it is a molecule within the cargo of the EVs that is responsible for the bystander effect. Previous work on BE has shown that alterations to the cargo of EVs are able to reduce the levels of damage in bystander cells (Xu *et al.,* 2014; Al-Mayah *et al.,* 2015; Al-Mayah *et al.,* 2012). Further there is evidence of irradiation altering the cargo of EVs extracted from whole blood samples (Yentrapalli *et al.,* 2017). Interestingly in that study, the levels of miR-34-5p were found to be increased, a microRNA that has been shown to be involved in conferring resistance to the drug cisplatin (Samuel *et al.,* 2016).

3.4.1.1 Increasing the dose of stress EVs Affects the level of cell viability but not DNA damage

In order to establish whether the bystander effect displays dose related effect cells were treated with 2 relative concentrations of EVs. EVs were extracted from MCF7 cells and re-suspended in PBS. Cells were treated with either 20µl of the EV suspension (1x) or 40 µl (2x) and then incubated for 24 hours before being assayed for DNA damage and cell viability. Cells treated with twice as many EVs from heat-treated cells showed a reduction in cell viability compared to cells treated with less EVs, but there was no difference seen in the levels of DNA damage. These data do suggest that the quantity of stress-derived EVs might affect the severity of the bystander effect displayed in the recipient cells. The lack of change in the levels of DNA damage might suggest that the cause of this damage and the reduction of cell viability occur via two separate pathways within the cell. It's possible that the factor carried by the EVs that induce damage acts at capacity with the quantity of EVs used in these experiments, therefore increasing the concentration will not increase the level of damage. Interestingly there are conflicting accounts of the effect of the varying the

stress dose on the damage observed in bystander cells. Several studies have shown that the dose of the stress administered to the cells does affect the levels of bystander effect observed (Asur *et al.,* 2009; Testi *et al.,* 2016; Jin *et al.,* 2011; Soleymanifard *et al.,* 2013; Toossi *et al.,* 2017; Purschke *et al.,* 2010). However, other studies on the bystander effect have shown that there is no dose relationship (Ponnaiya *et al.,* 2004; Baskar *et al.,* 2007; Shao *et al.,* 2005; Hu *et al.,* 2006). One such study showed no effect on the number of donor cells damaged on the bystander cells, suggesting that there is a separation between effects observed in the stressed cells and the effects observed in the bystander cell (Ponnaiya *et al.,* 2004). When the dose is able to affect the damage in the bystander cells it does seem that there is a limit at which the damage ceases to increase along with dose (Asur *et al.,* 2009; Purschke *et al.,* 2010). It is possible that these cells reach a point of saturation, being unable to send out anymore bystander signals, or potentially that the signals they do release are no longer able to reach or effect the bystander cells. Alternatively, the very high stresses may be causing many of the donor cells to die, meaning there are less stressed cells releasing bystander signals. Evidence for this hypothesis was shown in thermal bystander experiments, where bystander damage was shown to be reduced after a certain temperature treatment corresponding with a reduction of cell viability (Purschke *et al.,* 2010). Here however, it was the level of signalling, not stress, that was increased. One study increased gap junction signalling and subsequently observed an increase in micronuclei formation (Shao *et al.,* 2003) suggesting that increased bystander signalling would show a similar increase in damage. In another study, bystander effects were reduced when cell conditioned medium was diluted prior to being used to treat bystander cells (Baskar *et al.,* 2007). These data therefore, seem to suggest that increasing the levels of bystander signal should increase the levels of bystander effect observed. Whilst previous data have shown that the dose of the initial stress is linked to the levels of bystander damage, here I suggest that the dose of bystander signalling molecules (EVs) is also able to modulate the bystander

effect. Whilst the minimum level at which bystander effects will occur was not ascertained these data suggest that the EV induced bystander effect is not a binary response.

The dose response of the bystander effect is currently a contentious topic and more work is needed to understand the effects of stress and bystander signal dose. A greater understanding of the signalling pathways that control the bystander effect is therefore vital to learn whether these pathways are more active at more damaging stress conditions and whether these signals are reaching their targets and affecting them. Here it is suggested that doubling the number of EVs used to treat bystander cells does affect some measures of bystander damage, but not others. A wider range of EV concentrations should be used to treat the bystander cells, including lower concentrations than used here, to fully assess whether stress EVs induce damage in a dose dependant manner. It would also be useful to assess the effects of different EV concentrations on more sensitive measures of cell damage, in case the dose response is being missed by the assays used here. Further, the number of EVs released at different temperatures should be assessed to ascertain whether the release of EV bystander signals also acts in a dose dependant manner.

3.4.2 EVs frozen at -80°C seem to retain biological activity for a few weeks.

The correct way to store extracted EVs, and for how long they retain their function in these conditions has not been fully assessed. The best practice for EV storage laid out by the International Society of Extracellular Vesicles (ISEV) is to freeze EVs at -80°C (Witwer *et al.,* 2013). Data from 2014 showed that EVs stored at room temperature or -4°C overnight reduced function and storage at -20°C structural changes were observed (Lőrincz *et al.,* 2014). When these EVs were stored for a month at -80°C the structure had not changed, however they did show loss of function (Lőrincz *et al.,* 2014)

Here EVs frozen at -80°C were able to induce damage in bystander cells up to 2 weeks after freezing, however after 4 weeks no effect was observed. This data suggests that whilst EVs can be frozen, they may lose their function if stored too long. The ISEV recommendations suggest only testing fresh vs fresh or frozen vs frozen EVs (Witwer *et al.,* 2013). The data shown here supports this advice, as the length of time the EVs have been frozen for has been shown to potentially alter their biological effect. This fits with the previously published work on EVs that showed reduced function after being stored at 80°C for a month (Lőrincz *et al.,* 2014). It is unclear from the data what has caused the reduction in activity of frozen EVs after 4 weeks. It could be that the EVs themselves have degraded or that their content or cargo have been damaged. The structure of the EVs could be checked via Electron Microscopy to ensure that their membranes have not degraded. The activity of the cargo would be more difficult to assess, given the difficulty of purifying only EV-associated protein or nucleic acids, and as the factors involved in the effect remain unknown. As only DNA damage in recipient cells was assayed it's possible that other biological activity may be retained longer, or indeed may be lost sooner after the freezing process. Importantly future testing on the stability of frozen EVs should continue past the point at which EVs first begin to lose function in order to be certain that there are now inert and that it is not simply a problem with the sample thawed on that time point.

3.4.3 EV UPTAKE INHIBITORS HAVE DIFFERING EFFECTS ON THE BYSTANDER EFFECT

Whilst ultracentrifugation is the most commonly used method of EV extraction, the pellet recovered is not pure. It will contain a variety of different molecules that are also present in the pellet, along with the EVs (Witwer *et al.,* 2013). In order to try and confirm that it is EVs that are responsible for the bystander effect seen above EV treatment was repeated but cells were also treated with the EV uptake inhibitors: heparin and Dynasore. The data showed that Dynasore not only abrogated the damage from the bystander effect

but that the cells treated with heat derived EVs showed lower levels of damage than cells treated with control EVs. This would suggest that Dynasore treatment lowers the level of DNA damage below the baseline level of damage found in the cells treated with control EVs. This is an odd finding as if Dynasore itself protects against damage the effect should be seen in the control EV treated cells to. There are numerous different mechanisms by which EVs can enter cells (Mulcahy *et al.,* 2014). Dynasore is an inhibitor of dynamin, a GTPase involved in the scission of vesicles from membranes, it is thought to block EV uptake by the inhibition of endocytosis (Newton *et al.,* 2006). Heparin is thought to cause the aggregation of EVs and block their uptake by interfering with their ability to bind to the plasma membrane (Atai *et al.,* 2013).

Conformation of uptake inhibition was not carried out here, meaning the EVs may still have been able to enter the cells. This might explain why Dynasore but not heparin affected EV induced bystander damage. It may be that the uptake of the EVs responsible for the effect might be blocked by Dynasore but not heparin. It would be possible to test this by assessing vesicle uptake in bystander cells with and without treatment with both of the uptake inhibitors used here. Further, as neither heparin nor dynasore are specific inhibitors of EV uptake, it is possible that the effects seen in these experiments are in fact due to non-EV related effects of these molecules. Another method to decipher whether it is the EVs found in the sample that induce the bystander effect would be to block EV release from the donor cells and see whether the effect still occurs, or to boil or otherwise inactivate the EVs prior to treatment. If the effect still occurs when there are no active EVs it would suggest there is another molecule secreted by the cells during stress which is inducing these effects.

3.4.3.1 EVs seem to have a protective effect on a directly stressed population's viability.

MCF7 Cells were treated with Dynasore or amiloride, inhibitors of EV uptake, and then heat-treated at 45°C for 1 hour. The cells treated with Dynasore and amiloride showed a greater fold change in cell viability against untreated cells after heat treatment. These findings hint at a positive effect of the EVs within the population, as when uptake is blocked the cells show lower levels of survival. As stated above in relation to heparin and Dynasore, it's important to note that amiloride is not a specific inhibitor of EV uptake and acts by blocking micropinocytosis (Koivusalo *et al.,* 2010). As such the effects seen here could be due to off-target effects rather than EV uptake inhibition. It's possible that the EVs released during stress conditions are actually beneficial to the survival of the population, and that the bystander effect is simply a symptom of this protection. In order to test if recipients of heat shock EVs were better able to survive heat stress K562 cells were treated with EVs from heat and control treated cells. When these cells were subjected to further stress cells treated with heat shock derived EVs showed lower levels of DNA damage than cells treated with control EVs. This suggests that the HS EV treatment has increased the bystander population's ability to survive heat stresses. These data show that bystander cells are more resistant to heat treatment suggesting that the thermal bystander effect may be a way of reducing the effects of the heat stress on the population. This agrees with data showing that RIBE provides a protective effect against subsequent irradiation (Shankar *et al.,* 2006; Tang *et al.,* 2016; Ojima *et al.,* 2011). It would be interesting to test whether EVs released from cells after one stress are able to protect cells from another stress; for example, can EVs from heat-shocked cells protect cells from radiation-induced damage. It should be noted that both Dynasore and amiloride can sensitise cells to apoptosis (Cho *et al.,* 2005; Shen *et al.,* 2018) which could mean that inhibitor treatment doesn't block a protective EV signal but in fact simply sensitises the cells to the heat-stress. Here this effect was taken

into account as the data was compared to the survival in unstressed cells, however it would be useful to examine this effect using a method of uptake inhibition that does not affect cell survival.

The mechanism for this increase in resistance remains unknown. In bacteria, stress treatment is thought to induce mutation in an attempt to create a new strain with an increased ability to resist stress, a process known as Stress Induced Mutagenesis (Foster 2005; Foster 2007). However, bacterial populations can afford for a large percent of their population to die in order to increase their overall resistance to a stress, in animals this is not a viable strategy. It is more likely here, that some factor or factors carried by the EVs are able to create an environment within the bystander cells that allow them to better resist stress. It is already known that EVs can carry stress related proteins such as the HSPs (Kalra *et al.,* 2016; Krämer-Albers *et al.,* 2007), it could therefore be that these EVs carry cargo that is able to aid in stress resistance. It could also be that the EVs upregulate other stress resistance processes within the bystander cells. Further, it is thought that bystander effect is in part driven by NF-κB, which is known to be involved in the stress response and has been observed to have both pro- and anti-apoptotic effects in cancer cells (Hoesel & Schmid 2013), this could be related to the increased ability of the population to resist stress. It would be interesting to establish how long after EV treatment the adaptive effect is still present, in order to determine whether the change was short term, due to cargo delivered in the EVs or related to processes deregulated by that cargo, or long term, suggesting more permanent changes to the properties of the population.

3.4.4 EVs RELEASED FOLLOWING VERY HIGH TEMPERATURES CAN CAUSE BYSTANDER EFFECTS AFTER BRIEF TREATMENTS.

The EVs released after 70°C treatment were analysed using the nanoparticle tracking analysis (NTA) method, with their size and concentration being recorded. No difference

was found between the number of vesicles released from heat-treated cells, measured as particles/ml, or between the size of the vesicles released. This suggests that there is no morphological difference between stress and normal EVs that are involved with this effect. This suggests that size or concentration differences of EVs are not what cause the effect, further suggesting that it the effect is related to the cargo of the EVs. This agrees with other work from our lab which has shown that there is no significant change in the number of EVs released following stress (Bewicke-Copley *et al.,* 2017; Samuel *et al.,* 2017). However, one important consideration to take into account with these data is that the stress will very likely mean that there are fewer cells to release the EVs, meaning that whilst there is no overall difference, individual cells may be releasing more cells. Our previous work has however shown that EVs from stressed cells are smaller on average (Bewicke-Copley *et al.,* 2017; Samuel *et al.,* 2017). The data presented in Figure 3-9 is only from two biological replicates however, so care should be taken when making drawing any conclusions from it.

The previous experiments here have used low levels of heat, however early thermal bystander effects were observed following high heat treatments (Dąbrowska *et al.,* 2005). Bystander effects following brief high heat treatments were also assayed. Cells were heat shocked at 70°C for 10 seconds and then incubated for 3 hours. EVs were extracted and used to treat bystander cells for three hours after which the levels of cell viability were measured. Cells treated with EVs released by heat stressed cells showed significantly reduced levels of damage when compared against cells treated with control EVs, or cells that were not treated. Previous experiments presented here have shown bystander effects occurring after relatively low heat treatment for an hour or longer. This data, however, suggests that EVs released after short treatments with higher temperatures are capable of inducing the bystander effect. Here I show that EVs released after only 10 seconds of treatment were able to induce bystander effects. Further these EVs released within 3 hours of treatment were shown to be able to induce bystander damage, which fits with early

work on the RIBE which observed a medium transfer induced bystander only 1 hour post irradiation (Mothersill & Seymour 1997). This suggests that the stress induced changes to the secretome of the cell occur soon after treatment. Furthermore, the cells were only conditioned by the EVs for 3 hours before being assayed, suggesting that bystander effects may occur quite quickly following heat treatment. Care must be taken when interpreting these data however as the EVs were only extracted from one biological replicate. Previous studies on thermal bystander effect, including those presented above, have incubated bystander cells for 24 hours or longer before assessing the levels of damage (Purschke *et al.,* 2010; Purschke *et al.,* 2011; Dąbrowska *et al.,* 2005). One of the early studies on RIBE assessed the cells relatively early at 6 hours following irradiation (Hickman *et al.,* 1994), whilst another much later at 3 days (Prise *et al.,* 1998), however in these experiments the bystander cells were in the same culture vessel as the stressed cells, which could alter the time needed for effects to be observable. The timings of the bystander effect are as yet unknown, here and previously short treatments have shown bystander effects whilst many studies show effects occurring days after stress treatment. Whether the relatively short length of time cells needed to be cultured with stress-derived vesicles here is due to the high dose of the heat shock or whether a lower temperature treatment could also induce BE in these conditions is unknown. Further experiments could clarify this by extracting vesicles at different times after treatment with a variety of doses and culturing the bystander cells with EVs for varying times. This would better allow us to understand the speed at which these signals are produced by stressed cells and how long they take to act in bystander cells.

3.4.5 Further Work

Here EVs have been shown to have a role in the induction of the thermal and chemical bystander effect *in vitro.* However, the mechanism by which EVs are able to cause

bystander damage is not understood. In order to better understand the how the bystander effect is initiated. The cargo of the EVs is an obvious target for further study as alterations in cargo have been shown to reduce the bystander effect (Al-Mayah *et al.,* 2015). It would also be useful to know what biological processes are affected in the bystander cells themselves. There is evidence that *COX-2* expression is linked with radiation and chemically-induced bystander effect and that numerous pathways targeting its expression are activated in bystander cells (Zhou *et al.,* 2005; Asur *et al.,* 2010b; Asur *et al.,* 2010a). It seems likely that similar pathways would be activated in the thermal bystander effect. Analysis of the gene expression and protein phosphorylation in the bystander cells would help see what processes the HS EVs are activating.

3.4.6 Concluding remarks

The bystander effect is a potentially clinically interesting phenomenon where stressed cells are able to induce a stress response in nearby cells. In this chapter extracellular vesicles released from cells during heat stress have been shown to be able to induce damage and reduce cell viability in bystander populations. EV uptake inhibitors showed various effects on bystander damage, with inhibition of endocytosis abrogating the bystander effect. EV uptake inhibition was also shown to reduce cell viability following heat stress. This points to stress EVs as a mechanism of generating stress resistant populations in order to mitigate the damage caused by stress.

That cellular stress causes the release of EVs capable of inducing damage in cells could mean that when patients are treated with certain therapies, such as hyperthermia, their stressed cells release EVs that cause cellular damage. It is therefore important to consider the effects of these stress EVs when devising treatments. It's possible that treating patients with EV uptake inhibitors may help reduce bystander damage during treatment. Though as the uptake inhibitor heparin actually increased the levels of damage, more work is

necessary to know which inhibitors if any will abrogate the effect *in vivo*. Further the EV uptake inhibitors amiloride and Dynasore reduced cell viability following direct stress, suggesting that EV uptake may play a beneficial role in protecting the population from damage. More work is necessary to truly understand the potential risks of the bystander effect *in vivo*, and which steps, if any, should be put into place to alleviate these risks

4 CHAPTER 4 - THE EFFECTS OF CISPLATIN INDUCED EVS

4.1 INTRODUCTION

4.1.1 CHEMICALLY-INDUCED BYSTANDER EFFECTS

In the previous chapter EVs were demonstrated to be involved in the initiation of thermal bystander effects. The bystander effect has been observed following treatment with chemical agents in co-culture, medium transfer and EV transfer experiments (Samuel *et al.,* 2017; Asur *et al.,* 2009; Jin *et al.,* 2011). Bystander cells seem to be affected in numerous ways other than genetic damage and cell death, with bystander cells demonstrated to have greater invasive capacity and resistance to stress (Bewicke-Copley *et al.,* 2017; Samuel *et al.,* 2017). As EV are known to affect numerous biological processes including modulating disease (Tominaga *et al.,* 2015; Becker *et al.,* 2016; Beer & Wehman 2017; Yáñez-Mó *et al.,* 2015), it is possible that stress-derived vesicles might affect these processes differently.

4.1.2 CANCER RELATED CACHEXIA

Cancer-induced cachexia is unexplained weight loss, predominantly via reduction of muscle mass, observed in patients with cancer (Aoyagi *et al.,* 2015). Mice implanted with xenografts from cachexia inducing tumour types, such as lung cancers, have been shown to induce a cachexic phenotype (Zhang *et al.,* 2011; Zhang & Li 2012). Treatment of muscle cells with medium conditioned by cancer cells has however been demonstrated to induce muscle wasting (Zhang *et al.,* 2011). It is possible that EVs released by these cancer cells are able to propagate this effect.

4.1.3 EV EXTRACTION AND CHARACTERISATION TECHNIQUES

Ultracentrifugation is very commonly utilised as a method of EV extraction (Lötvall *et al.,* 2014; Momen-Heravi *et al.,* 2013). Cells, debris and larger vesicles are removed via centrifugation and then the sample filtered and centrifuged at 100,000-120,000 x g to pellet small EVs. Whilst this method of extraction has been and continues to be successfully used for this purpose, it does not provide a completely pure preparation of EVs, as other small molecules and complexes may be incorporated into the pellet (Gudbergsson *et al.,* 2015; Witwer *et al.,* 2013). Sucrose gradients can be used alongside ultracentrifugation in order to increase the purity of the preparation, however this has also been shown to reduce the yield of EVs (Gudbergsson *et al.,* 2015). Impure samples make it difficult to be sure that it is the EVs, not some other contaminant, that is causing an observed effect. Further in order to study the proteome of the EVs it is necessary to extract a large quantity of EVs whilst removing as many contaminating proteins as possible. One method for extracting EVs that could increase sample purity, without reducing yield, is size exclusion chromatography.

4.1.3.1 SIZE EXCLUSION CHROMATOGRAPHY

Size Exclusion Chromatography (SEC) is a method of separating particles based on their size. Particles travel through a stationary phase that contains numerous porous polymer beads. Smaller particles are able to enter these pores, slowing their progress through the column, whilst larger molecules cannot, allowing them to travel more quickly through the column. The outflow from the column is collected in desired volumes known as fractions. As smaller particles travel more slowly through the stationary phase they are found in the later fractions, whilst the larger, faster particles are found in the earlier fractions. This is shown in Figure 4-1.

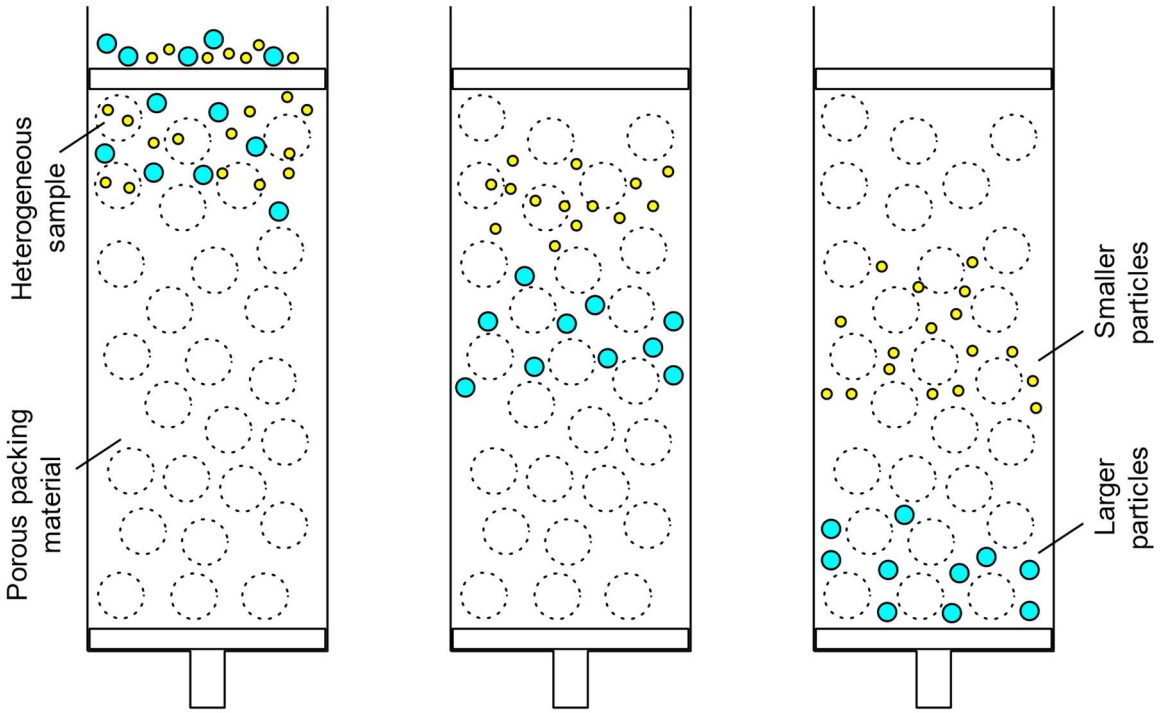

Figure 4-1: Size Exclusion Chromatography.

SEC is a method of separating particles in a heterogeneous sample by their size. The sample is run through a stationary phase comprised of porous beads. Smaller molecules are able to enter these pores, whilst the larger molecules cannot, slowing the progression of the smaller molecules through the stationary phase. As the larger molecules are not slowed they separate from the smaller molecules in the column. Numerous fractions are collected from the bottom of the column and differently sized molecules are found in different fractions.

4.1.3.2 Liquid-Chromatography Mass Spectrometry for proteomics

Liquid-Chromatography Mass Spectrometry (LC-MS) is a technique that allows the identification of molecules in a mixed sample by first separating the mixture by size using chromatography and then the contents quantified and identified using via mass spectrometry. Stable isotope-based labelling is a very accurate method of protein quantification (Ong *et al.,* 2002); however, it is a time-consuming and costly process. Label-free Quantification (LFQ), whilst less accurate, is relatively quick method of studying the proteome of cells and vesicles (Cox *et al.,* 2014; Asara *et al.,* 2008). One method of label free quantification known as MaxLFQ uses LC-MS along with peptide sequence databases to identify the proteins found within the sample. The proteins are first digested into peptide fragments which are then separated and quantified using LC-MS (Cox *et al.,* 2014).

The fingerprints of these fragments are then used to identify their parent proteins using the MaxQuant software (Tyanova, Temu & Cox 2016).

4.1.4 AIMS

In this chapter, the ability of EVs released from stress and unstressed A2780 cells to induce phenotypic effects in muscle cells will be assessed. In order to ensure that pure samples of EVs can be obtained SEC will be used to extract the EVs.

- Assess the ability of SEC to extract EVs without protein contaminants
- Identify differences in the proteomes in cells and EVs after cisplatin treatment

The ability of cancer EVs to induce cachexia will be tested both *in vitro* and *in vivo* with EVs extracted from both cisplatin and control treated cells

- Assess the ability of cancer EVs to alter muscle differentiation using C2C12 (mouse myoblast) cells
- Assess the effects of injecting cancer EVs on muscle mass and strength in healthy mice

Stress EVs have been shown to induce damage in bystander cells, but here I will test whether they are able to induce cachexia in both *in vitro* and *in vivo* models.

4.2 METHODS

4.2.1 SIZE EXCLUSION CHROMATOGRAPHY

4.2.1.1 MEDIA PREPARATION

Media was prepared as in the protocol for ultracentrifugation found in the methods chapter, section 2.1. However, after the medium was filtered it was then concentrated to 500 µl using Vivaspin® 20 concentration columns with a 100 kDa cut off filter (Fisher, 10774797). These tubes were centrifuged at 6000 x g or 3000 x g in fixed angle or swing out rotor respectively.

4.2.1.2 COLUMN PREPARATION

Columns were made up 2 to 24 hours prior to use. Empty chromatography columns (BioRad, 7321010) were filled with 14mls of sepharose (Fisher, 10217754) and 10 mls of cell culture grade PBS (Sigma, D8662). These columns were then left at room temperature to allow the sepharose to settle. Immediately prior to use an upper bed support was added to the column to reduce the disturbance to the sepharose during washes and sample addition. The column was washed through twice with PBS and then once with 0.03% v/v TWEEN® 20 (Fisher, BP337-500) in PBS. This detergent was added to stop particles within the sample from sticking to one another artificially increasing their size and therefore speed through the column. Column preparation is shown in Figure 4-2.

4.2.1.3 EV EXTRACTION

500 µl of concentrated medium was added to the column and allowed to fully enter the column before 10 mls of 0.03% v/v TWEEN® 20 in PBS were added. Immediately after the addition of the TWEEN® 20, 500 µl fractions were collected up to the desired fraction number. For EV extractions fractions 6-8 were pooled as the EV containing fractions. The protocol for EV extraction using SEC is shown in Figure 4-2.

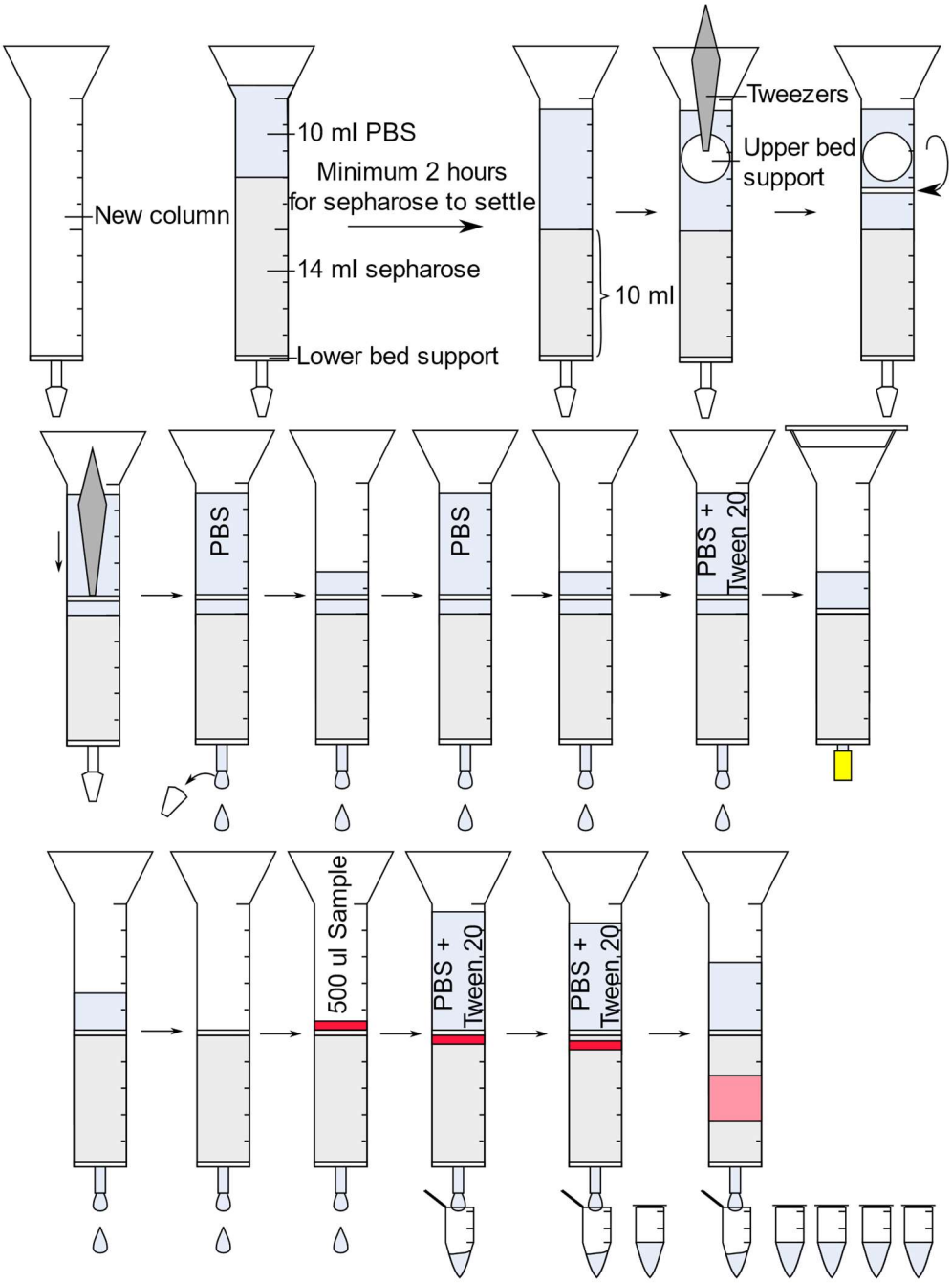

Figure 4-2: Size exclusion chromatography protocol.

Columns were made using sepharose as the stationary phase and allowed to settle for 2 hours - 1day. Prior to use, a top bed support was added, and the columns were washed 3 times, twice with PBS and once with 0.03% v/v TWEEN® 20 in PBS. 500 µl of concentrated sample was then added to the column. Once the sample had completely entered the stationary phase 10 ml of PBS + TWEEN® 20 was added to the column and 500 µl fractions were collected.

4.2.2 Cisplatin Treatment

Cells were treated with 40μM cisplatin (unless stated otherwise) diluted in PBS or an equivalent volume of pure PBS and incubated for 3 hours. Then the medium was removed from the cells and they were washed once with PBS to remove any residual cisplatin containing medium, fresh medium was added to the cells and they were returned to the incubator for two hours. The medium was then removed again, and the cells were washed with PBS to remove any cisplatin that may have remained in the mediu, or have been released from the cells, fresh EV-depleted medium was then added to the cells and they were returned to the incubator for the desired time before EV extraction.

4.2.3 Protein Analysis

4.2.3.1 Liquid chromatography-mass spectrometry

Cells were treated as outlined above and EVs were extracted from the cell conditioned medium 72 hours post treatment. Proteins were extracted from the cells and EVs as described in the methods section. The protein was sent Craig Kerr at the University of British Colombia who carried out the mass spectrometry.

The samples were boiled for 5 minutes and 20μg of each sample were added to 4 volumes of ice cold 80% Acetone and incubated for 4 hours at -20°C. The protein was pelleted at 16,000 rpm for 10 minutes. The pellets were washed twice with ice cold 80% Acetone before being heated to at 95 for 5 minutes and resuspended in 6M urea. The samples were then digested as follows: 2.6 μl id DTT was added to each 20μg sample and they were incubated at room temperature for 30 minutes. 2μl of 5.5mM iodacetamide was added and the sample was incubated at room temperature for a further 20 minutes. 0.2μg of LysC was added and incubated at room temperature for 3 hours. The samples were then diluted in 4 volumes of digestion buffer (50mM NH_4HCO_3) and 0.4 μg of trypsin were added and the samples were left over night at room temperature.

These samples were then analysed on an EasynLC-1000 chromatography system (Thermo) coupled to a Bruker Impact II Q-TOF mass spectrometer. Buffers A and B were 0.1% formic acid and 0.1% formic acid, 80% acetonitrile, respectively. Peptides were separated using a 165 min linear gradient of increasing Buffer B. The proteins were then quantified using the MaxQuant software version 1.5.5.1 and the output data was then processed with Perseus (Tyanova, Temu, Sinitcyn, *et al.,* 2016).

4.2.3.2 Volcano Plot Construction

Only proteins that were found in two out of three biological replicates were included in the fold change analysis in order for a p value to be calculated and LFQ values of 0 were excluded from the analysis. P values were calculated via a two tailed t-test. The fold change and p value were log2 and -log10 transformed respectively in R, which were then used to construct the volcano plots.

4.2.3.3 Gene Ontology (GO) term analysis

The gene names for all the proteins found to be up- or down-regulated by 2-fold or greater were uploaded to DAVID (Huang *et al.,* 2008; Huang *et al.,* 2009). The GO direct analysis for Biological Process and Molecular Function were downloaded. Bonferroni corrections were calculated by the DAVID software.

4.2.4 Animal work

4.2.4.1 Animals

The majority of the mice work was carried out by Abi Yates from the Department of Pharmacology at Oxford University. I assisted with the Day 0 and Day 21 behaviour analysis and the dissection of the mice and carried out the sectioning and staining of the tissues.

8.5-week-old male CD1 mice were purchased from Charles River and initial measurements of weight (g) and right hind limb circumference (cm) were recorded. Animals underwent preliminary strength tests, described below, and were arranged into 3

balanced groups. No significant differences between groups were observed in these tests when assessed using an ANOVA $p > 0.05$. In the control group, animals were treated with sterile saline (0.85% v/v). In the second group, animals were treated with EVs derived from A2780 cells. In the third group, animals were treated with EVs derived from A2780 cells that had been treated with cisplatin. The mice were randomly assigned numbers in order to blind the data analysis and the key was held only by the researcher who injected the mice. EVs were isolated by Size-Exclusion Chromatography 48 hours after treatment, concentration was determined using the ZetaView Nanoparticle Tracking Analyzer (ParticleMetrix, Germany) and normalised to $1x10^{10}$ particles/ml. Animals received 100µL of their respective injections intravenously every other day for 3 weeks. Weight was measured every 3 days and hind limb circumference was measured every week. Strength and motor tests were repeated after the 3 weeks were complete.

4.2.4.2 Behaviour

To evaluate any muscle wastage, the inverted screen and the weights test were performed as previously described (Deacon 2013). For the inverted screen, animals were placed in the centre of a $45cm^2$ square of wire mesh with 12mm squares of 1mm diameter. The screen was then inverted, and the time taken for the mouse to fall off onto a padded surface was recorded. Maximum experiment time was set at 60 seconds. For the weights test, 3 weights were used consisting of wired steel wool attached to a chain of 2, 3 and 4 links, corresponding to 33, 46 and 59g respectively. Animals were held at the base of the tail and lowered onto the lowest weight to allow grasping of the wired wool. Once forepaws had grasped the apparatus, the mouse was raised until the weight cleared the bench. If the weight was held for 3 or more seconds, the test was repeated with a larger weight. If after 3 attempts, with rest in between, the animal failed to hold the weight for the full 3 seconds, they were assigned the maximum weight achieved.

Weight lifting test

Screen hang test

Figure 4-3: Example images of behaviour tests. *The mice were assessed for functional strength using both the weight lifting test and the screen hang test. For the weight lifting test the mice were given three attempts to pick up progressively heavier weights if they succeeded in holding the weight for 3 seconds they were moved to the next weight. If they were unable to lift the weight after three attempts the maximum weight they could lift was recorded. In the screen hang test the mice were suspended upside-down for 60 seconds on a screen. If they were unable to hold onto the screen for 60 seconds, the time that they took to fall was recorded.*

4.2.4.3 TISSUE COLLECTION AND SECTIONING

Once behaviour tests were complete, mice were sacrificed via cardiac puncture then intracardially perfused with heparinised saline before being perfused with paraformaldehyde (PFA) (4% w/v, pH 7.4). Fixed liver, spleen and the right rear quadricep muscle were collected. Fixed tissue was left in PFA for 24 hours then they were cryoprotected with 30% w/v sucrose for a further 24 hours. Liver, Spleen and the muscle were mounted in optimal cutting temperature (OCT) compound. Transverse sections were taken from the belly of the muscle using a Leica CM1520 cryostat and then mounted onto slides and stored at -20°C.

4.2.4.4 ETHICS STATEMENT

Male CD-1 mice, X weeks of age, 32.6-41.5g, were housed under standard diurnal lighting conditions (12 hours) with ad libitum access to food and water. All procedures were carried out in accordance with the UK Animals (Scientific Procedures) Act, 1986 and licenced protocols were approved by local committees (LERP and ACER,

University of Oxford) and performed under licence number 30/3076. All efforts were made to adhere to the ARRIVE guidelines at all times.

4.2.5 STAINING

4.2.5.1 IMMUNOCYTOCHEMISTRY

C2C12 were grown in 96 well plates and treated as described. Cells were washed twice with PBS before being fixed in 3:1 methanol: acetic acid for 10 minutes at 4°C, washed once more in PBS and then stored in PBS at 4°C until staining. Cells were washed with PBS for three minutes with agitation then the PBS was removed and 100 µl of a 1% w/v BSA in PBS block solution was added to the well and incubated for 1 hour with agitation. An antibody cocktail was created for the primary antibodies against myosin heavy chain (MyHC, supplied by University of Iowa Developmental Studies Hybridoma Bank, gene MF20) and Ki67 (Abcam: ab15580) at a dilution of 1:500 and 1:2000 in 1% w/v BSA solution respectively. The block was removed from the cells and 100 µl of the antibody cocktail was added to each well and then incubated for 1 hr at room temperature. A secondary antibody cocktail was created for the secondary antibodies with Alexa Flour 488 anti-mouse (ThermoFisher A-11029) and tetramethylrhodamine (TRITC)-conjugated anti-rabbit (A16040) antibodies at a 1:1000 dilution in 1% w/v BSA solution. The primary antibody cocktail was removed, and the cells were wash 3 times with PBS for 5 minutes with agitation. 100 µl of the secondary antibody cocktail was added to each well and the cells were incubated for 30 minutes at room temperature in the dark. The secondary antibody cocktail was removed, and the nuclei were stained with 5 µl of 50 mg/ml Hoechst for 2 minutes before being washed three times in PBS for five minutes. The PBS was removed, and the fluorescence was measured using a plate reader. The following excitation/emission wavelengths were used: Hoechst (Nuclei) 360/460 nm, Alexa Fluor 488 (MyHC) 490/525

nm and TRITC (Ki67) 540/590 nm. The level of fluorescence for MyHC and Ki67 were normalised to Hoechst to control for cell number.

4.2.5.2 H&E STAINING

Slides were baked for 15 minutes then washed in PBS. Then they were stained with Haematoxylin for 4 minutes and washed thoroughly with water prior to being stained with Eosin for 30 seconds and being washed once again. The slides were then dehydrated using increasing concentrations of ethanol (1 x 85% v/v, 1 x 90% v/v, 2 x 100% v/v) and finally cleared with two five-minute washes in xylene and mounted with DPX permanent mounting medium. Photographs were taken on a GXM-L3201 LED microscope (GT Vision) using a GXCAM-FLUOMAX-S camera (GT Vision) and the GX Capture software (GT Vision). Fibre size was measured using the ImageJ image analysis software.

4.2.5.3 IMMUNOHISTOCHEMISTRY

The slides were baked in the oven at 37°C then washed in PBS. Cells were blocked with 1% v/v H_2O_2 in methanol for 10 minutes with agitation to block endogenous peroxidase activity. They were then washed twice with PBS and placed into sequenza clips and washed a further two times. The slides were then blocked with 120 µl of 1:20 avidin for 15 minutes and washed twice again in PBS. The slides were blocked with 120 µl of 1:20 biotin for 15 minutes and again washed twice with PBS. Slides were then blocked with 10% v/v serum in PBS for 1 hour to stop non-specific binding. Slides were the incubated overnight at 4°C with an anti-γH2AX antibody (Abcam: ab2893) diluted to 1:200 in 1% v/v serum in PBS. Slides were then washed 3 times with PBS before being incubated for 2 hours with the secondary antibody (vector laboratories: BA-1000) diluted 1:100 in 1% v/v serum in PBS. Slides were washed 3 times with PBS and then incubated in ABC mix (vector laboratories: VECTASTAIN® Elite® ABC-HRP Kit) for 1 hour at room temperature. Slides were washed 2 times in PBS and then placed into racks. The slides were washed in 0.1 M

phosphate buffer and then incubated with DAB until staining appeared. The slides were again washed with 0.1 M phosphate buffer and then counter stained with Haematoxylin as above. Photographs were taken on a GXM-L3201 LED microscope (GT Vision) using a GXCAM-FLUOMAX-S camera (GT Vision) and the GX Capture software (GT Vision).

4.3 RESULTS

4.3.1 EVS RELEASED DURING CHEMICAL STRESS ARE ALSO ABLE TO DRIVE THE BYSTANDER EFFECT

The bystander effect has been observed after many different stress conditions (Kadhim *et al.,* 2013; Purschke *et al.,* 2010; Asur *et al.,* 2009). Here I hypothesised that EVs from cisplatin treated cells would induce bystander damage in unstressed populations. In order to ascertain whether EVs were capable of inducing the bystander effect after chemical stress, EVs were extracted from cisplatin-treated cells and used to treat bystander cells. First, in order to demonstrate that cisplatin was able to damage cells A2780s were treated with increasing doses of cisplatin (0,10,20,40,100 μM) for three hours. The medium was then removed, the cells were washed with PBS and fresh medium was added to the cells. Two hours later the medium was removed, the cells were washed in PBS again and fresh medium was added. After 24 hours the cells were assayed for cell viability via the MTT assay Figure 4-4A. As the concentration of cisplatin increased the level of cell viability decreased. Cisplatin was therefore able to kill the A2780 cells. From these data the 40 μM concentration of cisplatin was chosen for future experiments.

Cells were treated with cisplatin as outlined above (A2780 cells: 40μM for 3 hours; HeLa cells: 40μM for 2 hours) and vesicles were extracted from the medium 24 hours post-treatment and were subsequently used to treat fresh cells. Vesicles from A2780 cells were used to treat A2780 cells and EVs from HeLa cells were used to treat HeLa cells. These cells were then assayed for cell viability with the MTT assay (Figure 4-4B) or harvested and assayed for DNA damage (Figure 4-4C). Treatment with EVs from cisplatin-treated cells reduced cell viability in A2780 cells and increased the levels of DNA damage observed in HeLa cells. This provides further evidence that the EVs released during stress are, at least

partly, responsible for the driving the damage in bystander cells, irrespective of the stress type.

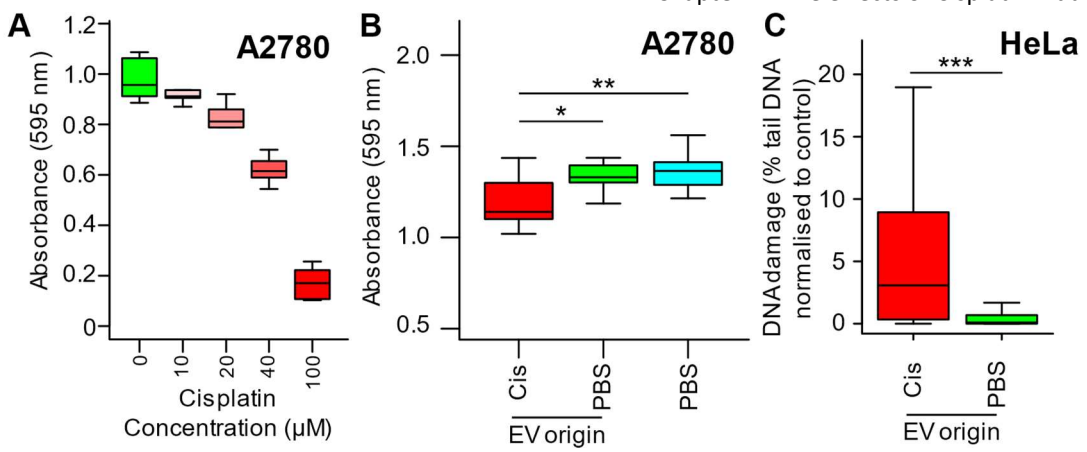

Figure 4-4: EVs released from cisplatin-treated cells are able to induce bystander damage.

*(**A**) A2780 cells were treated with increasing levels of cisplatin, after 24 hours the cell viability was estimated using the MTT assay. Then cells were treated with cisplatin (Red, 40μM for: A2780 3 hours; HeLa 2 hours) or control treated (green) and incubated for 24 hours. The medium was then removed from the cells, EVs were extracted and then used to treat bystander cells. The levels of cell viability (**B** – A2780s) and DNA damage (**C** – HeLa) in the bystander cells was assayed using the MTT assay or comet assay respectively. Box and whisker plots show median, upper and lower quartiles, error bars are 1.5x interquartile range; Differences were assessed with an ANOVA and post-hoc tukey test for MTT data and Mann-Whitney test for comet data, * p<0.05, ** p<0.01 and *** p<0.001. MTT data is from six wells of a 96 well plate (**A**) and ten wells of a 96 well plate (**B**). For comets at least 400 comets were scored across 2 biological replicates.*

4.3.2 EV EXTRACTION VIA SIZE EXCLUSION CHROMATOGRAPHY

Ultracentrifugation is the current gold standard for EV extraction, however the samples recovered from ultracentrifugation are not pure EVs and are often contaminated with proteins and other non-EV matter (Witwer *et al.,* 2013). Size-exclusion chromatography (SEC) allows the separation of molecules based on their size, with larger molecules being able to travel faster through the column than smaller molecules. In order to assess the ability of SEC to extract a pure sample of EVs from conditioned medium fractions 2, 4, 6-10, 12, 14, 16, 18 and 20 were assessed with NTA and the protein level of each fraction was assessed via the BCA assay. A2780s were cultured in EV-depleted medium for 24 hours before the medium was harvested, passed through the SEC column and twenty 500 µl fractions were collected. These fractions were assayed for EV and Protein content using NTA and BCA assay respectively, shown in Figure 4-5A. EVs were found in fractions 6-10, with the most appearing in fraction 7. There were also some particles detected in fractions 12, 16 and 20. Protein began to be seen in fraction 9, after

which the concentration increased until fraction 17. In order to confirm the identity of the particles found in fractions 6-8, EVs were isolated from cisplatin (40 μM) and PBS treated cells 72 hours after treatment using SEC and the proteins extracted and analysed with mass spectrometry. Gene Ontology (GO) term enrichment was carried out on the proteins found in these EVs. The top 10 most enriched cellular compartments from this analysis can be seen in Figure 4-5B. The top compartment enriched in the analysis was extracellular exosome, with the next two most highly enriched terms being cytosol and membrane. SEC was able to separate the majority of the EVs found in the conditioned medium from the protein in the medium. Whilst there was slight crossover of both EVs and protein, both were found at relatively low levels in these fractions. These data suggest that SEC is able to isolate a pure EV sample free from protein found within the cell conditioned medium.

A

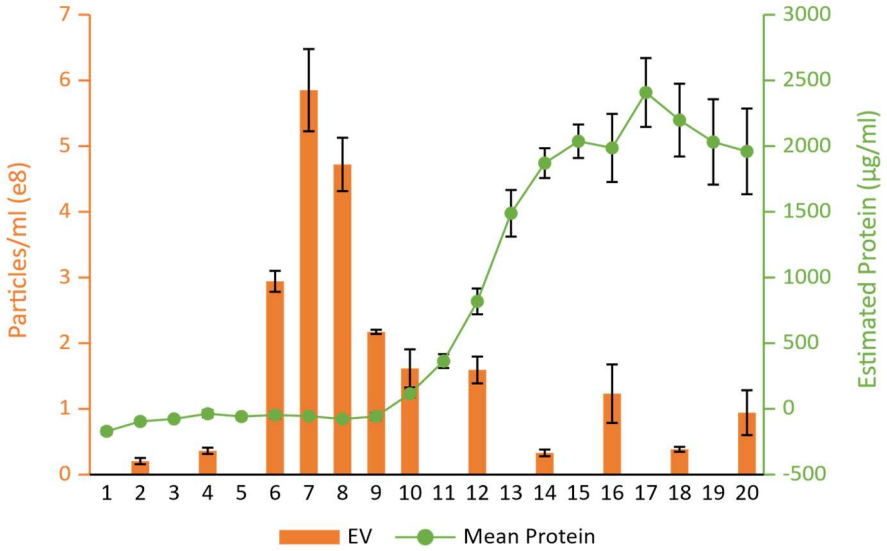

B

Cellular Comparetment	Fold Enrichment	PValue	Bonferroni
extracellular exosome	2.782	5.860E-186	5.310E-183
cytosol	2.352	5.503E-139	4.986E-136
membrane	2.553	3.297E-107	2.987E-104
nucleoplasm	2.108	1.812E-77	1.642E-74
focal adhesion	4.363	2.051E-63	1.858E-60
cell-cell adherens junction	4.560	1.886E-57	1.709E-54
cytoplasm	1.597	9.680E-57	8.770E-54
myelin sheath	6.064	1.797E-48	1.628E-45
extracellular matrix	4.188	9.146E-44	8.286E-41
intracellular ribonucleoprotein complex	5.687	4.018E-38	3.640E-35

Figure 4-5: Size Exclusion Chromatography allows EVs to be extracted from conditioned medium separate from the free protein found in the medium. *EVs were extracted from medium conditioned by A2780 cells using sepharose columns as outlined above. Twenty fractions of 500 µl were collected. (**A**) The fractions were analysed for EV content (orange) via NTA and their protein content (Green) via BCA assay. Data is from 3 biological replicates. Bars and scatter plot show the mean value for EV and protein concentration respectively, error bars are standard error of the mean. (**B**) The top ten cellular compartments associated with the proteins extracted from SEC EVs. The proteins associated with SEC isolated EVs were identified by mass spectrometry and a GO term enrichment analysis was carried out. Fold enrichment is the number of genes annotated with that term divided by the number of genes expected by the software to be annotated with that term.*

4.3.3 Proteins were identified in ovarian cancer cells and their EVs with and without cisplatin treatment

When cells undergo stress, numerous proteins are deregulated within the cells to attempt to combat it. Stress is also known to alter the cargo of EVs, and these changes can be linked with their function (Xu *et al.,* 2014; Xu *et al.,* 2015). Here the proteins were extracted from cells and EVs 72 hours after cisplatin or PBS treatment and the proteins were identified using mass spectrometry. The total number of proteins found in cisplatin and PBS treated cells and EVs are found in Figure 4-6(A, D), and the total number of proteins found in each of the three replicates for each treatment group is shown in Figure 4-6(C, F). The proteins found in two or more replicates of each treatment group are shown in Figure 4-6(B, E). For non-overlapping proteins in these Venn diagrams, a read was only counted if it was found in two or more replicates of one treatment group and none of the replicates for the other treatment group. Many of the identified proteins were found in both of the two treatment groups in EVs and Cells, however there are also proteins that were observed in only one group or the other. Cisplatin treatment alters the protein content of cells and cargo of EVs. The average LFQ for each sample grouping (Cis cell, PBS cell, Cis EV, PBS EV) were plotted against one another in Figure 4-6G. There appears to be no pattern in the protein levels between cisplatin and PBS treated cells, between the EVs from those cells or between the proteins in EVs and the protein in their parent cells.

Whilst the majority of the cellular proteins were observed in all three replicates most of the EV protein was only found in one replicate, with 683 cisplatin EV proteins out of 1,317 occurring in only one replicate and 629 PBS EV proteins out of 1165 occurring in only one replicate. This suggests that the protein cargo of EVs is heterologous, with relatively few common proteins compared to cells.

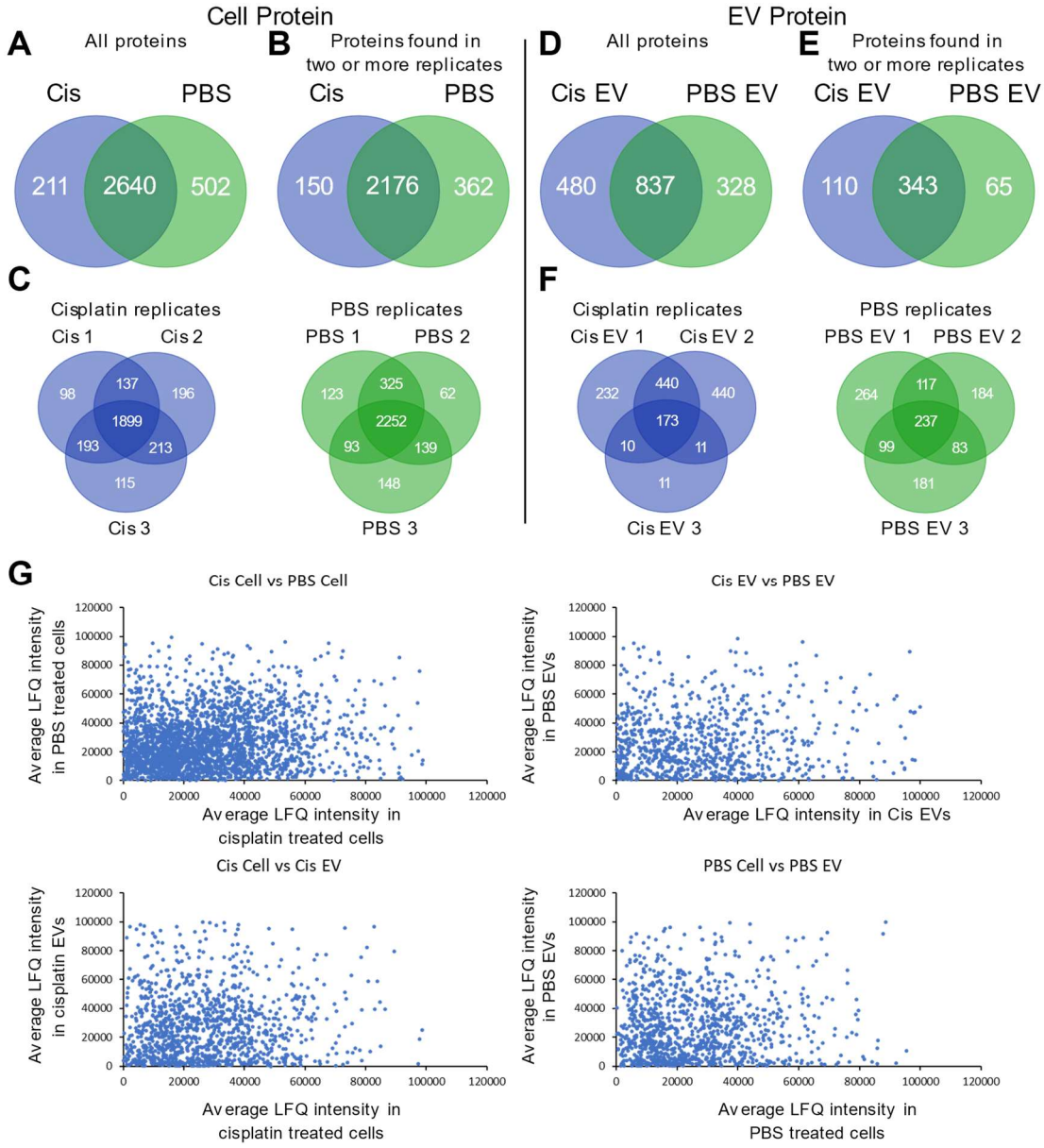

Figure 4-6: Proteins identified in A2780 cells and EVs after cisplatin and PBS treatment. *A2780 cells were treated with 40 µM cisplatin (blue) or an equivalent volume of PBS (green) for three hours, washed in fresh medium for 2 hours and then incubated in EV-depleted medium for 72 hours. At this time EVs were extracted from the medium using SEC and the proteins were extracted from both cells and EVs. The proteins were then identified using LC-MS.* ***A, D)*** *All the proteins found in at least one of the replicates in cisplatin or PBS treated cells.* ***B, E)*** *Proteins found in at least two of the replicates cisplatin or PBS treated groups. For non-overlapping proteins, a read was only counted if it was found in two or more replicates of one treatment group and none of the replicates for the other treatment group.* ***C, F)*** *All the proteins for each replicate in each treatment group.* ***G)*** *shows the relative LFQ intensity in the different treatment groups.*

4.3.4 Protein deregulation in cisplatin-treated cells identified by mass spectrometry

I hypothesised that the proteome of stress derived vesicles might be involved in the induction of bystander effects. To assess what changes occur in the proteome of cisplatin-treated A2780s, protein was extracted from cisplatin and PBS treated cells. The proteins within each population of cells was then identified and quantified via mass spectrometry. The fold change following cisplatin treatment and p value for this change was calculated for each protein. Figure 4-7A show a volcano plot of the identified proteins, proteins in orange have a 2-fold change either up or down, proteins in red had a p value of less than 0.05 and proteins in green had both. 497 proteins were shown to have increased expression following cisplatin treatment whilst 464 proteins decreased. Out of these proteins only 56 proteins that were upregulated had a p value of less than 0.05 and 44 down regulated proteins had a p value of less than 0.05. 1215 proteins were found to have a fold change in intensity less than 2-fold, with only 13 of these proteins having a p value of less than 0.05. The 10 most highly significanly up- and down-regulated proteins are shown in Figure 4-7B. Over 4.5% of the proteins identified via LC-MS were significantly deregulated in A2780s following treatment with cisplatin.

A

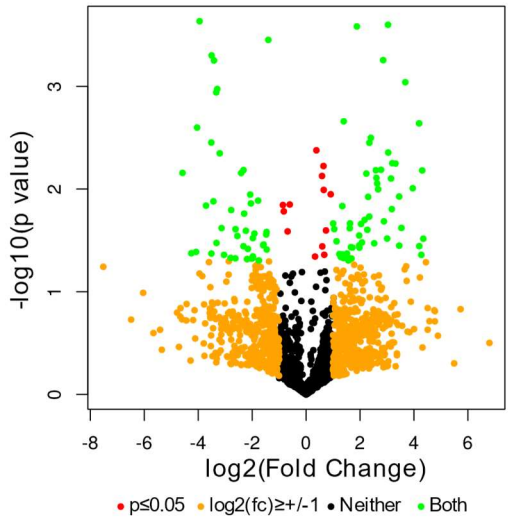

B

Top 10 Down Regulated Proteins			
Gene names	Fold Change	P value	Bonferroni
TEX1	0.06	2.32E-04	4.64E-03
DIS3	0.38	3.53E-04	7.05E-03
SLC25A4	0.09	5.00E-04	1.00E-02
PPCS	0.09	5.59E-04	1.12E-02
ALDH7A1	0.10	1.06E-03	2.12E-02
AK4	0.10	1.14E-03	2.29E-02
MESDC2	0.06	2.52E-03	5.04E-02
DUSP12	0.09	3.52E-03	7.05E-02
SIDT2	0.11	4.49E-03	8.98E-02
LRRC57	0.20	6.53E-03	1.31E-01

Top 10 Up Regulated Proteins			
Gene names	Fold Change	P Value	Bonferroni
SRI	8.21	2.51E-04	5.03E-03
GCN1L1	3.69	2.61E-04	5.22E-03
RAP1GDS1	7.25	5.56E-04	1.11E-02
PRKAR1A	12.81	9.12E-04	1.82E-02
MYO1C	2.63	2.19E-03	4.39E-02
PIK3R4	18.27	2.29E-03	4.59E-02
CUL1	5.29	3.17E-03	6.35E-02
S1A13	5.08	3.54E-03	7.09E-02
SIRT3	1.30	4.20E-03	8.39E-02
BANF1	8.26	4.41E-03	8.82E-02

Figure 4-7: Protein deregulation in cells following cisplatin treatment. *Protein was extracted from cells 3 days after treatment with either 40 μM cisplatin or PBS. The identities of the proteins present in the cells was determined using mass spectrometry. Three biological replicates of each treatment group were assayed. Proteins that did not appear in at least two of the three samples for each treatment were excluded from this analysis. The mean fold change of each protein was calculated and the means of the two samples were compared with a two tailed t-test.* ***A)*** *is a volcano plot showing the log2 of fold change of each protein against -log10 of the p value resulting from the t-test. Proteins with a fold change <= 0.5 or >= 2 are coloured orange, proteins with a p value of < 0.05 are coloured red and proteins that have both are coloured green. The gene names for the top ten most significantly down- and up-regulated proteins are shown in* ***B*** *with fold change, p value and a Bonferroni corrected p value. The Bonferroni value was calculated by multiplying the p value with the number of proteins in the two tables (20).*

4.3.5 GO Term Analysis of proteins deregulated in cells following cisplatin treatment

In order to determine what biological processes might have been altered within the cells, GO term analysis was carried out using DAVID. The gene names of the proteins found to increase or decrease by 2-fold or greater were uploaded to the DAVID analysis tool and the GO terms for biological processes and molecular functions were found. The top ten most highly significant GO terms are shown in Table 4-1‘poly(A) RNA binding’ respectively, whilst in the down regulated proteins the ‘viral transcription’ was the most significantly enriched term for biological process. The most significantly enriched term for molecule function was again ‘poly(A) RNA binding’ as in the upregulated proteins. KEGG pathway analysis was also carried out for these proteins and can be seen in Table 4-2. For all

significant Go terms see Appendix 7.1 & 7.2. These data suggest specific pathways that may become deregulated within cells following cisplatin treatment.

Down Regulated

Biological Function	Fold Enrichment	P Value	Bonferroni
viral transcription	7.73	1.61E-13	3.15E-10
mRNA splicing, via spliceosome	5.09	1.28E-12	2.51E-09
translational initiation	6.60	1.46E-12	2.85E-09
nuclear-transcribed mRNA catabolic process, nonsense-mediated decay	6.64	4.19E-11	8.18E-08
translation	4.17	8.22E-10	1.61E-06
viral process	3.65	7.61E-09	1.49E-05
protein folding	4.60	1.33E-08	2.60E-05
SRP-dependent cotranslational protein targeting to membrane	6.41	2.42E-08	4.73E-05
mRNA export from nucleus	6.02	5.70E-08	1.11E-04
rRNA processing	4.05	6.08E-08	1.19E-04
Molecular Function	**Fold Enrichment**	**P Value**	**Bonferroni**
poly(A) RNA binding	4.13	1.29E-44	9.10E-42
protein binding	1.39	6.95E-20	4.88E-17
RNA binding	3.65	4.87E-16	3.12E-13
structural constituent of ribosome	3.67	6.53E-07	4.59E-04
nucleotide binding	2.87	2.95E-06	2.07E-03
Ran GTPase binding	9.87	1.17E-05	8.22E-03
protein domain specific binding	3.38	1.40E-05	9.82E-03
protein transporter activity	5.66	2.20E-05	1.54E-02
unfolded protein binding	4.38	4.10E-05	2.84E-02
cadherin binding involved in cell-cell adhesion	2.81	4.18E-05	2.90E-02

Up Regulated

Biological Function	Fold Enrichment	P Value	Bonferroni
regulation of mRNA stability	6.84	7.55E-11	1.52E-07
cell-cell adhesion	4.03	1.92E-10	3.88E-07
mRNA splicing, via spliceosome	4.28	9.49E-10	1.92E-06
SRP-dependent cotranslational protein targeting to membrane	6.74	1.05E-09	2.11E-06
NIK/NF-kappaB signaling	8.00	3.59E-09	7.25E-06
translational initiation	5.14	1.11E-08	2.24E-05
regulation of cellular amino acid metabolic process	8.97	1.36E-08	2.75E-05
ER to Golgi vesicle-mediated transport	4.40	1.41E-07	2.85E-04
rRNA processing	3.78	1.96E-07	3.96E-04
nuclear-transcribed mRNA catabolic process, nonsense-mediated decay	5.03	2.49E-07	5.02E-04
Molecular Function	**Fold Enrichment**	**P Value**	**Bonferroni**
poly(A) RNA binding	3.93	3.93E-42	2.61E-39
protein binding	1.38	5.11E-19	3.40E-16
RNA binding	3.35	6.24E-14	4.15E-11
cadherin binding involved in cell-cell adhesion	4.01	4.98E-11	3.31E-08
structural constituent of ribosome	3.81	8.83E-08	5.87E-05
nucleotide binding	2.84	2.38E-06	1.58E-03
mRNA binding	4.23	1.22E-05	8.09E-03
threonine-type endopeptidase activity	11.75	1.89E-05	1.25E-02
ATP binding	1.63	6.19E-05	4.03E-02
tRNA binding	6.22	8.51E-05	5.50E-02

Table 4-1: GO term analysis of deregulated cellular protein following cisplatin treatment. *All the cellular proteins that were up- or down-regulated by 2-fold or greater following cisplatin treatment were analysed using the DAVID tool and the GO terms from Biological Function and Molecular Function were recorded. P value represents EASE score. Only the top ten GO terms found are shown. Fold enrichment is the number of genes annotated with that term divided by the number of genes expected by the software to be annotated with that term.*

Upregulated proteins				
Term	**Count**	**Genes**	**PValue**	**Bonferroni**
hsa03050:Proteasome	12	PSMA2, PSMB5, PSMB4, PSMB7, PSMA6, PSMB1, PSMD11, PSME2, PSMD3, PSME3, PSMA7, PSMD8	6.68E-07	1.54E-04
hsa03010:Ribosome	18	RPL35A, RPL17, RPS9, RPL23A, RPS4X, MRPL23, RPS19, MRPL28, RPL13A, RPS14, RPL34, MRPL17, MRPL16, RPS15, RPL3, RPL5, RPS11, RPS21	2.04E-05	4.69E-03
hsa01130:Biosynthesis of antibiotics	22	LDHB, DLST, ACO2, CYP51A1, ACO1, SUCLG2, PGD, PSPH, ALDH3A2, GPI, NME2, TPI1, GOT1, NME1-NME2, ADSL, IDI1, BPNT1, PAICS, MDH2, HSD17B7, UGP2, ALDH9A1	7.84E-05	1.79E-02
hsa03040:Spliceosome	16	TRA2B, SNRPD3, DDX39B, ALYREF, SNRPD1, WBP11, HSPA1A, SF3B5, SART1, HNRNPA3, SRSF2, DDX23, PRPF8, PQBP1, LSM4, LSM3	2.05E-04	4.60E-02
Downregulated proteins				
Term	**Count**	**Genes**	**PValue**	**Bonferroni**
hsa03013:RNA transport	26	XPO1, PABPC4, NUP93, NUP188, PNN, NDC1, EIF3D, EIF3A, RAE1, EIF1AX, EIF1AY, RANBP2, PABPC1, TPR, GEMIN6, EIF2B4, XPOT, UPF1, EIF2S3, RNPS1, NXF1, NUP155, EIF4A3, AAAS, UPF3B, CYFIP1	8.27E-09	1.72E-06
hsa01130:Biosynthesis of antibiotics	27	BCAT2, ADPGK, HK1, ASL, PKM, ISYNA1, AKR1A1, IDH2, PDHA1, SUCLA2, HADH, SHMT2, SUCLG1, AK3, FDPS, AK4, PFKM, PCK2, IDH3A, SDHA, ALDH7A1, G6PD, GFPT1, PCYOX1, PSAT1, CBS, PRPS1	1.45E-07	3.02E-05
hsa03015:mRNA surveillance pathway	16	PABPN1, SYMPK, UPF1, PABPC4, RNPS1, NXF1, PPP1CC, ETF1, PPP1CB, PNN, DAZAP1, EIF4A3, UPF3B, CPSF7, PABPC1, CSTF1	1.77E-06	3.68E-04
hsa03010:Ribosome	19	MRPS14, RPL14, RPL13, MRPL9, RPL38, RPL28, RPS7, MRPL11, RPS25, MRPL13, RPS27, RPS28, RPS17, RPL9, RPL8, RPL3, RPS13, RPL7A, RPS24	4.40E-06	9.16E-04
hsa01200:Carbon metabolism	15	SHMT2, ADPGK, SUCLG1, ESD, HK1, PFKM, IDH3A, PKM, SDHA, G6PD, IDH2, PDHA1, SUCLA2, PSAT1, PRPS1	1.08E-04	2.23E-02
hsa03040:Spliceosome	16	BCAS2, SNRPB2, SNW1, DDX5, SF3B4, CTNNBL1, HNRNPA3, PRPF19, EIF4A3, HNRNPM, SRSF5, DDX46, SRSF6, DHX16, HNRNPC, SNRPF	1.81E-04	3.70E-02

Table 4-2: KEGG pathway analysis of deregulated cellular protein following cisplatin treatment. *The KEGG pathways of the proteins analysed in Table 4-1 were also found. Only the pathways with a p values of under 0.05 after Bonferroni correction are shown above.*

4.3.6 Protein deregulation in EVs released from cisplatin-treated cells

The cargo of EVs can change due to the conditions within their parent cells, such as stress and disease, and are able to influence their function (Xu *et al.,* 2015; Yentrapalli *et al.,* 2017; Melo *et al.,* 2015; Jelonek *et al.,* 2015). In order to see what changes occur in the protein complement of EVs from cisplatin-treated cells EVs were extracted from cisplatin and PBS treated cells 72 hours post treatment in order to ensure sufficient release of EV cargo. The proteins were extracted from these EVs and then identified and quantified via mass spectrometry. The fold change following cisplatin treatment and p value of this change was calculated for each protein. Figure 4-8A shows a volcano plot of the identified proteins, proteins in orange have a 2-fold change either up or down, proteins in red had a p value of less than 0.05 and proteins in green had both. 65 proteins were shown to have increased expression in EVs following cisplatin treatment whilst 46 proteins decreased. Out of these proteins 0 proteins that were upregulated had a p value of less than 0.05 whilst 4 down regulated proteins had a p value of less than 0.05. 232 proteins were found to have changed in intensity by less than 2-fold fold in cisplatin EVs and 7 of these had a p value of below 0.05. The 10 most highly significanly up- and down-regulated proteins are shown in Figure 4-8B. Fewer proteins were identified in the EV protein samples than were observed in the cell protein and far fewer were significantly different betweent the cisplatin and PBS treatment groups.

A

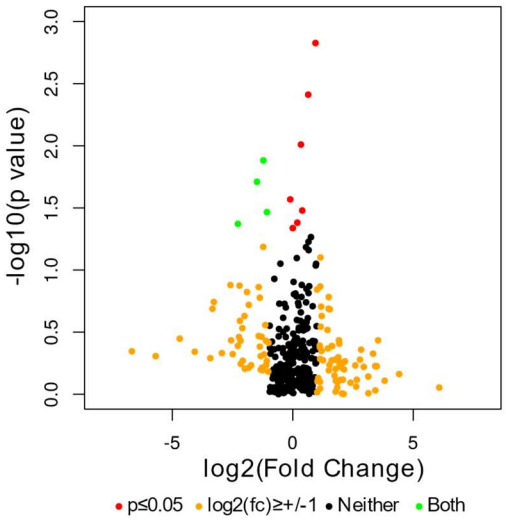

B

Top 10 Down Regulated Proteins			
Gene names	Fold Change	P value	Bonferroni
PDIA3	0.43	1.31E-02	2.63E-01
HIST1H4A	0.36	1.95E-02	3.90E-01
CKMT1A, CKMT1B	0.48	3.42E-02	6.84E-01
UBE2M	0.21	4.25E-02	8.50E-01
COX7A2	0.43	6.51E-02	1.30E+00
IARS	0.17	1.32E-01	2.64E+00
SEC61A1	0.22	1.34E-01	2.67E+00
OLA1	0.38	1.37E-01	2.75E+00
EEF1E1, EEF1E1-BLOC1S5	0.27	1.51E-01	3.01E+00
UBA1	0.39	1.67E-01	3.34E+00

Top 10 Up Regulated Proteins			
Gene names	Fold Change	P value	Bonferroni
NPEPPS	2.22	7.93E-02	1.59E+00
PSMB1	2.20	1.36E-01	2.72E+00
RPL11	2.01	1.44E-01	2.87E+00
MFGE8	2.81	1.65E-01	3.30E+00
ITGB1	2.26	1.97E-01	3.95E+00
RUVBL1	2.80	2.05E-01	4.10E+00
PTGFRN	2.90	2.07E-01	4.14E+00
HSPB1	2.30	2.35E-01	4.69E+00
SRRM2	2.23	2.86E-01	5.72E+00
DNAJA1	2.72	3.03E-01	6.07E+00

Figure 4-8: Protein deregulation in EVs from cisplatin-treated cells. *EVs were extracted from cells 3 days after treatment with 40 μM cisplatin or PBS and the protein cargo of these EVs was then extracted. The identities of the proteins present in the EVs were estimated using mass spectrometry. Three biological replicates of each treatment group were assayed. Proteins that did not appear in at least two of the three samples for each treatment were excluded from this analysis. The mean fold change of each protein was calculated and the means of the two samples were compared with a two tailed t-test.* ***A)*** *is a volcano plot showing the log2 of fold change of each protein against -log10 of the p value resulting from the t-test. Proteins with a fold change <= 0.5 or >= 2 are coloured orange, proteins with a p value of <= 0.05 are coloured red and proteins that have both are coloured green.* ***B)*** *shows the gene names for the top ten most significantly down- and up- regulated proteins with fold change, p value and a Bonferroni corrected p value. The Bonferroni values were calculated by multiplying the p value with the number of proteins in the two tables (20).*

4.3.7 GO Term Analysis of proteins deregulated in EVs released from cells following cisplatin treatment

In order to find what processes might be targeted by the protein cargo of EVs from cisplatin-treated cells, GO term analysis was carried out using DAVID on the deregulated EV proteins. The gene names of the proteins found to increase or decrease by 2-fold or greater were uploaded to the DAVID analysis tool and the GO terms for biological processes and molecular functions were found. The top ten most highly significant GO terms are shown in Table 4-3 As with the cellular protein the most significantly enriched term for molecular function is 'poly(A) RNA binding' in both the up- and down regulated proteins. The most significantly enriched term for biological processes are 'regulation of mRNA stability' and 'SRP-dependant cotranslational protein targeting to membrane' in the up- and down regulated proteins respectively. There were fewer GO terms found for the EV protein than were observed for the cell protein and the significance of these enrichments were lower with the EV proteins. KEGG pathway analysis found no terms were found to be significantly enriched in these proteins. For all significant Go terms see Appendix 7.3 & 7.4. This would suggest a more specialised role for these EVs, are their protein cargo is associated with fewer different pathways, than the cellular protein.

Down Regulated

Biological Function	Fold Enrichment	P Value	Bonferroni
SRP-dependent cotranslational protein targeting to membrane	19.85	1.05E-04	3.41E-02
viral transcription	16.66	2.07E-04	6.59E-02
rRNA processing	8.72	2.34E-03	5.37E-01
nuclear-transcribed mRNA catabolic process, Nonsense-mediated decay	12.54	3.72E-03	7.07E-01
cell-cell adhesion	6.88	5.43E-03	8.33E-01
translational initiation	10.90	5.51E-03	8.38E-01
IRES-dependent viral translational initiation	106.62	1.82E-02	9.98E-01
positive regulation of protein localization to Cajal body	93.29	2.08E-02	9.99E-01
positive regulation of establishment of protein localization To telomere	82.92	2.33E-02	1.00E+00
translation	5.90	2.84E-02	1.00E+00
Molecular Function	**Fold Enrichment**	**P Value**	**Bonferroni**
poly(A) RNA binding	5.65	1.01E-08	1.23E-06
ATP binding	3.01	1.25E-03	1.42E-01
GTPase binding	43.28	2.07E-03	2.24E-01
mRNA binding	12.00	4.21E-03	4.02E-01
cadherin binding involved in cell-cell adhesion	6.47	6.75E-03	5.62E-01
protein binding	1.37	1.00E-02	7.07E-01
transferase activity, transferring phosphorus-containing groups	150.05	1.30E-02	7.97E-01
RNA binding	4.11	1.34E-02	8.08E-01
creatine kinase activity	125.04	1.55E-02	8.52E-01
structural constituent of ribosome	6.76	2.00E-02	9.15E-01

Up Regulated

Biological Function	Fold Enrichment	P Value	Bonferroni
regulation of mRNA stability	20.07	1.24E-07	6.69E-05
cell-cell adhesion	8.58	8.40E-06	4.53E-03
translational initiation	13.20	1.34E-05	7.23E-03
nuclear-transcribed mRNA catabolic process, Nonsense-mediated decay	13.03	8.97E-05	4.73E-02
viral process	6.91	1.38E-04	7.18E-02
translation	7.15	3.98E-04	1.93E-01
purine nucleotide biosynthetic process	64.58	9.21E-04	3.92E-01
regulation of cellular amino acid metabolic process	20.26	9.65E-04	4.06E-01
positive regulation of telomerase RNA localization to Cajal body	51.67	1.45E-03	5.44E-01
antigen processing and presentation of exogenous peptide Antigen via MHC class I, TAP-dependent	16.40	1.78E-03	6.18E-01
Molecular Function	**Fold Enrichment**	**P Value**	**Bonferroni**
poly(A) RNA binding	6.44	1.10E-15	2.25E-13
cadherin binding involved in cell-cell adhesion	10.75	1.06E-08	2.14E-06
RNA binding	6.17	8.39E-07	1.70E-04
protein binding	1.51	1.45E-05	2.95E-03
ATP binding	3.13	2.85E-05	5.76E-03
ATPase activity	8.52	6.44E-04	1.23E-01
integrin binding	9.89	7.40E-03	7.79E-01
unfolded protein binding	9.44	8.41E-03	8.20E-01
structural constituent of ribosome	5.85	1.00E-02	8.70E-01
mRNA binding	8.31	1.19E-02	9.12E-01

Table 4-3: GO term analysis of EV protein deregulated following cisplatin treatment. *All the proteins that were up- or down-regulated by 2-fold or greater within the EVs were analysed using the DAVID tool and the GO terms from Biological Function and Molecular Function were recorded. P value represents EASE score. The top ten most significantly enriched GO terms are shown. Fold enrichment is the number of genes annotated with that term divided by the number of genes expected by the software to be annotated with that term.*

4.3.8 GO TERM ANALYSIS OF CELL PROTEINS ONLY FOUND WITH OR WITHOUT CISPLATIN TREATMENT

Numerous proteins were only found in either PBS or cisplatin-treated cells. In order to ascertain the functions these molecules might play in these cells the GO terms for the proteins that only occurred in one treatment group were found using DAVID as before. Only proteins that were found in 2 or more replicates were analysed. The top ten most significantly enriched GO terms can be seen in Table 4-4There were 362 proteins uniquely identified in PBS treated cells, whilst 150 were found in cisplatin-treated cells. The proteins only found in the PBS treated cells were linked to 86 biological process and 52 molecular functions whilst 29 biological processes and 9 molecular functions were identified linked to the proteins only found in cisplatin-treated cells. The majority of the GO terms associated with these proteins were not significantly enriched following a Bonferroni correction. Only the molecular function terms ‘protein binding’ and ‘poly(A) RNA binding’ were significantly enriched in the list of proteins only found in PBS treated cells. KEGG pathway analysis found only one significantly upregulated pathway, endocytosis, which was enriched in both sets of proteins. For all significant Go terms see Appendix 7.5. This suggests that the proteins only found in cells from one treatment group are not involved in specific pathways within these cells.involved in specific pathways within these cells.

GO terms for proteins in cisplatin-treated cells only

Biological Function	Fold Enrichment	P Value	Bonferroni
glutathione metabolic process	10.71	1.18E-03	6.48E-01
cell-cell adhesion	3.98	1.89E-03	8.12E-01
cellular response to nerve growth factor stimulus	15.48	2.11E-03	8.44E-01
G2/M transition of mitotic cell cycle	5.25	5.69E-03	9.93E-01
glutathione biosynthetic process	22.49	7.57E-03	9.99E-01
positive regulation of myoblast fusion	21.17	8.53E-03	9.99E-01
leukotriene biosynthetic process	17.99	1.17E-02	1.00E+00
translation	3.32	1.88E-02	1.00E+00
endocytosis	4.31	2.86E-02	1.00E+00
positive regulation of dopaminergic neuron differentiation	59.97	3.27E-02	1.00E+00
Molecular Function	**Fold Enrichment**	**P Value**	**Bonferroni**
protein binding	1.29	1.93E-04	5.35E-02
glutathione hydrolase activity	57.81	1.07E-03	2.64E-01
structural constituent of ribosome	4.17	3.09E-03	5.86E-01
gamma-glutamyltransferase activity	34.69	3.15E-03	5.93E-01
cadherin binding involved in cell-cell adhesion	3.19	1.27E-02	9.74E-01
structural constituent of cytoskeleton	5.26	1.50E-02	9.86E-01
2 iron, 2 sulfur cluster binding	13.87	1.93E-02	9.96E-01
transferrin receptor binding	28.91	6.67E-02	1.00E+00
oxidoreductase activity	2.89	9.39E-02	1.00E+00

GO terms for proteins in PBS treated cells only

Biological Function	Fold Enrichment	P Value	Bonferroni
nucleosome disassembly	14.88	2.88E-04	3.69E-01
protein transport	2.30	2.25E-03	9.73E-01
snRNA transcription from RNA polymerase II promoter	5.06	2.55E-03	9.83E-01
regulation of endocytosis	8.16	3.06E-03	9.93E-01
multivesicular body assembly	8.16	3.06E-03	9.93E-01
protein folding	3.09	3.08E-03	9.93E-01
mitotic nuclear division	2.65	3.87E-03	9.98E-01
autophagy	3.42	4.88E-03	1.00E+00
viral budding via host ESCRT complex	9.20	8.85E-03	1.00E+00
endosomal transport	4.60	9.67E-03	1.00E+00
Molecular Function	**Fold Enrichment**	**P Value**	**Bonferroni**
protein binding	1.31	6.77E-10	3.47E-07
poly(A) RNA binding	2.20	1.82E-07	9.29E-05
translation initiation factor activity	5.60	1.50E-03	5.37E-01
2 iron, 2 sulfur cluster binding	9.76	1.54E-03	5.47E-01
core promoter proximal region sequence-specific DNA binding	8.87	9.77E-03	9.93E-01
RNA polymerase II distal enhancer sequence-specific DNA binding	4.50	1.05E-02	9.96E-01
transcription coactivator activity	2.36	1.33E-02	9.99E-01
adenyl-nucleotide exchange factor activity	14.64	1.68E-02	1.00E+00
nucleoside kinase activity	14.64	1.68E-02	1.00E+00
m7G(5')pppN diphosphatase activity	13.31	2.03E-02	1.00E+00

Table 4-4: GO term analysis of cell protein found only in one treatment group.

All the proteins that were only found in one treatment group were analysed using the DAVID tool and the GO terms from Biological Function and Molecular Function were recorded. P value represents EASE score. The top ten most significantly enriched GO terms are shown. Fold enrichment is the number of genes annotated with that term divided by the number of genes expected by the software to be annotated with that term.

4.3.9 GO TERM ANALYSIS OF EV PROTEINS ONLY FOUND WITH OR WITHOUT CISPLATIN TREATMENT

As with the cellular proteins, some proteins were only found in EVs from either PBS or cisplatin-treated cells. Once again, the GO terms related to these proteins were found using DAVID. Only proteins that were found in 2 or more replicates were analysed. The top ten most significantly enriched GO terms can be seen in Table 4-5There were 110 proteins uniquely identified in EVs from PBS treated cells, whilst 110 were found in EVs from cisplatin-treated cells. The proteins only found in the control EVs were linked to 16 biological process and 8 molecular functions whilst 45 biological processes and 18 molecular functions were identified linked to the proteins only found in EVs released from cisplatin-treated cells. Only 5 of the GO terms were significantly enriched following a Bonferroni adjustment. The biological process terms ‘nuclear-transcribed mRNA catabolic process, nonsense-mediated decay’, ‘translational initiation’ and ‘SRP-dependant cotranslational protein targeting to membrane’ were significantly enriched in the proteins found only in cisplatin EVs, as were the molecular function terms ‘poly(A) RNA binding’ and ‘RNA binding’. No terms were significantly enriched in the proteins only found in the PBS EVs. Interestingly ‘SRP-dependant cotranslational protein targeting to membrane’ was the only significantly enriched term in the proteins down regulated in EVs following cisplatin treatment. KEGG pathway analysis found that VEGF signalling pathway was significantly enriched in the proteins only seen in EVs from cisplatin-treated cells. For all significant Go terms see Appendix 7.6. This suggests that this function may be both up and down regulated following cisplatin treatment.

GO terms for protein found in cisplatin EVs only

Biological Function	Fold Enrichment	P Value	Bonferroni
nuclear-transcribed mRNA catabolic process, nonsense-mediated decay	10.55	1.03E-05	7.53E-03
translational initiation	9.16	2.57E-05	1.87E-02
SRP-dependent cotranslational protein targeting to membrane	11.69	2.85E-05	2.08E-02
mRNA splicing, via spliceosome	6.36	8.17E-05	5.84E-02
rRNA processing	5.87	4.15E-04	2.64E-01
actin filament polymerization	24.14	5.72E-04	3.44E-01
viral transcription	8.41	7.16E-04	4.10E-01
translation	4.96	1.11E-03	5.60E-01
movement of cell or subcellular component	9.12	2.14E-03	7.94E-01
positive regulation of lamellipodium assembly	29.43	4.47E-03	9.63E-01
Molecular Function	**Fold Enrichment**	**P Value**	**Bonferroni**
poly(A) RNA binding	4.09	1.53E-10	3.69E-08
RNA binding	4.37	7.28E-06	1.76E-03
protein binding	1.32	4.13E-04	9.51E-02
ATP-dependent RNA helicase activity	12.25	7.15E-04	1.59E-01
structural constituent of ribosome	5.02	2.64E-03	4.72E-01
GTP binding	3.73	2.73E-03	4.84E-01
RNA helicase activity	36.75	2.86E-03	5.00E-01
GTPase activity	4.76	3.42E-03	5.64E-01
nucleotide binding	3.66	6.04E-03	7.69E-01
magnesium ion binding	4.68	8.94E-03	8.86E-01

GO terms for protein found in PBS EVs only

Biological Function	Fold Enrichment	P Value	Bonferroni
cell proliferation	4.44	1.05E-02	9.81E-01
endodermal cell fate commitment	90.28	2.16E-02	1.00E+00
negative regulation of single stranded viral RNA replication via double stranded DNA intermediumte	77.38	2.52E-02	1.00E+00
DNA cytosine deamination	77.38	2.52E-02	1.00E+00
positive regulation by host of viral genome replication	67.71	2.87E-02	1.00E+00
negative regulation of transposition	67.71	2.87E-02	1.00E+00
histone H2B ubiquitination	67.71	2.87E-02	1.00E+00
histone monoubiquitination	49.24	3.93E-02	1.00E+00
mRNA splicing, via spliceosome	4.88	4.69E-02	1.00E+00
positive regulation of receptor recycling	38.69	4.97E-02	1.00E+00
Molecular Function	**Fold Enrichment**	**P Value**	**Bonferroni**
protein binding	1.41	5.34E-04	7.31E-02
poly(A) RNA binding	3.04	8.38E-04	1.12E-01
hydrolase activity, acting on carbon-nitrogen (but not peptide) bonds, in cyclic amidines	47.96	4.03E-02	9.97E-01
NADPH binding	35.17	5.46E-02	1.00E+00
aminoacyl-tRNA ligase activity	31.03	6.16E-02	1.00E+00
calcium-dependent cysteine-type endopeptidase activity	25.12	7.56E-02	1.00E+00
cadherin binding involved in cell-cell adhesion	3.64	9.41E-02	1.00E+00
protein heterodimerization activity	2.84	9.54E-02	1.00E+00

Table 4-5: GO term analysis of EV protein found only in one treatment group. *All the EV proteins that were only found in one treatment group were analysed using the DAVID tool and the GO terms from Biological Function and Molecular Function were recorded. P value represents EASE score. The top ten most significantly enriched GO terms are shown. Fold enrichment is the number of genes annotated with that term divided by the number of genes expected by the software to be annotated with that term.*

4.3.10 RELATIVE ENRICHMENT OF PROTEINS IN EVS VS CELLS

In order to assess the differences in protein cargo enrichment between the cells and the EVs the fold changes of the proteins in the EVs and the cells following cisplatin treatment. Only Proteins found in 2 of the samples in each treatment group were included. Values were log 2 transformed before plotting. The fold change following cisplatin treatment of 319 proteins are shown in Figure 4-9. Spearman's rank correlation coefficient was calculated and found to be -0.09 (2 d.p.) with a p value of 0.09 (2 d.p.). This suggests there is a non-significant, weak negative correlation between the two samples. This means that enrichment of proteins in cells had little relation to the enrichment of those proteins in the EVs.

The ratio of enrichment of proteins in the EVs was found by dividing the fold change for EV protein by the fold change for cell protein. The GO terms for all proteins found to be more than 2 times more enriched in the EV samples were then found using DAVID. The top ten GO terms for these proteins are shown in Figure 4-9. There were 96 proteins found have a fold change in EVs 2 or more times higher than in cells. There were 113 GO terms for biological process associated with these proteins and 29 GO terms for molecular functions. The cellular compartment most significantly enriched in this list was the extracellular exosome. Therefore, the proteins with a fold change greater than 2 times higher in EVs than in cells are known to be associated with exosomes. The term 'SRP-dependant cotranslational protein targeting to membrane' is enriched in the proteins that are more enriched in EVs than cells post treatment with cisplatin. This term was also enriched in the proteins only found in cisplatin EVs. Other terms more highly enriched in cisplatin EVs than cisplatin-treated cells were numerous terms related to translation and transcription as well as 'NIK/NF-kappaB signalling'. KEGG pathway analysis of these proteins found 2 pathways were significantly enriched in these pathways: Ribosome and Spliceosome. Both of these KEGG pathways were also significantly enriched in the proteins

both up- and down regulated in cells following cisplatin treatment. For the full list of significantly enriched GO terms see Appendix 7.6 and KEGG pathways see Appendix 7.7.

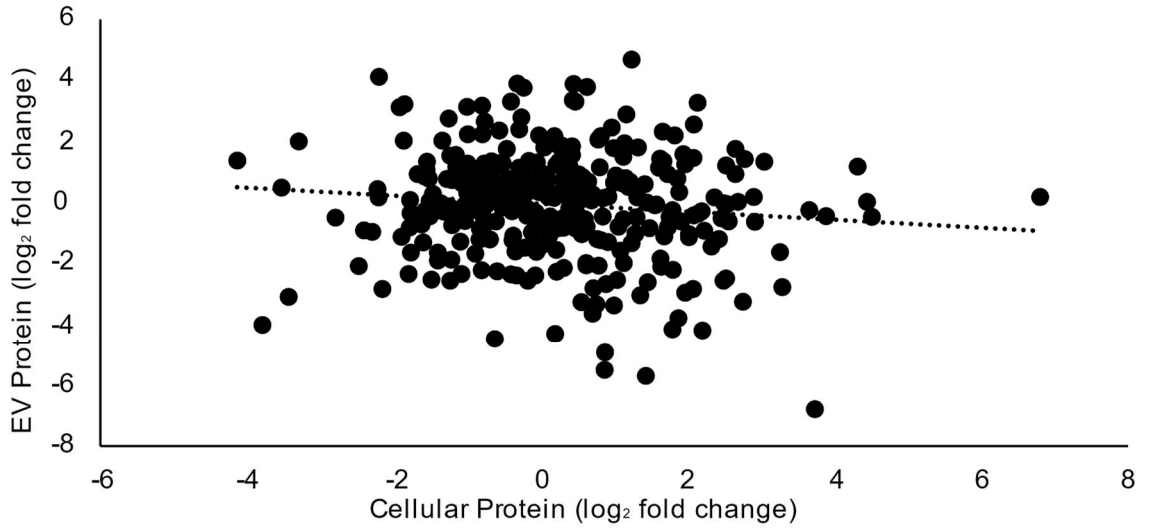

Biological Processes	Fold Enrichment	PValue	Bonferroni
translational initiation	20.04	1.86E-16	1.59E-13
SRP-dependent cotranslational protein targeting to membrane	18.89	2.85E-10	2.04E-07
viral transcription	15.86	1.63E-09	1.17E-06
nuclear-transcribed mRNA catabolic process, nonsense-mediated decay	14.93	2.95E-09	2.12E-06
NIK/NF-kappaB signaling	22.02	6.51E-09	4.68E-06
negative regulation of ubiquitin-protein ligase activity involved in mitotic cell cycle	20.47	1.18E-08	8.45E-06
regulation of mRNA stability	15.68	1.34E-08	9.63E-06
positive regulation of ubiquitin-protein ligase activity involved in regulation of mitotic cell cycle transition	19.12	2.03E-08	1.46E-05
anaphase-promoting complex-dependent catabolic process	18.39	2.77E-08	1.99E-05
translation	8.30	4.79E-08	3.44E-05
Molecular Function	Fold Enrichment	PValue	Bonferroni
poly(A) RNA binding	6.76	3.85E-27	1.07E-24
protein binding	1.57	3.72E-10	1.04E-07
structural constituent of ribosome	8.77	1.10E-07	3.06E-05
RNA binding	5.04	1.97E-07	5.49E-05
cadherin binding involved in cell-cell adhesion	7.28	2.00E-07	5.58E-05
translation initiation factor activity	15.97	3.48E-05	9.66E-03
unfolded protein binding	8.85	5.65E-04	1.46E-01
ATPase activity	6.21	8.96E-04	2.21E-01
ATP binding	2.17	1.61E-03	3.62E-01
GTPase activity	4.86	3.11E-03	5.81E-01
Cellular Compartment	Fold Enrichment	PValue	Bonferroni
extracellular exosome	3.83	4.97E-24	1.18E-21
membrane	4.02	1.21E-19	2.89E-17
cytosol	2.83	3.35E-14	7.98E-12
focal adhesion	7.55	7.06E-10	1.68E-07
eukaryotic 48S preinitiation complex	69.42	1.58E-08	3.75E-06
eukaryotic 43S preinitiation complex	69.42	1.58E-08	3.75E-06
myelin sheath	12.56	1.62E-08	3.84E-06
nucleoplasm	2.49	2.42E-08	5.75E-06
eukaryotic translation initiation factor 3 complex	61.26	3.22E-08	7.66E-06
extracellular matrix	7.62	1.23E-07	2.93E-05

Figure 4-9: The differences in protein enrichment in EVs and Cells. *All the proteins that had a fold change in EVs at least 2 times higher than in cells were analysed using the DAVID tool and the GO terms from Biological Function and Molecular Function were recorded. P value represents EASE score. The top ten most significantly enriched GO terms are shown. Fold enrichment is the number of genes annotated with that term divided by the number of genes expected by the software to be annotated with that term.*

4.3.11 ESTABLISHING THE C2C12 DIFFERENTIATION MODEL

C2C12 cells are mouse muscle precursor cell line that are often used to assess muscle differentiation *in vitro*. The levels of MyHC and Ki67 in differentiating cells to assess their levels in normal differentiation. Differentiation was induced in confluent C2C12s at day 0. These cells were then fixed on days 0-4 of differentiation and immunostained for MyHC, Ki67 and nuclear stained with Hoechst before the levels of fluorescence were read using a microplate reader. The level of fluorescence of MyHC and Ki67 were normalised to Hoechst in order to control for cell number. These data are shown in Figure 4-10. The levels of MyHC increased steadily from day 0 to day 4 of differentiation suggesting that the cells are differentiating into muscle cells. The levels of Ki67 increased on day 1 of differentiation before being reduced on days 2 and 3 and was highest on day 4 of the experiment. Addition of horse serum induces differentiation in C2C12 cells, with increasing amount of MyHC observed each day. The levels of proliferation were high on the first day of differentiation, lower the following two days before raising again on day 4.. The levels of MyHC increased steadily from day 0 to day 4 of differentiation suggesting that the cells are differentiating into muscle cells. The levels of Ki67 increased on day 1 of differentiation before being reduced on days 2 and 3 and was highest on day 4 of the experiment. Addition of horse serum induces differentiation in C2C12 cells, with increasing amount of MyHC observed each day. The levels of proliferation were high on the first day of differentiation, lower the following two days before raising again on day 4.

4.3.11.1 EVs FROM OVARIAN CANCER CELLS REDUCE THE LEVELS OF DIFFERENTIATION AND PROLIFERATION IN DIFFERENTIATING MUSCLE CELLS

Vesicles from Lewis Lung Carcinoma (LLC) tumour cells have been shown to induce cachexia-like symptoms in C2C12 cells (Zhang *et al.,* 2017). Here I hypothesised that EVs from ovarian cancer cells would also be able to induce muscle wasting and that if the EVs

were extracted from cisplatin treated cells this effect would be altered. In order to assess the effect of EVs from Ovarian cancer cells on C2C12s and whether any effect may be altered during cancer treatment, EVs were extracted from A2780 cells treated with either PBS or Cisplatin (40 μM) and then used to treat C2C12s. Differentiating C2C12s were treated with these EVs or PBS on day 2 and 3 of differentiation. These cells were then fixed on day 4 of differentiation and immunostained for MyHC, Ki67 and nuclear stained with Hoechst which was then read using a microplate reader. The level of fluorescence of MyHC and Ki67 were normalised to Hoechst in order to control for cell number. These data are shown in Figure 4-10. The levels of MyHC were significantly reduced following treatment with EVs from cancer cells, however PBS treatment had no effect on the levels of MyHC and Ki67. No differences were seen between the two vesicle groups. Cancer EVs reduced the level of differentiation and proliferation in these C2C12 cells and this effect is not altered when the cells were treated with EVs derived from cisplatin-treated cells.

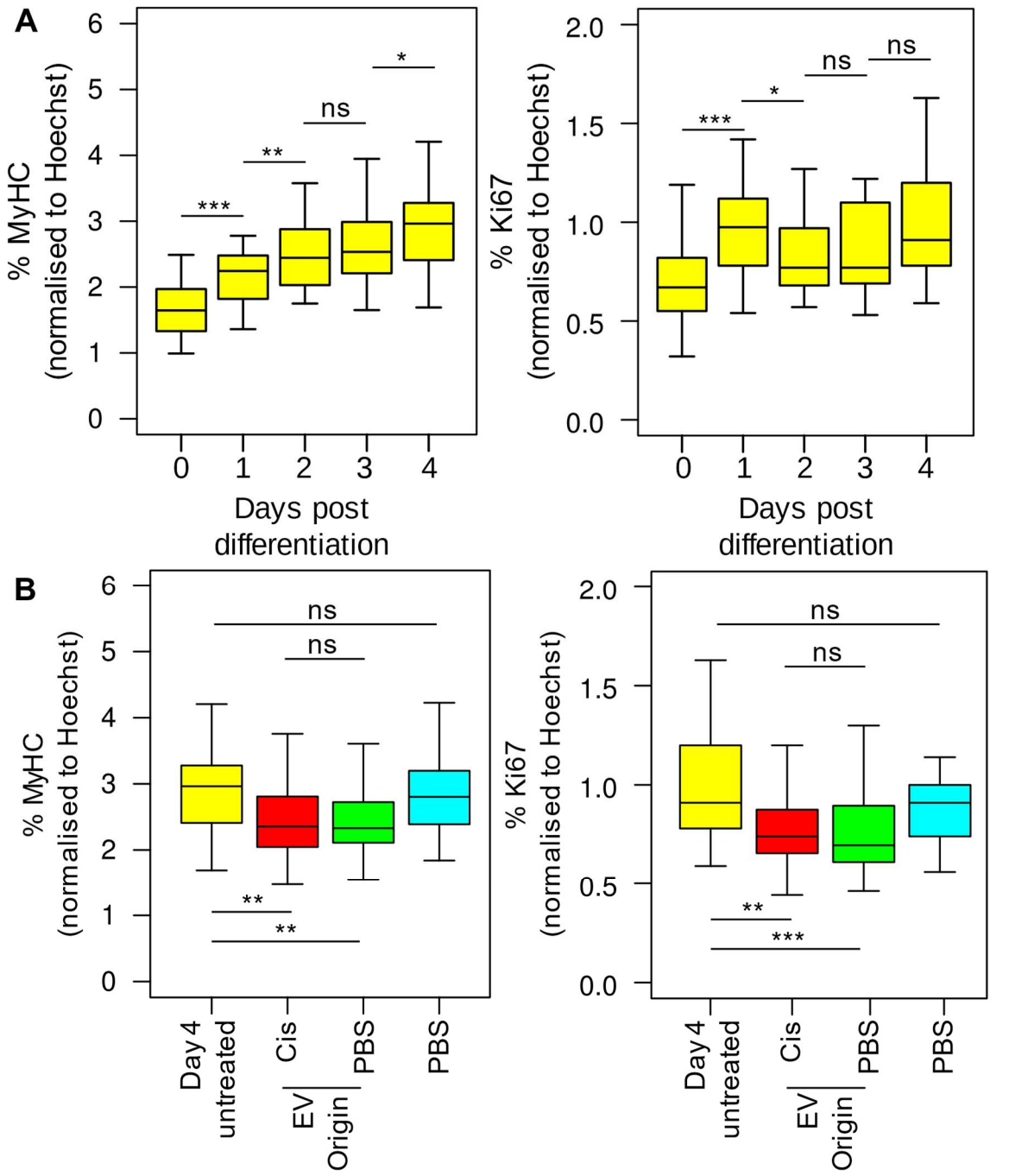

Figure 4-10: Cancer EVs reduce muscle cell differentiation and proliferation. *Differentiation was induced in C2C12 cells via the addition of medium supplemented with horse serum. On the fourth day of differentiation the cells were immunostained for MyHC, Ki67 and nuclear stained with Hoechst. The levels of fluorescence were then recorded on a microplate reader. The levels of MyHC and Ki67 for each well were normalised to the level of Hoechst in order to control for cell number.* ***A)*** *The levels of MyHC and Ki67 in untreated cells on days 0-4 of differentiation.* ***B)*** *These cells were treated with EVs from both Cisplatin (40 μM; red) and PBS (green) treated cells or PBS (blue) alone on days 2 and 3 of differentiation. Box and whisker plots show median, upper and lower quartiles, error bars are 1.5x interquartile range; * p<0.05, ** p<0.01 and *** p<0.001 measure using students ttest. Data from at least 30 biological replicates.*

4.3.12 Injection of Ovarian cancer EVs has no effect on the functional strength of mice

Above I demonstrated that cancer EV treatment *in vitro* caused reduced MyHC production in differentiating C2C12 cells. Here I hypothesised that treatment of animals using these EVs will reduce muscle mass and therefore reduce the functional strength of the mice relative to control treatment. In order to test whether cancer EVs were able to induce cachexia in mice, EVs were extracted from A2780 cells 48 hours after treatment with either cisplatin or PBS. Mice were then injected with these EVs or saline every other day for 21 days. The strength of the mice was assessed via inverted screen and weight lifting tests, outlined above, prior to injections and again after all injections had been completed. Each mouse was weighed every 3 days and the circumference of the right rear hind limb was observed every week. The change from baseline of these four variables is shown in Figure 4-11 ($p = 0.55$ AVOVA). The average mass of each mouse increased in all treatment groups over the course of the experiment however no significant differences were observed after 21 days ($p = 0.7$ ANOVA). The mice treated with cisplatin EVs showed the greatest average improvement in screen hang time, however this increase was not significant ($p = 0.11$ ANOVA). Finally, all the mice performed worse on the weight lifting test after 21 days however there was no difference between groups in their ability to lift the weights ($p = 0.81$ ANOVA). Statistical significance was assessed via ANOVA on the data set for the final reading. Treatment with the EVs appears to have had no effect on the strength of the mice over 21 days. Treatment with the EVs appears to have had no effect on the strength of the mice over 21 days. These data do not support the hypothesis that EVs would reduce strength and muscle mass in mice as there is no difference in the functional strength, or muscle size in the EV treated mice.

In order to see whether EV injection had altered the composition of immune cells in the animals the blood content of the mice was analysed using ABX-Pentra 60 (Horiba) after

they had been sacrificed. The concentration of white blood cells, red bloods cells and platelets were counted, and the composition of the white blood cells was assessed. Whilst the white blood cells do appear to have increased in mice treated with cisplatin EVs, no significant changes were observed in the composition of the blood cells or the relative levels of different white blood cells the between treatment groups (ANOVA $p = 0.058$, post hoc Tukey test $p = 0.16$ Cisplatin EV – PBS EV, $p = 0.06$ Cisplatin EV – Saline). Similarly, whilst the 75^{th} percentile for the monocytes was very high in the saline treated mice this was not significant when assessed with ANOVA ($p = 0.36$). EV treatment did appear to affect the whole blood counts.

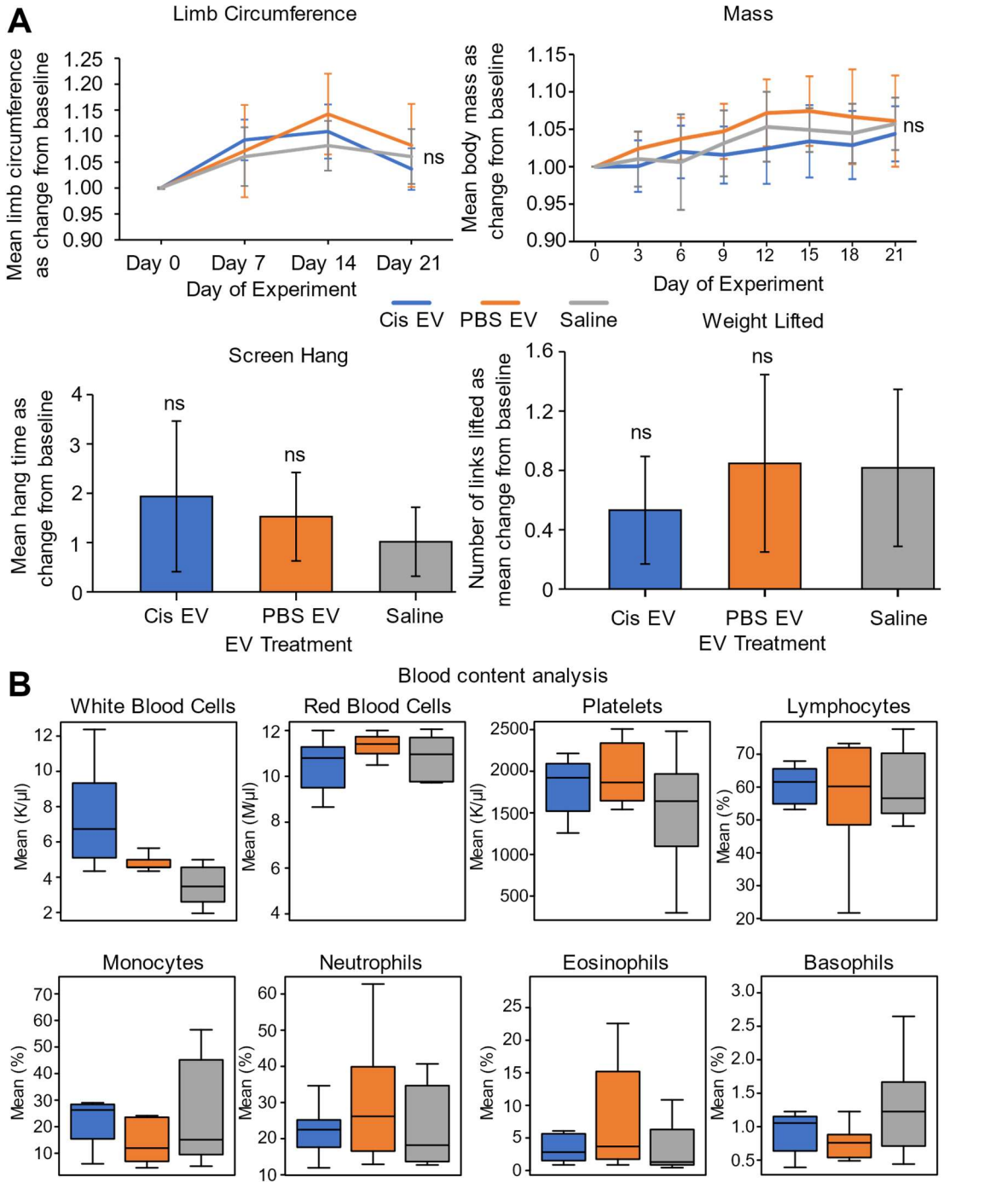

Figure 4-11: The effects of cancer EVs on the functional strength of mice. A) *Four measures of mouse strength and muscle were recorded before and after treatment with either saline (grey) or EVs from cisplatin (blue) or PBS (orange) treated ovarian cancer cells. The levels of each variable are displayed as average change from baseline.* ***B)*** *Blood was taken from the animals after sacrifice and the content was analysed. The PBS EV treatment group consisted of 6 mice and both the cisplatin EV and saline groups contained 8 mice. Statistical significance was assessed via an ANOVA carried out on the data from the final day of the experiment. Bars are mean change from baseline and error bars are standard deviation. Box and whisker plots show median, upper and lower quartiles, error bars are 1.5x interquartile range.*

4.3.13 MUSCLE FIBRE AREA WAS NOT AFFECTED BY TREATMENT WITH OVARIAN CANCER CELL DERIVED EVS

As cancer EVs were able to reduce muscle differentiation *in vitro* and have been shown to be involved in cachexia previously (Zhang *et al.,* 2017) I hypothesised that these EVs should also affect the development of muscle mass in mice. To see whether cancer EVs affected muscle fibre size mice were treated with saline or EVs from cells treated with cisplatin or PBS. The mice were treated every other day with $1x10^9$ EVs via tail vein injection. After 21 days the mice were sacrificed and the right rear quadricep was removed from the mice and transverse sections were taken from the mid-belly of the muscle. These sections were stained with haematoxylin and eosin. Images were taken of the muscles at 10x magnification and the area of the fibres was assessed using ImageJ. The median muscle fibre size for the mice in each treatment group are shown in Figure 4-12. Whilst the muscle fibres from mice treated with EVs were slightly larger than those from mice treated with saline, there were no significant differences measured via ANOVA. Therefore, it seems that treatment with EVs did not affect muscle fibre cross sectional area within the time of the experiment.

4.3.14 NO DNA DAMAGE WAS OBSERVED IN THE SPLEEN OF THE MICE

Work on the radiation-induced bystander effect has shown that irradiation in the head of a mouse can induce bystander effects in the spleen of the organism (Ilnytskyy *et al.,* 2009). As I have here demonstrated EVs are involved in the bystander effect *in vitro* I hypothesised that bystander effects should be found in mice that were treated with stress-derived EVs. Here I tested whether the EVs released from the cisplatin treated cells were able to induce bystander effects when injected into an organism. In order to test whether EVs extracted following cisplatin treatment were able to induce the bystander effect in these mice the levels of DNA damage in the spleen was assessed. Sections of spleen from

mice treated with saline or EVs from cisplatin or PBS treated cells were assessed for DNA damage via immunostaining for γH2AX, a histone protein known to be a marker of DNA damage. The percentage of nuclei that stained positive for γH2AX is shown in Figure 4-13. There was an increase in the level of nuclear γH2AX in the cisplatin EV treated mice, however this was not significant (p = 0.435 ANOVA, p = 0.45 Cis EV – PBS EV post hoc Tukey, p = 0.58 Cis EV- Saline post hoc Tukey). Whilst higher levels of DNA damage were observed in the spleens of mice treated with cisplatin EVs, this increase was not significant.

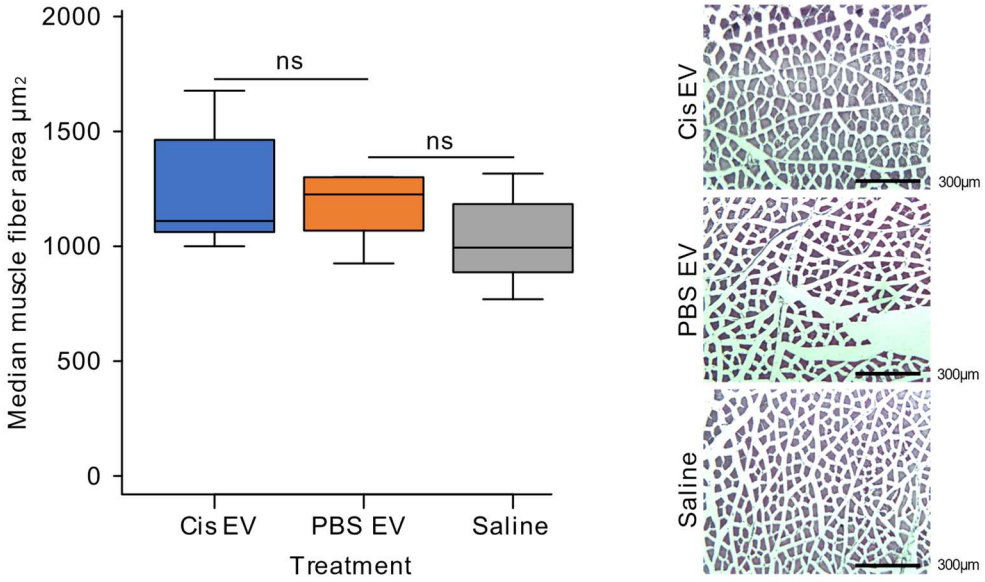

Figure 4-12: The effect of ovarian cancer EVs on muscle fibre cross sectional area in mice. *Mice were treated with saline or EVs from cisplatin or PBS treated cells every two days for 21 days. The mice were sacrificed and the right rear quadricep was fixed and harvested. The muscles were frozen in OCT and sections were cut on a cryostat. Sections were H&E stained and muscle fibre cross sectional area was measured using ImageJ. The median muscle fibre csa for each mouse was calculated. Box and whisker plots show median, upper and lower quartiles, error bars are 1.5x interquartile range. At least 650 fibres were counted for each mouse. Cis EV group had 7 biological replicates, PBS EV group had 6 biological replicates and the Saline group had 8 biological replicates. Significance was assessed via ANOVA.*

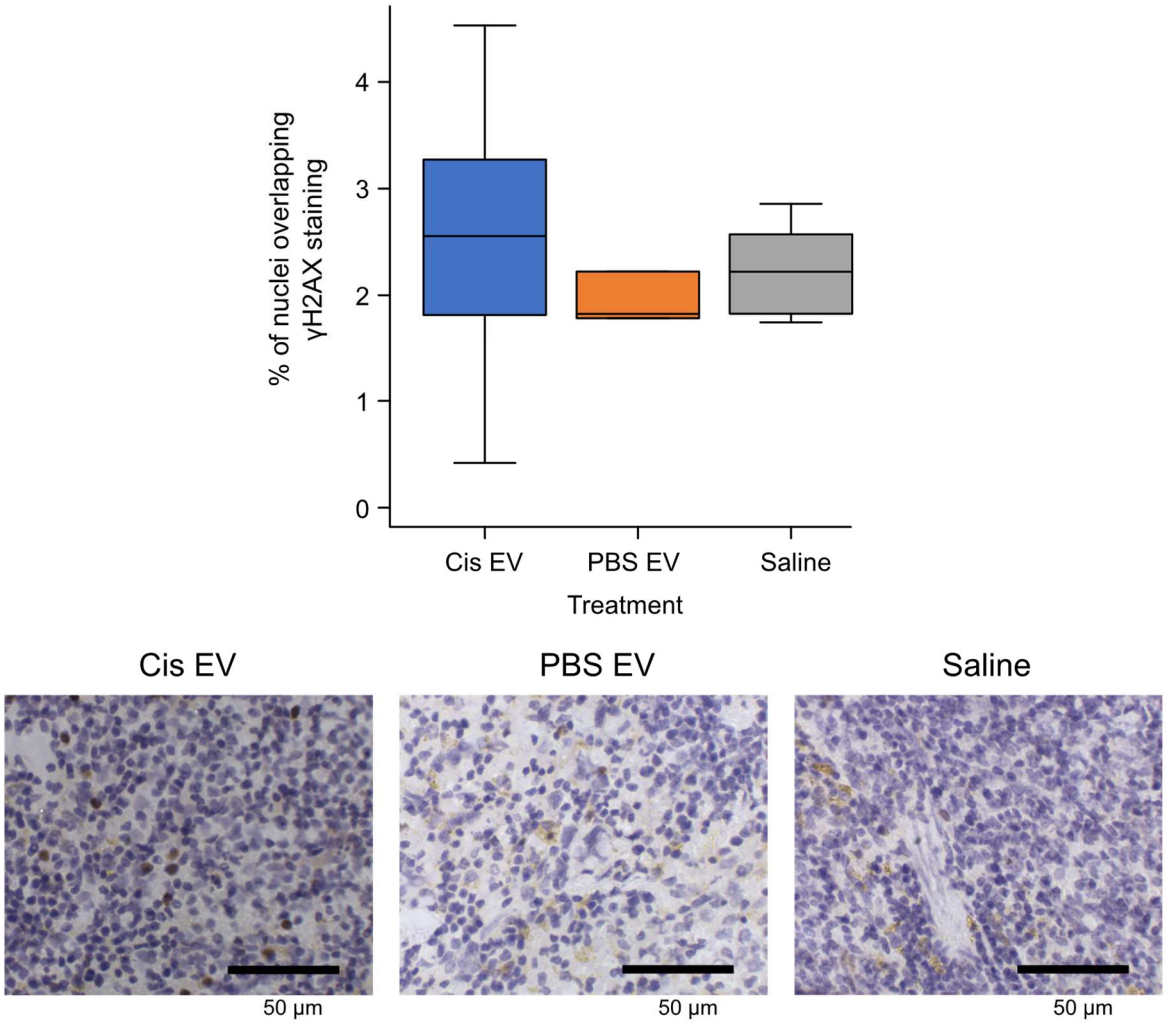

Figure 4-13: The effect of cisplatin EVs on the levels of DNA damage in the spleen.

Mice were treated with saline or EVs from cisplatin or PBS treated cells every two days for 21 days. The mice were sacrificed, and the spleen was fixed and harvested. The spleen was frozen in OCT and sections were cut on a cryostat. Sections were immunostained for γH2AX and the number of γH2AX containing nuclei were counted. The percentage of nuclei stained with γH2AX for each mouse was calculated. Box and whisker plots show median, upper and lower quartiles, error bars are 1.5x interquartile range. At least 200 cells were counted for each mouse. Cis EV group had 8 biological replicates, PBS EV group had 6 biological replicates and the Saline group had 8 biological replicates. Significance was assessed via ANOVA and post hoc tukey test.

4.4 Discussion

In this chapter the role of EVs in cancer induced cachexia has been assessed. Cancer EVs have been shown to reduce the levels of differentiation in mouse myoblast cells. Stressing the cells with cisplatin prior to extracting the EVs had no effect on this effect. However, no reduction in muscle mass was observed when these EVs were injected into mice. A screen of the protein cargo of these vesicles was also carried out which showed numerous differences in protein cargo, but functional analysis suggests the proteins in cisplatin and PBS treated cells and the EVs they release are involved in similar pathways.

4.4.1 EVs from Cisplatin-treated cells are able to induce bystander effects in Naïve populations.

Cisplatin is a platinum based chemotherapeutic used to treat a range of cancers, including ovarian carcinomas (Gómez-Ruiz *et al.,* 2012). Previously bystander effects have been observed following various chemical stresses, including chemotherapeutics (Samuel *et al.,* 2017; Asur *et al.,* 2009; Jin *et al.,* 2011). In radiation extracellular vesicles have been found to be involved with the induction of DNA damage in bystander cells and data in the previous chapter demonstrates that EVs are also involved in thermally-induced bystander effects. Here it has been shown that EVs released from cells treated with 40 µM Cisplatin were able to induce DNA damage and reduce cell viability when added to a naïve population. These data corroborate work in our own lab showing EVs from Cisplatin-treated cells having a multitude of effects on unstressed cells, including bystander effects in the form of reduced cell viability following treatment (Samuel *et al.,* 2017) and the previous work in the field suggesting that bystander effects are in part propagated via extracellular vesicles (Al-Mayah *et al.,* 2012; Bewicke-Copley *et al.,* 2017; Xu *et al.,* 2017).

4.4.2 SEC IS ABLE TO EXTRACT EVS FROM CELL CULTURE MEDIUM SEPARATE FROM PROTEIN CONTAMINATES

Ultracentrifugation is a technique widely used for EV extraction. However, these samples are likely to be contaminated with other molecules found in the medium that pellet at the same speed as the vesicles (Witwer *et al.,* 2013). There are a few different methods of extraction that are supposed to either increase purity such as buffering the EVs on a sucrose gradient (Gudbergsson *et al.,* 2015) or yield such as ExoSpin (Lane *et al.,* 2015). Size Exclusion Chromatography has more recently become a popular method of extraction (Corso *et al.,* 2017; Gámez-Valero *et al.,* 2016; Böing *et al.,* 2014; Lozano-Ramos *et al.,* 2015). Here EVs extracted from A2780 cells using SEC were observed by NTA in fraction 6 through to fraction 10. Free protein was first seen in fraction 10 at a relatively low level and it quickly increased until it peaked in fraction 18. This demonstrates that the majority of the EVs in the medium were able to be separated from the free protein also found in the medium. There were, however, some particles observed in the fractions after the protein levels, in fractions 12, 16 and fraction 20. The peaks in fractions 16 and 20 were only observed in samples from one column and appear to be due to either scratches in the device or very large objects/air bubbles causing artefacts on the video, which were measured as particles. Particles were observed in fraction 12 in all columns and were visible as particles in the videos, suggesting that there may still be some small vesicles being eluted along with the protein. Alternatively, these particles could in fact be protein aggregates which can also be detected via NTA (Filipe *et al.,* 2010). It is important to note that the vesicles did overlap slightly with the protein, and that only taking vesicles from fractions that did not contain protein may lead to potentially import vesicles being excluded. More work is needed to better understand the nature of the particles found after fraction 9. For example, an additional step to break up protein aggregates prior to analysis on the NTA.

The proteins found within the particles eluted in fractions 6-8 were identified via mass spectrometry and the GO terms for cellular compartment were found. These data show that the top three most significantly enriched GO terms 'extracellular exome', 'cytosol' and 'membrane'. This suggests that the protein cargo found within these vesicles is linked with proteins known to be found within exosomes as well as in the cell membrane and cytosol, both of which are likely to also be found within EVs. Therefore, it seems that the extracted particles are in fact extracellular vesicles not some other molecule or complex of roughly the same size.

4.4.3 GO TERM ANALYSIS OF THE PROTEIN CHANGES IN CISPLATIN-TREATED CELLS SUGGESTS A REDUCTION OF PROTEIN SYNTHESIS IN CISPLATIN-TREATED CELLS.

GO term analysis was carried out to determine what processes might be affected by the observed changes in the proteomes of the cells and EVs. Numerous GO terms were significantly enriched in the gene lists of the deregulated cellular proteins, however there is no clear pattern as to which processes were being up and down regulated. Numerous GO terms for biological processes and molecular functions were observed to be simultaneously enriched in both the up- and down-regulated protein populations such as 'translational initiation', 'poly(A) RNA binding' and 'nucleotide binding'.

Interestingly one of the biological processes up-regulated within the cells is 'NIK/NFkappaB signalling'. The activation of the transcription factor NFκB is known to be linked to resistance to chemotherapy (Godwin *et al.,* 2013; Montagut *et al.,* 2006) so it seems obvious that it would be up-regulated following chemotherapy treatment. Further this pathway is also known to be involved in the bystander effect, often seen to be up-regulated in the bystander cells (Zhou *et al.,* 2008; Prise *et al.,* 2009). The increase of the proteins related to NFκB signalling could mean that these proteins will be loaded into the

EVs released by these cells and might be able to induce the effect in bystander cells, however no such increase was observed in the EVs. It also seems that protein synthesis and transport might also be perturbed in the cisplatin-treated cells with the biological processes 'mRNA transport from the nucleus' and 'protein folding' both being significantly enriched in the down-regulated proteins along with the molecular functions 'unfolded protein binding', and 'protein transporter activity'. Cisplatin treatment is known to reduce protein synthesis (Heminger *et al.,* 1997; Sato *et al.,* 1996; Nicholas *et al.,* 2017) so it makes sense that processes related to it are down-regulated. The most highly enriched molecular function in the down-regulated proteins is 'Ran GTPase binding'. Ran GTPase is utilised for the translocation of RNA and proteins across the nuclear envelope and is involved with mitosis. Therefore, the deregulation here could also be related to the reduction in protein synthesis.

4.4.3.1 EVs from cisplatin-treated cells seem to be enriched in proteins that target mutant mRNA for degradation

Fewer proteins were identified in the EV samples with only 1651 proteins found in all the EV protein samples whilst 2688 proteins were found within the cell samples. Further whilst 2176 proteins were found in at least two samples of both treatment groups and 512 in two or more samples of one treatment group in cells, only 343 were found in at least two samples of both EV groups with only another 175 found in at least two samples of only one treatment group. This means that a lot of the proteins identified in the EVs were only seen in one of the samples tested in one or both treatment groups, suggesting that many of these proteins identified may not commonly be found in EVs and are only found here through chance.

Only 65 proteins were up-regulated 2-fold or more in EVs released by cisplatin cells and 45 were down regulated 2-fold or more, none of the proteins were significantly

enriched in cisplatin EVs following a Bonferroni correction. This could suggest that the protein cargo of the EVs is not related to its function and it could be the RNA or Lipid cargo or a combination of all three that induces effects. This would support work on the bystander effect which shows non-coding RNA molecules being important bystander signals (Xu *et al.,* 2014; Xu *et al.,* 2015). As with the GO term analysis for the cellular protein there is a lot of cross-over between the terms enriched in the up- and down-regulated proteins. For example, the biological processes 'translation' and 'cell-cell adhesion' appear in both lists as do the molecular functions 'mRNA binding' and 'poly(A) RNA binding'. Very few if the GO terms appear to be significantly enriched in either protein list however. Like in the GO terms for the cellular protein 'poly(A) RNA binding' is the most highly significant molecular function in both up- and down-regulated proteins, it is also the only significantly enriched downregulated molecular function in EVs. Interesting the GO terms 'regulation of mRNA stability' and 'nuclear-transcribed mRNA catabolic process, nonsense-mediated decay' were both significantly enriched in the EVs. The term 'nuclear-transcribed mRNA catabolic process, nonsense-mediated decay' refers to the pathway for preventing the translation of mRNA with nonsense mutations. It's possible that these are packaged into EVs following genotoxic stress to halt the production of erroneous protein in neighbouring recipient cells that may also have been affected by the stress, or in an attempt to prime cells for a future stress. A further 65 proteins were only found in EVs from PBS treated cells whilst 110 were found in EVs isolated from cisplatin-treated cells. When the GO terms analysis was run for these samples very few terms were significantly enriched. The protein only found in PBS treated cells were enriched for the molecular functions: 'protein binding' and 'poly(A) RNA binding' none were significantly upregulated for protein only found in cisplatin-treated cells. Proteins only found in EVs from cisplatin-treated cells were enriched in the biological process: 'nuclear-transcribed mRNA catabolic process, nonsense-mediated decay' and the molecular functions 'poly(A) RNA binding' and 'RNA binding' and the protein

only found in EVs from PBS treated cells weren't significantly enriched in any terms. These data suggest that the EVs may carry proteins that are involved in repressing translation in neighbouring cells. It is already known that numerous pathways are down regulated during stress, so it may be that EVs play a role in this facet of the stress response.

The proteins found in the EVs were often found in only one or two of the samples, suggesting they might not be very important to the function of the EVs. This also suggests that the EVs are highly heterogeneous as a population. It is important to note that non-stress-derived EVs will likely also be released following stress conditions, which will mean that some of the proteins observed in the cisplatin EV samples may not be related to stress. Further, these EVs were extracted from the cells 72 hours post stress, which may mean that the vesicles in these samples are from cells that have recovered from the stress. It would be possible to get a purer sample of stress EVs by extracting the EVs much sooner after stress treatment. For example, thermal bystander effects were observed above in 3.3.8.2 with EVs extracted only 3 hours after stress. However, this would likely require medium from far more cells in order to have enough vesicles in the medium after only three hours.

In order to generate a more robust dataset it would be necessary to take protein from a greater number of samples in order to see which proteins are commonly found in the EVs suggesting active loading, and which may have only been loaded into them by chance during their formation.

The relative enrichment of proteins following cisplatin treatment between cells and EVs was assessed to determine whether the protein changes in the EVs matched the changes in the cells. There was a weak negative correlation between the fold changes, however this was very low, and it seems likely that fold change of proteins in EVs in independent of the fold changes observed in the cells. Interestingly when the proteins whose fold change was 2 or more times higher in EVs were analysed for Go term enrichment analysis they were most significantly associated with the extracellular

exosome. This confirms that the EV proteins are more enriched in the EVs than in the cells. Many of the terms that were enriched in the other analyses were also found enriched in this protein list, such as 'poly(A) RNA binding' and 'viral transcription'. One interesting biological process that was enriched was 'NIK/NFkappaB signalling', which was found to be upregulated in the cells, but not the EVs after cisplatin treatment. However, it appears that the proteins whose fold change in EVs was over twice that of in cells are related to this process.

The proteomics data show a possible role of the protein cargo of cisplatin-treated cell derived EVs in targeting mutant mRNA for destruction. However, there is no evidence of any proteins that may be responsible for any effects that these EVs may cause in recipient cells.

4.4.4 EVs FROM CANCER CELLS REDUCE DIFFERENTIATION AND PROLIFERATION OF C2C12s

There is evidence that EVs from cancer cells are involved in the induction of cachexia in cancer patients (Zhang *et al.,* 2017). C2C12s are an immortalised mouse myoblast cell line that is often used to model muscle maturation *in vitro* (Zhang *et al.,* 2017; Bonetto *et al.,* 2015; Burattini *et al.,* 2004). There was a significant reduction in differentiation into muscle cells following treatment with EVs from A2780 cells. There was no difference in the effect of these EVs when cells were treated with cisplatin, suggesting the EVs of stressed cells show no difference in their ability to hinder muscle development. These data corroborated the findings above that showed EVs from lung cancer cells were able to reduce the differentiation of C2C12s (Zhang *et al.,* 2017). These findings suggest that EVs released from ovarian cell lines are able to reduce the level of muscle development observed after four days of differentiation in mouse myoblast cells. It is possible therefore

that EVs released by ovarian tumours could be responsible for the induction of cachexia in patients.

HSP70 and HSP90 carried within vesicles have shown to be important for the induction of cachexia (Zhang *et al.,* 2017). However, these proteins were not found to be enriched in the proteomics data. It could be that these EVs induced a reduction in muscle differentiation in a different way to the vesicles extracted from lung cancer cells. After treatment with lung cancer cells an increase in p38 phosphorylation was observed (Zhang *et al.,* 2017) and activation of p38 is known to be linked to muscle wasting (Yuan *et al.,* 2015; Zhang *et al.,* 2013; Zhang & Li 2012). In order to check whether ovarian cancer EVs induce muscle wasting via the same pathways the levels of p-p38 could be assessed following EV treatment. It is also possible that HSP70 and HSP90 are present in ovarian cancer EVs, but that they were simply not picked up by the proteomics screen.

4.4.5 EVs INJECTED INTO MICE SHOW NO FUNCTIONAL OR HISTOLOGICAL DIFFERENCES IN MUSCLE COMPARED TO MICE INJECTED WITH SALINE

After 21 days there were no significant differences in the results of limb circumference body mass the strength tests. Mice injected with cancer EVs were assayed for mass and limb circumference as well as being subjected to two different types of strength test. Surprisingly mouse limb circumference increased on average over the first two weeks before dropping again by week 3. The mice treated with EV from cancer cells showed the greatest drop in limb circumference whilst the saline treated mice showed a smaller reduction. The mass of the mice had also increased by the end of the experiment. The mice treated with EVs from cisplatin-treated cells showed the lowest mass increase throughout the experiment, however there were no significant differences in the final weight changes of the mice. On average treatment with EVs from cisplatin-treated cells seemed to slightly increase the time the mice could hang from the screen and PBS EV and

saline treated mice showed no improvement, however the three groups did not show any statistically significant differences in ability. All three groups showed reduced ability in the weight lifting test after 21 days, again with no significant differences in their ability to lift the weights. Mouse muscle fibre size was also assayed following the experiment, however this also showed no significant differences between the median muscle fibre size the mice in each treatment group. All this suggests that the EV treatment was insufficient to cause the mice to develop a cachexia phenotype. There is the possibility that had the experiment continued past 21 days that the reduction in hind leg circumference may have continued suggesting a that the mice were cachexic; however, the other measures of cachexia showed no sign of the EVs having an effect on the muscles of the mice.

The previous experiment showing that lung cancer EVs were able to induce cachexia did not inject EVs into healthy mice, but blocked EV release from the cell line that was implanted into the mice (Zhang *et al.,* 2017). It could be that it was the silencing of Rab27a and b that is responsible for the reduced cachexia, not the lack of EV release. This could be checked by seeing if the cachexia phenotype can be rescued in mice with the deficient cells via the addition of EVs from regular lung cancer cells. Further the xenograft model allows the xenograft to constantly release EVs whilst injecting the mice every two days drastically reduces the number of these potentially cachexia inducing signals. Whilst $1x10^9$ EVs has been shown previously to have an effect *in vivo* (Akbar *et al.,* 2017) it is possible that here the number of vesicles the mice were treated with was too low for any effect to be observed. It would be useful to know roughly how many EVs a tumour is able to release over time in order to better select the concentration of EVs to inject. The EVs used here were also extracted weekly and stored at 4C which may have impaired their function, which again is not a problem that would occur with EVs released from a xenograft. As well as the complications of injecting EVs the two strength tests in this study are not direct measures of strength unlike testing the mice with a grip strength meter, which means other factors

may have altered the performance of the mice. The data from these tests is supported by the histological data however, so this may not have affected the results.

The EVs have been shown to reduce the levels of differentiation in C2C12s, and EVs have been shown to be involved in cachexia (Zhang *et al.,* 2017). It therefore seems likely that these vesicles should have some effect *in vivo.* It is possible that with the relatively low levels of EVs utilised in these experiments that simply too few vesicles were able to interact with the muscles in the mice. One important thing to ascertain would be which tissues the injected EVs are taken up by in the mouse. This could be assessed by labelling the vesicles with a fluorescent dye (such as PKH67), sectioning numerous tissues including the muscles and liver and seeing where the vesicles could be found, and in what quantities. If the vesicles are unable to make it to the muscles, they are unlikely to affect muscle development.

The mice were also assessed for DNA damage in the spleen, in order to determine whether cisplatin EVs were able to induce bystander effects *in vivo*. However, there was no also no change in the levels of DNA damage observed across the three treatment groups. Whilst EVs have been implicated in the induction of bystander effect this has not been demonstrated in vivo (Al-Mayah *et al.,* 2012; Bewicke-Copley *et al.,* 2017; Xu *et al.,* 2017). Again, as above the treatment here may simply have been with too few EVs to be able to induce these affects. Interestingly there was a non-significant increase in the level of DNA damage in the mice treated with cisplatin EVs. It might be that if the mice were treated with a more physiologically-relevant number of EVs that this difference would become more pronounced. Preliminary work carried out by our collaborators suggests that there are around 1-2x10^{10} circulating EVs within a mouse. Here we injected 1x10^{9} EVs every other day which corresponds to around 5-10% of the total EVs in the mouse. With a mouse containing around 1.5 mls of blood this would correspond to a blood EV concentration of 1.3x10^{10}/ml which corresponds with out injection of 100µl of EVs at 1x10^{10}/ml. Whilst the

concentrations of the EVs injected here are comparable to the physiological levels in mice the turnover of EVs is relatively quick (Feng *et al.,* 2010) meaning that the injected EVs will be quickly used up or excreted by the organism, whilst EVs will be constantly released from a tumour, replenishing their levels as they are taken up by cells or excreted. It would be enlightening to know how many EVs are released by a tumour over a specific timeframe in order to accurately construct a dosing regimen.

There was a non-significant increase in the levels of white blood cells and monocytes in the mice treated with cisplatin EVs. Whilst these data are not significantly different it might be an interesting avenue of further research. It would be interesting to look at the blood composition of the mice over the course of the experiment, particularly before and shortly after injection to see whether the EVs are able to stimulate the immune system.

The data here seem to show that injection of cancer EVs is insufficient to induce cachexia in mice, contrary to previously published data (Zhang *et al.,* 2017). Whilst the work presented here attempted to induce muscle loss through addition of vesicles into healthy mice, the previous study showed that blocking EV release from a xenograft stopped cachexia from forming. This distinction in methodology may explain the differences in findings as it is difficult to mimic physiological EV levels and production when injecting them.

4.4.6 Concluding Remarks

In this chapter it has been demonstrated that EVs released from cells stressed with cisplatin are able to induce bystander effects in naïve cells. This is supports the data in the previous chapter suggesting that thermally-induced bystander effects can be induced with EVs, as well as with other literature on the subject (Samuel *et al.,* 2017; Al-Mayah *et al.,* 2015; Al-Mayah *et al.,* 2012; Xu *et al.,* 2015).

Size Exclusion Chromatography has been shown to be able to separate the EVs and protein components found in cell culture medium. This greater level of purity allows for more confidence that any observed effects are in fact due to EVs and not due to contaminants that are isolated alongside them.

A proteomics screen was carried out which suggested that whilst cisplatin and PBS treated cells have different a protein complement, the many of the pathways associated with the down-regulated proteins are similarly associated with the up-regulated proteins. There was evidence that cisplatin cells down-regulate pathways related to protein synthesis. The proteomes of the EVs were smaller and the differences in protein expression were much smaller than with cellular protein. However, EVs from cisplatin-treated cells do seem to contain proteins associated with blocking the expression of mutant mRNA, which might be an attempt to reduce the damage from the genotoxic stress.

Finally, EVs from PBS and cisplatin-treated ovarian cancer cells have been shown to reduce muscle cell differentiation and proliferation *in vitro* however, no cachexia or bystander effect was observed following injecting these EVs into mice for 21 days.

5 DISCUSSION

5.1 EVS AS BYSTANDER SIGNALS

5.1.1 EVS CAUSE EFFECTS IN BYSTANDER CELLS

In this thesis it has been demonstrated that EVs released following different stress treatments are able to induce bystander effects in unstressed populations. Previously this function of EVs had mostly been observed following radiation treatment. This suggests that EV induced bystander effects may be universal across different stress types. It has previously been shown that both RIBE and chemically-induced bystander effects involves the action of gap junction signalling (Zhou *et al.,* 2000; Zhou *et al.,* 2001; Shao *et al.,* 2003). This allows the construction of a unified model of bystander effects for all types of stress. It is already known that that the stressed cells are able to induce bystander effect in their immediate neighbours using gap junction signalling (Zhou *et al.,* 2000; Zhou *et al.,* 2001; Shao *et al.,* 2003) but the data presented here suggest they also secrete the EV signals, which will also be taken up in nearby cells, but are able to travel far from the original location of stress and induce bystander effects in distant tissues. This suggested model of bystander signalling can be observed in Figure 5-1. As EVs are known to be found in the circulation and that they can affect part of the body far from their origin (Hoshino *et al.,* 2015). It is probable, therefore, that these EVs are at least partially responsible for bystander effects observed far from the site of stress *in vivo*.

Most of the data on the bystander effect has come from *in vitro* studies. However, the data from *in vivo* experiments suggest that damage can be observed not only within an organism but between organisms, with data from studies in fish showing co-habiting the same tank as an irradiated fish, or eating irradiated worms was able to induce bystander effects (Mothersill *et al.,* 2006; Mothersill *et al.,* 2007; Smith *et al.,* 2013). This would

suggest that the signal responsible for inducing damage is protected in some way that would allow it to travel between organisms. Future work on *in vivo* bystander effect should attempt to look at the role of extracellular vesicles. Possibly trying to determine whether blocking the uptake of vesicles is able to reduce the levels of bystander damage. However, EVs are known to be involved in regular cellular processes as well, and simply blocking EV uptake could have off-target effects.

5.1.2 EVs ARE INVOLVED IN INCREASING SURVIVAL IN SUBSEQUENT STRESSES

The purpose of the bystander effect is unknown. Under most conditions cells attempt to either repair or remove damage cells. To respond to stressful conditions that are able to cause molecular damage and kill cells by releasing signals that do the same thing seems counter-productive. The data shown here demonstrates that stress EVs are able to increase the ability of cells to survive in stress. Therefore, it is possible that the bystander effect is an aspect of the response to stress, that induces a more resistant population of cells. This work has not assessed what mechanisms may be involved in the induction of the bystander effect in the bystander cells. Previous work has suggested a role for NF-κB signalling, which did show up in the proteome of cisplatin-treated cells, and was associated with protiens more highly enriched in EVs relative to cells (Zhou *et al.,* 2008). However, very little is known about the way in which EVs can induce the bystander effect. It would be enlightening to view the uptake of EVs into cells to determine where the EVs localise to within the cell, or whether they even need to undergo uptake at all. It could be that the signal is found on the outer leaflet of the membrane and it interacts with a receptor on the

surface of the cell. This could mean that the EV is then able to disassociate from the bystander cell and go on to target further cells.

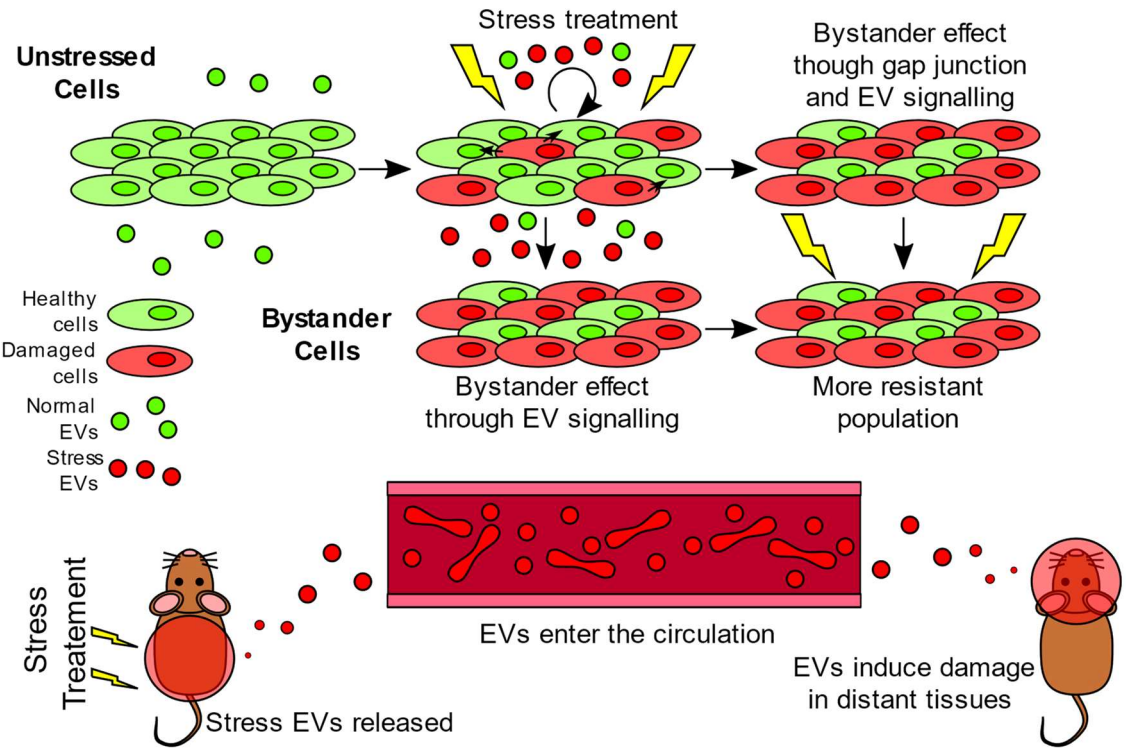

Figure 5-1: The proposed model for bystander signalling.

When cells become stressed they release a subtype of EVs that are taken up by both the cell population that released them, and also distant bystander cells. These stress EVs, along with gap junction signals, are then able to induce bystander effects in those cells. This population of bystander cells is then more resistant to subsequent stress than naïve cells. EVs are blood soluble and it therefore seems likely that it is these signals that are responsible for bystander effects observed in vivo. When stressed, the it is likely that the cells of the stressed tissues would release vesicles which are then carried to bystander tissues via the circulatory system.

5.1.3 The clinical implications of EV induced bystander effects

Bystander Effects are observed following treatments that are currently used in a clinical setting, chemotherapy and radiotherapy (Asur *et al.,* 2009; Al-Mayah *et al.,* 2012; Mancuso *et al.,* 2008), and as demonstrated here, following heat treatment which is currently undergoing trials to be used in a clinical setting (Mallory *et al.,* 2015). This means that the bystander effect could be relevant to the use of these treatments. If EVs released from tumour cells targeted by these therapies are able to induce damage and cell death in healthy cells in the patient this could lead to other problems arising in tissues far from the initial site of damage. Further, if these EVs are involved in developing more resistant

populations of cells they could be induce a tumour to become more resistant to therapy, and it has already been demonstrated that EVs released from cisplatin resistant cells are able to increase the resistance of other cell lines (Samuel *et al.,* 2017). More work is needed to know what affect, if any, stress EVs have inside of an organism. To date *in vivo* studies of the bystander effect have sought to check whether off targeted effects of treatment were found in the organisms, but they have not attempted to determine the long-term consequences of bystander effect on treatment or survival. This could ascertain whether the bystander damage is noticeable from a clinical perspective. It may be that the organism is able to survive with little to no adverse effects related to the bystander effect. If not, however, it could be that these therapies induce damaging off target effects. Bystander cells are also more resistant to stress, so stress EVs might be reducing the therapeutic potential of these treatments. Therefore, it would be useful to know whether uptake of these EVs could be blocked *in vivo* with uptake inhibitors like amiloride, in order to counter the damage and increased resistance in bystander cells and tissues.

5.2 EV EXTRACTIONS METHODS

Extracellular vesicles are hard to extract from both cell culture medium and from biofluids without also extracting contaminating factors such as protein. Here size exclusion chromatography has been shown to be able to extract protein free samples of EVs from cell culture medium. This agrees with a number of publications that also show SEC is capable of separating EVs and proteins.

However, there is still a crossover between EVs and proteins in the fractions that were taken from the column, with some fractions containing both EVs and free protein from the medium. This method could therefore lead to ignoring smaller vesicles, which might be still be important for the studied effect, but which are found in fractions contaminated with protein. The amount of EVs that co-elute with protein could be reduced

by increasing the length of the column which might allow for greater separation of the samples. However, if the proteins eluting here are in-fact a similar size to the EVs, large protein aggregates for example, then this technique would not be able to separate them further.

5.3 EVs TREATMENT ALONE WAS NOT SUFFICIENT TO INDUCE CACHEXIA

Whilst EVs released by cancer cell lines were able to reduce muscle differentiation *in vitro* no effect was observed in mice. As previously stated, blocking RAB27a and b in cells that were used for xenograft reduced the levels of cachexia observed after transplantation (Zhang *et al.,* 2017). Whilst it is possible that our data show that EV release is not related to cachexia, it is also possible that the EV treatment was insufficient to induce cachexia.

The levels of EVs in the blood of the mice was not assessed here, and it is possible therefore that the EVs were at a low concentration within the circulation of the mice. On top of this whilst a tumour is continuously secreting vesicles, injections pump all the sample into the organism at once. It might be that sustained signalling is required to induce cachexia, whilst here mice were only exposed to cancer vesicles in short bursts. *In vivo* effects have been observed shortly after EV injection (Akbar *et al.,* 2017), here it might be that after 21 days the mice have become desensitised to the EVs, it might be interesting to study the blood and levels of DNA damage 24 hours following the injection of EVs to see what short term effects may be observed. More information and new techniques are required to accurately simulate a complete tumour secretome in order to truly test the effects of cancer EVs in animals. Further HSP70 and HSP90 were shown to be involved in cancer EV induced cachexia (Zhang *et al.,* 2017), but these proteins were not found to be in the EV samples in the LC-MS data. Therefore, it may be that the vesicles collected here are different from cachexia-inducing vesicles.

The biodistribution of the EVs in the mice was not established in these experiments, however EVs are thought to localise to the liver shortly after injection (Wiklander *et al.,* 2015; Lai *et al.,* 2014). These studies suggest that EVs do not persist inside of the organism for a particularly long time after they are injected into the animal. Here the ability of EVs from cisplatin-stressed cells to induce bystander damage in the spleen was assessed, however the liver was not assayed for DNA damage. It has been shown previously that radiation-treatment can induce bystander effects in the spleen (Ilnytskyy *et al.,* 2009), whilst no such effect was observed in this study. As EVs are known to mainly localise to the liver it may be that the EVs used in this experiment did not travel to the spleen in sufficient numbers to induce bystander effects, future experiments should examine whether any bystander damage is seen within the liver. It would also be useful to track the spread of EVs throughout the organism to determine where they may travel before arriving in the liver and being removed.

Whilst the *in vivo* effects of EVs can be assessed by blocking their release, this could potentially affect other biological functions, which could be the real causative factor for observed effects. Similarly, attempting to block EV uptake could induce changes in a model through off target effects. A multifaceted approach would therefore be the best way to examine the roles of EVs *in vivo*. If blocking EV release and EV uptake show similar effects, it would reduce the chances that the observed change is due to an off-target effect. It is also important to understand where the vesicles localise to in the mice. It maybe that the vesicles are all taken up within the tail of the mice, close to the site of their injection and are not able to spread further into the mouse.

5.4 Conclusions

EVs from heat-treated cells are able to induce bystander effects in unstressed populations of cells. This work corroborates findings in on both chemical and radiation-

induced bystander effect and suggest that EV induced bystander effects are a unified response to stress conditions.

Size Exclusion Chromatography has been shown to be able to separate most of the EVs in cell culture medium from the proteins that are also found in the medium. This method of extraction therefore allows a relatively pure sample to be isolated for further analysis.

EVs from cancer cells have been shown to be able to slow the differentiation of muscle precursor cells *in vitro,* however no effect was observed when these EVs were injected into mice. It is probably that this result is due to the difficulties associated with simulating the secretome of a tumour.

6 REFERENCES

Abels, E.R. & Breakefield, X.O., 2016. Introduction to Extracellular Vesicles: Biogenesis, RNA Cargo Selection, Content, Release, and Uptake. *Cellular and Molecular Neurobiology*, 36(3), pp.1–12.

Abou El Hassan, M. *et al.,*, 2015. Cancer cells hijack PRC2 to modify multiple cytokine pathways. *PLoS ONE*, 10(6), pp.1–19.

Ackerman, D. & Simon, M.C., 2014. Hypoxia, lipids, and cancer: surviving the harsh tumor microenvironment. *Trends in Cell Biology*, 24(8), pp.472–478.

Akbar, N. *et al.,*, 2017. Endothelium-derived extracellular vesicles promote splenic monocyte mobilization in myocardial infarction. *JCI Insight*, 2(17), p.e93344.

Akers, J.C. *et al.,*, 2013. Biogenesis of extracellular vesicles (EV): Exosomes, microvesicles, retrovirus-like vesicles, and apoptotic bodies. *Journal of Neuro-Oncology*, 113(1), pp.1–11.

Al-Mayah, A.H.J. *et al.,*, 2017. Exosome-Mediated Telomere Instability in Human Breast Epithelial Cancer Cells after X Irradiation. *Radiation Research*, 187(187), pp.98–106.

Al-Mayah, A.H.J. *et al.,*, 2012. Possible Role of Exosomes Containing RNA in Mediating Nontargeted Effect of Ionizing Radiation. *Radiation Research*, 177(5), pp.539–545.

Al-Mayah, A.H.J. *et al.,*, 2015. The non-targeted effects of radiation are perpetuated by exosomes. *Mutation Research/Fundamental and Molecular Mechanisms of Mutagenesis*, 772, pp.38–45.

An, T. *et al.,*, 2015. Exosomes serve as tumour markers for personalized diagnostics owing to their important role in cancer metastasis. *Journal of Extracellular Vesicles*, 1(4), pp.1–15.

Andreu, Z. & Yáñez-Mó, M., 2014. Tetraspanins in extracellular vesicle formation and function. *Frontiers in Immunology*, 5(SEP), p.442.

Aoi, W. & Marunaka, Y., 2014. Importance of pH homeostasis in metabolic health and diseases: crucial role of membrane proton transport. *BioMed research international*.

Aoyagi, T. *et al.,*, 2015. Cancer cachexia, mechanism and treatment. *World journal of gastrointestinal oncology*, 7(4), pp.17–29.

Argilés, J.M. *et al.,*, 2003. Cancer cachexia: the molecular mechanisms. *International Journal of Biochemistry & Cell Biology*, 35(4), p.405.

Asano, K. *et al.,*, 2004. Masking of phosphatidylserine inhibits apoptotic cell engulfment

and induces autoantibody production in mice. *The Journal of experimental medicine*, 200(4), pp.459–67.

Asara, J.M. *et al.,*, 2008. A label-free quantification method by MS/MS TIC compared to SILAC and spectral counting in a proteomics screen. *Proteomics*, 8(5), pp.994–999.

Ashkenazi, A., 2008. Targeting the extrinsic apoptosis pathway in cancer. *Cytokine and Growth Factor Reviews*, 19(3–4), pp.325–331.

Asur, R. *et al.,*, 2010a. Bystander effects induced by chemicals and ionizing radiation: Evaluation of changes in gene expression of downstream MAPK targets. *Mutagenesis*, 25(3), pp.271–279.

Asur, R. *et al.,*, 2010b. Involvement of MAPK proteins in bystander effects induced by chemicals and ionizing radiation. *Mutation Research - Fundamental and Molecular Mechanisms of Mutagenesis*, 686(1–2), pp.15–29.

Asur, R., Thomas, R. a & Tucker, J.D., 2009. Chemical induction of the bystander effect in normal human lymphoblastoid cells. *Mutation research*, 676(1–2), pp.11–6.

Atai, N.A. *et al.,*, 2013. Heparin blocks transfer of extracellular vesicles between donor and recipient cells. *Journal of Neuro-Oncology*, 115(3), pp.343–351.

Aust, S. *et al.,*, 2015. Skeletal muscle depletion and markers for cancer cachexia are strong prognostic factors in epithelial ovarian cancer. *PLoS ONE*, 10(10), pp.1–13.

Azzam, E.I., De Toledo, S.M. & Little, J.B., 2003. Oxidative metabolism, gap junctions and the ionizing radiation-induced bystander effect. *Oncogene*, 22, pp.7050–7057.

Baietti, M.F. *et al.,*, 2012. Syndecan–syntenin–ALIX regulates the biogenesis of exosomes. *Nature Cell Biology*, 14(7), pp.677–685.

Bakthisaran, R., Tangirala, R. & Rao, C.M., 2014. Small heat shock proteins: role in cellular functions and pathology. *Biochimica et biophysica acta*, 1854(4), pp.291–319.

Bao, Y.P. *et al.,*, 2002. Mammalian, yeast, bacterial, and chemical chaperones reduce aggregate formation and death in a cell model of oculopharyngeal muscular dystrophy. *Journal of Biological Chemistry*, 277(14), pp.12263–12269.

Barry, M. *et al.,*, 2000. Granzyme B short-circuits the need for caspase 8 activity during granule-mediated cytotoxic T-lymphocyte killing by directly cleaving Bid. *Molecular and Cellular Biology*, 20(11), pp.3781–3794.

Baskar, R., Balajee, A.S. & Geard, C.R., 2007. Effects of low and high LET radiations on bystander human lung fibroblast cell survival. *International Journal of Radiation Biology*, 83(8), pp.551–559.

Becker, A. *et al.,*, 2016. Extracellular Vesicles in Cancer: Cell-to-Cell Mediators of

Metastasis. *Cancer Cell*, 30(6), pp.836–848.

Beer, K.B. & Wehman, A.M., 2017. Mechanisms and functions of extracellular vesicle release in vivo—What we can learn from flies and worms. *Cell Adhesion and Migration*, 11(2), pp.135–150.

Bertolotti, A. *et al.,*, 2000. Dynamic interaction of BiP and ER stress transducers in the unfolded-protein response. *Nature Cell Biology*, 2(6), pp.326–332.

Bewicke-Copley, F. *et al.,*, 2017. Extracellular vesicles released following heat stress induce bystander effect in unstressed populations. *Journal of Extracellular Vesicles*, 6(1), p.1340746.

Bing, C. *et al.,*, 2006. Adipose atrophy in cancer cachexia: morphologic and molecular analysis of adipose tissue in tumour-bearing mice. *British Journal of Cancer*, 95(8), pp.1028–1037.

Bodmer, J.L. *et al.,*, 2000. TRAIL receptor-2 signals apoptosis through FADD and caspase-8. *Nature Cell Biology*, 2(4), pp.241–243.

Bøhn, S.K. *et al.,*, 2012. Stress associated gene expression in blood cells is related to outcome in radiotherapy treated head and neck cancer patients. *BMC Cancer*, 12(1), p.426.

Böing, A.N. *et al.,*, 2014. Single-step isolation of extracellular vesicles by size-exclusion chromatography. *Journal of Extracellular Vesicles*, 3(1).

Bonaldo, P. & Sandri, M., 2013. Cellular and molecular mechanisms of muscle atrophy. *Disease models & mechanisms*, 6(1), pp.25–39.

Bonetto, A., Andersson, D.C. & Waning, D.L., 2015. Assessment of muscle mass and strength in mice. *BoneKEy Reports*, 4(AUGUST), p.732.

Braakman, I. & Bulleid, N.J., 2011. Protein folding and modification in the Mammalian endoplasmic reticulum. *Annual review of biochemistry*, 80, pp.71–99.

Brestoff, J.R. & Artis, D., 2015. Immune regulation of metabolic homeostasis in health and disease. *Cell*, 161(1), pp.146–160.

Bridge, G., Rashid, S. & Martin, S.A., 2014. DNA mismatch repair and oxidative DNA damage: Implications for cancer biology and treatment. *Cancers*, 6(3), pp.1597–1614.

Buchner, J. & Li, J., 2013. Structure, Function and Regulation of the Hsp90 Machinery. *Biomedical Journal*, 36(3), p.106.

Burattini, S. *et al.,*, 2004. C2C12 murine myoblasts as a model of skeletal muscle development: Morpho-functional characterization. *European Journal of Histochemistry*, 48(3), pp.223–233.

Calderwood, S.K. *et al.,*, 2006. Heat shock proteins in cancer: Chaperones of tumorigenesis. *Trends in Biochemical Sciences*, 31(3), pp.164–172.

Cao, X. *et al.,*, 2007. Granzyme B and Perforin Are Important for Regulatory T Cell-Mediated Suppression of Tumor Clearance. *Immunity*, 27(4), pp.635–646.

Caron, E. & Hall, A., 1998. Identification of Two Distinct Mechanisms of Phagocytosis Controlled by Different Tho GTPases. *Science*, 282(November), pp.1717–1721.

Chargaff, E. & Randolph, W., 1946. The biological significance of the thromboplastic protein of blood. *Journal of Biological Chemistry*, 166(7), pp.189–197.

Chen, S. *et al.,*, 2009. Up-regulation of ROS by mitochondria-dependent bystander signaling contributes to genotoxicity of bystander effects. *Mutation research*, 666(1–2), pp.68–73.

Chen, X., Shen, J. & Prywes, R., 2002. The luminal domain of ATF6 senses endoplasmic reticulum (ER) stress and causes translocation of ATF6 from the er to the Golgi. *Journal of Biological Chemistry*, 277(15), pp.13045–13052.

Chen, Y. & Brandizzi, F., 2014. IRE1: ER stress sensor and cell fate executor. *Trends in Cell Biology*, 23(11), pp.22–25.

Cheng, E.H.Y. *et al.,*, 2001. BCL-2, BCL-X L sequester BH3 domain-only molecules preventing BAX- and BAK-mediated mitochondrial apoptosis. *Molecular Cell*, 8(3), pp.705–711.

Cheng, M.Y. *et al.,*, 1989. Mitochondrial heat-shock protein hsp60 is essential for assembly of proteins imported into yeast mitochondria. *Nature*, 337(6208), pp.620–625.

Cheung, W.L. *et al.,*, 2003. Apoptotic phosphorylation of histone H2B is mediated by mammalian sterile twenty kinase. *Cell*, 113(4), pp.507–517.

Chiaruttini, N. *et al.,*, 2015. Relaxation of Loaded ESCRT-III Spiral Springs Drives Membrane Deformation. *Cell*, 163(4), pp.866–879.

Cho, Y.L. *et al.,*, 2005. Amiloride potentiates TRAIL-induced tumor cell apoptosis by intracellular acidification-dependent Akt inactivation. *Biochemical and Biophysical Research Communications*, 326(4), pp.752–758.

Ciccia, A. & Elledge, S.J., 2010. The DNA Damage Response: Making It Safe to Play with Knives. *Molecular Cell*, 40(2), pp.179–204.

Clayton, A. *et al.,*, 2005. Induction of heat shock proteins in B-cell exosomes. *Journal of cell science*, 118(Pt 16), pp.3631–8.

Cocucci, E. & Meldolesi, J., 2015. Ectosomes and exosomes: Shedding the confusion between extracellular vesicles. *Trends in Cell Biology*, 25(6), pp.364–372.

Coin, F. *et al.,*, 2008. Nucleotide Excision Repair Driven by the Dissociation of CAK from

TFIIH. *Molecular Cell*, 31(1), pp.9–20.

Coleman, M.L. *et al.,*, 2001. Membrane blebbing during apoptosis results from caspase-mediated activation of ROCK I. *Nature cell biology*, 3(4), pp.339–345.

Colombo, M. *et al.,*, 2013. Analysis of ESCRT functions in exosome biogenesis, composition and secretion highlights the heterogeneity of extracellular vesicles. *Journal of cell science*, 126(Pt 24), pp.5553–65.

Corso, G. *et al.,*, 2017. Reproducible and scalable purification of extracellular vesicles using combined bind-elute and size exclusion chromatography. *Scientific Reports*, 7(1), pp.1–10.

Costa Verdera, H. *et al.,*, 2017. Cellular uptake of extracellular vesicles is mediated by clathrin-independent endocytosis and macropinocytosis. *Journal of Controlled Release*, 266(September), pp.100–108.

Couch, Y. *et al.,*, 2017. Inflammatory Stroke Extracellular Vesicles Induce Macrophage Activation. *Stroke*.

Cox, J. *et al.,*, 2014. Accurate Proteome-wide Label-free Quantification by Delayed Normalization and Maximal Peptide Ratio Extraction, Termed MaxLFQ. *Molecular & Cellular Proteomics*, 13(9), pp.2513–2526.

Crawford, N., 1971. The Presence of Contractile Proteins in Platelet Microparticles Isolated from Human and Animal Platelet-free Plasma. *British Journal of Haematology*, 21(1), pp.53–69.

Croft, D.R. *et al.,*, 2005. Actin-myosin-based contraction is responsible for apoptotic nuclear disintegration. *Journal of Cell Biology*, 168(2), pp.245–255.

Dąbrowska, A., Goś, M. & Janik, P., 2005. “Bystander effect” induced by photodynamically or heat-injured ovarian carcinoma cells (OVP10) in vitro. *Medical science monitor : international medical journal of experimental and clinical research*, 11(9), pp.BR316-R324.

Damke, H. *et al.,*, 1994. Induction of mutant dynamin specifically blocks endocytic coated vesicle formation. *Journal of Cell Biology*, 127(4), pp.915–934.

Deacon, R.M.J., 2013. Measuring the Strength of Mice. *Journal of Visualized Experiments*, (76), pp.1–4.

Deans, C. & Wigmore, S.J., 2005. Systemic inflammation, cachexia and prognosis in patients with cancer. *Current opinion in clinical nutrition and metabolic care*, 8, pp.265–269.

Dejean, L.M. *et al.,*, 2005. Oligomeric Bax Is a Component of the Putative Cytochrome c Release Channel MAC, Mitochondrial Apoptosis-induced Channel. *Molecular biology*

of the cell, 16(8), pp.2424–2432.

Dejean, L.M. *et al.,*, 2006. Regulation of the mitochondrial apoptosis-induced channel, MAC, by BCL-2 family proteins. *Biochimica et Biophysica Acta - Molecular Basis of Disease*, 1762(2), pp.191–201.

Desai, S. *et al.,*, 2014. Damaging and protective bystander cross-talk between human lung cancer and normal cells after proton microbeam irradiation. *Mutation research*, 763–764(January), pp.39–44.

Deshpande, A. *et al.,*, 1996. Alpha-particle-induced sister chromatid exchange in normal human lung fibroblasts: evidence for an extranuclear target. *Radiation research*, 145(3), pp.260–267.

Dewys, W.D. *et al.,*, 1980. Prognostic effect of weight loss prior tochemotherapy in cancer patients. *The American Journal of Medicine*, 69(4), pp.491–497.

Doherty, G.J. & McMahon, H.T., 2009. Mechanisms of Endocytosis. *Annual Review of Biochemistry*, 78(1), pp.857–902.

Dvorak, H.F. *et al.,*, 1981. Tumor shedding and coagulation. *Science*, 212(4497), pp.923–924.

Ekström, K. *et al.,*, 2012. Characterization of mRNA and microRNA in human mast cell-derived exosomes and their transfer to other mast cells and blood CD34 progenitor cells. *Journal of Extracellular Vesicles*, 1(0), pp.1–12.

Elmore, S., 2007. Apoptosis: a review of programmed cell death. *Toxicologic pathology*, 35(4), pp.495–516.

Ermolaeva, M.A. *et al.,*, 2008. Function of TRADD in tumor necrosis factor receptor 1 signaling and in TRIF-dependent inflammatory responses. *Nature Immunology*, 9(9), pp.1037–1046.

Evans, W.J., 2010. Skeletal muscle loss: cachexia, sarcopenia, and inactivity. *The American journal of clinical nutrition*, 91(4), p.1123S–1127S.

Fadda, E., 2016. Role of the XPA protein in the NER pathway: A perspective on the function of structural disorder in macromolecular assembly. *Computational and Structural Biotechnology Journal*, 14, pp.78–85.

Fearon, K.C.H. & Moses, A.G.W., 2002. Cancer cachexia. *International Journal of Cardiology*, 85(1), pp.73–81.

Feder, M.E. & Hofmann, G.E., 1999. Heat-Shock Proteins, Molecular Chaperones, and the Stress Response: Evolutionary and Ecological Physiology. *Annual Review Physiology*, 61, pp.243–282.

Feller, G., 2010. Protein stability and enzyme activity at extreme biological temperatures. *Journal of physics. Condensed matter : an Institute of Physics journal*, 22(32), pp.323101–321018.

Feng, D. *et al.,*, 2010. Cellular internalization of exosomes occurs through phagocytosis. *Traffic*, 11(5), pp.675–687.

Filipe, V., Hawe, A. & Jiskoot, W., 2010. Critical evaluation of nanoparticle tracking analysis (NTA) by NanoSight for the measurement of nanoparticles and protein aggregates. *Pharmaceutical Research*, 27(5), pp.796–810.

Foster, P.L., 2007. *Stress-Induced Mutagenesis in Bacteria*,

Foster, P.L., 2005. Stress responses and genetic variation in bacteria. *Mutation research*, 569(1–2), pp.3–11.

Fox, K.M. *et al.,*, 2009. Estimation of cachexia among cancer patients based on four definitions. *Journal of Oncology*, 2009.

Franzen, C. a. *et al.,*, 2014. Characterization of uptake and internalization of exosomes by bladder cancer cells. *BioMed Research International*, 2014, p.619829.

Fulda, S. *et al.,*, 2010. Cellular stress responses: cell survival and cell death. *International Journal of Cell Biology*, 2010, p.23.

Gaillard, H., García-Muse, T. & Aguilera, A., 2015. Replication stress and cancer. *Nature Reviews Cancer*, 15(5), pp.276–280.

Gámez-Valero, A. *et al.,*, 2016. Size-Exclusion Chromatography- based isolation minimally alters Extracellular Vesicles' characteristics compared to precipitating agents. *Nature Publishing Group*, (September), pp.1–9.

Giampietri, C. *et al.,*, 2015. Cancer microenvironment and endoplasmic reticulum stress response. *Mediators of Inflammation*, 2015.

Godwin, P. *et al.,*, 2013. Targeting Nuclear Factor-Kappa B to Overcome Resistance to Chemotherapy. *Frontiers in Oncology*, 3(May), pp.1–10.

Gómez-Ruiz, S. *et al.,*, 2012. On the discovery, biological effects, and use of cisplatin and metallocenes in anticancer chemotherapy. *Bioinorganic Chemistry and Applications*, 2012, pp.15–17.

Gregory, C.D. & Devitt, A., 2004. The macrophage and the apoptotic cell: An innate immune interaction viewed simplistically? *Immunology*, 113(1), pp.1–14.

Griesemer, M. *et al.,*, 2014. BiP Clustering Facilitates Protein Folding in the Endoplasmic Reticulum. *PLoS Computational Biology*, 10(7).

Gudbergsson, J.M. *et al.,*, 2015. Systematic review of factors influencing extracellular

vesicle yield from cell cultures. *Cytotechnology*.

Guo, P. *et al.,*, 2010. Sequential action of Caenorhabditis elegans Rab GTPases regulates phagolysosome formation during apoptotic cell degradation. *Proceedings of the National Academy of Sciences of the United States of America*, 107(42), pp.18016–18021.

Guo, W. *et al.,*, 2017. Exosomes: New players in cancer (Review). *Oncology reports*, 38(2), pp.665–675.

Habash, R.W.Y. *et al.,*, 2011. Principles, applications, risks and benefits of therapeutic hyperthermia Riadh. *Frontiers in Bioscience*, 3, pp.1169–1181.

Hakem, R., 2008. DNA-damage repair; the good, the bad, and the ugly. *The EMBO Journal*, 27(4), pp.589–605.

Hall, E.J., 2003. The Bystander Effect. *Health physics*, 85(1), pp.31–35.

Hanahan, D. & Weinberg, R.A., 2011. Hallmarks of cancer: The next generation. *Cell*, 144(5), pp.646–674.

Hanayama, R. *et al.,*, 2002. Identification of a factor that links apoptotic cells to phagocytes. *Nature*, 417(May), pp.182–187.

Hanson, P.I. *et al.,*, 2008. Plasma membrane deformation by circular arrays of ESCRT-III protein filaments. *Journal of Cell Biology*, 180(2), pp.389–402.

Haraszti, R.A. *et al.,*, 2016. High-resolution proteomic and lipidomic analysis of exosomes and microvesicles from different cell sources. *Journal of Extracellular Vesicles*, 5(1), pp.1–14.

Harding, C., Heuser, J. & Stahl, P., 1983. Receptor-mediated endocytosis of transferrin and recycling of the transferrin receptor in rat reticulocytes. *Journal of Cell Biology*, 97(2), pp.329–339.

Harding, H.P., Zhang, Y., *et al.,*, 2000. Perk is essential for translational regulation and cell survival during the unfolded protein response. *Molecular Cell*, 5(5), pp.897–904.

Harding, H.P., Novoa, I., *et al.,*, 2000. Regulated Translation Initiation Controls Stress-Induced Gene Expression in Mammalian Cells. *Molecular Cell*, 6(5), pp.1099–1108.

Hargett, L.A. & Bauer, N.N., 2013. On the origin of microparticles: From “platelet dust” to mediators of intercellular communication. *Pulmonary circulation*, 3(2), pp.329–340.

Hartl, F.U., Bracher, A. & Hayer-Hartl, M., 2011. Molecular chaperones in protein folding and proteostasis. *Nature*, 475(1), pp.324–332.

Hatayama, T. *et al.,*, 2001. Role of hsp105 in Protection against Stress-Induced Apoptosis in Neuronal PC12 Cells. *Biochemical and Biophysical Research Communications*, 288(3),

pp.528–534.

Haughey, N.J. *et al.,*, 2002. Disruption of neurogenesis by amyloid b -peptide , and perturbed neural progenitor cell homeostasis , in models of Alzheimer ' s disease. *Journal of Neurochemistry*, 83, pp.1509–1524.

Hawkins, L.A. & Devitt, A., 2013. Current Understanding of the Mechanisms for Clearance of Apoptotic Cells - A Fine Balance. *Journal of Cell Death*, 6, pp.57–68.

Hei, T.K. *et al.,*, 2008. Mechanism of radiation-induced bystander effects: a unifying model. *The Journal of pharmacy and pharmacology*, 60(8), pp.943–50.

Heminger, K.A. *et al.,*, 1997. Cisplatin inhibits protein synthesis in rabbit reticulocyte lysate by causing an arrest in elongation. *Archives of Biochemistry and Biophysics*, 344(1), pp.200–207.

Herskovits, J.S. *et al.,*, 1993. Effects of mutant rat dynamin on endocytosis. *Journal of Cell Biology*, 122(3), pp.565–578.

Hetz, C., 2012. The unfolded protein response: controlling cell fate decisions under ER stress and beyond. *Nature Reviews Molecular Cell Biology*, 13(2), pp.89–102.

Hewson, C. *et al.,*, 2016. Extracellular vesicle associated long non-coding RNAs functionally enhance cell viability. *Non-coding RNA Research*, 1(1), pp.3–11.

Hickman, A.W. *et al.,*, 1994. Alpha-particle-induced p53 protein expression in a rat lung epithelial cell strain. *Cancer research*, 54(22), pp.5797–5800.

Hirao, A. & Kong, Y., 2000. DNA Damage – Induced Activation of p53 by the Checkpoint Kinase Chk2. *Science*, 287(March), pp.1824–1827.

Hirata, H. *et al.,*, 1998. Caspases are activated in a branched protease cascade and control distinct downstream processes in Fas-induced apoptosis. *The Journal of experimental medicine*, 187(4), pp.587–600.

Hoesel, B. & Schmid, J.A., 2013. The complexity of NF-κB signaling in inflammation and cancer. *Molecular Cancer*, 12(1), p.1.

Hoffmann, J.H. *et al.,*, 2004. Identification of a redox-regulated chaperone network. *The EMBO Journal*, 23, pp.160–168.

Hoshino, A. *et al.,*, 2015. Tumour exosome integrins determine organotropic metastasis. *Nature*, 527(7578), pp.329–35.

Hsu, H. *et al.,*, 1996. TRADD-TRAF2 and TRADD-FADD interactions define two distinct TNF receptor 1 signal transduction pathways. *Cell*, 84(2), pp.299–308.

Hu, B. *et al.,*, 2006. The time and spatial effects of bystander response in mammalian cells induced by low dose radiation. *Carcinogenesis*, 27(2), pp.245–251.

Huang, D.W., Sherman, B.T. & Lempicki, R.A., 2009. Bioinformatics enrichment tools: Paths toward the comprehensive functional analysis of large gene lists. *Nucleic Acids Research*, 37(1), pp.1–13.

Huang, D.W., Sherman, B.T. & Lempicki, R.A., 2008. Systematic and integrative analysis of large gene lists using DAVID bioinformatics resources. *Nature Protocols*, 4, p.44.

Huang, K. *et al.,*, 2016. Cleavage by caspase 8 and mitochondrial membrane association activate the BH3-only protein bid during TRAIL-induced apoptosis. *Journal of Biological Chemistry*, 291(22), pp.11843–11851.

Huang, X. *et al.,*, 2013. Characterization of human plasma-derived exosomal RNAs by deep sequencing. *BMC genomics*, 14, p.319.

Hugel, B. *et al.,*, 2005. Membrane microparticles: two sides of the coin. *Physiology*, 20, pp.22–27.

Hurley, J.H., 2010. The ESCRT complexes. *Critical reviews in biochemistry and molecular biology*, 45(6), pp.463–87.

Hutchinson, F., 1966. The Molecular Basis for Radiation Effects on Cells The Molecular Basis for Radiation. *Cancer Research*, 26(1), pp.2045–2052.

Ichim, G. & Tait, S.W.G., 2016. A fate worse than death: apoptosis as an oncogenic process. *Nature Reviews Cancer*, 16(8), pp.539–548.

Ilnytskyy, Y., Koturbash, I. & Kovalchuk, O., 2009. Radiation-induced bystander effects in vivo are epigenetically regulated in a tissue-specific manner. *Environmental and Molecular Mutagenesis*, 113(December 2008), p.50:105-113.

Iyer, R.R. *et al.,*, 2008. The MutSα-proliferating cell nuclear antigen interaction in human DNA mismatch repair. *Journal of Biological Chemistry*, 283(19), pp.13310–13319.

Iyer, S.S. *et al.,*, 2009. Necrotic cells trigger a sterile inflammatory response through the Nlrp3 inflammasome. *Proceedings of the National Academy of Sciences of the United States of America*, 106(48), pp.20388–93.

Jackson, S.P. & Bartek, J., 2009. The DNA-damage response in human biology and disease. *Nature*, 461(7267), pp.1071–8.

Jacobs, A.L. & Schär, P., 2012. DNA glycosylases: In DNA repair and beyond. *Chromosoma*, 121(1), pp.1–20.

Jain, R. *et al.,*, 2015. Analysis of the pH-dependent stability and millisecond folding kinetics of horse cytochrome c. *Archives of Biochemistry and Biophysics*, 585, pp.52–63.

Jänicke, R.U. *et al.,*, 1998. Caspase-3 is required for DNA fragmentation and morphological changes associated with apoptosis. *The Journal of biological chemistry*, 273(16),

pp.9357–9360.

Jasin, M. & Rothstein, R., 2013. Repair of strand breaks by homologous recombination. *Cold Spring Harbor perspectives in biology*, 5(11).

Jeevanandam, M. *et al.,*, 1984. Cancer cachexia and protein metabolism. *The Lancet*, 1(8392), pp.1423–6.

Jella, K.K. *et al.,*, 2014. Exosomes are involved in mediating radiation induced bystander signaling in human keratinocyte cells. *Radiation research*, 181(2), pp.138–45.

Jelonek, K. *et al.,*, 2015. Ionizing radiation affects protein composition of exosomes secreted in vitro from head and neck squamous cell carcinoma. , 62(2), pp.265–272.

Jersmann, H.P.A. *et al.,*, 2003. Phagocytosis of apoptotic cells by human macrophages: Analysis by multiparameter flow cytometry. *Cytometry*, 51A(1), pp.7–15.

Jiang, X. & Wang, X., 2000. Cytochrome c promotes caspase-9 activation by inducing nucleotide binding to Apaf-1. *Journal of Biological Chemistry*, 275(40), pp.31199–31203.

Jin, C. *et al.,*, 2011. Induction of the bystander effect in Chinese hamster V79 cells by actinomycin D. *Toxicology Letters*, 202(3), pp.178–185.

Johnstone, R.M. *et al.,*, 1987. Vesicle formation during reticulocyte maturation. Association of plasma membrane activities with released vesicles (exosomes). *Journal of Biological Chemistry*, 262(19), pp.9412–9420.

Kadhim, M. *et al.,*, 2013. Non-targeted effects of ionising radiation-Implications for low dose risk. *Mutation Research - Reviews in Mutation Research*, 752(2), pp.84–98.

Kajimoto, T. *et al.,*, 2013. Ongoing activation of sphingosine 1-phosphate receptors mediates maturation of exosomal multivesicular endosomes. *Nature communications*, 4, p.2712.

Kälin, S. *et al.,*, 2010. Macropinocytotic uptake and infection of human epithelial cells with species B2 adenovirus type 35. *Journal of virology*, 84(10), pp.5336–5350.

Kalra, H., Drummen, G.P.C. & Mathivanan, S., 2016. Focus on extracellular vesicles: Introducing the next small big thing. *International Journal of Molecular Sciences*, 17(2).

Kampinga, H.H. & Craig, E.A., 2010. The HSP70 chaperone machinery: J proteins as drivers of functional specificity. *Nature Reviews. Molecular Cell Biology*, 11(8), pp.579–92.

Kawahara, T. *et al.,*, 1997. Endoplasmic reticulum stress-induced mRNA splicing permits synthesis of transcription factor Hac1p/Ern4p that activates the unfolded protein response. *Molecular Biology of the Cell*, 8(10), pp.1845–62.

Klumperman, J. & Raposo, G., 2014. The complex ultrastructure of the endolysosomal

system. *Cold Spring Harbor Perspectives in Biology*, 6(10).

Koivusalo, M. *et al.,*, 2010. Amiloride inhibits macropinocytosis by lowering submembranous pH and preventing Rac1 and Cdc42 signaling JCB: Correction. *J. Cell Biol*, 188(4), pp.547–563.

Końca, K. *et al.,*, 2003. A cross-platform public domain PC image-analysis program for the comet assay. *Mutation Research - Genetic Toxicology and Environmental Mutagenesis*, 534(1–2), pp.15–20.

Kotas, M.E. & Medzhitov, R., 2015. Homeostasis, Inflammation, and Disease Susceptibility. *Cell*, 160(5), pp.816–827.

Kothakota, S. *et al.,*, 1997. Caspase-3-Generated Fragment of Gelsolin: Effector of Morphological Change in Apoptosis. *Science*, 278(5336), pp.294–298.

Kowal, J. *et al.,*, 2016. Proteomic comparison defines novel markers to characterize heterogeneous populations of extracellular vesicle subtypes. *Proceedings of the National Academy of Sciences of the United States of America*, 113(8), pp.E968-77.

Kowal, J., Tkach, M. & Théry, C., 2014. Biogenesis and secretion of exosomes. *Current Opinion in Cell Biology*, 29(1), pp.116–125.

Kozutsumi, Y. *et al.,*, 1988. The presence of malfolded proteins in the endoplasmic reticulum signals the induction of glucose-regulated proteins. *Nature*, 332(6163), pp.462–464.

Krämer-Albers, E.-M.M. *et al.,*, 2007. Oligodendrocytes secrete exosomes containing major myelin and stress-protective proteins: Trophic support for axons? *Proteomics - Clinical Applications*, 1(11), pp.1446–1461.

Kress, M. *et al.,*, 1979. Simian virus 40-transformed cells express new species of proteins precipitable by anti-simian virus 40 tumor serum. *Journal of Virology*, 31(2), pp.472–483.

Krokan, H.E. & Bjoras, M., 2013. Base excision repair. *Cold Spring Harbor perspectives in biology*, 5(4), p.a012583.

Kuehn, M.J. & Kesty, N.C., 2005. Bacterial outer membrane vesicles and the host-pathogen interaction. *Genes & development*, 19(22), pp.2645–55.

Kuerbitz, S.J. *et al.,*, 1992. Wild-type p53 is a cell cycle checkpoint determinant following irradiation. *Proceedings of the National Academy of Sciences of the United States of America*, 89(16), pp.7491–5.

Kumar, N.B. *et al.,*, 2010. Cancer cachexia: Traditional therapies and novel molecular mechanism-based approaches to treatment. *Current Treatment Options in Oncology*,

11(3–4), pp.107–117.

Kunkel, T.A., 2004. DNA Replication Fidelity. *Journal of Biological Chemistry*, 279(17), pp.16895–16898.

Labreck, C.J. *et al.,*, 2017. The Protein Chaperone ClpX Targets Native and Non-native Aggregated Substrates for Remodeling , Disassembly , and Degradation with ClpP. *Frontiers in Molecular Biosciences*, 4(May), pp.1–13.

Lai, C.P. *et al.,*, 2014. Dynamic Biodistribution of Extracellular Vesicles In Vivo Using a Multimodal Imaging Reporter. *ACS Nano*, 8(1), pp.483–494.

Lane, D.P. & Crawford, L. V, 1979. T antigen is bound to a host protein in SV40-transformed cells. *Nature*, 278, pp.261–263.

Lane, R.E. *et al.,*, 2015. Analysis of exosome purification methods using a model liposome system and tunable-resistive pulse sensing. *Scientific reports*, 5, p.7639.

Larson, M.C. *et al.,*, 2012. Phosphatidylethanolamine is externalized at the surface of microparticles. *Biochimica et Biophysica Acta - Molecular and Cell Biology of Lipids*, 1821(12), pp.1501–1507.

Lauber, K. *et al.,*, 2003. Apoptotic cells induce migration of phagocytes via caspase-3-mediated release of a lipid attraction signal. *Cell*, 113(6), pp.717–730.

Lee Hamm, L., Nakhoul, N. & Hering-Smith, K.S., 2015. Acid-base homeostasis. *Clinical Journal of the American Society of Nephrology*, 10(12), pp.2232–2242.

Little, J.B., 2003. Genomic instability and bystander effects: a historical perspective. *Oncogene*, 22(45), pp.6978–6987.

Liu, X. *et al.,*, 1997. DFF, a heterodimeric protein that functions downstream of caspase-3 to trigger DNA fragmentation during apoptosis. *Cell*, 89(2), pp.175–184.

Lőrincz, Á.M. *et al.,*, 2014. Effect of storage on physical and functional properties of extracellular vesicles derived from neutrophilic granulocytes. *Journal of extracellular vesicles*, 3(0), p.25465.

Lötvall, J. *et al.,*, 2014. Minimal experimental requirements for definition of extracellular vesicles and their functions: a position statement from the International Society for Extracellular Vesicles. *Journal of extracellular vesicles*, 3, p.26913.

Lozano-Ramos, I. *et al.,*, 2015. Size exclusion chromatography-based enrichment of extracelluar vesicles from urine samples. *Journal of Extracellular Vesicles*, accepted f, pp.1–11.

Luo, J., Solimini, N.L. & Elledge, S.J., 2009. Principles of Cancer Therapy: Oncogene and Non-oncogene Addiction. *Cell*, 136(5), pp.823–837.

Lyng, F.M. *et al.,*, 2006. The involvement of calcium and MAP kinase signaling pathways in the production of radiation-induced bystander effects. *Radiation research*, 165(4), pp.400–409.

Lyng, F.M., Seymour, C.B. & Mothersill, C., 2000. Production of a signal by irradiated cells which leads to a response in unirradiated cells characteristic of initiation of apoptosis. *British journal of cancer*, 83(9), pp.1223–1230.

Magnoni, R. *et al.,*, 2014. The Hsp60 folding machinery is crucial for manganese superoxide dismutase folding and function. *Free Radical Research*, 48(2), pp.168–179.

Mak, R.H. & Cheung, W., 2006. Energy homeostasis and cachexia in chronic kidney disease. *Pediatric Nephrology*, 21(12), pp.1807–1814.

Malhotra, V. & Perry, M.C., 2003. Classical chemotherapy: mechanisms, toxicities and the therapeutic window. *Cancer biology & therapy*, 2(4 Suppl 1), pp.4–6.

Mallory, M. *et al.,*, 2015. Therapeutic hyperthermia: The old, the new, and the upcoming. *Critical Reviews in Oncology/Hematology*, 97, pp.56–64.

Mancuso, M. *et al.,*, 2008. Oncogenic bystander radiation effects in Patched heterozygous mouse cerebellum. *Proceedings of the National Academy of Sciences of the United States of America*, 105(34), pp.12445–12450.

Martinez-Caballero, S. *et al.,*, 2009. Assembly of the mitochondrial apoptosis-induced channel, MAC. *Journal of Biological Chemistry*, 284(18), pp.12235–12245.

Mashima, T., Naito, M. & Tsuruo, T., 1999. Caspase-mediated cleavage of cytoskeletal actin plays a positive role in the process of morphological apoptosis. *Oncogene*, 18(15), pp.2423–2430.

Matts, R.L. *et al.,*, 1992. Interactions of the Heme-regulated eIF-2a Kinase with Heat Shock Proteins in Rabbit Reticulocyte Lysates. *The Journal of biological chemistry*, 261(25), pp.18160–18167.

Maurel, M. *et al.,*, 2014. Getting RIDD of RNA: IRE1 in cell fate regulation. *Trends in Biochemical Sciences*, 39(5), pp.245–254.

Mazurov, D., Barbashova, L. & Filatov, A., 2013. Tetraspanin protein CD9 interacts with metalloprotease CD10 and enhances its release via exosomes. *FEBS Journal*, 280(5), pp.1200–1213.

Melo, S.A. *et al.,*, 2015. Cancer Exosomes Perform Cell-Independent MicroRNA Biogenesis and Promote Tumorigenesis. *Cancer Cell*, 26(5), pp.707–721.

Momen-Heravi, F. *et al.,*, 2013. Current methods for the isolation of extracellular vesicles. *Biological chemistry*, 394(10), pp.1253–62.

Monk, J.P. *et al.,*, 2006. Assessment of tumor necrosis factor alpha blockade as an intervention to improve tolerability of dose-intensive chemotherapy in cancer patients. *Journal of Clinical Oncology*, 24(12), pp.1852–1859.

Montagut, C. *et al.,*, 2006. Activation of nuclear factor-κ B is linked to resistance to neoadjuvant chemotherapy in breast cancer patients. *Endocrine Related Cancer*, 13(2), pp.607–616.

Montecalvo, A. *et al.,*, 2012. Mechanism of transfer of functional microRNAs between mouse dendritic cells via exosomes. *Blood*, 119(3), pp.756–766.

Morelli, A.E. *et al.,*, 2004. Endocytosis, intracellular sorting, and processing of exosomes by dendritic cells. *Blood*, 104(10), pp.3257–3266.

Mosser, D.D. & Morimoto, R.I., 2004. Molecular chaperones and the stress of oncogenesis. *Oncogene*, 23(16), pp.2907–2918.

Mothersill, C. *et al.,*, 2007. Characterization of a radiation-induced stress response communicated in vivo between zebrafish. *Environmental Science and Technology*, 41(9), pp.3382–3387.

Mothersill, C. *et al.,*, 2006. Communication of radiation-induced stress or bystander signals between fish in vivo. *Environmental Science and Technology*, 40(21), pp.6859–6864.

Mothersill, C. & Seymour, C.B., 1998. Cell-cell contact during gamma irradiation is not required to induce a bystander effect in normal human keratinocytes: evidence for release during irradiation of a signal controlling survival into the medium. *Radiation research*, 149(3), pp.256–262.

Mothersill, C. & Seymour, C.B., 1997. Medium from irradiated human epithelial cells but not human fibroblasts reduces the clonogenic survival of unirradiated cells. *International journal of radiation biology*, 71(4), pp.421–427.

Mulcahy, L.A., Pink, R.C. & Carter, D.R.F., 2014. Routes and mechanisms of extracellular vesicle uptake. *Journal of extracellular vesicles*, 3, pp.1–14.

Müller, M. *et al.,*, 1998. p53 Activates the CD95 (APO-1/Fas) Gene in Response to DNA Damage by Anticancer Drugs. *The Journal of Experimental Medicine*, 188(11), pp.2033–2045.

Muralidharan-Chari, V. *et al.,*, 2009. ARF6-regulated shedding of tumor-cell derived plasma membrane microvesicles. *Current Biology*, 19(22), pp.1875–1885.

Muralidharan-Chari, V. *et al.,*, 2010. Microvesicles: mediators of extracellular communication during cancer progression. *Journal of cell science*, 123(Pt 10), pp.1603–1611.

Mutschelknaus, L. *et al.*,, 2016. Exosomes derived from squamous head and neck cancer promote cell survival after ionizing radiation. *PLoS ONE*, 11(3).

Nabhan, J.F. *et al.*,, 2012. Formation and release of arrestin domain-containing protein 1-mediated microvesicles (ARMMs) at plasma membrane by recruitment of TSG101 protein. *Proceedings of the National Academy of Sciences of the United States of America*, 109(11), pp.4146–51.

Nagasawa, H. & Little, J.B., 1992. Induction of Sister Chromatid Exchanges by Extremely Low Doses of α -Particles. *Cancer Research*, 02115(4), pp.6394–6396.

Naik, E. *et al.*,, 2007. Ultraviolet radiation triggers apoptosis of fibroblasts and skin keratinocytes mainly via the BH3-only protein Noxa. *Journal of Cell Biology*, 176(4), pp.415–424.

Nathan, D.F., Vos, M.H. & Lindquist, S., 1997. In vivo functions of the Saccharomyces cerevisiae Hsp90 chaperone. *Proceedings of the National Academy of Sciences of the United States of America*, 94(24), pp.12949–56.

Neurath, H. *et al.*,, 1944. The Chemistry of Protein Denaturation. *Chemical Reviews*, 34(2), pp.157–265.

Newton, A.J., Kirchhausen, T. & Murthy, V.N., 2006. Inhibition of dynamin completely blocks compensatory synaptic vesicle endocytosis. *Proceedings of the National Academy of Sciences of the United States of America*, 103(47), pp.17955–17960.

Nicholas, B.D. *et al.*,, 2017. Protein Synthesis Inhibition and Activation of the c-Jun N-Terminal Kinase Are Potential Contributors to Cisplatin Ototoxicity. *Frontiers in Cellular Neuroscience*, 11(September), pp.1–14.

Nika, J., Rippel, S. & Hannig, E.M., 2001. Biochemical analysis of the eIF2βγ complex reveals a structural function for eIF2α in catalyzed nucleotide exchange. *Journal of Biological Chemistry*, 276(2), pp.1051–1056.

Nunes, J.M. *et al.*,, 2015. Action of the Hsp70 chaperone system observed with single proteins. *Nature Communications*, 6.

Ojima, M. *et al.*,, 2011. Radiation-induced bystander effects induce radioadaptive response by low-dose radiation. *Radiation Protection Dosimetry*, 146(1–3), pp.276–279.

Okamura, K. *et al.*,, 2000. Dissociation of Kar2p/BiP from an ER sensory molecule, Ire1p, triggers the unfolded protein response in yeast. *Biochemical and Biophysical Research Communications*, 279(2), pp.445–450.

Oliveira, D.L. *et al.*,, 2010. Characterization of yeast extracellular vesicles: evidence for the participation of different pathways of cellular traffic in vesicle biogenesis. *PloS one*,

5(6), p.e11113.

Ong, S.-E. *et al.,*, 2002. Stable Isotope Labeling by Amino Acids in Cell Culture, SILAC, as a Simple and Accurate Approach to Expression Proteomics. *Molecular & Cellular Proteomics*, 1(5), pp.376–386.

Ostrowski, M. *et al.,*, 2010. Rab27a and Rab27b control different steps of the exosome secretion pathway. *Nature cell biology*, 12(1), pp.19-30; sup pp 1–13.

Pan, B.T. *et al.,*, 1985. Electron microscopic evidence for externalization of the transferrin receptor in vesicular form in sheep reticulocytes. *Journal of Cell Biology*, 101(3), pp.942–948.

Pan, B.T. & Johnstone, R.M., 1983. Fate of the transferrin receptor during maturation of sheep reticulocytes in vitro: Selective externalization of the receptor. *Cell*, 33(3), pp.967–978.

Pan, L. *et al.,*, 2016. Exosomes-mediated transfer of long noncoding RNA ZFAS1 promotes gastric cancer progression. *Journal of Cancer Research and Clinical Oncology*, 0(0), p.0.

Panganiban, R.A.M., Snow, A.L. & Day, R.M., 2013. Mechanisms of radiation toxicity in transformed and non-transformed cells. *International Journal of Molecular Sciences*, 14(8), pp.15931–15958.

Pasupuleti, N. *et al.,*, 2010. The anti-apoptotic function of human αA-crystallin is directly related to its chaperone activity. *Cell Death and Disease*, 1(3), pp.e31-12.

Peinado, H. *et al.,*, 2017. Pre-metastatic niches: organ-specific homes for metastases. *Nature Reviews Cancer*.

Penna, F. *et al.,*, 2010. Anti-cytokine strategies for the treatment of cancer-related anorexia and cachexia. *Expert Opinion on Biological Therapy*, 10(8), pp.1241–1250.

Perez-Hernandez, D. *et al.,*, 2013. The intracellular interactome of tetraspanin-enriched microdomains reveals their function as sorting machineries toward exosomes. *Journal of Biological Chemistry*, 288(17), pp.11649–11661.

Pflaum, J., Schlosser, S. & MÃ¼ller, M., 2014. p53 Family and Cellular Stress Responses in Cancer. *Frontiers in Oncology*, 4(October), pp.1–15.

Ponnaiya, B. *et al.,*, 2004. Biological Responses in Known Bystander Cells Relative to Known Microbeam-Irradiated Cells. *Radiation Research*, 162(4), pp.426–432.

Porporato, P.E., 2016. Understanding cachexia as a cancer metabolism syndrome. *Oncogenesis*, 5(2), pp.e200-10.

Prada, I. & Meldolesi, J., 2016. Binding and fusion of extracellular vesicles to the plasma membrane of their cell targets. *International Journal of Molecular Sciences*, 17(8).

Prado, C.M.M. *et al.,*, 2009. Sarcopenia as a determinant of chemotherapy toxicity and time to tumor progression in metastatic breast cancer patients receiving capecitabine treatment. *Clinical Cancer Research*, 15(8), pp.2920–2926.

Prise, K.M. *et al.,*, 1998. Studies of bystander effects in human fibroblasts using a charged particle microbeam. *International journal of radiation biology*, 74(6), pp.793–798.

Prise, K.M., O'Sullivan, J.M. & O 'sullivan, J.M., 2009. Radiation-induced bystander signalling in cancer therapy. *Nature reviews. Cancer*, 9(5), pp.351–360.

Privalov, P.L. & Privalov, P.L., 1990. Cold Denaturation of Protein. *Critical Reviews in Biochemistry and Molecular Biology*, 25(5), pp.281–306.

Purschke, M. *et al.,*, 2011. Cell-cycle-dependent Active Thermal Bystander Effect (ATBE). *Lasers in Surgery and Medicine*, 43(3), pp.230–235.

Purschke, M. *et al.,*, 2010. Thermal injury causes DNA damage and lethality in unheated surrounding cells: active thermal bystander effect. *The Journal of Investigative Dermatology*, 130(1), pp.86–92.

Puthalakath, H. *et al.,*, 2007. ER Stress Triggers Apoptosis by Activating BH3-Only Protein Bim. *Cell*, 129(7), pp.1337–1349.

Quail, D. & Joyce, J., 2013. Microenvironmental regulation of tumor progression and metastasis. *Nature medicine*, 19(11), pp.1423–1437.

Raiborg, C. & Stenmark, H., 2009. The ESCRT machinery in endosomal sorting of ubiquitylated membrane proteins. *Nature*, 458(7237), pp.445–52.

Randow, F. & Seed, B., 2001. Endoplasmic reticulum chaperone gp96 is required for innate immunity but not cell viability. *Nature Cell Biology*, 3(10), pp.891–896.

Rastogi, R.P., Richa & Sinha, R.P., 2009. Apoptosis: Molecular mechanisms and pathogenicity. *EXCLI Journal*, 8, pp.155–181.

Ravichandran, K.S. & Lorenz, U., 2007. Engulfment of apoptotic cells: signals for a good meal. *Nature Reviews Immunology*, 7(december), pp.964–974.

Ray, P.D., Huang, B.-W. & Tsuji, Y., 2012. Reactive oxygen species (ROS) homeostasis and redox regulation in cellular signaling. *Cell Signal*, 24(5), pp.981–990.

Record, M. *et al.,*, 2011. Exosomes as intercellular signalosomes and pharmacological effectors. *Biochemical pharmacology*, 81(10), pp.1171–82.

Reid, M.B. & Li, Y.P., 2001. Tumor necrosis factor-alpha and muscle wasting: a cellular perspective. *Respiratory research*, 2(5), pp.269–72.

Richarme, G. & Kohiyama, M., 1993. Specificity of the Escherichia coli chaperone DnaK (70-kDa heat shock protein) for hydrophobic amino acids. *Journal of Biological Chemistry*,

268(32), pp.24074–24077.

Richter, K., Haslbeck, M. & Buchner, J., 2010. The Heat Shock Response: Life on the Verge of Death. *Molecular Cell*, 40(2), pp.253–266.

Ross, P.J. *et al.,*, 2004. Do patients with weight loss have a worse outcome when undergoing chemotherapy for lung cancers? *British Journal of Cancer*, 90(10), pp.1905–1911.

Rydén, M. & Arner, P., 2007. Fat loss in cachexia-is there a role for adipocyte lipolysis? *Clinical Nutrition*, 26(1), pp.1–6.

Saibil, H., 2013. Chaperone machines for protein folding, unfolding and disaggregation. *Nature Reviews Molecular Cell Biology*, 14(10), pp.630–642.

Samuel, P. *et al.,*, 2017. Cisplatin induces the release of extracellular vesicles from ovarian cancer cells that can induce invasiveness and drug resistance in bystander cells. *Philosophical Transactions of the Royal Society B: Biological Sciences*.

Samuel, P. *et al.,*, 2016. Over-expression of miR-31 or loss of KCNMA1 leads to increased cisplatin resistance in ovarian cancer cells. *Tumor Biology*, 37(2), pp.2565–2573.

Sato, P.H., Rosenberg, J.M. & Sato, R.I., 1996. Differences in the inhibition of translation by cisplatin, transplatin, and certain related compounds. *Biochemical Pharmacology*, 52(12), pp.1895–1902.

Segundo, C. *et al.,*, 1999. Surface molecule loss and bleb formation by human germinal center B cells undergoing apoptosis: role of apoptotic blebs in monocyte chemotaxis. *Blood*, 94(3), pp.1012–1020.

Shankar, B., Pandey, R. & Sainis, K., 2006. Radiation-induced bystander effects and adaptive response in murine lymphocytes. *International journal of radiation biology*, 82(8), pp.537–48.

Shao, C. *et al.,*, 2005. Bystander signaling between glioma cells and fibroblasts targeted with counted particles. *International Journal of Cancer*, 116(1), pp.45–51.

Shao, C. *et al.,*, 2003. Role of gap junctional intercellular communication in radiation-induced bystander effects in human fibroblasts. *Radiation research*, 160(3), pp.318–323.

Shen, B. *et al.,*, 2011. Protein targeting to exosomes/microvesicles by plasma membrane anchors. *Journal of Biological Chemistry*, 286(16), pp.14383–14395.

Shen, F. *et al.,*, 2018. Dynasore suppresses proliferation and induces apoptosis of the non-small-cell lung cancer cell line A549. *Biochemical and Biophysical Research Communications*, 495(1), pp.1158–1166.

Silva, J. *et al.,*, 2012. Analysis of exosome release and its prognostic value in human

colorectal cancer. *Genes Chromosomes and Cancer*, 51(4), pp.409–418.

Slee, E.A. *et al.,*, 1999. Ordering the Cythochrome-c-initiated Caspase Cascade: Hierarchical Activation of Caspases-2, -3, -6, -7, -8, and -10 in Caspase-9-dependent Manner. *The Journal of Cell Biology*, 144(2), pp.281–292.

Slee, E.A., Adrain, C. & Martin, S.J., 2001. Executioner Caspase-3, -6, and -7 Perform Distinct, Non-redundant Roles during the Demolition Phase of Apoptosis. *Journal of Biological Chemistry*, 276(10), pp.7320–7326.

Smith, H.A. & Kang, Y., 2014. The Metastasis-Promoting Roles of Tumor-Associated Immune Cells. *Journal of Molecular Medicine*, 91(4), pp.411–429.

Smith, R.W. *et al.,*, 2013. The induction of a radiation-induced bystander effect in fish transcends taxonomic group and trophic level. *International journal of radiation biology*, 89(4), pp.225–33.

Soleymanifard, S. *et al.,*, 2013. The role of target and bystander cells in dose-response relationship of radiation-induced bystander effects in two cell lines. *Iranian Journal of Basic Medical Sciences*, 16(2), pp.177–183.

Srdic, D. *et al.,*, 2016. Cancer cachexia, sarcopenia and biochemical markers in patients with advanced non-small cell lung cancer - chemotherapy toxicity and prognostic value. *Supportive Care in Cancer*, 24(11), pp.4495–4502.

Stennicke, H.R. *et al.,*, 1998. Pro-caspase-3 is a major physiologic target of caspase-8. *Journal of Biological Chemistry*, 273(42), pp.27084–27090.

Stuffers, S. *et al.,*, 2009. Multivesicular endosome biogenesis in the absence of ESCRTs. *Traffic*, 10(7), pp.925–937.

Sun, L. *et al.,*, 2015. Site-1 protease cleavage site is important for the ER stress-induced activation of membrane-associated transcription factor bZIP28 in Arabidopsis. *Science China Life Sciences*, 58(3), pp.270–275.

Takayama, S., Reed, J.C. & Homma, S., 2003. Heat-shock proteins as regulators of apoptosis. *Oncogene*, 22, pp.9041–9047.

Tang, H. *et al.,*, 2016. Interaction between Radioadaptive Response and Radiation-Induced Bystander Effect in Caenorhabditis elegans : A Unique Role of the DNA Damage Checkpoint. *Radiation Research*, 186(6), pp.662–668.

Taylor, R.C., Cullen, S.P. & Martin, S.J., 2008. Apoptosis: controlled demolition at the cellular level. *Nature reviews. Molecular cell biology*, 9(3), pp.231–241.

Testi, S. *et al.,*, 2016. Vincristine-induced bystander effect in human lymphocytes. *Mutation Research - Fundamental and Molecular Mechanisms of Mutagenesis*, 789, pp.39–47.

Thery, C. *et al.,*, 2001. Proteomic Analysis of Dendritic Cell-Derived Exosomes: A Secreted Subcellular Compartment Distinct from Apoptotic Vesicles. *The Journal of Immunology*, 166(12), pp.7309–7318.

Théry, C., Zitvogel, L. & Amigorena, S., 2002. Exosomes: composition, biogenesis and function. *Nature reviews. Immunology*, 2(8), pp.569–79.

Thust, R. *et al.,*, 2004. Cytogenetic detection of a trans-species bystander effect: Induction of sister chormatid exchanges in murine 3T3 cells by ganciclovir metabolized in HSV thymidine kinase gene-transfected Chinese hamster ovary cells. *Mutagenesis*, 19(1), pp.27–33.

Tirode, F. *et al.,*, 1999. Reconstitution of the transcription factor TFIIH: Assignment of functions for the three enzymatic subunits, XPB, XPD, and cdk7. *Molecular Cell*, 3(1), pp.87–95.

Tkach, M., Kowal, J. & Théry, C., 2018. Why the need and how to approach the functional diversity of extracellular vesicles. *Philosophical transactions of the Royal Society of London. Series B, Biological sciences*, 373(1737), p.20160479.

Tominaga, N., Katsuda, T. & Ochiya, T., 2015. Micromanaging of tumor metastasis by extracellular vesicles. *Seminars in Cell and Developmental Biology*, 40, pp.52–59.

Toossi, M.T.B. *et al.,*, 2017. Assessment of the dose-response relationship of radiation-induced bystander effect in two cell lines exposed to high doses of ionizing radiation (6 and 8 Gy). *Cell Journal*, 19(3), pp.434–442.

Trajkovic, K. *et al.,*, 2008. Ceramide triggers budding of exosome vesicles into multivesicular endosomes. *Science (New York, N.Y.)*, 319(5867), pp.1244–7.

Turner, C. *et al.,*, 2003. Macrophage-mediated clearance of cells undergoing caspase-3-independent death. *Cell Death and Differentiation*, 10(3), pp.302–312.

Twiddy, D. *et al.,*, 2006. Caspase-7 is directly activated by the ∼700-kDa apoptosome complex and is released as a stable XIAP-caspase-7 ∼200-kDa complex. *Journal of Biological Chemistry*, 281(7), pp.3876–3888.

Tyanova, S., Temu, T., Sinitcyn, P., *et al.,*, 2016. The Perseus computational platform for comprehensive analysis of (prote)omics data. *Nature Methods*, 13(9), pp.731–740.

Tyanova, S., Temu, T. & Cox, J., 2016. The MaxQuant computational platform for mass spectrometry-based shotgun proteomics. *Nature Protocols*, 11(12), pp.2301–2319.

Uma, S., Thulasiraman, V. & Matts, R.L., 1999. Dual role for Hsc70 in the biogenesis and regulation of the heme-regulated kinase of the alpha subunit of eukaryotic translation initiation factor 2. *Molecular and cellular biology*, 19(9), pp.5861–5871.

Valadi, H. *et al.,*, 2007. Exosome-mediated transfer of mRNAs and microRNAs is a novel mechanism of genetic exchange between cells. *Nature cell biology*, 9(6), pp.654–9.

Vanhoutte, G. *et al.,*, 2016. Cachexia in cancer: what is in the definition? *BMJ Open Gastroenterology*, 3(1), p.e000097.

Vanni, I. *et al.,*, 2017. Exosomes: a new horizon in lung cancer. *Drug Discovery Today*, 00(00), pp.1–10.

Vaughan, V.C., Martin, P. & Lewandowski, P.A., 2013. Cancer cachexia: Impact, mechanisms and emerging treatments. *Journal of Cachexia, Sarcopenia and Muscle*, 4(2), pp.95–109.

Velichko, A.K. *et al.,*, 2012. Dual effect of heat shock on DNA replication and genome integrity. *Molecular Biology of the Cell*, 23(17), pp.3450–3460.

Verweij, F.J. *et al.,*, 2011. LMP1 association with CD63 in endosomes and secretion via exosomes limits constitutive NF-κB activation. *The EMBO journal*, 30(11), pp.2115–2129.

Villarroya-Beltri, C. *et al.,*, 2014. Sorting it out: Regulation of exosome loading. *Seminars in Cancer Biology*, 28(1), pp.3–13.

Villarroya-Beltri, C. *et al.,*, 2013. Sumoylated hnRNPA2B1 controls the sorting of miRNAs into exosomes through binding to specific motifs. *Nature communications*, 4, p.2980.

Vousden, K.H. & Lu, X., 2002. Live or let die: The cell's response to p53. *Nature Reviews Cancer*, 2(8), pp.594–604.

Walter, P. & Ron, D., 2012. The Unfolded Protein Response: From stress pathway to homeostatic regulation. *Science*, 334(2011), pp.1081–1086.

Wang, C. & Youle, R.J., 2009. The role of mitochondria in apoptosis. *Annual review of genetics*, 43, pp.95–118.

Wang, M. *et al.,*, 2009. Role of the unfolded protein response regulator GRP78/BiP in development, cancer, and neurological disorders. *Antioxidants & redox signaling*, 11(9), pp.2307–16.

Wang, M. & Kaufman, R.J., 2014. The impact of the endoplasmic reticulum protein-folding environment on cancer development. *Nature Reviews Cancer*, 14(9), pp.581–597.

Webber, A.J. & Johnson, S.A., 1970. Platelet participation in blood coagulation aspects of hemostasis. *The American Journal of Pathology*, 60(1), pp.19–42.

Welton, J.L. *et al.,*, 2016. Proteomics analysis of vesicles isolated from plasma and urine of prostate cancer patients using a multiplex, aptamer-based protein array. *Journal of Extracellular Vesicles; Vol 5 (2016) incl supplements*, 1, pp.1–18.

Whitley, D., Goldberg, S.P. & Jordan, W.D., 1999. Heat shock proteins: a review of the molecular chaperones. *Journal of vascular surgery*, 29(4), pp.748–51.

Wickman, G.R. *et al.,*, 2013. Blebs produced by actin-myosin contraction during apoptosis release damage-associated molecular pattern proteins before secondary necrosis occurs. *Cell death and differentiation*, 20(10), pp.1293–305.

Wiklander, O.P.B. *et al.,*, 2015. Extracellular vesicle in vivo biodistribution is determined by cell source, route of administration and targeting. *Journal of Extracellular Vesicles*, 4(2015), pp.1–13.

Witwer, K.W. *et al.,*, 2013. Standardization of sample collection, isolation and analysis methods in extracellular vesicle research. *Journal of extracellular vesicles*, 2.

Wolf, P., 1967. The nature and significance of platelet products in human plasma. *British journal of haematology*, 13(3), pp.269–288.

Wu, J. *et al.,*, 2017. Heat Shock Proteins and Cancer. *Trends in Pharmacological Sciences*, 38(3), pp.226–256.

Xu, J. *et al.,*, 2017. Exosomes containing differential expression of microRNA and mRNA in osteosarcoma that can predict response to chemotherapy. *Oncotarget*, 8(44), pp.1–11.

Xu, S. *et al.,*, 2015. Exosome-mediated microRNA transfer plays a role in radiation-induced bystander effect. *RNA biology*, 6286(12), pp.1355–1363.

Xu, S. *et al.,*, 2014. MiR-21 is involved in radiation-induced bystander effects. *RNA biology*, 11(9), pp.1161–1170.

Yáñez-Mó, M.M. *et al.,*, 2015. Biological properties of extracellular vesicles and their physiological functions. *Journal of Extracellular Vesicles*, 4(2015), pp.1–60.

Yang, X. *et al.,*, 1998. Granzyme B mimics apical caspases. *Journal of Biological Chemistry*, 273(51), pp.34278–34283.

Yang, X. *et al.,*, 2001. Reconstitution of Caspase 3 Sensitizes MCF-7 Breast Cancer Cells to Doxorubicin- and Etoposide-induced Apoptosis Reconstitution of Caspase 3 Sensitizes MCF-7 Breast Cancer Cells to. *Cancer Research*, pp.348–354.

Yentrapalli, R. *et al.,*, 2017. Quantitative changes in the protein and miRNA cargo of plasma exosome-like vesicles after exposure to ionizing radiation. *International Journal of Radiation Biology*, 0(0), pp.1–37.

Yoshioka, Y. *et al.,*, 2013. Comparative marker analysis of extracellular vesicles in different human cancer types. *Journal of extracellular vesicles*, 2, pp.1–9.

Yuan, L. *et al.,*, 2015. Muscle-specific E3 ubiquitin ligases are involved in muscle atrophy of

cancer cachexia: An in vitro and in vivo study. *Oncology Reports*, 33(5), pp.2261–2268.

Zhan, R. *et al.,*, 2009. Heat shock protein 70 is secreted from endothelial cells by a non-classical pathway involving exosomes. *Biochemical and Biophysical Research Communications*, 387(2), pp.229–233.

Zhang, G. *et al.,*, 2013. Signaling mechanism of tumor cell-induced up-regulation of E3 ubiquitin ligase UBR2. *FASEB Journal*, 27(7), pp.2893–2901.

Zhang, G. *et al.,*, 2017. Tumor induces muscle wasting in mice through releasing extracellular Hsp70 and Hsp90. *Nature Communications*, 8(1), p.589.

Zhang, G., Jin, B. & Li, Y.-P., 2011. C/EBPβ mediates tumour-induced ubiquitin ligase atrogin1/MAFbx upregulation and muscle wasting. *The EMBO Journal*, 30(20), pp.4323–4335.

Zhang, G. & Li, Y.-P., 2012. p38β MAPK upregulates atrogin1/MAFbx by specific phosphorylation of C/EBPβ. *Skeletal Muscle*, 2(1), p.20.

Zhou, H. *et al.,*, 2009. Consequences of cytoplasmic irradiation: studies from microbeam. *Journal of radiation research*, 50 Suppl A(1), pp.A59-65.

Zhou, H. *et al.,*, 2002. Effects of irradiated medium with or without cells on bystander cell responses. *Mutation Research - Fundamental and Molecular Mechanisms of Mutagenesis*, 499(2), pp.135–141.

Zhou, H. *et al.,*, 2000. Induction of a bystander mutagenic effect of alpha particles in mammalian cells. *Proceedings of the National Academy of Sciences of the United States of America*, 97(5), pp.2099–104.

Zhou, H. *et al.,*, 2005. Mechanism of radiation-induced bystander effect: role of the cyclooxygenase-2 signaling pathway. *Proceedings of the National Academy of Sciences of the United States of America*, 102(41), pp.14641–6.

Zhou, H. *et al.,*, 2008. Mitochondrial function and nuclear factor-kappaB-mediated signaling in radiation-induced bystander effects. *Cancer research*, 68(7), pp.2233–40.

Zhou, H. *et al.,*, 2001. Radiation risk to low fluences of alpha particles may be greater than we thought. *Proceedings of the National Academy of Sciences of the United States of America*, 98(25), pp.14410–5.

Zong, W. *et al.,*, 2001. BH3-only proteins that bind pro-survival Bcl-2 family members fail to induce apoptosis in the absence of Bax and Bak service BH3-only proteins that bind pro-survival Bcl-2 family members fail to induce apoptosis in the absence of Bax and Bak. *Genes and Development*, pp.1481–1486.

Zou, H. *et al.,*, 1999. An APAf-1 · cytochrome C multimeric complex is a functional

apoptosome that activates procaspase-9. *Journal of Biological Chemistry*, 274(17), pp.11549–11556.

7 APPENDICES

7.1 GO TERMS ASSOCIATED WITH PROTEINS DEREGULATED IN CELLS FOLLOWING CISPLATIN TREATMENT.

Downregulated cell protein				
Biological Processes	**Count**	**Genes**	**PValue**	**Bonferroni**
GO:0019083~viral transcription	23	RPL14, RPL13, NUP93, NUP188, RPL38, NUP155, RPL28, RPS7, NDC1, RPS25, RPS27, AAAS, RPS28, RPS17, RAE1, RPL9, RPL8, RPL3, RPS13, RANBP2, RPL7A, TPR, RPS24	1.61E-13	3.15E-10
GO:0000398~mRNA splicing, via spliceosome	30	SNRPB2, SART3, SF3B4, YBX1, PNN, CTNNBL1, HNRNPA3, PRPF19, HNRNPM, DDX46, DHX16, PABPC1, HNRNPC, GEMIN6, BCAS2, PABPN1, SF1, RNPS1, SNW1, DDX5, EIF4A3, SRSF5, UPF3B, SRSF6, GTF2F2, CPSF7, SNRPF, HNRNPH1, CSTF1, RBM15	1.28E-12	2.51E-09
GO:0006413~translational initiation	24	ABCF1, ABCE1, RPL14, RPL13, EIF2S3, RPL38, RPL28, RPS7, RPS25, EIF3D, RPS27, EIF3A, RPS28, RPS17, EIF1AX, RPL9, EIF1AY, RPL8, RPL3, RPS13, RPL7A, PABPC1, EIF2B4, RPS24	1.46E-12	2.85E-09
GO:0000184~nuclear-transcribed mRNA catabolic process, nonsense-mediated decay	21	UPF1, RPL14, RPL13, RNPS1, RPL38, ETF1, RPL28, RPS7, RPS25, EIF4A3, RPS27, RPS28, UPF3B, RPS17, RPL9, RPL8, RPL3, RPS13, RPL7A, PABPC1, RPS24	4.19E-11	8.18E-08
GO:0006412~translation	28	ABCF1, MRPS14, RPL14, RPL13, PABPC4, RPL38, RPS25, MRPL11, RPS27, MRPL13, RPS28, RPL9, RPL8, RPL3, SLC25A2, RPL7A, RPS24, SLC25A4, SARS, SLC25A6, MRPS24, MRPL9, RPL28, GTF2H2, RPS7, RPS17, FARSB, RPS13	8.22E-10	1.61E-06
GO:0016032~viral process	29	XPO1, VIM, NUP93, NUP188, SCRIB, NDC1, CUL2, DYNLL1, RAE1, RANBP1, RANBP2, ZYX, TPR, ABCE1, MSH6, SLC25A4, UBR4, FDPS, SNW1, NXF1, NUP155, SGTA, AAAS, PLCG1, IPO7, PSMA4, IPO5, RBM15, DYNC1I2	7.61E-09	1.49E-05
GO:0006457~protein folding	22	TXNL1, FKBP9, GRPEL1, TXN2, CSNK2B, CCT2, MESDC2, PDIA4, LMAN1, CDC37, TRAP1, CCT5, CCT4, DNAJB11, GNB2, PPID, PFDN4, SIL1, HSPE1, RANBP2, DNAJB1, DNAJC1	1.33E-08	2.60E-05
GO:0006614~SRP-dependent cotranslational protein targeting to membrane	16	RPL14, RPL13, RPL38, SRPRB, RPL28, RPS7, RPS25, RPS27, RPS28, RPS17, RPL9, RPL8, RPL3, RPS13, RPL7A, RPS24	2.42E-08	4.73E-05
GO:0006406~mRNA export from nucleus	16	UPF1, NUP93, EIF5A, RNPS1, NUP188, NXF1, NUP155, NDC1, EIF4A3, SRSF5, UPF3B, AAAS, SRSF6, RAE1, RANBP2, TPR	5.70E-08	1.11E-04

GO:0006364~rRNA processing	23	TBL3, EXOSC6, RPL14, EMG1, RPL13, EXOSC5, RPL38, RPL28, RPS7, DIS3, RPS25, EIF4A3, SBDS, RPS27, RPS28, DKC1, RPS17, RPL9, RPL8, RPL3, RPS13, RPL7A, RPS24	6.08E-08	1.19E-04
GO:0006409~tRNA export from nucleus	9	NDC1, XPOT, AAAS, RAE1, NUP93, NUP188, RANBP2, NUP155, TPR	1.37E-06	2.68E-03
GO:0007077~mitotic nuclear envelope disassembly	10	NDC1, CDK1, AAAS, RAE1, NUP93, NEK9, NUP188, RANBP2, NUP155, TPR	1.85E-06	3.61E-03
GO:0075733~intracellular transport of virus	10	NDC1, XPO1, AAAS, RAE1, NUP93, NUP188, RANBP2, NUP155, TPR, KPNA2	6.74E-06	1.31E-02
GO:0006405~RNA export from nucleus	10	EIF4A3, SRSF5, UPF3B, SRSF6, NUP188, RNPS1, RANBP1, NXF1, NUP155, TPR	1.28E-05	2.47E-02
GO:0010827~regulation of glucose transport	8	NDC1, AAAS, RAE1, NUP93, NUP188, RANBP2, NUP155, TPR	2.06E-05	3.95E-02
Downregulated cell protein				
Molecular Function	**Count**	**Genes**	**PValue**	**Bonferroni**
GO:0044822~poly(A) RNA binding	126	RPL14, ZC3HAV1, RPL13, RBM4, EIF5A, SART3, PNN, DDX18, TRMT1L, EIF1AX, TARDBP, LUC7L2, PTBP3, API5, PABPN1, ACTN4, EMG1, SUCLG1, MYH9, PPP1CC, HUWE1, RCC2, RPS17, RPS13, MYBBP1A, MRPL44, ADD1, HMGB1, HMGB2, MRPS14, PABPC4, PRRC2B, PRRC2C, KNOP1, DAZAP1, RPS25, HNRNPA3, PPAN, PFN1, HNRNPM, EIF3D, RPS27, EIF3A, RPS28, DDX46, MACF1, BRIX1, RPL8, RPL3, HSPE1, PABPC1, RPL7A, HNRNPC, SEC23IP, RPS24, HNRNPAB, TBL3, MRPS24, FDPS, RNPS1, SNW1, NXF1, UBE2L3, DDX5, RPS7, SRSF5, UPF3B, CCT4, PPIB, PTCD3, SRSF6, CPNE3, TRIP6, HNRNPH1, METTL16, CSTF1, PHF6, ABCF1, TCOF1, TSNAX, YLPM1, YBX3, PDIA4, YBX1, PKM, RBM4B, SBDS, DKC1, TRMT6, QKI, ZYX, TPR, LBR, KHDRBS1, EXOSC6, HIST1H1B, SLC3A2, SF1, CCDC47, MRPL9, HLTF, UBE2N, EIF4A3, TRAP1, IPO5, ARCN1, CPSF7, KPNA2, GLRX3, TUFM, MTDH, SF3B4, MRPL11, MRPL13, EZR, CCDC124, DHX16, AATF, SSRP1, UPF1, NUCKS1, ETF1, RPL28, ILF2, UBTF, RBM15	1.29E-44	9.10E-42
GO:0005515~protein binding	331	TUBB2B, VAPA, RPL14, TUBB2A, RPL13, CCT2, TPD52, SART3, B2M, MAP3K7, CUL2, GTF2H2C, DDX18, DNAJB11, AGPS, EIF1AX, PLOD3, EIF1AY, LUC7L2, TMEM14C, EIF2B4, FTL, OPA1, KIF5B, MYH1, EMG1, STRN4, WNK1, UBR4, EIF2S3, MAGED2, MYH9, DCTN4, LETM1, HUWE1, RCC2, RFC1, RAB18, SURF4, RPS13, NEK9, MYBBP1A, MCTS1, MRPL44, CPSF3L, AHCY, TXN2, PABPC4, HSD17B12, UBA6, DUSP12, PPT1, PRRC1, PRRC2B, ASL, COIL, CDC37, TIPRL, SCRIB, RPS25, HNRNPA3, PLAA, PFN1, RPS27, RPS28, MACF1, GORASP2, RAC1, AGRN, PABPC1, SEC23IP, TUBB4A, HNRNPAB, FAM111B, PHB, FDXR, NXF1, UBE2L3, OCIAD1, DDX5, VDAC2, RPS7, CCT5, SRSF5, CCT4, UPF3B, AIDA, RNF4,	6.95E-20	4.88E-17

		PTCD3, SRSF6, AHSA1, ABCF1, RAB5C, ATP5B, COPS3, TSNAX, TCOF1, QARS, NFKB2, PDIA4, YBX1, PKM, RBM4B, MCCC2, LONP1, PBXIP1, DYNLL1, DNAJC13, DYNLL2, QKI, USP14, SYMPK, ABCE1, CCNK, SLC25A4, SLC25A6, EXOSC5, SF1, SLC3A2, MRPL9, NDUFA13, GTF2H2, TRAP1, EIF4A3, G6PD, GNB2, MED9, RRM1, PFDN4, FARSB, CNOT11, SIL1, EEF1D, DYNC1I2, TUFM, PREP, MTDH, LANCL1, HK1, EEA1, HDGFRP2, SF3B4, MIF, MRPL11, PRPF19, NUMA1, MRPL13, EZR, DHX16, RAB11A, AATF, TCEA1, BCL9, BCAS2, SSRP1, SHMT2, UPF1, NUB1, CSNK2B, ETF1, PCK2, CAPN2, RPL28, SGTA, SDHA, UBTF, ILF2, RAB34, RBM15, XPO1, ILKAP, ZC3HAV1, AP1G1, CRABP2, RBM4, EIF5A, CBX3, COX5B, CTNNBL1, PRKAR2A, GHITM, TARDBP, PGRMC1, PMS2, RPRD1A, DNAJC1, API5, CUTA, PABPN1, ACTN4, TOR1AIP1, BASP1, PPP1CC, PPP1CB, PSMA1, PSMA4, SIX1, PAF1, PDCD6IP, FLAD1, SNRPF, DYNLRB1, PRPS1, HMGB1, HMGB2, GNE, SNRPB2, NEDD8, ARPC4, LMAN1, PTRH2, EIF3D, HNRNPM, EIF3A, ISYNA1, GSTK1, RPL9, RPL3, HSPE1, RPL7A, HNRNPC, TBL3, EPB41, CCDC25, WDR5, AK3, ARID3B, RNPS1, SNW1, DENR, SUGT1, CTR9, EPS15, LAMP2, PLEKHA5, PLCG1, PPIB, PPID, POLD1, GTF2F2, CYFIP1, CPNE3, DNAJB1, TRIP6, HNRNPH1, CSTF1, GLYR1, FABP5, PHF6, HP1BP3, YLPM1, UCHL1, ESD, EDC4, PRDX3, SPRY4, HMOX2, SBDS, DKC1, GSN, PSMD2, ZYX, RANBP2, TPR, CSK, SUCLA2, CLINT1, LBR, KHDRBS1, SEC23A, CDK1, PRKCI, COX4I1, CCDC47, IPO9, PFKM, HLTF, HMGA2, MCM4, MCM5, TUT1, UBE2N, PPM1G, ALDH7A1, PSME1, IPO7, IPO4, IPO5, CPSF7, KPNA2, COPE, GLRX3, GALNT2, PPP4R1, NDUFB9, USP9X, VIM, NUP93, HCFC1, HAT1, RPA1, ANXA6, AKR1A1, TMED2, AP3M1, LARS, PAFAH1B3, VPS35, MYCBP, HSPA4, GEMIN6, NEFL, TNPO3, GPS1, MSH6, DNM1L, NCDN, SNX27, MAP1A, DPYSL2, NUP155, MEMO1, MGST3, NCSTN, DIS3, CLPTM1, DR1, TMEM43, SYNM, FAF1, CBS		
GO:0003723~RNA binding	54	XPO1, RPL14, RPL13, RBM4, EIF5A, QARS, YBX1, TRMT1L, DDX18, DKC1, RAE1, TARDBP, QKI, PTBP3, RANBP2, PABPN1, KHDRBS1, EMG1, SARS, EXOSC5, SF1, TUT1, PSMA1, FARSB, SNRPF, PABPC4, RPL38, DAZAP1, HNRNPA3, RPS25, EIF3D, HNRNPM, EIF3A, RPS28, RPL9, RPL8, BRIX1, RPL3, PABPC1, RPL7A, HNRNPC, HNRNPAB, UPF1, RNPS1, NXF1, ETF1, RPL28, RPS7, DIS3, SRSF5, ILF2, SRSF6, HNRNPH1, CSTF1	4.87E-16	3.12E-13
GO:0003735~structural constituent of ribosome	22	MRPS14, SLC25A4, RPL14, RPL13, SLC25A6, MRPS24, MRPL9, RPL38, RPL28, RPS7, MRPL11, MRPL13, RPS27, RPS28, RPS17, RPL9, RPL8, RPL3, RPS13, SLC25A2, RPL7A, RPS24	6.53E-07	4.59E-04

GO:0000166~nucleotide binding	27	PABPN1, RBM4, SNRPB2, PABPC4, RNPS1, NXF1, SART3, VDAC2, SF3B4, DAZAP1, TUT1, HNRNPA3, HNRNPM, RBM4B, SRSF5, UPF3B, SRSF6, TARDBP, POLD1, CPSF7, PTBP3, HNRNPC, PABPC1, HNRNPH1, RBM15, HNRNPAB, RPS24	2.95E-06	2.07E-03
GO:0008536~Ran GTPase binding	8	XPOT, XPO1, IPO7, IPO4, IPO5, IPO9, RANBP1, RANBP2	1.17E-05	8.22E-03
GO:0019904~protein domain specific binding	19	XPO1, HMGB2, VAPA, CSNK2B, PRKCI, CBX3, BASP1, MYH9, PPP1CC, HNRNPM, LAMP2, EZR, AIDA, RFC1, RCC2, DYNLL1, GSN, FAF1, NEFL	1.40E-05	9.82E-03
GO:0008565~protein transporter activity	11	AP1G1, IPO7, IPO4, IPO5, TSNAX, AP3D1, IPO9, VPS35, TIMM13, KPNA2, TNPO3	2.20E-05	1.54E-02
GO:0051082~unfolded protein binding	13	TRAP1, GRPEL1, CCT5, CCT4, PPIB, DNAJB11, PFDN4, SIL1, CCT2, HSPE1, DNAJB1, LMAN1, CDC37	4.10E-05	2.84E-02
GO:0098641~cadherin binding involved in cell-cell adhesion	22	ZC3HAV1, RPL14, KIF5B, VAPA, SLC3A2, EIF2S3, HCFC1, MYH9, SCRIB, EPS15, PKM, PFN1, EZR, MACF1, TMOD3, RANBP1, RPL7A, DNAJB1, EEF1D, AHSA1, CLINT1, ADD1	4.18E-05	2.90E-02
Upregulated cell protein				
Biological Processes	**Count**	**Genes**	**PValue**	**Bonferroni**
GO:0043488~regulation of mRNA stability	20	EXOSC2, HSPA1A, PSMA7, PSMA2, EIF4G1, PSMB5, PSMB4, NUP214, PSMB7, PSMA6, PSMB1, PSMD11, PSME2, SERBP1, ANP32A, PSMD3, HSPB1, PSME3, TNPO1, PSMD8	7.55E-11	1.52E-07
GO:0098609~cell-cell adhesion	31	RTN4, CNN3, VAPB, EIF2A, EPS15L1, HSPA1A, CAPZB, LARP1, BZW2, BZW1, DDX3X, RPL34, SND1, ARHGAP1, PCMT1, NUDC, PLEC, ZC3H15, RPL23A, FLNB, YWHAE, VASP, EIF4G1, TJP1, PRDX6, SERBP1, TMPO, NOP56, DBN1, YKT6, PAICS	1.92E-10	3.88E-07
GO:0000398~mRNA splicing, via spliceosome	27	RALY, POLR2L, SNRPD3, TRA2B, SNRPD1, SF3B5, POLR2B, SART1, HNRNPA3, HNRNPL, SRRT, DDX23, CLP1, PRPF8, LSM4, LSM3, DDX39A, DHX9, CSTF2, DDX39B, HNRNPA2B1, ALYREF, SRSF2, HNRNPUL1, PSPC1, CPSF2, CPSF1	9.49E-10	1.92E-06
GO:0006614~SRP-dependent cotranslational protein targeting to membrane	18	RPL35A, RPL17, SRP68, RPS9, RPL23A, RPS4X, SEC63, RPS19, RPL13A, RPL34, RPS14, RPS15, RPL3, RPL5, RPS11, RPS21, SEC61A1, SRP9	1.05E-09	2.11E-06
GO:0038061~NIK/NF-kappaB signaling	15	PSMA7, PSMA2, PSMB5, PSMB4, PSMB7, PSMB1, PSMA6, PSMD11, PSME2, UBA3, UBE2M, PSMD3, PSME3, CUL1, PSMD8	3.59E-09	7.25E-06
GO:0006413~translational initiation	20	RPL35A, RPL17, RPS9, EIF2A, RPL23A, RPS4X, EIF2B1, LARP1, EIF4G1, EIF4G3, RPS19, RPL13A, RPS14, RPL34, RPS15, DDX3Y, RPL3, RPL5, RPS11, RPS21	1.11E-08	2.24E-05
GO:0006521~regulation of cellular amino acid metabolic process	13	PSMA7, PSMB5, PSMA2, PSMB4, PSMB7, PSMB1, PSMA6, PSMD11, PSME2, PSMD3, PSME3, NQO1, PSMD8	1.36E-08	2.75E-05

GO:0006888~ER to Golgi vesicle-mediated transport	20	ARFGAP1, COPA, DYNC1LI2, VAPB, NAPA, TMED9, ERGIC1, DCTN1, BCAP31, CUL3, HYOU1, TMED7, COPG2, ANK3, MCFD2, ARF4, SEC22B, GOSR1, YKT6, GOLGB1	1.41E-07	2.85E-04
GO:0006364~rRNA processing	23	RPL35A, RPL17, EXOSC2, RPS9, RPL23A, LAS1L, WBP11, DIEXF, RPS4X, FBL, MRTO4, PA2G4, RPS19, RPL13A, RPS14, RPL34, RPS15, RPL3, NPM3, RPL5, RPS11, NOP56, RPS21	1.96E-07	3.96E-04
GO:0000184~nuclear-transcribed mRNA catabolic process, nonsense-mediated decay	17	PPP2R1A, RPL35A, RPL17, RPS9, RPL23A, RPS4X, EIF4G1, RPS19, RPL13A, RPL34, RPS14, PPP2CA, RPS15, RPL3, RPL5, RPS11, RPS21	2.49E-07	5.02E-04
GO:0008380~RNA splicing	20	RBFOX1, PPP2R1A, RBFOX2, SNRPD3, RBFOX3, DDX39B, SNRPD1, WBP11, IWS1, RRAGC, SRSF2, C1QBP, DDX23, PPP1R8, PPP2CA, SFPQ, PRPF8, ZRANB2, LSM4, LUC7L3	2.54E-07	5.12E-04
GO:0019083~viral transcription	16	NUP133, RPL35A, RPL17, RPS9, RPL23A, RPS4X, NUP214, RPS19, RPL13A, RPL34, RPS14, RPS15, RPL3, RPL5, RPS11, RPS21	6.21E-07	1.25E-03
GO:0006412~translation	24	RPL35A, RPL17, RPS9, RPL23A, RPS4X, SLC25A12, EIF4G1, MRPL23, RPS19, MRPL28, SLC25A24, RPL13A, RPS14, RPL34, MRPL17, RPS15, MRPL16, RPL3, HARS, RPL5, DHPS, RPS11, RPS21, SLC25A15	9.35E-07	1.89E-03
GO:0002479~antigen processing and presentation of exogenous peptide antigen via MHC class I, TAP-dependent	12	PSMA2, PSMB5, PSMB4, PSMB7, PSMA6, PSMB1, PSMD11, PSME2, PSMD3, PSME3, PSMA7, PSMD8	1.38E-06	2.77E-03
GO:0051437~positive regulation of ubiquitin-protein ligase activity involved in regulation of mitotic cell cycle transition	13	PSMA7, PSMB5, PSMA2, PSMB4, PSMB7, PSMB1, PSMA6, PSMD11, PSME2, PSMD3, PSME3, CUL1, PSMD8	1.40E-06	2.82E-03
GO:0031145~anaphase-promoting complex-dependent catabolic process	13	PSMA7, PSMB5, CUL3, PSMA2, PSMB4, PSMB7, PSMB1, PSMA6, PSMD11, PSME2, PSMD3, PSME3, PSMD8	2.14E-06	4.31E-03
GO:0006396~RNA processing	14	ATXN1, HNRNPL, DHX9, HNRNPUL1, SNRPD3, RBM3, PNPT1, SNRPD1, LSM4, WBP11, SSB, HNRNPDL, RTCA, ADAR	3.45E-06	6.94E-03
GO:0051436~negative regulation of ubiquitin-protein ligase activity involved in mitotic cell cycle	12	PSMA2, PSMB5, PSMB4, PSMB7, PSMA6, PSMB1, PSMD11, PSME2, PSMD3, PSME3, PSMA7, PSMD8	4.67E-06	9.38E-03
GO:0060071~Wnt signaling pathway, planar cell polarity pathway	13	PSMA7, PSMB5, PSMA2, PSMB4, AP2B1, PSMB7, PSMB1, PSMA6, PSMD11, PSME2, PSMD3, PSME3, PSMD8	1.09E-05	2.17E-02

GO:0006418~tRNA aminoacylation for protein translation	9	IARS, CARS, YARS, AARS, GARS, HARS, EPRS, DARS2, PPA1	1.36E-05	2.71E-02
GO:0006457~protein folding	18	PDIA3, AARS, TMX3, CCT3, MOGS, CALR, CCT7, PFDN2, ERP44, TBCA, PFDN5, TBCD, MPDU1, DNAJC7, QSOX2, NUDC, HSPA9, FKBP2	1.49E-05	2.96E-02
GO:0000209~protein polyubiquitination	18	UBE2V2, PSMA7, PSMA2, LNPEP, PSMB5, CUL3, PSMB4, PSMB7, PSMA6, PSMB1, PSMD11, PSME2, UBR5, PSMD3, PSME3, PSMD8, TRIP12, CUL1	1.99E-05	3.93E-02
GO:0043161~proteasome-mediated ubiquitin-dependent protein catabolic process	19	CSNK1A1, NSFL1C, MTA1, PSMA7, PSMA2, PSMB5, CUL3, PSMB4, PSMB7, PSMA6, PSMB1, PSMD11, UBE2K, PSME2, PPP2CB, PSMD3, PSME3, PSMD8, CUL1	2.00E-05	3.95E-02
Upregulated cell protein				
Molecular Function	**Count**	**Genes**	**PValue**	**Bonferroni**
GO:0044822~poly(A) RNA binding	126	RALY, DYNC1LI1, FLYWCH2, RPL17, SNRPD3, RBM3, SRP68, XRCC6, SNRPD1, CCT3, SART1, TOP1, DDX23, SND1, TIA1, TPT1, LSM4, LSM3, NQO1, LUC7L3, GNL3, DDX39A, RBFOX2, GTPBP1, RPL35A, CHTOP, YARS, DDX39B, HNRNPA2B1, CTNNA1, MRTO4, PA2G4, RPS19, RPS14, TIAL1, SERBP1, RPS15, HSPB1, EDF1, RPS11, MDH2, PUS1, DIAPH1, PNPT1, IGF2BP2, PRRC2A, CALR, PUS7, MANF, HNRNPA3, HNRNPL, HIST1H4A, DDX3X, RPL3, BTF3, NPM3, RPL5, RPS21, DHX9, P4HB, ZC3H15, CSTF2, ZC3H18, LGALS1, NTPCR, RPS9, SSB, RPL23A, SRSF2, HDAC2, CIRBP, HSPD1, SMC1A, ADAR, RTN4, IBA57, PDIA3, DEK, LARP1, BZW1, RTF1, ANP32A, HIST1H1E, HIST1H1D, SSBP1, DIEXF, LAS1L, RPS4X, NCL, FLNB, EIF4G1, EIF4G3, TBCA, ADK, UCHL5, MATR3, FAM98B, TRA2B, BCCIP, WBP11, POLR2B, SEC63, SRRT, PRPF8, CSDE1, CEBPZ, TNPO1, RTCA, HSPA9, PLEC, IMMT, ALYREF, HNRNPDL, YWHAE, FBL, LRP1, MRPL28, RPL13A, HNRNPUL1, TSFM, IFIT5, SFPQ, PSPC1, ZRANB2, NOP56, GOLGB1	3.93E-42	2.61E-39
GO:0005515~protein binding	343	LDHB, SNCG, DYNC1LI1, RPL17, HM13, PDLIM7, VAPB, THOP1, PPP2R5D, SRP68, XRCC6, SNCA, CCT3, ANKLE2, WDR82, SART1, CUL3, ACBD3, ATP2B4, APOE, NT5C2, PQBP1, LSM4, LSM3, FAS, CAB39, CUL1, LUC7L3, PLD3, CHTOP, YARS, RAP1GDS1, CTNNA1, ERGIC1, DCTN1, SPAG9, NME2, PPP1CA, RPS19, RPS14, UBR5, SERBP1, MED17, RPS15, RPS11, ARL8B, MRPL48, CHORDC1, DBN1, TMX3, CHCHD2, ARF6, IGF2BP2, PRRC2A, HSPA1A, CALR, BANF1, CALU, HNRNPA3, TPI1, PFN2, DRAP1, WDHD1, NUDC, TIGAR, DHX9, UFSP2, ZC3H15, MAP2K1, ZC3H18, LGALS1, RPS9, EPRS, TFCP2, OXSR1, LACTB2, PTPN11, NCKAP1, CCT7, SRSF2, WDR61, ARF4, UBA3, FNBP4, PCNA, ADAR, RTN4, COPS2, PDIA3, NIF3L1, FAM3C, EIF2A, TERF2IP, LNPEP,	5.11E-19	3.40E-16

		MTHFD1, HSPH1, AP2B1, GBAS, ANP32A, TICAM2, GSTZ1, RAB6A, ARHGEF4, CTBP1, HIST1H1E, ACO1, EXOSC2, POLR1C, DARS2, CYB5B, KLHDC4, FLNB, ATP6V1C1, PFDN2, CLIC4, PFDN5, RIPK1, MTAP, CAND1, SRP9, POLR2L, BCCIP, POLR2B, SUMO3, SRRT, NUP214, PPP2CA, PPP2CB, MPDU1, CSDE1, ABCD3, PCMT1, TRIP12, FEN1, AGL, PLEC, CSNK1A1, CAPN7, MAT2A, IMMT, NSFL1C, HNRNPDL, EIF2B1, YWHAE, IWS1, NAE1, CAPN1, MRPL23, ERP44, RPS6KA3, TJP1, LRP1, MRPL28, HNRNPUL1, PPP1R8, PSMD11, SFPQ, POLDIP2, DPM1, NOP56, UBXN7, PAICS, UBXN4, NCLN, DNM2, GOLGB1, RALY, RBM3, SNRPD3, CNOT3, SNRPD1, UBQLN4, UBQLN2, COX5A, VCL, TOP1, DDX23, ANK3, SND1, TIA1, TIMM9, TPT1, DNAJC7, RPRD1B, NQO1, NQO2, GNL3, DDX39A, RBFOX1, NUP133, RPL35A, RBFOX2, CARS, STMN2, DFFA, DDX39B, HNRNPA2B1, STK26, MTA1, TECR, POR, BCAP31, MRTO4, PSMA2, SUZ12, PA2G4, PSMA6, EDF1, HSPB1, VAMP3, VAMP2, VPS26A, PACS1, SRI, ARFGAP1, MYL6, DIAPH1, GLUD1, PNPT1, PTK7, COPS7A, UBE2V2, NAPA, PSMA7, RRAGD, RRAGC, PSMB5, HNRNPL, PSMB4, PSMB7, PSMB1, DDX3X, HIST1H4A, RPL3, BTF3, NPM3, RPL5, CLASP2, SEC61A1, MRPS27, P4HB, CSTF2, FOCAD, MYO1C, SSB, RPL23A, MYL12B, TSN, MYL12A, CORO1C, LAMP1, TXNDC12, HDAC2, PRKAR1A, RHOT1, NELFB, RAP1A, RHOT2, CIRBP, RAP1B, HSPD1, SMC1A, XPO7, PDCD6, CLTB, PRKAG1, EPS15L1, PIP5K1A, PTMA, TMF1, LARP1, GSS, RTF1, ARHGAP1, PSMD3, NDUFS3, PPP2R1A, IK, SSBP1, PIGT, DIEXF, STXBP3, TBCEL, RPS4X, MCM3, PMM2, NCL, HMGA1, VASP, ARL3, EIF4G1, TBCB, C1QBP, TBCA, PRDX6, UBE2K, PSME2, TBCD, UBE2M, UCHL5, PSME3, UCHL3, DHPS, KPNA3, CPSF2, CPSF1, EPN1, UGP2, MATR3, FKBP2, UQCRB, MYDGF, TRA2B, ASNS, WBP11, ESYT1, SEC63, RPA3, IARS, CHD1L, PRPF8, TMED1, SEC22B, PIK3R4, TNPO1, CHD4, HSPA9, GBA, WDFY1, NDUFA9, ALYREF, TMED9, ANXA5, SMC3, FBL, ATXN1, SCFD1, IFIT1, PSPC1, ZRANB2, APIP, CRK, RCN1		
GO:0003723~RNA binding	52	RALY, RBM3, SNRPD1, CNP, TIA1, LSM3, RBFOX1, RBFOX2, ACO1, RBFOX3, HNRNPA2B1, EXOSC2, RPS4X, NCL, EIF4G1, SUZ12, EIF4G3, PSMA6, RPS14, UBR5, TIAL1, RPS15, CPSF2, SRP9, PUS1, SKIV2L, PNPT1, PUS7, HNRNPL, HNRNPA3, DDX3X, RPL34, PRPF8, DDX3Y, RPL3, RPL5, RTCA, CSTF2, SSB, TSN, FBL, ATXN1, MRPL23, IFIT1, HNRNPUL1, PPP1R8, IFIT5, ZRANB2, CIRBP, NOP56, SRBD1, ADAR	6.24E-14	4.15E-11
GO:0098641~cadherin binding involved in cell-cell adhesion	33	RTN4, CNN3, VAPB, HSPA1A, EIF2A, EPS15L1, CAPZB, VCL, LARP1, BZW2, BZW1, DDX3X, RPL34, SND1, ARHGAP1, PCMT1, NUDC, PLEC, ZC3H15, RPL23A, CTNNA1, FLNB, YWHAE,	4.98E-11	3.31E-08

		VASP, EIF4G1, TJP1, PRDX6, SERBP1, TMPO, NOP56, DBN1, YKT6, PAICS		
GO:0003735~structural constituent of ribosome	24	RPL35A, RPL17, MRPS34, NDUFA7, RPS9, RPL23A, RPS4X, MRTO4, SLC25A12, MRPL23, RPS19, MRPL28, SLC25A24, RPL13A, RPS14, RPL34, MRPL17, RPS15, MRPL16, RPL3, RPL5, RPS11, RPS21, SLC25A15	8.83E-08	5.87E-05
GO:0000166~nucleotide binding	28	RALY, TRA2B, RBM3, HINT2, IGF2BP2, HNRNPA3, HNRNPL, SRRT, CHD1L, TIA1, NT5C2, RBFOX1, RBFOX2, CSTF2, RBFOX3, ALYREF, HNRNPA2B1, SSB, RPL23A, HNRNPDL, NCL, MRPL23, SRSF2, TIAL1, SFPQ, PSPC1, CIRBP, MATR3	2.38E-06	1.58E-03
GO:0003729~mRNA binding	15	RBFOX1, RBFOX2, CSTF2, TRA2B, RBFOX3, IGF2BP2, SSB, EIF2A, TSN, CALR, HNRNPA3, C1QBP, RPL13A, PPP1R8, LUC7L3	1.22E-05	8.09E-03
GO:0004298~threonine-type endopeptidase activity	7	PSMA2, PSMB5, PSMB4, PSMB7, PSMA6, PSMB1, PSMA7	1.89E-05	1.25E-02
GO:0005524~ATP binding	69	ATP5D, DYNC1LI1, DYNC1LI2, PRKAG1, XRCC6, DTYMK, CCT3, PIP5K1A, GSS, MTHFD1, HSPH1, ACTG2, ATP2B4, DDX23, CLP1, DDX39A, CARS, YARS, SUCLG2, ACTA2, STK26, AARS, DDX39B, DARS2, MCM3, ATP6V1A, NME2, UBE2K, ADK, RIPK1, UBE2M, HARS, CHORDC1, BTAF1, POMK, GLUD1, SKIV2L, PTK7, ASNS, HSPA1A, IARS, CHD1L, DDX3X, DDX3Y, ABCD3, PIK3R4, RTCA, CHD4, HSPA9, CSNK1A1, DHX9, MAT2A, MAP2K1, MYO1C, NTPCR, GARS, EPRS, OXSR1, SMC3, ATAD1, CCT7, HYOU1, RPS6KA3, NME2P1, NME1-NME2, UBA3, HSPD1, SMC1A, PAICS	6.19E-05	4.03E-02

7.2 KEGG PATHWAY ANALYSIS OF CELLULAR PROTEINS

Upregulated proteins				
Term	**Count**	**Genes**	**PValue**	**Bonferroni**
hsa03050:Proteasome	12	PSMA2, PSMB5, PSMB4, PSMB7, PSMA6, PSMB1, PSMD11, PSME2, PSMD3, PSME3, PSMA7, PSMD8	6.68E-07	1.54E-04
hsa03010:Ribosome	18	RPL35A, RPL17, RPS9, RPL23A, RPS4X, MRPL23, RPS19, MRPL28, RPL13A, RPS14, RPL34, MRPL17, MRPL16, RPS15, RPL3, RPL5, RPS11, RPS21	2.04E-05	4.69E-03
hsa01130:Biosynthesis of antibiotics	22	LDHB, DLST, ACO2, CYP51A1, ACO1, SUCLG2, PGD, PSPH, ALDH3A2, GPI, NME2, TPI1, GOT1, NME1-NME2, ADSL, IDI1, BPNT1, PAICS, MDH2, HSD17B7, UGP2, ALDH9A1	7.84E-05	1.79E-02

hsa03040:Spliceosome	16	TRA2B, SNRPD3, DDX39B, ALYREF, SNRPD1, WBP11, HSPA1A, SF3B5, SART1, HNRNPA3, SRSF2, DDX23, PRPF8, PQBP1, LSM4, LSM3	2.05E-04	4.60E-02
Downregulated proteins				
Term	**Count**	**Genes**	**PValue**	**Bonferroni**
hsa03013:RNA transport	26	XPO1, PABPC4, NUP93, NUP188, PNN, NDC1, EIF3D, EIF3A, RAE1, EIF1AX, EIF1AY, RANBP2, PABPC1, TPR, GEMIN6, EIF2B4, XPOT, UPF1, EIF2S3, RNPS1, NXF1, NUP155, EIF4A3, AAAS, UPF3B, CYFIP1	8.27E-09	1.72E-06
hsa01130:Biosynthesis of antibiotics	27	BCAT2, ADPGK, HK1, ASL, PKM, ISYNA1, AKR1A1, IDH2, PDHA1, SUCLA2, HADH, SHMT2, SUCLG1, AK3, FDPS, AK4, PFKM, PCK2, IDH3A, SDHA, ALDH7A1, G6PD, GFPT1, PCYOX1, PSAT1, CBS, PRPS1	1.45E-07	3.02E-05
hsa03015:mRNA surveillance pathway	16	PABPN1, SYMPK, UPF1, PABPC4, RNPS1, NXF1, PPP1CC, ETF1, PPP1CB, PNN, DAZAP1, EIF4A3, UPF3B, CPSF7, PABPC1, CSTF1	1.77E-06	3.68E-04
hsa03010:Ribosome	19	MRPS14, RPL14, RPL13, MRPL9, RPL38, RPL28, RPS7, MRPL11, RPS25, MRPL13, RPS27, RPS28, RPS17, RPL9, RPL8, RPL3, RPS13, RPL7A, RPS24	4.40E-06	9.16E-04
hsa01200:Carbon metabolism	15	SHMT2, ADPGK, SUCLG1, ESD, HK1, PFKM, IDH3A, PKM, SDHA, G6PD, IDH2, PDHA1, SUCLA2, PSAT1, PRPS1	1.08E-04	2.23E-02
hsa03040:Spliceosome	16	BCAS2, SNRPB2, SNW1, DDX5, SF3B4, CTNNBL1, HNRNPA3, PRPF19, EIF4A3, HNRNPM, SRSF5, DDX46, SRSF6, DHX16, HNRNPC, SNRPF	1.81E-04	3.70E-02
Protein only in cisplatin-treated cells				
Term	**Count**	**Genes**	**PValue**	**Bonferroni**
hsa04144:Endocytosis	11	CHMP3, ARPC3, CAPZA2, HSPA6, RHOA, RUFY1, SNX1, HLA-B, EHD1, ARFGEF2, VPS36	2.73E-04	3.62E-02
Protein only in PBS treated cells				
Term	**Count**	**Genes**	**PValue**	**Bonferroni**
hsa04144:Endocytosis	15	STAMBP, PARD3, CHMP4A, FAM21A, CHMP7, VPS37A, ARPC5, IGF2R, RBSN, ACAP2, RAB5A, PDGFRA, STAM, VPS28, ARAP1	2.55E-04	4.63E-02

7.3 GO TERMS ASSOCIATED WITH PROTEINS DEREGULATED IN EVS FOLLOWING CISPLATIN TREATMENT.

Downregulated EV protein

Biological Processes	Count	Genes	PValue	Bonferroni
SRP-dependent cotranslational protein targeting to membrane	5	RPL13A, RPL8, RPL3, RPS9, SEC61A1	1.05E-04	3.41E-02
Downregulated EV protein				
Molecular Function	**Count**	**Genes**	**PValue**	**Bonferroni**
poly(A) RNA binding	17	SRSF1, PDIA3, HIST1H1B, XRCC6, RPS9, SSB, TCERG1, HIST1H4A, UBA1, RPL13A, PCBP2, RPL8, RPL3, SPTBN1, TPR, NQO1, ENO1	1.01E-08	1.23E-06
Upregulated EV protein				
Biological Processes	**Count**	**Genes**	**PValue**	**Bonferroni**
regulation of mRNA stability	8	EIF4G1, PSMC6, SET, PSMB1, PSMC3, ANP32A, HSPB1, PSMD6	1.24E-07	6.69E-05
cell-cell adhesion	9	ALDOA, EIF4G1, DDX3X, KIF5B, ATIC, RARS, SLC3A2, KTN1, RUVBL1	8.40E-06	4.53E-03
translational initiation	7	EIF4G1, EIF3A, RPS16, DDX3Y, RPL3, RPL11, RPL4	1.34E-05	7.23E-03
nuclear-transcribed mRNA catabolic process, nonsense-mediated decay	6	EIF4G1, RPS16, RBM8A, RPL3, RPL11, RPL4	8.97E-05	4.73E-02
Upregulated EV protein				
Molecular Function	**Count**	**Genes**	**PValue**	**Bonferroni**
poly(A) RNA binding	28	GLRX3, ALDOA, FKBP4, SNRPD1, STIP1, CALR, TOP1, EIF3A, DDX3X, RBM8A, SRRM2, RPL3, DHX15, ANP32A, RPL11, RPL4, EEF1A1, TCP1, SLC25A5, CKAP4, SLC3A2, KTN1, FBL, FXR1, EIF4G1, RPS16, VCP, HSPB1	1.10E-15	2.25E-13
cadherin binding involved in cell-cell adhesion	12	ALDOA, EIF4G1, TLN1, DDX3X, KIF5B, ATIC, RARS, SLC3A2, KTN1, CLIC1, RUVBL1, ITGB1	1.06E-08	2.14E-06
RNA binding	13	SNRPD1, FBL, FXR1, EIF4G1, EIF3A, DDX3X, RPS16, RBM8A, DDX3Y, FARSB, RPL3, RPL11, RPL4	8.39E-07	1.70E-04
protein binding	51	LDHB, TLN1, SNRPD1, POSTN, MTHFD1, TOP1, RBM8A, ANP32A, RPL11, PSMD6, KIF5B, SLC25A5, SLC3A2, KTN1, CLIC1, EIF4G1, RPS16, RARS, SURF4, FARSB, HSPB1, PTGFRN, RUVBL1, GLRX3, ALDOA, FKBP4, STIP1, CALR, ITGB1, EIF3A, PFN2, SET, PSMB1, DDX3X, DNAJA1, RPL3, DHX15, RPL4, EEF1A1, TCP1, NASP, FBL, SMC3, FXR1, PSMC6, CCT5, VCP, PYGL, PSMC3, PCNA, H3F3A	1.45E-05	2.95E-03
ATP binding	18	TCP1, KIF5B, FKBP4, SMC3, PFAS, MTHFD1, PSMC6, CCT5, DDX3X, VCP, PYGL, PSMC3, RARS, DDX3Y, DNAJA1, FARSB, DHX15, RUVBL1	2.85E-05	5.76E-03

7.4 KEGG PATHWAY ANALYSIS OF EV PROTEINS

Upregulated proteins				
Term	**Count**	**Genes**	**PValue**	**Bonferroni**
hsa03050:Proteasome	4	PSMC6, PSMB1, PSMC3, PSMD6	2.66E-03	2.07E-01
hsa01130:Biosynthesis of antibiotics	6	ALDOA, LDHB, ATIC, GFPT1, ADH5, PFAS	1.06E-02	6.06E-01
hsa03013:RNA transport	5	EIF4G1, EEF1A1, EIF3A, RBM8A, FXR1	2.32E-02	8.70E-01
hsa03010:Ribosome	4	RPS16, RPL3, RPL11, RPL4	5.50E-02	9.93E-01
hsa00010:Glycolysis / Gluconeogenesis	3	ALDOA, LDHB, ADH5	6.75E-02	9.98E-01
hsa04141:Protein processing in endoplasmic reticulum	4	VCP, CKAP4, DNAJA1, CALR	9.19E-02	1.00E+00
Downregulated proteins				
Term	**Count**	**Genes**	**PValue**	**Bonferroni**
hsa03010:Ribosome	4	RPL13A, RPL8, RPL3, RPS9	2.05E-02	6.74E-01
hsa03018:RNA degradation	3	DIS3, WDR61, ENO1	4.36E-02	9.10E-01
Protein only in Evs from cisplatin-treated cells				
Term	**Count**	**Genes**	**PValue**	**Bonferroni**
hsa04370:VEGF signaling pathway	6	NRAS, KRAS, RAC2, PLCG1, MAPK14, RAC1	2.68E-04	4.10E-02
hsa04664:Fc epsilon RI signaling pathway	6	NRAS, KRAS, RAC2, PLCG1, MAPK14, RAC1	4.47E-04	6.73E-02
hsa05205:Proteoglycans in cancer	8	NRAS, CTTN, KRAS, PLCG1, MAPK14, RAC1, PPP1CC, FGF2	2.81E-03	3.55E-01
hsa04810:Regulation of actin cytoskeleton	8	NRAS, KRAS, RAC2, RAC1, ARPC4, PPP1CC, FGF2, NCKAP1	3.78E-03	4.47E-01
hsa04722:Neurotrophin signaling pathway	6	NRAS, KRAS, PLCG1, MAPK14, RAC1, ARHGDIA	5.58E-03	5.82E-01
hsa03010:Ribosome	6	RPL13, RPL22, RPL9, RPL26, RPL27, RPL38	9.38E-03	7.70E-01
hsa03015:mRNA surveillance pathway	5	UPF1, GSPT1, PABPC4, ALYREF, PPP1CC	1.09E-02	8.19E-01
hsa04015:Rap1 signaling pathway	7	NRAS, KRAS, RAC2, PLCG1, MAPK14, RAC1, FGF2	1.46E-02	9.00E-01
hsa05231:Choline metabolism in cancer	5	NRAS, KRAS, RAC2, PLCG1, RAC1	1.55E-02	9.13E-01
hsa05131:Shigellosis	4	CTTN, MAPK14, RAC1, ARPC4	2.29E-02	9.73E-01
hsa03013:RNA transport	6	EIF3B, UPF1, PABPC4, ALYREF, EIF2S3, GEMIN5	2.38E-02	9.76E-01

hsa04071:Sphingolipid signaling pathway	5	NRAS, KRAS, RAC2, MAPK14, RAC1	2.73E-02	9.87E-01
hsa04662:B cell receptor signaling pathway	4	NRAS, KRAS, RAC2, RAC1	2.79E-02	9.88E-01
hsa04650:Natural killer cell mediated cytotoxicity	5	NRAS, KRAS, RAC2, PLCG1, RAC1	2.88E-02	9.90E-01
hsa05100:Bacterial invasion of epithelial cells	4	CTTN, SEPT1, RAC1, ARPC4	3.81E-02	9.98E-01
hsa04666:Fc gamma R-mediated phagocytosis	4	RAC2, PLCG1, RAC1, ARPC4	4.59E-02	9.99E-01
hsa01130:Biosynthesis of antibiotics	6	PGLS, FDPS, IDI1, IDH3A, PPAT, PRPS1	5.12E-02	1.00E+00
hsa04014:Ras signaling pathway	6	NRAS, KRAS, RAC2, PLCG1, RAC1, FGF2	6.40E-02	1.00E+00
hsa04660:T cell receptor signaling pathway	4	NRAS, KRAS, PLCG1, MAPK14	7.51E-02	1.00E+00
hsa05130:Pathogenic Escherichia coli infection	3	CTTN, TUBB6, ARPC4	8.50E-02	1.00E+00
hsa00230:Purine metabolism	5	POLR2H, NUDT5, GMPS, PPAT, PRPS1	8.69E-02	1.00E+00
hsa01200:Carbon metabolism	4	PGLS, ESD, IDH3A, PRPS1	9.30E-02	1.00E+00
hsa04919:Thyroid hormone signaling pathway	4	NRAS, KRAS, ATP1B3, PLCG1	9.49E-02	1.00E+00
hsa04010:MAPK signaling pathway	6	NRAS, KRAS, RAC2, MAPK14, RAC1, FGF2	9.56E-02	1.00E+00
hsa05223:Non-small cell lung cancer	3	NRAS, KRAS, PLCG1	9.96E-02	1.00E+00
Protein only in Evs from PBS treated cells				
Term	**Count**	**Genes**	**PValue**	**Bonferroni**
hsa05203:Viral carcinogenesis	4	HIST1H2BM, HIST1H2BD, HIST1H2BL, SCRIB	5.81E-02	9.65E-01

7.5 GO TERMS ASSOCIATED WITH PROTEINS FOUND IN ONLY ONE TREATMENT GROUP

Protein in only Cisplatin-treated cells

Molecular Function	Count	Genes	PValue	Bonferroni
GO:0005515~protein binding	98	MPZL1, HMGN2, PRPF4B, CHMP3, RPS27L, GGT1, CBX8, ANK1, SLC25A23, FSTL5, MLKL, GNG5, RAB21, ARGLU1, DBNL, TWF2, STRN3, VTI1B, SYNJ2BP, OPTN, DPCD, TIMM8A, CHID1, SNRPE, MRPL43, CRELD2, CCDC12, MTX2, SNX1, NIFK, GSTCD, RRM2B, ARFGEF2, ARPC3, PROCR, EIF1AD, CD276, FDXR, SAP18, UBE2L6, PLGRKT, CDKN1A, METTL13, SARM1, MYH11, POP4, CYP2S1, MAX, GPC3, TPP1, HMOX1, CCDC43, RHOA, CEACAM1, RAP2B, NOL9, FLOT1, TPX2, UBE2H, SLIT2, GTF2H1, PPM1F, SENP3, EML1, MED8, CD81, RIN1, KIAA1191, IFT88, SEC23B, UBE2Z, FHL3, HK2, AKAP9, SFN, MRPL12, SAFB, TBC1D5, HSPA6, RPIA, EHD1, VPS36, USP32, EXOC1, RUFY1, SCOC, IFIT3, PREB, SON, CSNK1D, CSNK1E, MBOAT7, GOLPH3, TMTC3, DPM3, GDF15, AACS, RCN2	1.93E-04	5.35E-02
Protein in only PBS treated cells				
Molecular Function	**Count**	**Genes**	**PValue**	**Bonferroni**
GO:0005515~protein binding	236	MEF2C, XRCC4, TMEM19, MEF2A, LSM7, CHMP7, VPS51, NSRP1, CIAPIN1, FAH, INTS7, PIK3C3, STAM, NUP37, EIF2B2, NSMAF, STAG2, EIF2B5, IKBKAP, ROCK1, TOX4, MARK2, UHRF1, NME3, PDGFRA, ACP1, PEA15, VRK1, KRAS, HIP1, UNC45A, WDR59, LAMTOR5, ZC3H14, DVL2, ZNF622, ZC3H13, KIF3A, SREK1, MAP2K4, SRA1, CREBBP, TRIO, YTHDC2, FXR2, PRPSAP1, PTPN12, NOTCH3, CNIH4, HSPA14, TMEM41A, MAB21L1, MAB21L2, FAM96B, SPIN1, TCOF1, CCNT1, VPS37A, BAG5, FXN, BAG3, PARG, FAM129A, COX17, TUBB3, TFIP11, STX4, HIST1H1C, ZC3H7B, EXOSC4, DNAJC21, PDCL3, ANKRD28, RRM2, NCK1, RAB5A, FKBP15, CAND2, PARVB, SRGAP2, TF, PARD3, EXOC7, PPP6R3, POLR2C, NUFIP2, NCAPH, RBSN, GATAD2A, WDR12, GATAD2B, SNAP23, USP34, KIF21A, RBM26, HSD17B8, EIF4ENIF1, SHMT1, TBX2, TTC17, MEF2D, MEOX2, COG7, PYGM, YAF2, GSK3B, POLDIP3, USP47, CWC22, PES1, LUC7L, TRMT112, GNA13, RNMT, CHMP4A, CLPB, TTC9C, CNOT1, LZTFL1, CNOT6, FNTB, TBC1D15, CISD2, NUDCD3, PACSIN3, SMARCD2, SMARCD1, AKR7A2, ORC2,	6.77E-10	3.47E-07

		SCAMP1, ATG9A, NUDT1, BST2, NUDT4, PDXP, CLPX, DCUN1D1, TRIM33, IGBP1, MCMBP, CLIP1, MFAP1, SNRPC, SEPT6, PPP5C, BLM, IFITM3, ARPC5, LIN28B, LLGL1, CXXC1, ZFC3H1, PEF1, NIPBL, METTL1, GMPPA, OTUD7B, CLASP1, STRBP, ERCC6L, RAB8B, MRC2, INTS12, ATG3, ARMC1, LIN7A, C8ORF37, NOSIP, UACA, SALL4, SMARCC1, SALL1, POLD2, AHCYL1, PTPN1, AHCYL2, ABL2, EIF4E2, GPATCH8, DAP3, NDUFAF4, C9ORF78, ARHGAP17, THADA, PDCD1, DSTN, AKT1, SLC1A5, CASP3, GPKOW, CAMSAP2, CASP7, EDC3, PCBP2, CDK12, MKL2, VPS11, C11ORF68, ANKS1A, RING1, STXBP1, MINK1, MRPS6, COQ9, CDK7, RB1, UBE2C, SMU1, NCOA2, CRKL, MRPS9, IGF2R, CARM1, PPP4R2, KMT2A, ARID2, N4BP1, REL, KIF6, SH3GLB1, POU2F3, POU2F1, GTF3C1, TERF2, GEMIN4, SCO2, STAMBP, GMDS, DRG1, MRGBP, ZBED1, PSMG2, SP3, VPS28, SETD2, ARAP1		
GO:0044822~poly(A) RNA binding	51	TRMT2A, TCOF1, CNOT1, NSRP1, CISD2, GRWD1, PCBP2, DDX24, EIF1, C11ORF68, BST2, HIST1H1C, ZC3H7B, STXBP1, DNAJC21, EIF1B, SARS2, MARK2, CRKL, MRPS9, LLPH, MFAP1, SNRPC, RBM33, LIN28B, NUFIP2, ZFC3H1, PEF1, MRPL14, SPATS2, STRBP, NSUN5, NMD3, RBM26, ZNF622, EIF4ENIF1, ZC3H14, ZC3H13, SREK1, YTHDC2, FXR2, TRIM56, NOSIP, POLDIP3, NOP16, PTPN1, PES1, GPATCH8, EIF4E2, REPIN1, DAP3	1.82E-07	9.29E-05
Protein in only Evs from Cisplatin-treated cells				
Biological Processes	**Count**	**Genes**	**PValue**	**Bonferroni**
GO:0000184~nuclear-transcribed mRNA catabolic process, nonsense-mediated decay	8	UPF1, GSPT1, RPL13, RPL22, RPL9, RPL26, RPL27, RPL38	1.03E-05	0.007534
GO:0006413~translational initiation	8	EIF3B, RPL13, RPL22, RPL9, RPL26, RPL27, EIF2S3, RPL38	2.57E-05	0.018748
GO:0006614~SRP-dependent cotranslational protein targeting to membrane	7	RPL13, RPL22, RPL9, SRP68, RPL26, RPL27, RPL38	2.85E-05	0.020776
Protein in only Evs from Cisplatin-treated cells				
Molecular Function	**Count**	**Genes**	**PValue**	**Bonferroni**

GO:0044822~poly(A) RNA binding	29	HDLBP, RPL13, SRSF11, SRP68, PABPC4, HDGF, SKIV2L2, YBX1, NUFIP2, DDX27, RBM28, GEMIN5, UPF1, SUB1, ALYREF, RPL26, DDX1, FDPS, RPL27, PPP1CC, HNRNPR, DDX6, ATXN2, TRAP1, GSPT1, RPL22, ARCN1, SNRPA, KPNA2	1.53E-10	3.69E-08
GO:0003723~RNA binding	15	HDLBP, UPF1, RPL13, PABPC4, RPL26, RPL38, HNRNPR, YBX1, NUFIP2, ATXN2, TROVE2, EIF3B, RPL22, RPL9, SNRPA	7.28E-06	0.001761

7.6 GO TERMS FOR PROTEINS WITH HIGHER RELATIVE ENRICHMENT IN EVS THAN IN CELLS FOLLOWING CISPLATIN TREATMENT

Biological Processes	Count	Genes	PValue	Bonferroni
GO:0006413~translational initiation	17	RPLP2, RPL24, EIF3C, EIF3D, EIF3CL, EIF3A, RPS16, RPS17, EIF3H, RPL3, RPS12, RPL5, EIF3I, RPL11, UBA52, RPS23, RPS27A	1.86E-16	1.59E-13
GO:0006614~SRP-dependent cotranslational protein targeting to membrane	11	RPS16, RPS17, RPS12, RPL3, RPLP2, RPL5, RPL24, RPL11, UBA52, RPS27A, RPS23	2.85E-10	2.04E-07
GO:0019083~viral transcription	11	RPS16, RPS17, RPS12, RPL3, RPLP2, RPL5, RPL24, RPL11, UBA52, RPS27A, RPS23	1.63E-09	1.17E-06
GO:0000184~nuclear-transcribed mRNA catabolic process, nonsense-mediated decay	11	RPS16, RPS17, RPS12, RPL3, RPLP2, RPL5, RPL24, RPL11, UBA52, RPS27A, RPS23	2.95E-09	2.12E-06
GO:0038061~NIK/NF-kappaB signaling	9	PSMD13, PSMC5, PSMB1, PSMC3, UBC, UBB, PSMD6, UBA52, RPS27A	6.51E-09	4.68E-06
GO:0051436~negative regulation of ubiquitin-protein ligase activity involved in mitotic cell cycle	9	PSMD13, PSMC5, PSMB1, PSMC3, UBC, UBB, PSMD6, UBA52, RPS27A	1.18E-08	8.45E-06
GO:0043488~regulation of mRNA stability	10	PSMD13, PSMC5, PSMB1, PSMC3, UBC, UBB, PSMD6, UBA52, RPS27A, HSPA8	1.34E-08	9.63E-06
GO:0051437~positive regulation of ubiquitin-protein ligase activity involved in regulation of mitotic cell cycle transition	9	PSMD13, PSMC5, PSMB1, PSMC3, UBC, UBB, PSMD6, UBA52, RPS27A	2.03E-08	1.46E-05
GO:0031145~anaphase-promoting complex-dependent catabolic process	9	PSMD13, PSMC5, PSMB1, PSMC3, UBC, UBB, PSMD6, UBA52, RPS27A	2.77E-08	1.99E-05

GO:0006412~translation	13	SLC25A6, RPLP2, RPL24, RPS16, RPS17, RPS12, FARSB, RPL3, RPL11, RPL5, UBA52, RPS23, RPS27A	4.79E-08	3.44E-05
GO:0060071~Wnt signaling pathway, planar cell polarity pathway	9	PSMD13, PSMC5, PSMB1, PSMC3, UBC, UBB, PSMD6, UBA52, RPS27A	9.26E-08	6.65E-05
GO:0000086~G2/M transition of mitotic cell cycle	10	KHDRBS1, NES, DYNLL1, UBC, MAPRE1, UBB, TUBA1A, DYNC1H1, UBA52, RPS27A	1.61E-07	1.16E-04
GO:0000209~protein polyubiquitination	11	PSMD13, PSMC5, PSMB1, HUWE1, PSMC3, UBC, NPEPPS, UBB, PSMD6, UBA52, RPS27A	1.91E-07	1.37E-04
GO:0001731~formation of translation preinitiation complex	6	EIF3C, EIF3D, EIF3CL, EIF3A, EIF3H, EIF3I	2.43E-07	1.74E-04
GO:0002223~stimulatory C-type lectin receptor signaling pathway	9	PSMD13, PSMC5, PSMB1, PSMC3, UBC, UBB, PSMD6, UBA52, RPS27A	2.60E-07	1.86E-04
GO:0019068~virion assembly	5	PPIA, UBC, UBB, UBA52, RPS27A	6.36E-07	4.57E-04
GO:0033209~tumor necrosis factor-mediated signaling pathway	9	PSMD13, PSMC5, PSMB1, PSMC3, UBC, UBB, PSMD6, UBA52, RPS27A	6.38E-07	4.58E-04
GO:0090263~positive regulation of canonical Wnt signaling pathway	9	PSMD13, PSMC5, PSMB1, PSMC3, UBC, UBB, PSMD6, UBA52, RPS27A	7.26E-07	5.21E-04
GO:0006364~rRNA processing	11	RPS16, RPS17, RPS12, RPL3, RPLP2, RPL5, RPL24, RPL11, UBA52, RPS27A, RPS23	7.70E-07	5.53E-04
GO:0006446~regulation of translational initiation	6	EIF3C, EIF3D, EIF3CL, EIF3A, EIF3H, EIF3I	2.55E-06	1.83E-03
GO:0007017~microtubule -based process	6	DYNLL1, DYNLL2, TUBA3C, TUBA1A, TUBA1B, TUBA1C	2.55E-06	1.83E-03
GO:0042769~DNA damage response, detection of DNA damage	6	RFC5, UBC, DNAJA1, UBB, UBA52, RPS27A	2.55E-06	1.83E-03
GO:0050852~T cell receptor signaling pathway	9	PSMD13, PSMC5, PSMB1, PSMC3, UBC, UBB, PSMD6, UBA52, RPS27A	3.53E-06	2.53E-03
GO:0042276~error-prone translesion synthesis	5	RFC5, UBC, UBB, UBA52, RPS27A	4.82E-06	3.46E-03
GO:0070987~error-free translesion synthesis	5	RFC5, UBC, UBB, UBA52, RPS27A	4.82E-06	3.46E-03
GO:0090090~negative regulation of canonical Wnt signaling pathway	9	PSMD13, PSMC5, PSMB1, PSMC3, UBC, UBB, PSMD6, UBA52, RPS27A	7.22E-06	5.17E-03
GO:0006297~nucleotide-excision repair, DNA gap filling	5	RFC5, UBC, UBB, UBA52, RPS27A	1.29E-05	9.23E-03
GO:0038095~Fc-epsilon receptor signaling pathway	9	PSMD13, PSMC5, PSMB1, PSMC3, UBC, UBB, PSMD6, UBA52, RPS27A	1.37E-05	9.82E-03

GO:0061418~regulation of transcription from RNA polymerase II promoter in response to hypoxia	5	CUL2, UBC, UBB, UBA52, RPS27A	2.44E-05	1.74E-02
GO:0043161~proteasome-mediated ubiquitin-dependent protein catabolic process	9	PSMD13, PSMC5, PSMB1, PSMC3, UBC, UBB, PSMD6, UBA52, RPS27A	3.54E-05	2.51E-02
GO:0019058~viral life cycle	5	PPIA, UBC, UBB, UBA52, RPS27A	3.70E-05	2.62E-02
GO:0010939~regulation of necrotic cell death	4	UBC, UBB, UBA52, RPS27A	4.74E-05	3.34E-02
GO:0032479~regulation of type I interferon production	4	UBC, UBB, UBA52, RPS27A	6.13E-05	4.31E-02
GO:0002756~MyD88-independent toll-like receptor signaling pathway	4	UBC, UBB, UBA52, RPS27A	6.13E-05	4.31E-02
GO:0000398~mRNA splicing, via spliceosome	9	HNRNPM, HNRNPK, SRSF6, SRRM2, DHX15, HNRNPC, HNRNPA1, HSPA8, SF3A3	6.66E-05	4.67E-02
GO:0019985~translesion synthesis	5	RFC5, UBC, UBB, UBA52, RPS27A	6.76E-05	4.74E-02
Molecular Function	Count	Genes	PValue	Bonferroni
GO:0044822~poly(A) RNA binding	47	GLRX3, GANAB, STRAP, STIP1, SERPINH1, GOT2, EIF3C, HNRNPM, EIF3D, EIF3A, HNRNPK, EIF3H, SRRM2, RPL3, DHX15, RPL5, RPL11, HNRNPC, DYNC1H1, LBR, KPNB1, RPS27A, HSPA8, RBM25, RPS23, KHDRBS1, TCP1, ACTN4, SLC3A2, KTN1, RPL24, ILF3, MYH9, HNRNPA1, FLNA, SF3A3, RPS16, HUWE1, ARF1, RPS17, SRSF6, PPIA, IPO5, UBC, RPS12, MAP4, MAPRE1	3.85E-27	1.07E-24
GO:0005515~protein binding	85	NAMPT, TLN1, ATP5B, FERMT2, RPLP2, CUL2, LONP1, DYNLL1, DYNLL2, H2AFY, RPL11, TUBA1A, DYNC1H1, PSMD6, TUBA1B, KPNB1, LBR, RPS27A, TUBA1C, KHDRBS1, ACTN4, MYH1, KIF5B, SLC25A6, TOR1AIP1, SLC3A2, KTN1, CLIC1, MYH9, MCM5, FLNA, RFC5, ALDH7A1, RPS16, HUWE1, IPO7, IPO5, FARSB, UBC, SURF4, UBB, MAPRE1, UBA52, GLRX3, ECH1, AHCY, STRAP, STIP1, ITGB1, MIF, EIF3C, ANXA6, EIF3D, HNRNPM, EIF3A, STT3A, HNRNPK, PSMB1, EIF3H, DHX15, RPL3, TUBA3C, DNAJA1, RAB11A, RPL5, EIF3I, HNRNPC, RPS23, CHD4, RBM25, HSPA8, TCP1, ILF3, RPL24, COTL1, HNRNPA1, SF3A3, CCT5, PSMC5, ATP2A2, ARF1, SRSF6, PSMC3, PPIA, MAP4	3.72E-10	1.04E-07

GO:0003735~structural constituent of ribosome	12	RPS16, RPS17, SLC25A6, RPS12, RPL3, RPLP2, RPL5, RPL24, RPL11, UBA52, RPS27A, RPS23	1.10E-07	3.06E-05
GO:0003723~RNA binding	17	HNRNPA1L2, KHDRBS1, ILF3, RPL24, HNRNPA1, SF3A3, EIF3D, HNRNPM, EIF3A, HNRNPK, RPS16, SRSF6, RPL3, FARSB, RPL5, RPL11, HNRNPC	1.97E-07	5.49E-05
GO:0098641~cadherin binding involved in cell-cell adhesion	13	TLN1, TWF1, HNRNPK, KIF5B, SLC3A2, KTN1, RPL24, CLIC1, MAPRE1, MYH9, ITGB1, FLNA, HSPA8	2.00E-07	5.58E-05
GO:0003743~translation initiation factor activity	6	EIF3C, EIF3D, EIF3CL, EIF3A, EIF3H, EIF3I	3.48E-05	9.66E-03

7.7 KEGG PATHWAYS FOR PROTEINS WITH HIGHER RELATIVE ENRICHMENT IN EVS THAN IN CELLS FOLLOWING CISPLATIN TREATMENT

Term	Count	Genes	PValue	Bonferroni
hsa03010:Ribosome	11	RPS16, RPS17, RPS12, RPL3, RPLP2, RPL5, RPL24, RPL11, UBA52, RPS27A, RPS23	2.52E-06	2.62E-04
hsa03040:Spliceosome	10	HNRNPA1L2, HNRNPM, HNRNPK, SRSF6, DHX15, HNRNPC, HNRNPA1, RBM25, HSPA8, SF3A3	1.64E-05	1.70E-03
hsa03050:Proteasome	5	PSMD13, PSMC5, PSMB1, PSMC3, PSMD6	1.45E-03	1.40E-01
hsa05130:Pathogenic Escherichia coli infection	5	TUBA3C, TUBA1A, TUBA1B, ITGB1, TUBA1C	2.51E-03	2.30E-01
hsa03013:RNA transport	8	EIF3C, EIF3D, EIF3CL, EIF3A, STRAP, EIF3H, EIF3I, KPNB1	3.13E-03	2.78E-01
hsa04962:Vasopressin-regulated water reabsorption	4	DYNLL1, DYNLL2, RAB11A, DYNC1H1	1.31E-02	7.48E-01
hsa04145:Phagosome	6	TUBA3C, DYNC1H1, TUBA1A, TUBA1B, ITGB1, TUBA1C	2.89E-02	9.53E-01
hsa00350:Tyrosine metabolism	3	GOT2, ADH5, MIF	5.89E-02	9.98E-01
hsa04540:Gap junction	4	TUBA3C, TUBA1A, TUBA1B, TUBA1C	7.68E-02	1.00E+00